Revitalizing lignin

Revitalizing lignin

On lignin applications in materials and additives

Monika Aleksandra Jędrzejczyk

Revitalizing lignin

On lignin applications in materials and additives

Monika Aleksandra Jędrzejczyk

Revitalizing lignin

On lignin applications in materials and additives

DISSERTATION

to obtain the degree of Doctor at Maastricht University,
on the authority of the Rector Magnificus, Prof. dr. Pamela Habibović
in accordance with the decision of the Board of Deans,
to be defended in public
on Tuesday 14th of March 2023, at 16:00 hours

by

Monika Aleksandra Jędrzejczyk

Supervisors
Dr. Katrien Bernaerts
Prof. Andrij Pich

Assessment committee
Prof. dr. Maarten Honing (Chair)
Dr. Hanne Diliën
Dr. Richard Gosselink, *Wageningen Food & Biobased Research*
Prof. dr. Wim Thielemans, *Katholieke Universiteit Leuven*

Table of contents

Hello darkness, my old friend…

Simon & Garfunkel - The Sound of Silence

CHAPTER 1

Introduction

Transitioning toward bioeconomy

In academia, industry, and society, we are witnessing a great transition: from a linear economy to a circular economy. The concept of the circular economy is nothing new - it was introduced in the 1960s, followed defining it by the Ellen MacArthur Foundation in 2012 as 'an industrial economy that is restorative or regenerative by intention and design'.[1] This concept has a variety of ways in which it can be implemented: by repair, by reuse, by renewal, by refurbishment, by remanufacture, by maintenance, by upgrading, by recycling, and by cascading. As a result of this, the use of renewable resources gained more interest, as well as the entire development of a biobased economy to produce sustainable fuels, chemicals, and materials.[2] This transition is gaining momentum, which can be seen not only as an increasing social demand to shift into a more sustainable direction due to climate change, but also as its reflection in policymaking and industrial implementation.[3-5] Examples of such initiatives are United Nations 2030 Agenda for Sustainable Development and the Sustainable Development Goals, European Commission's European Green Deal and Bioeconomy strategy, US National Bioeconomy Blueprint, and China's 14th five-year plan.[6-11] What is important is not only assess the environmental and techno-economic impact of the biobased economy, but also their social aspects and support of those efforts by standardization and certification.[3, 12-15]

The core of the bioeconomy is its feedstock, which can include agricultural and forest biomass (e.g., crops, wood, and grasses), algae and fishery biomass, or waste biomass (e.g., food waste and municipal waste).[16, 17] Certain biomass feedstocks serve the purpose of food and feed production (e.g., crops and agricultural produce) while others are not (e.g., miscanthus, forestry biomass, nonedible plants, food, and municipal waste); there are also some feedstocks (e.g., palm oil, triticale, maize, soya, and coconut), which can be used as both depending on the market opportunities.[17] However, the competition with edible feedstock as well as water consumption associated with their production is problematic.[18, 19] In that respect, lignocellulosic biomass is an important feedstock, especially given that it is the most abundant renewable material on earth.[20]

Introducing lignin

Cellulose (35-80%), hemicellulose (5-35%), and lignin (15-35%) are the main components of the lignocellulosic biomass, and their ratio depends on the biomass source.[21] Lignin content is the highest in hardwood, decreasing in softwood and grasses.[21] There are multiple possibilities for lignocellulosic biomass conversion, using both cellulose and hemicellulose (to ethanol, furfural derivatives, sugar platforms, ethylene glycol, acetone, ethylene),[19, 22-27] and using lignin (technical or fractionated lignin, or llignin converted to monomers and oligomers after depolymerization).[19, 28-30] This research focuses on the biggest source of bioaromatic compounds - lignin. Lignin is an amorphous material consisting of highly branched aromatic macromolecules based on three basic phenylpropanoid components (coumaryl, coniferyl, and sinapyl alcohols) enzymatically cross-linked during their biosynthesis and bonded by various types of ether, ester, and carbon-carbon linkages (Figure 1).[31-33] Lignin has various functionalities: phenolic and aliphatic hydroxyl groups, methoxy moieties, carboxylic acids, and unsaturated carbon-carbon bonds. [21, 34] In hardwood, syringyl and guaiacyl units are most abundant (approx. 25-50% and 45-75%, respectively), while for softwoods guaiacyl units are predominant (approx. 90-95%).[21, 34] Grasses contain mostly guaiacyl and syringyl units (approx. 35-80% and 20-55%, respectively), and they incorporate p-hydroxyphenyl units in their structure (approx. 5-35%).[21, 34] In Nature, lignin provides lignocellulosic materials with inner strength, rigidity, and dimensional stability due to covalent and non-covalent interactions with cellulose and hemicellulose, water impermeability and its transport within the plant, and it also has UV-blocking, antioxidant, antimicrobial, and antifungal properties.[35-37]
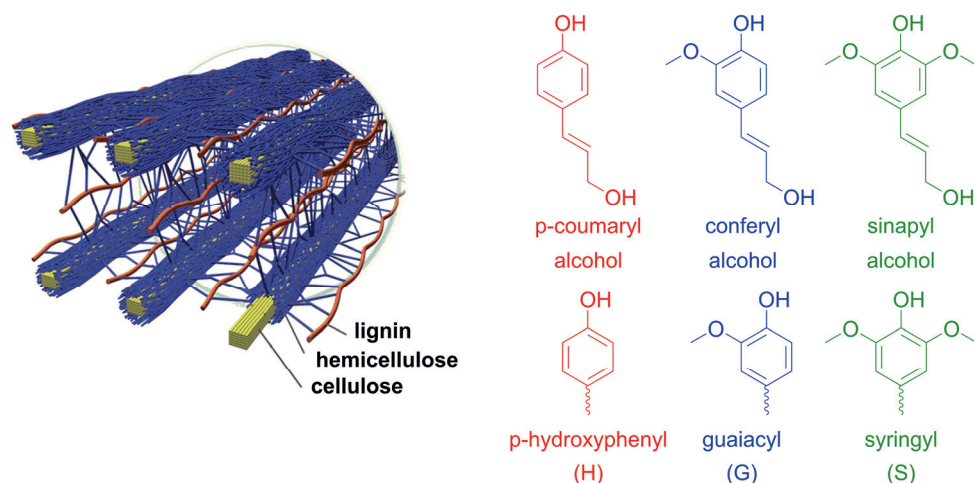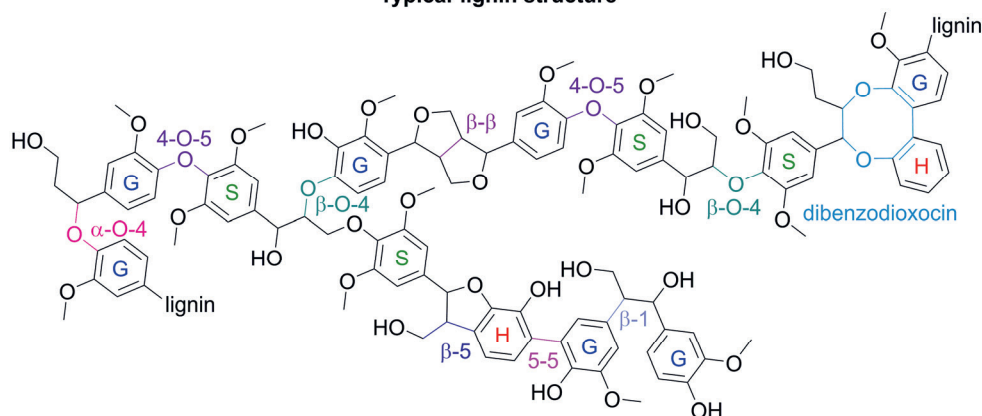
Figure 1 *Lignin composition and bonds present in its structure. Adapted from ref. 35 and 37*

Isolation of technical lignins

The purpose of a biomass refinery is to separate and convert biomass feedstock into marketable products. Currently, lignin is often considered as a by-product of the paper industry and lignocellulose bioethanol production, and it has relatively low value and quality due to the harsh processing conditions.[38] From the 70 million tons of lignin produced annually, only 5% is not used as an energy source.[39] In order to valorize lignin and widen the spectrum of its use, added-value applications are currently being developed, and lignin biorefineries converting lignin into high-value products are drawing more and more attention.[40-45] There are multiple technical lignins available on the market, including kraft lignin, lignosulfonates, soda lignin,

organosolv lignin, and steam-explosion lignin obtained in second-generation ethanol biorefineries.[46-49]

The majority of technical lignin is obtained via the kraft process as a side stream of paper production. In this process, lignocellulosic biomass is treated with a solution of sodium hydroxide and (sodium) sulfide at elevated temperatures, between 150 and 170 °C.[50, 51] After the biomass fractionation, there are two streams: solid cellulose stream and 'black liquor' containing dissolved lignin and hemicellulose components. However, the majority of the 'black liquor' is used as a source of energy, and only a small portion is furtherly processed to isolate kraft lignin. The isolation step involves neutralization and precipitation of solid kraft lignin. Due to the harsh processing conditions, this kind of lignin is highly condensed, insoluble, and possesses sulfur (1-3%), which limits its applications in, for example, resins synthesis. On the other hand, this method leads to the highest extent of lignin removal and provides the best quality of the remaining cellulose fibers.[52]

Alternatively, the sulfite process can be used to produce lignosulfonates, also known as sulfonated lignin. This process can be carried out in a broad pH range (2-13), between 140 and 160 °C, by using sulfurous acid and/or a sulfite salt (magnesium, calcium, sodium, or ammonium).[40, 51, 53] Lignosulfonates are water soluble in a broad pH range due to the presence of sulfonates, making it more difficult to isolate from the spent liquor than precipitating the kraft lignin. For this purpose, membrane filtration is the most employed method of lignosulfonates separation, next to the Howard process using lime.[53] Lignosulfonates can also be produced from kraft lignin after sulfonation.[53]

Another important process of lignin isolation from biomass is soda pulping. Similar to the kraft process, it uses alkaline (typically sodium hydroxide) solution treatment under high pressure between 140 and 170 °C, but it does not use sulfides, which makes the isolated lignin sulfur-free.[47, 54] This isolation process is less efficient than the kraft processing, and it is used primarily to isolate lignin from herbaceous feedstocks.[40] This kind of lignin is usually hard to filter and centrifuge because of the high content of carboxylic acid moiety, therefore, it is often coagulated to ensure better filterability.[40]

Another common process to isolate lignin from biomass is the organosolv process.[30] It involves lignin dissolution in solvents such as alcohols, organic acids, ketones, polyols, and ethers, in elevated temperatures, between 100 and 250 °C, while mineral acids or bases can be used as a catalyst to control the pulping rate and increase the yield.[47, 50, 51, 55, 56] Organosolv lignin is often isolated via precipitation in a non-solvent such as water. This kind of lignin has a high solubility in polar organic solvents and one of the lowest carbohydrates and ash content, making it

the highest-purity lignin available on the market.[30] Moreover, this process is considered to be more environmentally friendly due to the milder conditions and lack of toxic chemicals used during this process.[30]

Lignin can also be obtained as a residue from bioethanol production using the steam explosion process and/or after hydrolytic degradation of the cellulosic and hemicellulosic components.[46, 47, 54] In this process, biomass is subjected to high-pressure steam and carried out at temperatures ranging from 180 to 250 °C to cause hemicellulose autohydrolysis, followed by explosive decompression to atmospheric pressure resulting in disruption of the biomass.[57] Lignin can be isolated after neutral washing to remove hemicellulose sugars, followed by the alkali process, or after cellulose enzymatic hydrolysis using cellulases and hemicellulases enzymes.[47, 57] This process is considered a suitable pretreatment method for enzymatic hydrolysis of cellulose for monomeric sugar and ethanol production in an environmentally and cost-effective way.[47]

'Lignin-first' biorefineries

Nowadays, we can observe the emergence of 'lignin-first' biorefineries whose primary focus is isolating lignin for the production of renewable aromatic compounds.[49, 58] In 'cellulose-first' processes, such as kraft and sulfide processes, the lignin structure is irreversibly altered, and the conversion of those lignins into value-added chemicals is greatly limited due to lignin condensation and/or the presence of sulfur. 'Lignin-first' biorefineries prioritize lignin isolation and/or depolymerization, while cellulose is considered a residual stream, which should also be valorized, leading to the fullest utilization of the available lignocellulosic biomass, such as woody and herbaceous biomass.[49, 59] Usually, 'lignin-first' processes involve three steps: (1) lignin isolation from the whole biomass using an organic solvent through solvolysis or acid-catalyzed reactions, (2) catalytic depolymerization and stabilization of the isolated lignin intermediates to prevent condensation of reactive species generated by lignin depolymerization, and (3) further depolymerization, which happens if lignin intermediates are not fully depolymerized at the stabilization stage.[49] There are several approaches described in the literature that fall under this lignin biorefinery scheme, including reductive catalytic fractionation (RCF), diol-assisted fractionation (DAF), and aldehyde-assisted fractionation (AAF).[49, 59, 60]

The core principle of RCF is lignin stabilization by reacting it with a hydrogen donor (usually H_2 gas or H_2 donor solvent) at elevated temperatures (between 180 and 280 °C) in the presence of a redox-active catalyst through hydrogenation and hydrogenolysis.[61] Usually, catalysts such as Pd/C, Pt/C, Rh/C, Ru/C, Ru/Al$_2$O$_3$, Raney-Ni, Ni/SiO$_2$, and copper-chromite, are used in the RCF process, sometimes

in the presence of acidic or basic promoters.[50, 59, 61, 62] The stabilization mechanism in this case usually involves nucleophilic protection of the benzylic carbocations formed at the C_α of the original β-O-4 bonds which are destroyed during an organosolv isolation process.[63] The main products of RCF are the following streams: (1) lignin oil, which is a mixture of phenolic monomers, dimers, and lignin oligomers, (2) carbohydrate pulp (mainly cellulose), and (3) water-soluble sugars (originating mainly from hemicellulose).[59] Depending on the applied processing conditions and the used catalyst, the main products of RCF include 4-propylcyclohexanol, 4-propylcyclohexanediol, 4-ethylsyringol, 4-ethanolsyringol, 4-propylsyringol, 4-propenylsyringol, 4-propanolsyringol, 4-propylguaiacol, 4-propenylguaiacol, methoxypropylsyringol, and methoxypropylguaiacol.[59] Depending on the feedstock, the monomer yield usually does not exceed 30% for softwoods, 40-55% for hardwoods, and 25-40% for herbaceous crops.[50]

In DAF, diols such as ethylene glycol are used to form protective groups on the S, G, and H-aldehydes, which are intermediate products of the acid-catalyzed depolymerization.[64, 65] In this way, the highly selective formation of the corresponding stable cyclic acetals results in suppressing lignin intermediates recondensation.[66] Alternatively, AAF utilizes the already existing 1,3-diols (α- and γ-hydroxyl groups) on lignin side chains. Upon reaction with aldehyde, such as formaldehyde, a 1,3-dioxane structure is formed, which prevents condensation reactions similar to DAF.[67, 68] In both approaches, the protective acetal moiety can be converted to the corresponding phenolic monomers after hydrogenolysis.

Lignin conversions

Thermal conversion of lignin
Thermal conversion is the most widely industrially applied method of lignin conversion to chemicals and fuels.[51] Most reported routes of lignin thermal conversions are pyrolysis, gasification, and hydrothermal liquefaction. In pyrolysis, lignin is treated at elevated temperature (between 300 and 800 °C) and usually under elevated pressure for short (2-3 s, fast pyrolysis) or longer (above 30 min, slow pyrolysis) periods of time in the absence or in the presence of small amounts of oxygen.[51, 63, 69, 70] Products of pyrolysis are combustible gases (such as hydrogen, methane, ethane, ethylene, carbon monoxide, and carbon dioxide), bio-oil (composed of alcohols, aldehydes, phenolic monomers), and bio-char (containing carbonous material, ash, inorganics).[46, 51, 63] Pyrolysis processes can be divided into two different stages: the first stage of pyrolysis, between 150 and 400 °C, where ether linkages are destroyed (including β-O-4 bonds), and the secondary stage of pyrolysis, between 400 and 800 °C, where most of the bonds in lignin and

depolymerized lignin monomers break down and the gasification starts.[38, 70-72] The products of the first stage of pyrolysis include 4-methylguaiacol, syringol, coniferyl alcohol, vanillin, and isoeugenol, while the second stage of pyrolysis yields in the formation of products such as catechol, pyrogallol, cresols, vanillin, guaiacol, and o-quinone methide, and ultimately carbon monoxide, acetylene, coke, and polycyclic aromatic hydrocarbons.[38, 70-72]

Fast pyrolysis is another variant of lignin thermal conversion methods, more effective in converting lignin into bio-oil than slow pyrolysis.[51] The product composition strongly depends on the operating conditions such as temperature, heating rate, residence time, and used feedstock.[38, 69, 73] Temperature is the most crucial parameter: at lower temperatures, the products consist mostly of aldehydes, styrenes, guaiacol hydroxyl, and toluols, while at higher temperatures cresols, catechols, hydroxyphenols, and biochar are mainly obtained.[51] Pyrolysis can also be combined with catalysts, such as zeolites, metal oxides, and metal chlorides to improve its performance.[38, 63] Usually, pyrolysis results in a conversion of approximately 40% of lignin into bio-oil containing approximately 20% phenolic compounds.[73] Although pyrolysis can be an effective method for converting lignin, the low selectivity of this process, harsh operating conditions, and difficulties in products separation limit its application.[38, 71]

Next to pyrolysis, gasification is another common thermal processing method. Here, lignin is subjected to very high temperatures, above 800 °C, under elevated pressure, in an oxidative environment (such as air, oxygen, or steam) to produce a mixture of hydrogen, carbon monoxide (syngas), and combustible gasses such as methane.[46, 48, 51, 52, 70, 71, 74] Gasification products can be used in the conventional Fischer-Tropsch synthesis to be converted to various chemicals and fuels. The biggest drawback of gasification is undesirable tar formation, which limits its application.

Because harsh conditions are usually applied in pyrolysis and gasification processes, an alternative approach was developed, namely hydrothermal liquefaction. In this process, lignin is converted to simple molecules in aqueous media at elevated temperature and pressure (between 150 and 450 °C, between 5 and 25 MPa) in subcritical or supercritical conditions.[69, 70, 75] The main products of hydrothermal liquefaction are bio-oil containing phenol, catechol, cresols, guiacol, aromatic aldehydes, ketones, and acids among other primary and substituted phenolic compounds, obtained after lignin hydrolysis, due to a fracture of lignin ether and carbon-carbon bonds, cleavage of methoxy moieties and benzene ring alkylation.[69, 70, 75] Conversion of lignin to bio-oil is improved compared with pyrolysis and gasification, up to 60-80% conversion.[69, 70] This solution can also utilize catalysis to improve the conversion rate, and the use of catalysts such as ZrO_2, K_2CO_3, and

NaOH was reported.[69, 70] Similar to pyrolysis, this process results in a mixture of monomers which are difficult to fractionate.[69] Even though this process is more environmentally friendly than pyrolysis due to the milder conditions and the possibility of using wet feedstock, it is facing difficulties with scale up and industrialization due to the problems with reproducing lab scale conditions (heat transfer and heat sinking issues).[69, 74, 76]

Acid-catalyzed lignin depolymerization

Acids play an important role in lignin isolation from biomass, but they can also be used in acid-catalyzed lignin depolymerization techniques. This process is usually performed at elevated temperatures, between 140 and 370 °C, a pressure between 2 and 25Mpa, and in aqueous or alcoholic solutions.[29, 38, 50] Acids such as HCl, H_2SO_4, acetic acid, formic acid, Lewis acids such as metal chlorides, metal triflates, and acidic zeolites are often reported in this depolymerization technique.[29, 50] The mechanism of acid-catalyzed lignin depolymerization is that under acidic conditions, β-O-4 bonds are broken and converted to substituted (with aldehyde, aceto, acid, alkene, or alkane) phenol, methoxyphenols, and catechols as well as condensed, charred lignin as a byproduct.[29, 50, 51, 73] This process usually results in low conversion toward monomers, typically less than 20%, but there are some examples of higher conversion.[29, 50] Because of low monomer yields, repolymerization of lignin, harsh reaction conditions, use of corrosive chemicals, generation of a significant amount of waste, and environmental pollutants, further developments of acid-catalyzed depolymerization are limited.[38]

Base-catalyzed lignin depolymerization

Alternatively, base-catalyzed lignin depolymerization is another widely studied lignin depolymerization technique. Similarly to acid-catalyzed depolymerization, base-catalyzed depolymerization is performed at elevated temperatures, between 240 and 330 °C, pressure 3-90 MPa, in aqueous solution or organic solvents such as alcohols, glycols, or tetrahydrofuran.[29, 51] Bases such as NaOH, KOH, K_2CO_3, $Ca(OH)_2$, LiOH, CsOH, CaO, MgO, $Mg(OH)_2$, basic zeolites were reported in this approach.[29, 38, 73] In base-catalyzed depolymerization, monomers are obtained as a result of cleavage of β-O-4 bonds involving ionized lignin hydroxyl groups, which are converted to an oxirane intermediate, which readily opens in the presence of a nucleophile (base) to corresponding monomers such as syringol, guiacol or coniferyl alcohol.[38, 73] Products of this process are a mixture of phenolic products containing substituted (with alkyl chains, aldehyde, or acetophenone) phenols, methoxyphenols, catechol, and vanillin.[29, 73] Similarly to acid-catalyzed depolymerization, base-catalyzed depolymerization results in low conversion of lignin to monomers, usually below 10%, and the highest reported values did not exceed 20%.[29, 73] The biggest drawbacks of base-catalyzed lignin depolymerization

are very low efficiency, severe charring and repolymerization of lignin, harsh reaction conditions, low product selectivity, and difficulties in monomers separation from the reaction mixture. [29, 51] These factors are hampering the development of base-catalyzed depolymerization.[29, 51]

Reductive lignin depolymerization

Reductive depolymerization is a process where lignin C-O bonds are cleaved in the presence of a redox catalyst and a reducing agent (mainly in the form of hydrogen gas), unlike in acid and base-catalyzed depolymerizations, here reactive intermediates are stabilized by a hydrogen donor therefore charring is significantly reduced.[29, 69, 77, 78] There are different kinds of reductive lignin depolymerization: mild hydroprocessing, harsh hydroprocessing, liquid phase reforming, and bifunctional hydroprocessing.[29, 73, 77, 78] In hydroprocessing, the monomer yield and degree of deoxygenation depends on the severity of the conditions (temperature, hydrogen pressure) and the type of catalyst.[29, 50] In mild hydroprocessing, the operating conditions are milder than in harsh hydroprocessing, typically below 300 °C and below 35 bar of hydrogen gas pressure, this process is performed in organic solvents (alcohols, dioxane, tetrahydrofuran) or water in the presence of a metal-based catalyst.[29, 77, 78] Examples of the catalysts used in mild hydroprocessing are metals such as Ru, Pd, Pt, Rh, NiMo, NiFe supported on C, Al_2O_3, or zeolites, Ni Raney, CoMo, $CoMoO_x$, NiMo, $CuMgAlO_x$, CuPMO.[29, 50, 57, 63, 69, 73, 74] A pool of products of mild lignin hydroprocessing include various methoxyphenols, often substituted in para position with alcohols or alkyl chains. [29, 50, 57, 63, 69, 73, 74] The yields of mild hydroprocessing usually are below 20%, but there are reports of significantly increased monomer yields when Lewis acids or bases are used as an additive.[29]

Lignin hydroprocessing

Harsh hydroprocessing is conducted in more severe conditions than mild hydroprocessing, usually at above 300 °C and 35 bar of hydrogen gas pressure.[29, 73, 79] This process can be performed in alcohols or solvent-free, also in the presence of a metal-based catalyst, similar to mild hydroprocessing catalysts.[29, 73, 79] Typical catalysts in harsh hydroprocessing include: Ru supported on C, TiO_2, or Al_2O_3; Pd supported on C or Al_2O_3; CoMo NiMo, Cu, Ni, W, and NiW supported on C, SiO_2, Al_2O_3, and zeolites.[29, 73, 79] Unlike in mild hydroprocessing, the severity of the process leads to a wider pool of products where the methoxy functionality in lignin monomers is not always preserved, typical products include phenol, alkylated phenols, catechol, deoxygenated aromatic compounds, and sometimes alkanes.[29, 73, 79] The monomer yields of harsh hydroprocessing usually range between 20 and 30%, but higher yields were also reported.[29, 50] Liquid phase reforming is an alternative approach in which hydrogen gas is replaced with a hydrogen donating agent, such as tetralin, alcohols, or formic acid, and the entire

process is carried out in an inert atmosphere at elevated temperatures up to 400 °C.[29, 50, 73] The use of catalysts such as Ru, Pt, Pd, MoC on C support, CuMgO$_x$, Ni Raney, Pt/Al$_2$O$_3$, Ni/SiO$_2$ were reported in this approach to yield various products including substituted methoxyphenols, catechols, alkylphenols, deoxygenated aromatics, and cycloalkanes.[29, 50, 73] The monomer yield often was between 20 and 30%, but some reports also presented up to 80% conversion of lignin to monomers.[29, 50]

Bifunctional hydroprocessing is a combined approach where tandem reductive depolymerization and hydrodeoxygenation take place to form aromatic compounds, and cyclic alkanes form lignin monomers.[29, 50, 51, 63, 77] This process is also performed at elevated temperatures of 150-320 °C with 20-70 bar of hydrogen gas in the presence of a catalyst such as Ru/C, Ru/Al$_2$O$_3$, Ru/zeolites, Ph/C, Ph/Al$_2$O$_3$, Ph/zeolites, Pt/C, Pt/Al$_2$O$_3$, Pt/zeolites, Pd/C, Pd/Al$_2$O$_3$, Pd/zeolites, Ni/SiO$_2$, Ni/zeolites, Ni Raney, NiW, CoMo, CoMoS, NiMo, PtMo, PtCo/C, PdFe, Fe/C, CoC$_x$/C, RuRe.[29, 50, 51, 63, 77] This process can yield up to 70% of hydrocarbons, such as alkanes, cycloalkanes, aromatic hydrocarbons (BTX), phenols, cyclohexanols, but yields between 20-30% are the most common.[29, 50, 63]

Oxidative lignin depolymerization

Lignin depolymerization using the oxidative route is another widely reported possibility, where lignin conversion to monomers involves the use of an oxidizing agent. This process leads to more valuable monomers than reductive lignin depolymerization, and it is often performed under milder conditions, mostly in alkaline media (use of acidic media, organic solvents, or ionic liquids was also reported), in the presence of an appropriate metal catalyst, in the temperature range of 60 - 225 °C, and a pressure of oxygen gas or air between 2 and 30 bar.[29, 50, 70, 73, 78, 80-82] Commonly used oxidizing agents are air, oxygen gas, and hydrogen peroxide, but occasionally other oxidants such as nitrobenzene, metal oxides, ozone, chlorine, chlorine dioxide, peroxyacids were reported.[29, 50, 73, 77, 78, 80] The use of Cu, Fe, Co, Mn, Zn, La, V, Re, Nb salts or complexes, Pd and Pt supported on Al$_2$O$_3$, TiO$_2$, or SiO$_2$, metalloporphyrins, MTO, TEMPO, Shiff base complexes, Frémy's salt and Perovskite-type oxide catalysts were reported as a catalyst.[29, 38, 50, 52, 57, 61, 70, 73, 77, 78, 80-82] The main target of oxidative lignin depolymerization is vanillin, which can be obtained via side chain cleavage together with other phenolic compounds. [29, 50, 73, 78, 81, 82] When stronger oxidant, higher temperature, pressure, and longer reaction time are used, the main observed products are aliphatic carboxylic acids and diacids, obtained via the oxidation of the aromatic ring and aromatic ring opening.[29, 50, 73, 78, 81, 82] Products of oxidative lignin depolymerization from the phenolic pool are vanillin, syringylaldehyde, p-hydroxybenzaldehyde, veratraldehyde, vanillic, syringic, ferulic, and benzoic

acids, phenol, guaiacol, syringol, vanillyl alcohol, cresols, acetophenone, and benzoquinone. [29, 38, 50, 57, 61, 70, 73, 74, 77, 78, 80-82] Aliphatic acids and diacids such as formic, acetic, succinic, oxalic, and malonic acid, among others, can also be obtained via this depolymerization route.[29, 38, 50] Monomer yields of oxidative lignin depolymerization usually do not exceed 20% for the production of phenolic monomers, but the aliphatic acids and diacids can be produced with higher yields, up to 60%.[29, 38, 50, 80]

Biological lignin depolymerization

Lignin degradation in a natural environment is hindered due to the complex structure and heterogeneity of lignin, lack of its water solubility, and absence of hydrolyzable bonds, making this process long and resulting in a wide variety of products. In nature, enzymatic systems present in certain fungi and bacteria are able to degrade lignin.[83] Though bacteria such as Actinobacteria, Proteobacteria, and Firmicutes can degrade lignin, the most robust in lignin degradation are white-, red-, and soft-rot fungi species.[48, 84] Key enzymes in lignin degradation are *peroxidases* and *laccases*, which can oxidatively break down lignin to small aromatic molecules, such as ferulic, p-coumaric, and gallic acids; and *β-etherases* and aromatic ring-cleaving *dioxygenases,* which further convert depolymerized lignin in upper and lower pathways into catechol, vanillic, protocatechuic, muconic and pyruvic acids, and benzoyl-, acetyl-, or succinyl-CoA.[73, 85, 86] Those enzymes can be used to convert lignin into a variety of products, including lipids for biodiesel production, vanillin, vanillyl alcohol, lactic acid, and polyhydroxyalkanoates.[52, 71, 73, 84-86]

Lignin fractionation

Technical lignins are often heterogeneous - polydisperse, contaminated with sugars, and possessing variable amounts of functional group distributions. The extent of lignin heterogeneity depends on the isolation method and processing conditions. Lignin can be subjected to fractionation to obtain more homogeneous fractions and make it more suitable for utilization in various applications, such as polymeric materials. Techniques such as organic solvent extraction, precipitation, and membrane separation are the most common methodologies used in lignin fractionation.[87-89]

Extraction

The majority of efforts in lignin fractionation are put into extraction techniques. It can be performed either as a single step using one solvent, as a sequential cascade of various solvents, as a mixture of solvents or as a cascade of solvent mixtures. The principle of this fractionation technique is related to differences in lignin solubility with different molecular weights in organic solvents; the ability of the solvent to dissolve

lignin is correlated with the hydrogen bonding capacity and cohesive energy of the solvent.[89, 90] A single solvent fractionation process is the most straightforward variant, where lignin is treated with only one solvent to obtain the soluble and insoluble fractions. Methanol, ethanol, propanol, butanol, ethylene glycol, tetrahydrofuran, ethyl acetate, acetone methyl ethyl ketone, dichloromethane, 2-butanone dioxane, and pyridine are commonly used in this fractionation technique as they can partially dissolve lignin.[89-91] To narrow down the dispersity of the resulting lignin fractions, a cascade of solvents with varying polarities can be applied. The cascade is designed in a way that the solubility of lignin in organic solvents gradually increases, and as a result, lignin fractions with even narrower dispersities are obtained. Alternatively, a mixture of solvents and their cascade can also be used to separate lignin. The solubility of lignin in the mixed solution can be tuned by adjusting the ratio of the solvents. Solvent mixtures used in these methods are ethanol/glycerol, acetone/glycerol, acetone/hexanes, and ethyl acetate/petroleum ether.[89] Mixtures of solvents such as ethanol, acetone, and tetrahydrofuran with water were also reported.[89] Conventional organic solvents used in this approach are often volatile, flammable, explosive, and/or toxic, therefore, it is important to investigate more eco-friendly alternative solvents for lignin dissolution and extraction, such as deep eutectic solvents or ionic liquids.[91]

Precipitation

Alternatively, lignin precipitation is also commonly used to fractionate lignin. Usually, it is performed by gradient pH precipitation. The first step is lignin dissolution in basic solution, where it forms stable colloids due to the negative charge of lignin, hydrophilic van der Waals, hydrogen bonding forces, and repulsive forces. Upon protonation by decreasing the pH of the lignin solution, the negative charge on lignin molecules is neutralized, and the colloids start to aggregate and precipitate.[89, 92] High molecular weight lignin starts to precipitate at relatively high pH, while low molecular weight is stable in more neutral to acidic conditions, which is connected to a higher concentration of negatively charged groups (phenolic OH and COOH) compared to low molecular weight lignin. Therefore, the polydispersities of both high and low molecular weight lignin fractions are reduced upon this fractionation method, where high molecular weight lignin is recovered at high pH and low molecular weight lignin is recovered at low pH. It was also reported that lignin could be fractionated using organic solvents mixtures, where lignin fractions are dissolved in organic solvent (e.g., acetone) and precipitated with the addition of antisolvent (such as water or hexanes).[87, 93]

Membrane technology

Another common approach in lignin fractionation is a membrane separation. Depending on the desired separation degree, one or multiple diafiltration steps can

be performed (e.g., micro-, ultra-, and nanofiltration cascade). The principle of the membrane separation is that dissolved lignin is filtered at elevated pressure through the membrane with a well-defined molecular weight cut-off, resulting in fractionation to high molecular weight lignin retentate and low molecular weight lignin permeate.[41, 92] Both ceramic and polymeric membranes can be used in this approach, however, ceramic membranes are more suitable due to better pH and temperature resistance.[92] It is a very convenient method to separate lignosulphonates, whose separation is hindered due to the very good solubility in water and organic solvents.[92, 94] Recently, the separation of depolymerized lignin oils was also demonstrated using membrane technology.[95] Despite the operational difficulties of membrane separation (e.g., membrane fouling and need of membrane separation setup maintenance), this method is very promising in biorefineries because it is a low energy consuming, versatile separation method, and the resulting fractions are characterized by narrow molecular weight distributions and well-defined physiochemical characteristics.[41, 88]

Exploring lignin applications

Currently, lignin is mainly considered as a by-product of the paper industry and lignocellulose bioethanol production, and this kind of lignin has relatively low value and quality.[38] Therefore, it is currently primarily used as an energy source.[39] In order to valorize lignin and improve its use, added-value applications are being developed, and lignin biorefineries converting lignin into higher-value products are drawing more and more attention.[40, 41] There are certain limitations of using unmodified lignin, such as the presence of impurities, low reactivity, its complex structure, its heterogeneity, and polydispersity. That is why lignin depolymerization and fractionation techniques are attracting both academic and industry interests.[29, 38, 41, 87, 90, 94, 96-102] Also, lignin often requires functionalization before it can be used as a starting material for polymer production.[35, 36, 97, 103-105] In the fields of polymeric materials, lignin can be used as a precursor or as an additive in various types of resins, including lignin-phenol-formaldehyde resins, polyurethanes, and epoxy resins for adhesives and coatings.[40, 106-118] Lignin can also be implemented in the development of polymeric blends and composites, smart materials, additives, and carbonous materials, or as a feedstock for the production of various chemicals and fuels. [21, 35, 36, 119]

Chemicals and fuels

The key lignin-originating chemicals and fuels are obtained from various depolymerization processes, described in the previous parts of the introduction. The most important products discussed below are vanillin, syringaldehyde, aromatic and

aliphatic acids and diacids, aromatic compounds, such as benzene, toluene, and xylene (BTX), fuels, and fuel additives.

The most important chemical originating from lignin depolymerization is vanillin, which is currently the only chemical produced from lignin at the industrial scale by Borregaard through lignosulfonate catalytic oxidation.[29, 50, 75, 120] On a lab scale, it is mostly obtained via oxidative treatment, but it can also be obtained by biological methods using microorganisms.[29, 57, 71, 75] Vanillin is commonly used in food and cosmetics industries as flavoring and fragrance compounds, in polymer synthesis as a precursor in epoxy resins, as an inhibitor and antifoaming agent, or as a starting material in the synthesis of fine chemicals, agrochemicals, and pharmaceutical products.[48, 57, 75, 97, 121] Similarly to vanillin, syringaldehyde can also be used in food, cosmetics, and chemical synthesis.[75] This compound is obtained from hardwood lignin, with abundant S units, using the same depolymerization techniques as for vanillin production (originating from G units).[75, 78] Separation and purification of both vanillin and syringaldehyde are complex and expensive, which makes producing lignin in biobased routes more expensive compared to petrochemical routes.[75, 78]

Other promising lignin-based products are vanillic, syringic, p-hydroxybenzoic, coumaric, ferulic, and caffeinic acids. They can be produced either via oxidative lignin depolymerization using stronger oxidants (such as hydrogen peroxide), via oxidation of the corresponding aldehydes or via biological conversion; despite the difficulties in their separation, they still have a good potential to be commercially produced from lignin.[46, 71, 75, 78, 122] The above-mentioned acids are biologically active compounds with UV-blocking and antioxidant properties, and they have a potential to be used in polymer synthesis, in food, cosmetics, and pharmaceutical industries, as well as a starting material in chemical synthesis.[46, 75, 122] Aliphatic acids, such as formic, acetic, succinic, oxalic, malonic, fumaric, malic, and tartaric acids can be obtained in high yields from oxidative lignin depolymerization in more severe conditions using strong oxidants (like hydrogen peroxide).[29, 75, 78] These compounds are widely used in polymer synthesis, chemical, food, and pharmaceutical industries.[75, 78]

Many efforts are put into lignin depolymerization to phenolic monomers using numerous thermal and thermochemical depolymerization routes described earlier. Lignin-derived phenol, 4-propylsyringol, 4-propylguiacol, 4-propylcatechol, 4-propanolsyringol, 4-propanolguiacol, and 4-propanolcatechol are considered to be the most promising from a commercialization perspective.[48, 75, 78, 121, 123] These chemicals have great potential to be used in polymer and chemical synthesis, as well as antioxidants, flavors, and fragrances.[48, 75]

BTX are commonly used chemicals in numerous existing industrial technologies as a precursor to fine chemicals and materials.[21, 46, 61, 78, 121] Drop-in lignin bases BTX can be obtained via hydrodeoxygenation of bio-oils or via catalytic depolymerization routes, but not yet on the commercial scale due to the safety issues, connected with harsh conditions, use of hydrogen, and the high lignin-based BTX price.[46, 48, 57, 61, 78]

Lignin-based fuels and fuel additives can be obtained via thermal and thermochemical lignin depolymerization.[78, 121, 21, 46, 120] Examples of lignin-based fuels and fuel additives are syngas used to produce methanol and Fischer-Tropsch fuel, aliphatic and aromatic compounds (BTX, cresols, aliphatic, aromatic and cyclic hydrocarbons, paraffin, and naphthalenes among others) obtained from lignin oil hydrodeoxygenation or via catalytic depolymerization routes.[21, 57, 61, 75, 78] At the moment, the production of lignin-based fuels and fuel additives is economically questionable.[61]

Materials

As demonstrated above, a lot of effort was put into developing lignin-based chemicals and fuels. At the same time, lignin-based materials were also extensively developed. Those applications include developments in the field of polymeric materials, additives, and carbonous materials, discussed in the next parts of this introduction. However, the spectrum of lignin use is broader and includes composite materials, dispersants, flocculants, adsorbents, fertilizers, animal feed, and energy storage, among other applications.[46, 124-127]

Lignin modifications

In order to extend the spectrum of lignin applications, lignin can be furthermore functionalized to introduce new functionalities and reactive sites or to modify lignin's polarity to increase miscibility with other materials.[35, 103, 104, 128, 129] Lignin modification strategies can be divided into the following categories: aromatic ring transformations, hydroxyl groups transformations, methoxy group transformations, and carboxylic group transformations.[128] Figure 2 visualizes the most common modifications of lignin, whose purpose is summarized in Table 1.
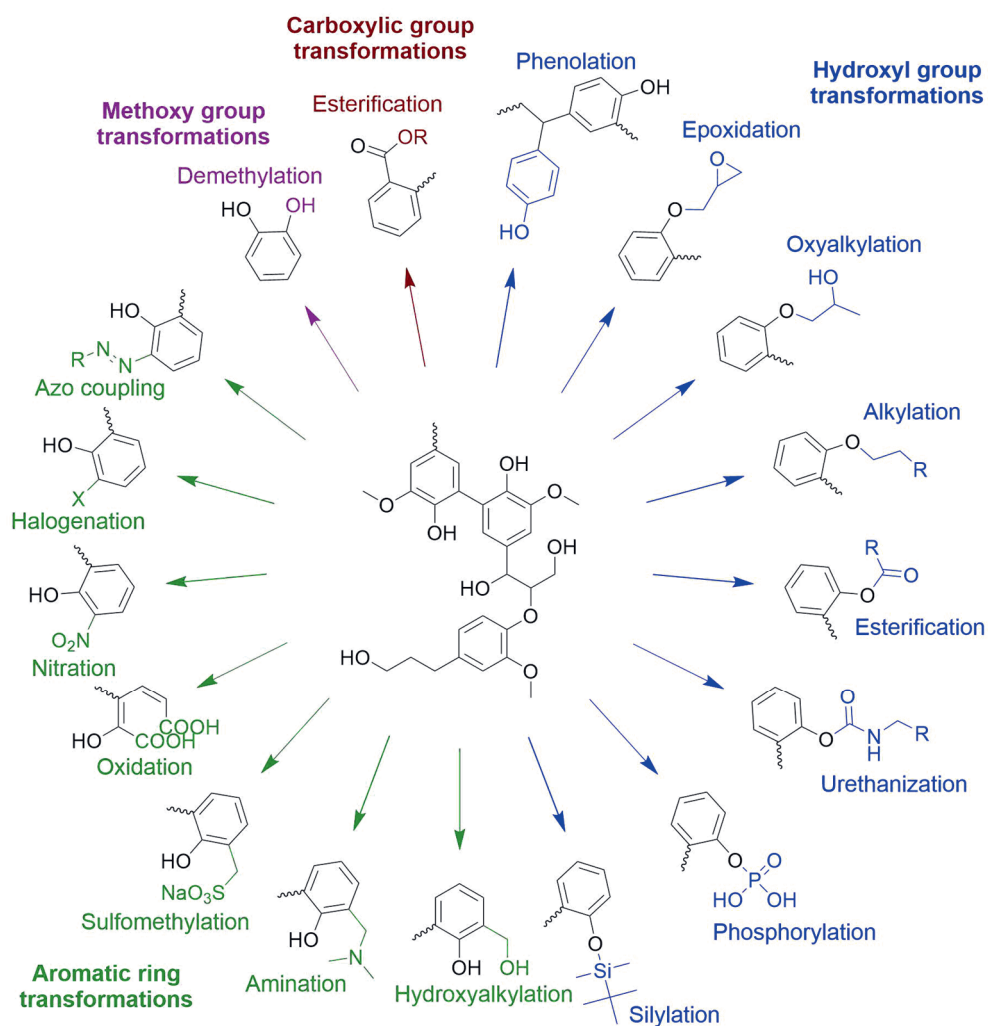
Figure 2 *Most common lignin modification strategies. Adapted from ref. 128*

Table 1 *Applications of modified lignin*

Modification position	Modification type	Applications	Ref.
Aromatic ring transformations	Hydroxyalkylation	Lignin-phenol-formaldehyde resins	35, 36, 103, 129
	Amination	Surfactants, coagulants, emulsifiers, coagulants, exchange resins, curing agents	35, 36, 103, 129
	Sulfomethylation	Surfactants, binders, dispersants, ion-exchange resins, coatings, additives in cement and concrete	35, 103
	Oxidation	Dispersants	103
	Nitration	Additive in polyurethane resins	35, 36
	Halogenation	Bioactive compound in herbi-, fungi-, or insecticides	103
	Azo-coupling	Novel polymeric materials (grafting from strategies)	128
Hydroxyl groups transformations	Phenolation	Lignin lignin-phenol-formaldehyde resins and polyurethane resins	35, 103, 129
	Epoxidation	Epoxy resins	103, 129
	Oxyalkylation	Lignin-based polyols for polyurethane resins	35, 36, 103
	Alkylation	Plasticizers, polymeric blends	35, 36, 103, 129
	Esterification	Polymeric blends, lignin-based polyesters	35, 36, 103, 129
	Urethanization	Polyurethane and lignin-urea-formaldehyde resins.	35, 129
	Phosphorylation	Flame retardants	103
	Silylation	Flame retardants	103
Methoxy group transformation	Demethylation	Polymeric resins, especially lignin-phenol-formaldehyde resins	35
Carboxylic group transformation	Esterification	Polymeric blends, lignin-based polyesters	35, 103

Lignin in polymeric materials

One of the most important applications of lignin is in polymeric materials. The most promising use of lignin on the commercial scale includes phenolic resins used as wood adhesives, polyurethane and epoxy resins, and polymeric blends, where lignin is mainly used as an additive.[104, 125, 127, 130, 131]

Lignin is the most straightforward biobased component that can be used in phenol-formaldehyde resins due to the structural similarities of lignin and cross-linked phenolic resins.[132] Therefore, a lot of research was focused on phenol replacement by lignin in phenolic resins, commonly used for engineered wood products.[104, 132-135] Other applications of phenolic resins include coatings, electronics, and construction materials.[36] Phenol-formaldehyde resins are synthesized by electrophilic substitution of phenol in the ortho and para positions with formaldehyde,

followed by acid or base-catalyzed step-growth polymerization to yield oligomers, which can then be cross-linked at elevated temperature.[133, 134] Due to the requirements of this chemical approach, less substituted lignin originating from softwood or grasses possessing low molecular weight and narrow dispersity is preferred.[132, 136, 137] Because of lower reactivity toward formaldehyde compared with phenol, lignin modifications such as phenolation or hydroxyalkylation are employed to improve it.[133, 134, 136-139] Usually, less than 50% of phenol can be substituted by lignin in this kind of resins due to the reactivity deterioration, but there are some examples of a higher degree of substitution up to 70%, or even 100% replacement.[131-134, 138, 139] This application is one of the best developed: there are already lignin-containing phenolic resins available on the market.[134, 135, 139]

Lignin was also reported as a replacement of bisphenol A in epoxy resins.[98, 127, 140, 141] Epoxy resins are widely used as adhesives, coatings, composites, and materials for electronics.[98, 130, 141] Epoxides are polymerized using anionic or cationic polymerization techniques to yield an epoxy polymer.[135, 136] Epoxy resins can be cross-linked by multifunctional amines, acids, anhydrides, alcohols, thiols, and phenols. [135, 136, 141] Therefore, lignin can be used both as a building block in epoxy polymer synthesis after its epoxidation and as a cross-linker. [135, 136] Up to 50% of lignin can be incorporated into the epoxy resin, which is similar to phenolic resins.[104, 141]

Another important example of commercial use of lignin use in polymeric material is polyurethanes. Polyurethanes are widely used as adhesives, coatings, sealants, and insulating materials.[131, 136, 137, 142] Polyurethanes are formed by polyaddition of isocyanate and polyol components.[131, 137, 142] Depending on the structure of the polyol and the isocyanate, the resulting polymer can be either an elastomer, thermoplastic, or thermoset. Lignin can be incorporated in polyurethane either as a polyol or as a cross-linker.[133, 136, 137, 140, 142, 143] Addition of lignin in polyurethanes leads to increased rigidity and brittleness.[133] Up to 20% of unmodified lignin was reported to be successfully incorporated in polyurethanes, but when modified lignin is used, this amount can be significantly higher, up to 70%.[113, 131, 136, 137, 140] Modifications such as oxyalkylation, demethylation, amination, and esterification are commonly applied.[137, 142, 143]

Lignin was reported to be blended with multiple polymers. Due to the complex lignin structure and behavior, blending lignin with other polymers is often challenging.[132, 144] Although lignin shows thermoplastic behavior at lower temperatures, at elevated temperatures it often undergoes condensation, it self-cross-links and acts like a thermoset.[132] In general, lignin shows good compatibility with polar polymers due to the interactions with hydroxyl groups present in the lignin structure.[132] Therefore, there are three major strategies for blending lignin with other polymers:

blending materials as such, using compatibilizers or plasticizers, or chemical modification of lignin to improve dispersibility.[40, 132, 144, 145] Those modifications often include esterification or alkylation to decrease the polarity of lignin.[133, 144] Examples of polymers which can be blended with lignin include polyethylene oxide (PEO), polyethylene terephthalate (PET), poly(vinyl alcohol) (PVA), ethylene vinyl acetate (EVA), polyvinyl acetate (PVAc), polyvinyl chloride (PVC), polylactic acid (PLA), polycaprolactone (PCL), poly(methyl methacrylate) (PMMA), polyacrylonitrile (PAN), polyvinylpyrrolidone (PVP), polyhydroxyalkanoates (PHAs), polyurethanes (PUs), polyamides (PAs), polystyrene (PS), polyethylene (PE), polypropylene (PP), poly(butylene adipate-co-terephthalate) (PBAT), poly(hydroxybutyrate-co-valerate) (PHVB), rubbers, starch, cellulose, gelatin, chitosan, and proteins.[40, 132, 133, 144, 145] In most cases, no more than 20-30% of lignin can be added to the blend due to the significant deterioration of mechanical properties upon adding higher amounts of lignin.[132, 133]

Next to the development of the most industrially relevant applications, academic research is also focused on the exploration of novel functional materials where lignin can be incorporated. Examples of such smart materials include stimuli-responsive materials (triggered by light, temperature, pH, moisture, mechanical force, electric or magnetic field), shape-memory materials, self-healing materials, vitrimers, nanomaterials, nanocomposites, and functional hydrogels.[36, 146, 147]

Lignin as an additive
Lignin is a highly functional material with various valuable intrinsic properties such as antioxidant, UV-blocking, antimicrobial, and antifungal, among others.[35, 36, 132] Therefore, lignin can be used as an additive to other materials for property improvement. Lignins obtained from different feedstocks and processes using different isolation techniques can show differences in performance.[132] The most important and common application of lignin as an additive are antioxidants. Lignin's antioxidant properties originate from the presence of phenolic hydroxyl groups capable of stabilizing radicals via resonance, therefore for this particular application high amount of phenolic hydroxyl groups combined with low molecular weight is preferred.[35, 102, 103, 132, 148] Applications of lignin in food and feed, biodiesel, lubricants, and polymeric materials were reported.[148-152]

Lignin contains UV chromophore functional groups such as quinones and methoxy-substituted phenoxy groups, which can be conjugated with double bonds or carbonyl functional groups which can absorb a broad spectrum of UV light in the range of 250-400 nm and give lignin a brown color.[153] Therefore, lignin can be used as a UV-blocker in sunscreen creams, polymeric films and blends, paints, and varnishes.[36, 150, 153, 154] Lignin can also be used as an additive in constructions materials (concrete, bitumen, and asphalt), as a filler in feed and feed, as a

surfactant, as a dispersant, as a viscosity modifier, as a flame retardant, as an antistatic agent, and as an insect repellent agent.[35, 36, 39, 40, 71, 96, 103, 133, 137, 155-157]

Lignin-based carbonous materials
Next to the above-mentioned applications, lignin can also be used as a precursor in carbonous materials synthesis, such as carbon fibers, activated carbons, or templated carbons with micro and/or mesopores.[119] Those materials primarily consist of carbon and have multiple applications in various fields of industry. Among numerous polymeric precursors in their manufacture, lignin can be used as a promising biobased precursor.

Carbon fibers are considered materials of the future.[158] They have numerous high-value applications, including automotive, aerospace, and construction materials due to their superior mechanical properties and lightweight.[57, 130, 136, 159] Currently, 90% of carbon fibers are obtained from PAN. Carbon fibers can also be obtained using lignin and another polymeric such as PAN, PEO, PET, PP, PVA, PLA, or thermoplastic polyurethane (TPU) as precursors.[119, 131-133, 136, 159] These blends are extruded into fibers, which are then thermally stabilized and carbonized to yield carbon fibers.[57, 132, 135, 136, 159] Often, limited amounts of lignin can be incorporated in the blends and lignin tends to char and degrade before it is able to flow and be spinned into fibers. To overcome those issues addition of plasticizers (for example PVA), the use of depolymerized, pyrolytic, or fractionated lignin was employed to improve fibers' spinnability and overall quality. In order to obtain high-quality fibers, it is beneficial to use lignin with low molecular weight, low glass transition temperature, and very high purity, free of inorganics.[159] Nonetheless, lignin-based carbon fibers' performance is still inferior compared with PAN-based carbon fibers.[133] On the other hand, the addition of lignin can decrease the costs and the environmental impact of carbon fibers fabrication, which is promising for their further development and utilization.[130, 131, 133]

Other carbonous materials, such as activated carbons and templated carbons with micro and/or mesoporous structures are widely applied in applications heavily dependent on their high porosity and adsorptive properties. Such applications include adsorbents, systems suitable for filtration, gas separation, energy storage, and catalyst supports.[39, 119, 133, 160-163] Porous carbons can be categorized as micro-, meso-, and macroporous, where the pore diameter is below 2 nm, between 2 and 50 nm, and above 50 nm, respectively. Carbon material porosity depends on the synthesis method and surface functionality. Lignin is a very good candidate to be used as a precursor to obtain carbonous materials due to its high carbon content functionality and high char yield after carbonization.[119] Activated carbons are predominantly macroporous materials fabricated using either chemical or physical activation strategies.[36, 133, 164-166] In chemical activation, the precursor is impregnated

with the activating agent, such as KOH, NaOH, H_3PO_4, $ZnCl_2$, K_2CO_3 or Na_2CO_3, and carbonized at elevated temperature (450-900 °C) yielding etching of the pores in the carbonized material.[36, 133, 164-166] In physical activation, the precursor is carbonized and activated by performing carbonization in the oxidative environment at elevated temperatures (900-1200 °C) to yield porous material. [36, 133, 164-166] However, both methods lead to the synthesis of mainly microporous materials with ununiform porosity. Therefore, to obtain mesoporous materials with more controlled porosity, templating strategies for the fabrication of porous carbons were developed as an alternative. Both soft templates, such as amphiphilic block copolymers, and hard templates, for instance, zeolites and silica nanoparticles, can be used to obtain carbonous materials.[119, 167-169] In those approaches, the precursor is cross-linked in the presence of the template, followed by carbonization and template removal (only in hard templating, in soft templating the template is removed during carbonization).[119, 167-169] Unfortunately, using lignin as the only carbon source leads to materials with compromised surface area and pore volume, therefore lignin is mixed with state-of-the-art precursors such as phenol-, resorcinol- or phloroglucinol-formaldehyde resins.[170, 171]

Chapter 1

Aim and outlook of this thesis

Although many efforts have been put into exploring the possible applications for technical lignins, there is very limited knowledge regarding the use of depolymerized and fractionated lignins in the field of polymeric materials. Such lignin fractions diverge significantly from the technical lignins in terms of composition, molecular weight, and functionality. As a result, those fractions have different physicochemical properties compared to the technical lignins, especially their solubility in organic solvents, which is greatly improved. Up until recently, lignin depolymerization research was mostly conducted on the laboratory scale and focused primarily on studying the depolymerization process itself, not per se on the valorization of its product, which usually is a mixture of monomeric and oligomeric compounds. Although the properties of depolymerized lignins are promising, their performance in marketable applications is still not fully explored.

Therefore, the main goal of this work is to valorize and benchmark lignin fractions in numerous applications, including adhesives, coatings, additives, and carbonous materials adsorbents. This objective is of utmost importance in order to build up an understanding of how lignin can be used in the value chain of upscaling of lignin biorefineries and fractionation technology. The lignin fractions used in this study originate from various feedstocks and processing methods and include isolation of technical lignins, solvolysis of technical lignin, 'lignin-first' process, and separation of lignin fractions. The first question which arises is: how to incorporate those lignin fractions in the polymeric materials? In this thesis, several proofs-of-concept are established using novel synthetic approaches, which include chemical modification of said lignin fractions. The obtained lignin-based products are compared with state-of-the-art equivalents in terms of their properties and performance. Currently, very little is known regarding the relationship between the structure and properties of the lignins obtained in depolymerization and fractionation processes and their performance in real-life applications. This emerging question is addressed in this thesis. The development of lignin-based adhesives, coatings, additives, and carbonous materials adsorbents is discussed in the following chapters:

Lignin-based wood adhesives are studied in Chapter 2. This chapter explores the use of two lignin fractions, namely technical soda lignin and its product of mild solvolysis in the synthesis of thiol-yne thermally cured networks. By adding monomeric reactive diluent, the network performance can be tuned. The influence of an additional post-curing step is also investigated.

In Chapter 3, tandem thiol-yne UV curable and thermal Claisen rearrangement curing of lignin-based metal coatings is studied. In this chapter, a mixture of lignin monomers and oligomers originating from the RCF process is benchmarked against

the depolymerization mixture after fractionation by extraction and membrane separation. Such obtained coatings show very promising corrosion resistance.

Another application explored in Chapter 4 is as an antioxidant additive. Here, the antioxidant properties of lignin fractions with varying molecular weights and origins are assessed. Additionally, those lignin fractions are esterified in order to increase their miscibility with vegetable oils, in which this kind of additives are commonly used to increase their thermo-oxidative stability.

The last discussed application is as adsorbent. In Chapter 5, fully lignin-based mesoporous carbons are synthesized using thermal cross-linking via Claisen rearrangement in the presence of a polymeric template followed by carbonization. Such prepared mesoporous carbons are shown to be effective in removal of water contaminations such as humic acid.

The conclusions, outlook, recommendations, and valorization addendum of this thesis are presented in Chapter 6.

Chapter 1

References

1.   Morseletto, P., Restorative and regenerative: Exploring the concepts in the circular economy. *J. Ind. Ecol.* **2020,** *24* (4), 763-773.

2.   Lewandowski, I.; Gaudet, N.; Lask, J.; Maier, J.; Tchouga, B.; Vargas-Carpintero, R., *Bioeconomy: Shaping the Transition to a Sustainable, Biobased Economy*. Springer International Publishing: Cham, 2018; p 1-356.

3.   Rafiaani, P.; Kuppens, T.; Dael, M. V.; Azadi, H.; Lebailly, P.; Passel, S. V., Social sustainability assessments in the biobased economy: Toward a systemic approach. *Renewable Sustainable Energy Rev.* **2018,** *82*, 1839-1853.

4.   Bennich, T.; Belyazid, S., The Route to Sustainability—Prospects and Challenges of the Bio-Based Economy. *Sustainability* **2017,** *9* (6), 887.

5.   Yang, L.; Wang, X.-C.; Dai, M.; Chen, B.; Qiao, Y.; Deng, H.; Zhang, D.; Zhang, Y.; Villas Bôas de Almeida, C. M.; Chiu, A. S. F.; Klemeš, J. J.; Wang, Y., Shifting from fossil-based economy to bio-based economy: Status quo, challenges, and prospects. *Energy* **2021,** *228*, 120533.

6.   Transforming our world: the 2030 Agenda for Sustainable Development. https://sdgs.un.org/2030agenda (accessed 15.15.2021).

7.   The 17 goals. https://sdgs.un.org/goals (accessed 15.12.2021).

8.   A European Green Deal. https://ec.europa.eu/info/strategy/priorities-2019-2024/european-green-deal_en (accessed 15.12.2021).

9.   Bioeconomy strategy. https://ec.europa.eu/info/research-and-innovation/research-area/environment/bioeconomy/bioeconomy-strategy_en (accessed 15.12.2021).

10.   House, T. W., National bioeconomy blueprint, April 2012. *Ind. Biotechnol.* **2012,** *8* (3), 97-102.

11.   Issue Brief - China's 14th five-year plan. https://www.cn.undp.org/content/china/en/home/library/environment_energy/issue-brief---china-s-14th-five-year-plan.html (accessed 15.12.2021).

12.   Bennich, T.; Belyazid, S.; Stjernquist, I.; Diemer, A.; Seifollahi-Aghmiuni, S.; Kalantari, Z., The bio-based economy, 2030 Agenda, and strong sustainability – A regional-scale assessment of sustainability goal interactions. *J. Clean. Prod.* **2021,** *283*, 125174.

13.   Ladu, L.; Blind, K., Overview of policies, standards and certifications supporting the European bio-based economy. *Curr. Opin. Green Sustain* **2017,** *8*, 30-35.

14.   Majer, S.; Wurster, S.; Moosmann, D.; Ladu, L.; Sumfleth, B.; Thrän, D., Gaps and Research Demand for Sustainability Certification and Standardisation in a Sustainable Bio-Based Economy in the EU. *Sustainability* **2018,** *10* (7), 2455.

15.   Morone, P., Sustainability Transition toward a Biobased Economy: Defining, Measuring and Assessing. *Sustainability* **2018,** *10* (8), 2631.

16.   Ubando, A. T.; Felix, C. B.; Chen, W.-H., Biorefineries in circular bioeconomy: A comprehensive review. *Bioresour. Technol.* **2020,** *299*, 122585.

17.   Wohlfahrt, J.; Ferchaud, F.; Gabrielle, B.; Godard, C.; Kurek, B.; Loyce, C.; Therond, O., Characteristics of bioeconomy systems and sustainability issues at the territorial scale. A review. *J. Clean. Prod.* **2019,** *232*, 898-909.

18.   Finley, J. W.; Seiber, J. N., The Nexus of Food, Energy, and Water. *J. Agric. Food Chem.* **2014,** *62* (27), 6255-6262.

19.   Cherubini, F.; Strømman, A. H., Chemicals from lignocellulosic biomass: opportunities, perspectives, and potential of biorefinery systems. *Biofuels, Bioprod. Biorefin.* **2011,** *5* (5), 548-561.

20.   Octave, S.; Thomas, D., Biorefinery: Toward an industrial metabolism. *Biochimie* **2009,** *91* (6), 659-664.

21.   Azadi, P.; Inderwildi, O. R.; Farnood, R.; King, D. A., Liquid fuels, hydrogen and chemicals from lignin: A critical review. *Renewable Sustainable Energy Rev.* **2013,** *21*, 506-523.

22.	Avanthi, A.; Kumar, S.; Sherpa, K. C.; Banerjee, R., Bioconversion of hemicelluloses of lignocellulosic biomass to ethanol: an attempt to utilize pentose sugars. *Biofuels* **2017,** *8* (4), 431-444.

23.	Saha, B., Hemicellulose Bioconversion. *J. Ind. Microbiol. Biotechnol.* **2003,** *30*, 279-291.

24.	Rivas, S.; Raspolli Galletti, A. M.; Antonetti, C.; Licursi, D.; Santos, V.; Parajó, J. C., A Biorefinery Cascade Conversion of Hemicellulose-Free Eucalyptus Globulus Wood: Production of Concentrated Levulinic Acid Solutions for γ-Valerolactone Sustainable Preparation. *Catalysts* **2018,** *8* (169), 1-16.

25.	Peng, X.; Luan, Z.; Chen, F.; Tian, B.; Jia, Z., Adsorption of humic acid onto pillared bentonite. *Desalination* **2005,** *174* (2), 135-143.

26.	Peng, F.; Ren, J. L.; Xu, F.; Sun, R.-C., Chemicals from Hemicelluloses: A Review. In *Sustainable Production of Fuels, Chemicals, and Fibers from Forest Biomass*, American Chemical Society: 2011; Vol. 1067, pp 219-259.

27.	Steinbach, D.; Kruse, A.; Sauer, J., Pretreatment technologies of lignocellulosic biomass in water in view of furfural and 5-hydroxymethylfurfural production- A review. *Biomass Convers. Biorefin.* **2017,** *7* (2), 247-274.

28.	Narron, R. H.; Kim, H.; Chang, H.-m.; Jameel, H.; Park, S., Biomass pretreatments capable of enabling lignin valorization in a biorefinery process. *Curr. Opin. Biotechnol.* **2016,** *38*, 39-46.

29.	Schutyser, W.; Renders, T.; Van den Bosch, S.; Koelewijn, S. F.; Beckham, G. T.; Sels, B. F., Chemicals from lignin: an interplay of lignocellulose fractionation, depolymerisation, and upgrading. *Chem. Soc. Rev.* **2018,** *47* (3), 852-908.

30.	Zakzeski, J.; Bruijnincx, P. C. A.; Jongerius, A. L.; Weckhuysen, B. M., The Catalytic Valorization of Lignin for the Production of Renewable Chemicals. *Chem. Rev.* **2010,** *110* (6), 3552-3599.

31.	Vanholme, R.; Demedts, B.; Morreel, K.; Ralph, J.; Boerjan, W., Lignin Biosynthesis and Structure. *Plant Physiol.* **2010,** *153* (3), 895-905.

32.	Dixon, R. A.; Barros, J., Lignin biosynthesis: old roads revisited and new roads explored. *Open Biol.* **2019,** *9* (12), 190215.

33.	Tobimatsu, Y.; Schuetz, M., Lignin polymerization: how do plants manage the chemistry so well? *Curr. Opin. Biotechnol.* **2019,** *56*, 75-81.

34.	Schutyser, W., Renders, T., Van den Bossche, G., Van den Bosch, S., Koelewijn, S.-F., Ennaert, T. and Sels, B.F., Catalysis in Lignocellulosic Biorefineries: The Case of Lignin Conversion. In *Nanotechnology in Catalysis*, 2017; pp 537-584.

35.	Figueiredo, P.; Lintinen, K.; Hirvonen, J. T.; Kostiainen, M. A.; Santos, H. A., Properties and chemical modifications of lignin: Toward lignin-based nanomaterials for biomedical applications. *Prog. Mater Sci.* **2018,** *93*, 233-269.

36.	Kai, D.; Tan, M. J.; Chee, P. L.; Chua, Y. K.; Yap, Y. L.; Loh, X. J., Toward lignin-based functional materials in a sustainable world. *Green Chem.* **2016,** *18* (5), 1175-1200.

37.	Brandt, A.; Gräsvik, J.; Hallett, J. P.; Welton, T., Deconstruction of lignocellulosic biomass with ionic liquids. *Green Chem.* **2013,** *15* (3), 550-583.

38.	Chio, C.; Sain, M.; Qin, W., Lignin utilization: A review of lignin depolymerization from various aspects. *Renewable Sustainable Energy Rev.* **2019,** *107*, 232-249.

39.	Erfani Jazi, M.; Narayanan, G.; Aghabozorgi, F.; Farajidizaji, B.; Aghaei, A.; Kamyabi, M. A.; Navarathna, C. M.; Mlsna, T. E., Structure, chemistry and physicochemistry of lignin for material functionalization. *SN Appl. Sci.* **2019,** *1* (9), 1-19.

40.	Doherty, W. O. S.; Mousavioun, P.; Fellows, C. M., Value-adding to cellulosic ethanol: Lignin polymers. *Ind. Crops Prod.* **2011,** *33* (2), 259-276.

41.	Gillet, S.; Aguedo, M.; Petitjean, L.; Morais, A. R. C.; da Costa Lopes, A. M.; Łukasik, R. M.; Anastas, P. T., Lignin transformations for high value applications: toward targeted modifications using green chemistry. *Green Chem.* **2017,** *19* (18), 4200-4233.

42.   Garlapati, V. K.; Chandel, A. K.; Kumar, S. P. J.; Sharma, S.; Sevda, S.; Ingle, A. P.; Pant, D., Circular economy aspects of lignin: Toward a lignocellulose biorefinery. *Renewable Sustainable Energy Rev.* **2020,** *130*, 109977.

43.   Balakshin, M. Y.; Capanema, E. A.; Sulaeva, I.; Schlee, P.; Huang, Z.; Feng, M.; Borghei, M.; Rojas, O. J.; Potthast, A.; Rosenau, T., New Opportunities in the Valorization of Technical Lignins. *ChemSusChem* **2020,** *14*, 1016–1036.

44.   Becker, J.; Wittmann, C., A field of dreams: Lignin valorization into chemicals, materials, fuels, and health-care products. *Biotechnol. Adv.* **2019,** *37* (6), 107360.

45.   Glasser, W. G., About Making Lignin Great Again-Some Lessons From the Past. *Front. Chem.* **2019,** *7*, 565.

46.   Bajwa, D. S.; Pourhashem, G.; Ullah, A. H.; Bajwa, S. G., A concise review of current lignin production, applications, products and their environmental impact. *Ind. Crops Prod.* **2019,** *139*, 111526.

47.   Liao, J. J.; Latif, N. H. A.; Trache, D.; Brosse, N.; Hussin, M. H., Current advancement on the isolation, characterization and application of lignin. *Int. J. Biol. Macromol.* **2020,** *162*, 985-1024.

48.   Ponnusamy, V. K.; Nguyen, D. D.; Dharmaraja, J.; Shobana, S.; Banu, J. R.; Saratale, R. G.; Chang, S. W.; Kumar, G., A review on lignin structure, pretreatments, fermentation reactions and biorefinery potential. *Bioresour. Technol.* **2019,** *271*, 462-472.

49.   Abu-Omar, M. M.; Barta, K.; Beckham, G. T.; Luterbacher, J. S.; Ralph, J.; Rinaldi, R.; Román-Leshkov, Y.; Samec, J. S. M.; Sels, B. F.; Wang, F., Guidelines for performing lignin-first biorefining. *Energy Environ. Sci.* **2021,** *14* (1), 262-292.

50.   Van den Bosch, S.; Koelewijn, S. F.; Renders, T.; Van den Bossche, G.; Vangeel, T.; Schutyser, W.; Sels, B. F., Catalytic Strategies Toward Lignin-Derived Chemicals. *Top. Curr. Chem.* **2018,** *376* (5), 36.

51.   Ahmad, E.; Pant, K. K., Lignin Conversion: A Key to the Concept of Lignocellulosic Biomass-Based Integrated Biorefinery. In *Waste Biorefinery*, 2018; pp 409-444.

52.   Poveda-Giraldo, J. A.; Solarte-Toro, J. C.; Cardona Alzate, C. A., The potential use of lignin as a platform product in biorefineries: A review. *Renewable Sustainable Energy Rev.* **2021,** *138*, 110688.

53.   Aro, T.; Fatehi, P., Production and Application of Lignosulfonates and Sulfonated Lignin. *ChemSusChem* **2017,** *10* (9), 1861-1877.

54.   Lobato-Peralta, D. R.; Duque-Brito, E.; Villafán-Vidales, H. I.; Longoria, A.; Sebastian, P. J.; Cuentas-Gallegos, A. K.; Arancibia-Bulnes, C. A.; Okoye, P. U., A review on trends in lignin extraction and valorization of lignocellulosic biomass for energy applications. *J. Clean. Prod.* **2021,** *293*, 126123.

55.   Zhu, J.; Yan, C.; Zhang, X.; Yang, C.; Jiang, M.; Zhang, X., A sustainable platform of lignin: From bioresources to materials and their applications in rechargeable batteries and supercapacitors. *Prog. Energy Combust. Sci.* **2020,** *76*, 100788-100812.

56.   Kouris, P. D.; Huang, X.; Ouyang, X.; van Osch, D. J. G. P.; Cremers, G. J. W.; Boot, M. D.; Hensen, E. J. M., The Impact of Biomass and Acid Loading on Methanolysis during Two-Step Lignin-First Processing of Birchwood. *Catalysts* **2021,** *11* (6), 750.

57.   Zevallos Torres, L. A.; Lorenci Woiciechowski, A.; de Andrade Tanobe, V. O.; Karp, S. G.; Guimarães Lorenci, L. C.; Faulds, C.; Soccol, C. R., Lignin as a potential source of high-added value compounds: A review. *J. Clean. Prod.* **2020,** *263*, 121499.

58.   Paone, E.; Tabanelli, T.; Mauriello, F., The rise of lignin biorefinery. *Curr. Opin. Green Sustain* **2020,** *24*, 1-6.

59.   Koranyi, T. I.; Fridrich, B.; Pineda, A.; Barta, K., Development of 'Lignin-First' Approaches for the Valorization of Lignocellulosic Biomass. *Molecules* **2020,** *25* (12), 2815.

60.   Renders, T.; Van den Bosch, S.; Koelewijn, S. F.; Schutyser, W.; Sels, B. F., Lignin-first biomass fractionation: the advent of active stabilisation strategies. *Energy Environ. Sci.* **2017,** *10* (7), 1551-1557.

61.   Kumar, A.; Jindal, M.; Maharana, S.; Thallada, B., Lignin Biorefinery: New Horizons in Catalytic Hydrodeoxygenation for the Production of Chemicals. *Energy Fuels* **2021,** *35* (21), 16965-16994.

62.   Renders, T.; Van den Bossche, G.; Vangeel, T.; Van Aelst, K.; Sels, B., Reductive catalytic fractionation: state of the art of the lignin-first biorefinery. *Curr. Opin. Biotechnol.* **2019,** *56*, 193-201.

63.   Ha, J.-M.; Hwang, K.-R.; Kim, Y.-M.; Jae, J.; Kim, K. H.; Lee, H. W.; Kim, J.-Y.; Park, Y.-K., Recent progress in the thermal and catalytic conversion of lignin. *Renewable Sustainable Energy Rev.* **2019,** *111*, 422-441.

64.   Deuss, P. J.; Lancefield, C. S.; Narani, A.; de Vries, J. G.; Westwood, N. J.; Barta, K., Phenolic acetals from lignins of varying compositions via iron(iii) triflate catalysed depolymerisation. *Green Chem.* **2017,** *19* (12), 2774-2782.

65.   De Santi, A.; Galkin, M. V.; Lahive, C. W.; Deuss, P. J.; Barta, K., Lignin-First Fractionation of Softwood Lignocellulose Using a Mild Dimethyl Carbonate and Ethylene Glycol Organosolv Process. *ChemSusChem* **2020,** *13* (17), 4468-4477.

66.   Deuss, P. J.; Scott, M.; Tran, F.; Westwood, N. J.; de Vries, J. G.; Barta, K., Aromatic Monomers by in Situ Conversion of Reactive Intermediates in the Acid-Catalyzed Depolymerization of Lignin. *J. Am. Chem. Soc.* **2015,** *137* (23), 7456-7467.

67.   Shuai, L.; Amiri, M. T.; Questell-Santiago, Y. M.; Héroguel, F.; Li, Y.; Kim, H.; Meilan, R.; Chapple, C.; Ralph, J.; Luterbacher, J. S., Formaldehyde stabilization facilitates lignin monomer production during biomass depolymerization. *Science* **2016,** *354* (6310), 329-333.

68.   Lan, W.; Amiri, M. T.; Hunston, C. M.; Luterbacher, J. S., Protection Group Effects During α,γ-Diol Lignin Stabilization Promote High-Selectivity Monomer Production. *Angew. Chem. Int. Ed.* **2018,** *57* (5), 1356-1360.

69.   Cao, L.; Yu, I. K. M.; Liu, Y.; Ruan, X.; Tsang, D. C. W.; Hunt, A. J.; Ok, Y. S.; Song, H.; Zhang, S., Lignin valorization for the production of renewable chemicals: State-of-the-art review and future prospects. *Bioresour. Technol.* **2018,** *269*, 465-475.

70.   Liu, X.; Bouxin, F. P.; Fan, J.; Budarin, V. L.; Hu, C.; Clark, J. H., Recent Advances in the Catalytic Depolymerization of Lignin toward Phenolic Chemicals: A Review. *ChemSusChem* **2020,** *13* (17), 4296-4317.

71.   Nguyen, L. T.; Phan, D.-P.; Sarwar, A.; Tran, M. H.; Lee, O. K.; Lee, E. Y., Valorization of industrial lignin to value-added chemicals by chemical depolymerization and biological conversion. *Ind. Crops Prod.* **2021,** *161*, 113219.

72.   Kawamoto, H., Lignin pyrolysis reactions. *J. Wood Sci.* **2017,** *63* (2), 117-132.

73.   Rajesh Banu, J.; Kavitha, S.; Yukesh Kannah, R.; Poornima Devi, T.; Gunasekaran, M.; Kim, S. H.; Kumar, G., A review on biopolymer production via lignin valorization. *Bioresour. Technol.* **2019,** *290*, 121790.

74.   Cao, Y.; Chen, S. S.; Zhang, S.; Ok, Y. S.; Matsagar, B. M.; Wu, K. C.; Tsang, D. C. W., Advances in lignin valorization toward bio-based chemicals and fuels: Lignin biorefinery. *Bioresour. Technol.* **2019,** *291*, 121878.

75.   Ren, T.; Qi, W.; Su, R.; He, Z., Promising Techniques for Depolymerization of Lignin into Value-added Chemicals. *ChemCatChem* **2019,** *11* (2), 639-654.

76.   Cao, Y.; Zhang, C.; Tsang, D. C. W.; Fan, J.; Clark, J. H.; Zhang, S., Hydrothermal Liquefaction of Lignin to Aromatic Chemicals: Impact of Lignin Structure. *Ind. Eng. Chem. Res.* **2020,** *59* (39), 16957-16969.

77.   Rishikesh, M. S.; Harish, S.; Mahendran Prasanth, S.; Gnana Prakash, D., A comprehensive review on lignin obtained from agro-residues: potential source of useful chemicals. *Biomass Convers. Biorefin.* **2021**.

78.   Wong, S. S.; Shu, R.; Zhang, J.; Liu, H.; Yan, N., Downstream processing of lignin derived feedstock into end products. *Chem. Soc. Rev.* **2020,** *49* (15), 5510-5560.

79.   Van den Bosch, S.; Renders, T.; Kennis, S.; Koelewijn, S. F.; Van den Bossche, G.; Vangeel, T.; Deneyer, A.; Depuydt, D.; Courtin, C. M.; Thevelein, J. M.; Schutyser, W.;

Sels, B. F., Integrating lignin valorization and bio-ethanol production: on the role of Ni-Al2O3catalyst pellets during lignin-first fractionation. *Green Chem.* **2017,** *19* (14), 3313-3326.

80.	Cheng, C.; Wang, J.; Shen, D.; Xue, J.; Guan, S.; Gu, S.; Luo, K. H., Catalytic Oxidation of Lignin in Solvent Systems for Production of Renewable Chemicals: A Review. *Polymers* **2017,** *9* (6), 240.

81.	Liu, C.; Wu, S.; Zhang, H.; Xiao, R., Catalytic oxidation of lignin to valuable biomass-based platform chemicals: A review. *Fuel Process. Technol.* **2019,** *191*, 181-201.

82.	Liu, Y.; Nie, Y.; Lu, X.; Zhang, X.; He, H.; Pan, F.; Zhou, L.; Liu, X.; Ji, X.; Zhang, S., Cascade utilization of lignocellulosic biomass to high-value products. *Green Chem.* **2019,** *21*, 3499-3535.

83.	Janusz, G.; Pawlik, A.; Sulej, J.; Świderska-Burek, U.; Jarosz-Wilkołazka, A.; Paszczyński, A., Lignin degradation: microorganisms, enzymes involved, genomes analysis and evolution. *FEMS Microbiol. Rev.* **2017,** *41* (6), 941-962.

84.	Weng, C.; Peng, X.; Han, Y., Depolymerization and conversion of lignin to value-added bioproducts by microbial and enzymatic catalysis. *Biotechnol. Biofuels* **2021,** *14* (1), 84.

85.	Li, C.; Chen, C.; Wu, X.; Tsang, C. W.; Mou, J.; Yan, J.; Liu, Y.; Lin, C. S. K., Recent advancement in lignin biorefinery: With special focus on enzymatic degradation and valorization. *Bioresour. Technol.* **2019,** *291*, 121898.

86.	Li, M.; Wilkins, M., Lignin bioconversion into valuable products: fractionation, depolymerization, aromatic compound conversion, and bioproduct formation. *Syst. Microbiol. Biomanuf.* **2020,** *1* (2), 166-185.

87.	Cui, C.; Sun, R.; Argyropoulos, D. S., Fractional Precipitation of Softwood Kraft Lignin: Isolation of Narrow Fractions Common to a Variety of Lignins. *ACS Sustain. Chem. Eng.* **2014,** *2* (4), 959-968.

88.	Gigli, M.; Crestini, C., Fractionation of industrial lignins: opportunities and challenges. *Green Chem.* **2020,** *22* (15), 4722-4746.

89.	Pang, T.; Wang, G.; Sun, H.; Sui, W.; Si, C., Lignin fractionation: Effective strategy to reduce molecule weight dependent heterogeneity for upgraded lignin valorization. *Ind. Crops Prod.* **2021,** *165*, 113442.

90.	Duval, A.; Vilaplana, F.; Crestini, C.; Lawoko, M., Solvent screening for the fractionation of industrial kraft lignin. *Holzforschung* **2016,** *70* (1), 1-10.

91.	Rashid, T.; Sher, F.; Rasheed, T.; Zafar, F.; Zhang, S.; Murugesan, T., Evaluation of current and future solvents for selective lignin dissolution–A review. *J. Mol. Liq.* **2021,** *321*, 114577.

92.	Sadeghifar, H.; Ragauskas, A., Perspective on Technical Lignin Fractionation. *ACS Sustain. Chem. Eng.* **2020,** *8* (22), 8086-8101.

93.	Sadeghifar, H.; Wells, T.; Le, R. K.; Sadeghifar, F.; Yuan, J. S.; Jonas Ragauskas, A., Fractionation of Organosolv Lignin Using Acetone:Water and Properties of the Obtained Fractions. *ACS Sustain. Chem. Eng.* **2016,** *5* (1), 580-587.

94.	Humpert, D.; Ebrahimi, M.; Czermak, P., Membrane Technology for the Recovery of Lignin: A Review. *Membranes* **2016,** *6* (42), 1-13.

95.	Polizzi, V.; Servaes, K.; Vandezande, P.; Kouris, P. D.; Panaite, A. M.; Jacobs, G.; Hensen, E. J. M.; Boot, M. D.; Vanbroekhoven, K., Molecular weight-based fractionation of lignin oils by membrane separation technology. *Holzforschung* **2020,** *74* (2), 166-174.

96.	Liu, W.-J.; Jiang, H.; Yu, H.-Q., Thermochemical conversion of lignin to functional materials: a review and future directions. *Green Chem.* **2015,** *17* (11), 4888-4907.

97.	Sun, Z.; Fridrich, B.; de Santi, A.; Elangovan, S.; Barta, K., Bright Side of Lignin Depolymerization: Toward New Platform Chemicals. *Chem. Rev.* **2018,** *118* (2), 614-678.

98.	Upton, B. M.; Kasko, A. M., Strategies for the Conversion of Lignin to High-Value Polymeric Materials: Review and Perspective. *Chem. Rev.* **2016,** *116* (4), 2275-2306.

99.	Boeriu, C. G.; Fiţigău, F. I.; Gosselink, R. J. A.; Frissen, A. E.; Stoutjesdijk, J.; Peter, F., Fractionation of five technical lignins by selective extraction in green solvents and characterisation of isolated fractions. *Ind. Crops Prod.* **2014,** *62*, 481-490.

100.   Matsakas, L.; Raghavendran, V.; Yakimenko, O.; Persson, G.; Olsson, E.; Rova, U.; Olsson, L.; Christakopoulos, P., Lignin-first biomass fractionation using a hybrid organosolv – Steam explosion pretreatment technology improves the saccharification and fermentability of spruce biomass. *Bioresour. Technol.* **2019,** *273*, 521-528.

101.   Talebi Amiri, M.; Dick, G. R.; Questell-Santiago, Y. M.; Luterbacher, J. S., Fractionation of lignocellulosic biomass to produce uncondensed aldehyde-stabilized lignin. *Nat. Protoc.* **2019,** *14* (3), 921-954.

102.   Majira, A.; Godon, B.; Foulon, L.; Putten, J. C.; Cézard, L.; Thierry, M.; Pion, F.; Bado-Nilles, A.; Pandard, P.; Jayabalan, T.; Aguié-Béghin, V.; Ducrot, P. H.; Lapierre, C.; Marlair, G.; Gosselink, R. J. A.; Baumberger, S.; Cottyn, B., Enhancing the Antioxidant Activity of Technical Lignins by Combining Solvent Fractionation and Ionic-Liquid Treatment. *ChemSusChem* **2019,** *12* (21), 4799-4809.

103.   Eraghi Kazzaz, A.; Hosseinpour Feizi, Z.; Fatehi, P., Grafting strategies for hydroxy groups of lignin for producing materials. *Green Chem.* **2019,** *21* (21), 5714-5752.

104.   Glasser, W. G., About Making Lignin Great Again—Some Lessons From the Past. *Front. Chem.* **2019,** *7* (565), 1-17.

105.   Laurichesse, S.; Avérous, L., Chemical modification of lignins: Toward biobased polymers. *Prog. Polym. Sci.* **2014,** *39* (7), 1266-1290.

106.   de Haro, J.; Magagnin, L.; Turri, S.; Griffini, G., Lignin-Based Anticorrosion Coatings for the Protection of Aluminum Surfaces. *ACS Sustain. Chem. Eng.* **2019,** *7* (6), 6213-6222.

107.   de Haro, J. C.; Allegretti, C.; Smit, A. T.; Turri, S.; D'Arrigo, P.; Griffini, G., Biobased Polyurethane Coatings with High Biomass Content: Tailored Properties by Lignin Selection. *ACS Sustain. Chem. Eng.* **2019,** *7* (13), 11700-11711.

108.   Emerson, J. A.; Garabedian, N. T.; Burris, D. L.; Furst, E. M.; Epps, T. H., Exploiting Feedstock Diversity To Tune the Chemical and Tribological Properties of Lignin-Inspired Polymer Coatings. *ACS Sustain. Chem. Eng.* **2018,** *6* (5), 6856-6866.

109.   Ghorbani, M.; Konnerth, J.; van Herwijnen, H. W. G.; Zinovyev, G.; Budjav, E.; Requejo Silva, A.; Liebner, F., Commercial lignosulfonates from different sulfite processes as partial phenol replacement in PF resole resins. *J. Appl. Polym. Sci.* **2018,** *135* (8), 45893-45904.

110.   Hajirahimkhan, S.; Xu, C. C.; Ragogna, P. J., Ultraviolet Curable Coatings of Modified Lignin. *ACS Sustain. Chem. Eng.* **2018,** *6* (11), 14685-14694.

111.   Hao, C.; Liu, T.; Zhang, S.; Brown, L.; Li, R.; Xin, J.; Zhong, T.; Jiang, L.; Zhang, J., A High-Lignin-Content, Removable, and Glycol-Assisted Repairable Coating Based on Dynamic Covalent Bonds. *ChemSusChem* **2019,** *12* (5), 1049-1058.

112.   Laine, C.; Willberg-Keyriläinen, P.; Ropponen, J.; Liitiä, T., Lignin and lignin derivatives as components in biobased hot melt adhesives. *J. Appl. Polym. Sci.* **2019,** *136* (38), 47983-47994.

113.   Lang, J. M.; Shrestha, U. M.; Dadmun, M., The Effect of Plant Source on the Properties of Lignin-Based Polyurethanes. *Front. Energy Res.* **2018,** *6* (4), 1-12.

114.   Li, J.; Wang, W.; Zhang, S.; Gao, Q.; Zhang, W.; Li, J., Preparation and characterization of lignin demethylated at atmospheric pressure and its application in fast curing biobased phenolic resins. *RSC Advances* **2016,** *6* (71), 67435-67443.

115.   Li, R. J.; Gutierrez, J.; Chung, Y.-L.; Frank, C. W.; Billington, S. L.; Sattely, E. S., A lignin-epoxy resin derived from biomass as an alternative to formaldehyde-based wood adhesives. *Green Chem.* **2018,** *20* (7), 1459-1466.

116.   Raquez, J. M.; Deléglise, M.; Lacrampe, M. F.; Krawczak, P., Thermosetting (bio)materials derived from renewable resources: A critical review. *Prog. Polym. Sci.* **2010,** *35* (4), 487-509.

117.   Scarica, C.; Suriano, R.; Levi, M.; Turri, S.; Griffini, G., Lignin Functionalized with Succinic Anhydride as Building Block for Biobased Thermosetting Polyester Coatings. *ACS Sustain. Chem. Eng.* **2018,** *6* (3), 3392-3401.

118.   Wei, C.; Zhu, X.; Peng, H.; Chen, J.; Zhang, F.; Zhao, Q., Facile Preparation of Lignin-Based Underwater Adhesives with Improved Performances. *ACS Sustain. Chem. Eng.* **2019,** *7* (4), 4508-4514.

119.   Chatterjee, S.; Saito, T., Lignin-Derived Advanced Carbon Materials. *ChemSusChem* **2015,** *8* (23), 3941-3958.

120.   Margellou, A.; Triantafyllidis, K., Catalytic Transfer Hydrogenolysis Reactions for Lignin Valorization to Fuels and Chemicals. *Catalysts* **2019,** *9* (1), 43.

121.   Patil, V.; Adhikari, S.; Cross, P.; Jahromi, H., Progress in the solvent depolymerization of lignin. *Renewable Sustainable Energy Rev.* **2020,** *133*, 110359.

122.   Wendisch, V. F.; Kim, Y.; Lee, J.-H., Chemicals from lignin: Recent depolymerization techniques and upgrading extended pathways. *Curr. Opin. Green Sustain* **2018,** *14*, 33-39.

123.   Haldar, D.; Purkait, M. K., Lignocellulosic conversion into value-added products: A review. *Process Biochem.* **2020,** *89*, 110-133.

124.   Espinoza-Acosta, J. L.; Torres-Chávez, P. I.; Olmedo-Martínez, J. L.; Vega-Rios, A.; Flores-Gallardo, S.; Zaragoza-Contreras, E. A., Lignin in storage and renewable energy applications: A review. *J. Energy Chem.* **2018,** *27* (5), 1422-1438.

125.   Yu, O.; Kim, K. H., Lignin to Materials: A Focused Review on Recent Novel Lignin Applications. *Appl. Sci.* **2020,** *10* (13), 4626.

126.   Norgren, M.; Edlund, H., Lignin: Recent advances and emerging applications. *Curr. Opin. Colloid Interface Sci.* **2014,** *19* (5), 409-416.

127.   Kienberger, M., Potential Applications of Lignin. In *Economics of Bioresources: Concepts, Tools, Experiences*, Krozer, Y.; Narodoslawsky, M., Eds. Springer International Publishing: Cham, 2019; pp 183-193.

128.   Ganewatta, M. S.; Lokupitiya, H. N.; Tang, C., Lignin Biopolymers in the Age of Controlled Polymerization. *Polymers* **2019,** *11* (7), 1176.

129.   Bertella, S.; Luterbacher, J. S., Lignin Functionalization for the Production of Novel Materials. *Trends in Chemistry* **2020,** *2* (5), 440-453.

130.   Vásquez-Garay, F.; Carrillo-Varela, I.; Vidal, C.; Reyes-Contreras, P.; Faccini, M.; Teixeira Mendonça, R., A Review on the Lignin Biopolymer and Its Integration in the Elaboration of Sustainable Materials. *Sustainability* **2021,** *13* (5), 2697.

131.   Karunarathna, M. S.; Smith, R. C., Valorization of Lignin as a Sustainable Component of Structural Materials and Composites: Advances from 2011 to 2019. *Sustainability* **2020,** *12* (2), 734.

132.   Collins, M. N.; Nechifor, M.; Tanasa, F.; Zanoaga, M.; McLoughlin, A.; Strozyk, M. A.; Culebras, M.; Teaca, C. A., Valorization of lignin in polymer and composite systems for advanced engineering applications - A review. *Int. J. Biol. Macromol.* **2019,** *131*, 828-849.

133.   Duval, A.; Lawoko, M., A review on lignin-based polymeric, micro- and nano-structured materials. *React. Funct. Polym.* **2014,** *85*, 78-96.

134.   Gao, Z.; Lang, X.; Chen, S.; Zhao, C., Mini-Review on the Synthesis of Lignin-Based Phenolic Resin. *Energy Fuels* **2021,** *35* (22), 18385-18395.

135.   Wang, Y. Y.; Meng, X.; Pu, Y.; Ragauskas, A. J., Recent Advances in the Application of Functionalized Lignin in Value-Added Polymeric Materials. *Polymers* **2020,** *12* (10), 2277.

136.   Xu, C.; Ferdosian, F., Conversion of Lignin into Bio-Based Chemicals and Materials. In *Green Chemistry and Sustainable Technology*, Liang-Nian He, R. D. R., Dangsheng Su, Fritz Haber, Pietro Tundo, Z. Conrad Zhang, Ed. Springer Nature: 2017; pp 1-164.

137.   Dessbesell, L.; Paleologou, M.; Leitch, M.; Pulkki, R.; Xu, C., Global lignin supply overview and kraft lignin potential as an alternative for petroleum-based polymers. *Renewable Sustainable Energy Rev.* **2020,** *123*, 109768.

138.   Kalami, S.; Arefmanesh, M.; Master, E.; Nejad, M., Replacing 100% of phenol in phenolic adhesive formulations with lignin. *J. Appl. Polym. Sci.* **2017,** *134* (30), 45124-45133.

139.   Karthauser, J.; Biziks, V.; Mai, C.; Militz, H., Lignin and Lignin-Derived Compounds for Wood Applications-A Review. *Molecules* **2021,** *26* (9), 2533.

140.   Sternberg, J.; Sequerth, O.; Pilla, S., Green chemistry design in polymers derived from lignin: review and perspective. *Prog. Polym. Sci.* **2021,** *113*, 101344-101348.

141.   Gioia, C.; Colonna, M.; Tagami, A.; Medina, L.; Sevastyanova, O.; Berglund, L. A.; Lawoko, M., Lignin-Based Epoxy Resins: Unravelling the Relationship between Structure and Material Properties. *Biomacromolecules* **2020,** *21* (5), 1920-1928.

142.   Li, H.; Liang, Y.; Li, P.; He, C., Conversion of biomass lignin to high-value polyurethane: A review. *J. Bioresour. Bioprod.* **2020,** *5* (3), 163-179.

143.   Wang, B.; Ma, S.; Xu, X.; Li, Q.; Yu, T.; Wang, S.; Yan, S.; Liu, Y.; Zhu, J., High-Performance, Biobased, Degradable Polyurethane Thermoset and Its Application in Readily Recyclable Carbon Fiber Composites. *ACS Sustain. Chem. Eng.* **2020,** *8* (30), 11162-11170.

144.   Kun, D.; Pukánszky, B., Polymer/lignin blends: Interactions, properties, applications. *Eur. Polym. J.* **2017,** *93*, 618-641.

145.   Sen, S.; Patil, S.; Argyropoulos, D. S., Thermal properties of lignin in copolymers, blends, and composites: a review. *Green Chem.* **2015,** *17* (11), 4862-4887.

146.   Moreno, A.; Sipponen, M. H., Lignin-based smart materials: a roadmap to processing and synthesis for current and future applications. *Mater. Horiz.* **2020,** *7* (9), 2237-2257.

147.   Zhao, S.; Abu-Omar, M. M., Materials Based on Technical Bulk Lignin. *ACS Sustain. Chem. Eng.* **2021,** *9* (4), 1477-1493.

148.   Alzagameem, A.; Khaldi-Hansen, B. E.; Buchner, D.; Larkins, M.; Kamm, B.; Witzleben, S.; Schulze, M., Lignocellulosic Biomass as Source for Lignin-Based Environmentally Benign Antioxidants. *Molecules* **2018,** *23* (10), 2664-2689.

149.   Domenek, S.; Louaifi, A.; Guinault, A.; Baumberger, s., Potential of Lignins as Antioxidant Additive in Active Biodegradable Packaging Materials. *J. Polym. Environ.* **2013,** *21* (3), 692-701.

150.   Kai, D.; Chua, Y. K.; Jiang, L.; Owh, C.; Chan, S. Y.; Loh, X. J., Dual functional anti-oxidant and SPF enhancing lignin-based copolymers as additives for personal and healthcare products. *RSC Advances* **2016,** *6* (89), 86420-86427.

151.   Sadeghifar, H.; Argyropoulos, D. S., Correlations of the Antioxidant Properties of Softwood Kraft Lignin Fractions with the Thermal Stability of Its Blends with Polyethylene. *ACS Sustain. Chem. Eng.* **2015,** *3* (2), 349-356.

152.   Chandrasekaran, S. R.; Murali, D.; Marley, K. A.; Larson, R. A.; Doll, K. M.; Moser, B. R.; Scott, J.; Sharma, B. K., Antioxidants from Slow Pyrolysis Bio-Oil of Birch Wood: Application for Biodiesel and Biobased Lubricants. *ACS Sustain. Chem. Eng.* **2016,** *4* (3), 1414-1421.

153.   Sadeghifar, H.; Ragauskas, A., Lignin as a UV Light Blocker-A Review. *Polymers* **2020,** *12* (5), 1134.

154.   Zhang, Y.; Naebe, M., Lignin: A Review on Structure, Properties, and Applications as a Light-Colored UV Absorber. *ACS Sustain. Chem. Eng.* **2021,** *9* (4), 1427-1442.

155.   Sivagurunathan, P.; Raj, T.; Mohanta, C. S.; Semwal, S.; Satlewal, A.; Gupta, R. P.; Puri, S. K.; Ramakumar, S. S. V.; Kumar, R., 2G waste lignin to fuel and high value-added chemicals: Approaches, challenges and future outlook for sustainable development. *Chemosphere* **2021,** *268*, 129326.

156.   Özel, M.; Demir, F.; Aikebaier, A.; Kwiczak-Yiğitbaşı, J.; Baytekin, H. T.; Baytekin, B., Why Does Wood Not Get Contact Charged? Lignin as an Antistatic Additive for Common Polymers. *Chem. Mater.* **2020,** *32* (17), 7438-7444.

157.   Vachon, J.; Assad-Alkhateb, D.; Baumberger, S.; van Haveren, J.; Gosselink, R. J. A.; Monedero, M.; Bermudez, J. M., Use of lignin as additive in polyethylene for food protection: Insect repelling effect of an ethyl acetate phenolic extract. *Compos. Part C* **2020,** *2*, 100044.

158.   Advancement, T. I. f. S. Carbon Fiber: The Material of the Future? https://ifsa.my/articles/carbon-fiber-the-material-of-the-future (accessed 31.01.2022).

159.   Qu, W.; Yang, J.; Sun, X.; Bai, X.; Jin, H.; Zhang, M., Toward producing high-quality lignin-based carbon fibers: A review of crucial factors affecting lignin properties and conversion techniques. *Int. J. Biol. Macromol.* **2021,** *189*, 768-784.

Chapter 1

160.   Navarro-Suárez, A. M.; Saurel, D.; Sánchez-Fontecoba, P.; Castillo-Martínez, E.; Carretero-González, J.; Rojo, T., Temperature effect on the synthesis of lignin-derived carbons for electrochemical energy storage applications. *J. Power Sources* **2018**, *397*, 296-306.

161.   Xin, W.; Song, Y., Mesoporous carbons: recent advances in synthesis and typical applications. *RSC Advances* **2015**, *5* (101), 83239-83285.

162.   Benzigar, M. R.; Talapaneni, S. N.; Joseph, S.; Ramadass, K.; Singh, G.; Scaranto, J.; Ravon, U.; Al-Bahily, K.; Vinu, A., Recent advances in functionalized micro and mesoporous carbon materials: synthesis and applications. *Chem. Soc. Rev.* **2018**, *47* (8), 2680-2721.

163.   Titirici, M. M.; White, R. J.; Brun, N.; Budarin, V. L.; Su, D. S.; del Monte, F.; Clark, J. H.; MacLachlan, M. J., Sustainable carbon materials. *Chem. Soc. Rev.* **2015**, *44* (1), 250-290.

164.   Supanchaiyamat, N.; Jetsrisuparb, K.; Knijnenburg, J. T. N.; Tsang, D. C. W.; Hunt, A. J., Lignin materials for adsorption: Current trend, perspectives and opportunities. *Bioresour. Technol.* **2019**, *272*, 570-581.

165.   González-García, P., Activated carbon from lignocellulosics precursors: A review of the synthesis methods, characterization techniques and applications. *Renewable Sustainable Energy Rev.* **2018**, *82*, 1393-1414.

166.   Yang, D.-P.; Li, Z.; Liu, M.; Zhang, X.; Chen, Y.; Xue, H.; Ye, E.; Luque, R., Biomass-Derived Carbonaceous Materials: Recent Progress in Synthetic Approaches, Advantages, and Applications. *ACS Sustain. Chem. Eng.* **2019**, *7* (5), 4564-4585.

167.   Malgras, V.; Tang, J.; Wang, J.; Kim, J.; Torad, N. L.; Dutta, S.; Ariga, K.; Hossain, M. S. A.; Yamauchi, Y.; Wu, K. C. W., Fabrication of Nanoporous Carbon Materials with Hard- and Soft-Templating Approaches: A Review. *J. Nanosci. Nanotechnol.* **2019,** *19* (7), 3673-3685.

168.   Inagaki, M.; Toyoda, M.; Soneda, Y.; Tsujimura, S.; Morishita, T., Templated mesoporous carbons: Synthesis and applications. *Carbon* **2016**, *107*, 448-473.

169.   Enterría, M.; Figueiredo, J. L., Nanostructured mesoporous carbons: Tuning texture and surface chemistry. *Carbon* **2016**, *108*, 79-102.

170.   Saha, D.; Warren, K. E.; Naskar, A. K., Soft-templated mesoporous carbons as potential materials for oral drug delivery. *Carbon* **2014**, *71*, 47-57.

171.   Herou, S.; Ribadeneyra, M. C.; Madhu, R.; Araullo-Peters, V.; Jensen, A.; Schlee, P.; Titirici, M., Ordered mesoporous carbons from lignin: a new class of biobased electrodes for supercapacitors. *Green Chem.* **2019**, *21* (3), 550-559.

CHAPTER 2

Renewable thiol-yne "click" networks based on propargylated lignin for adhesive resin applications
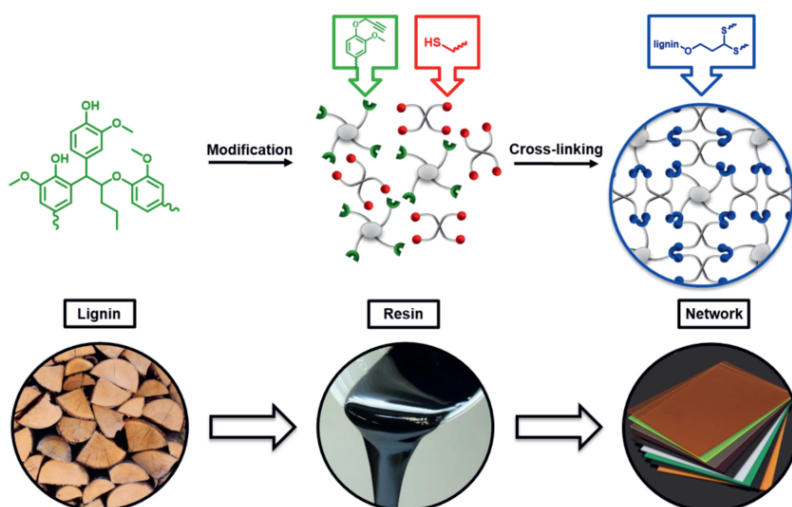
In this chapter, the development of a lignin-based resins for wood adhesion applications was demonstrated. We investigated two lignin fractions: commercial Protobind 1000 lignin and methanol soluble Protobind 1000 lignin fraction after mild solvolysis. Although lignin has previously been incorporated into various cross-linked systems, this is the first report on lignin-based thermosets obtained via thiol-yne "click" chemistry. In this approach, lignin was functionalized with terminal alkyne groups followed by cross-linking with a multifunctional thiol, resulting in polymeric network formation. The influence of the curing conditions on the resin characteristics and performance was studied by varying the amount of reactive monomeric diluent. Additionally, a post-curing strategy utilizing the Claisen rearrangement was investigated. These resins were tested as a wood adhesive and were proven to possess a desirable performance, comparable to state-of-the-art phenol-formaldehyde resins. Lignin-based thiol-yne resins turn out to be an alternative to phenol-formaldehyde resins, currently used as adhesives and coatings. Although it is possible to use lignin in phenol-formaldehyde resins, lignin addition compromises the resin's performance. The main benefits over the phenol-formaldehyde approach are that higher lignin loadings are possible to achieve and no volatiles are emitted during the resin processing and use.

Introduction

Traditionally, thermoset resins such as phenol-formaldehyde (PF), urea-formaldehyde, melamine-formaldehyde, isocyanate, and polyurethane resins are used as adhesives for wood bonding.[1] Despite their very good performance, there are environmental concerns because of toxic formaldehyde or isocyanate release during the wood bonding and their production relying on petroleum-based resources. There is an urgent need seen by academia, industry, and policymakers for a change toward formaldehyde-free, more environment-friendly adhesives produced from renewable resources, such as lignin, tannin, proteins, carbohydrates, and vegetable oils.[2, 3]

Lignin is an amorphous material consisting of highly branched aromatic macromolecules based on three basic phenylpropanoid components (coumaryl, coniferyl, and sinapyl alcohols) enzymatically cross-linked during their biosynthesis.[4] Lignin provides lignocellulosic materials with strength, rigidity, and dimensional stability due to the chemical bonding with cellulose and hemicellulose, water impermeability, and transport within the plant, and it also has antioxidant, antimicrobial, and antifungal properties.[5, 6] Although lignin is considered as a by-product of the paper industry and lignocellulose bioethanol production, it can be produced through a range of different isolation, fractionation and/or depolymerization process technologies, as reviewed by Liu *et al.* and Chio *et al.*.[7, 8, 9] Lignin products have been valorized in applications such as adhesives, coatings, fuels, antioxidant additives, and as a platform for chemicals and polymers among others.[6, 9-13]

The lignin structure exhibits a resemblance to PF networks; therefore, a lot of research was concentrated on lignin as a phenol replacement in PF resins. Unfortunately, lignin has a low reactivity toward formaldehyde, and only partial replacement of phenol with lignin leads to the acceptable performance of those resins, usually lower than 50% for unmodified lignin and lower than 70% for hydroxymethylated or phenolated lignin.[14-16] The exception to this is the work performed by Kalami *et al.*[17] In their study, 100% of phenol was replaced by lignin with acceptable performance. Feedstock from which lignin is isolated is crucial for its performance in lignin-phenol-formaldehyde (LPF) resins. Lignin originating from annual crops has a high concentration of *p*-hydroxyphenyl units, which are more reactive toward formaldehyde than guaiacyl and syringyl units, abundant in softwoods and hardwoods.[18] Phenol replacement, however, partially solves the problem since these resins are still prone to emitting formaldehyde during processing and use. An alternative for phenolic resins where not only phenol is replaced with lignin, but also toxic formaldehyde is replaced with a more environment-friendly thiol cross-linker is presented in this study.

The use of lignin in thermoset resins has been extensively investigated.[11, 19] One of the possibilities is to use "click" chemistry strategies in polymeric network formation, as reviewed by Buono *et al*.[20] The chemistries such as alkyne-azide cycloaddition,[21, 22] furan–maleimide Diels–Alder cycloaddition,[23] thiol-ene,[24-28] and thiol-maleimide reactions have been reported.[29] Thiol-yne chemistry has never been employed as a cross-linking technique to prepare lignin-based polymeric networks or wood adhesives. Jin *et al*. described the use of thiol-yne chemistry to graft 1,2,4-triazole groups on lignin for the preparation of lignin-based metal ion adsorbents.[30] Propargylated lignin was reported to self-cross-link via the Claisen rearrangement.[31-33]

In this research, the focus is on the synthesis of lignin-based resins applied as wood adhesives. Currently, PF resins are widely used for this purpose. We aim to develop a more sustainable alternative using thiol-yne chemistry instead (Scheme 1). Here, we use lignin-based monomers as a reactive diluent of functionalized lignin-based resin in order to decrease the formulation viscosity and tune the material properties. Additionally, we investigated two curing strategies: thermal thiol-yne curing with and without post-curing, which is done via the Claisen rearrangement. Two lignin fractions were tested in this study: commercially available Protobind 1000 lignin and methanol soluble Protobind 1000 lignin fraction after mild solvolysis. These fractions were selected due to ongoing valorization, scale-up initiatives, and/or coming commercialization of these types of lignin, and their application development is required.[34]

Chapter 2

Thiol-yne curing approach:
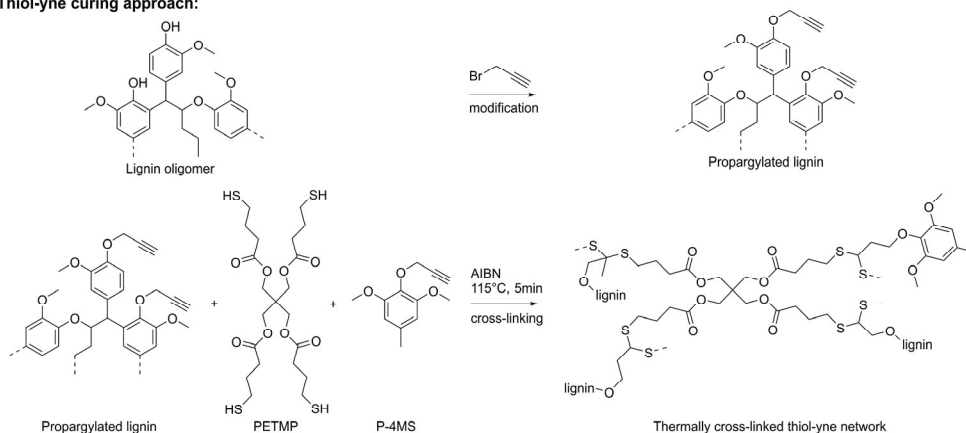
Claisen rearrangement post-curing approach:
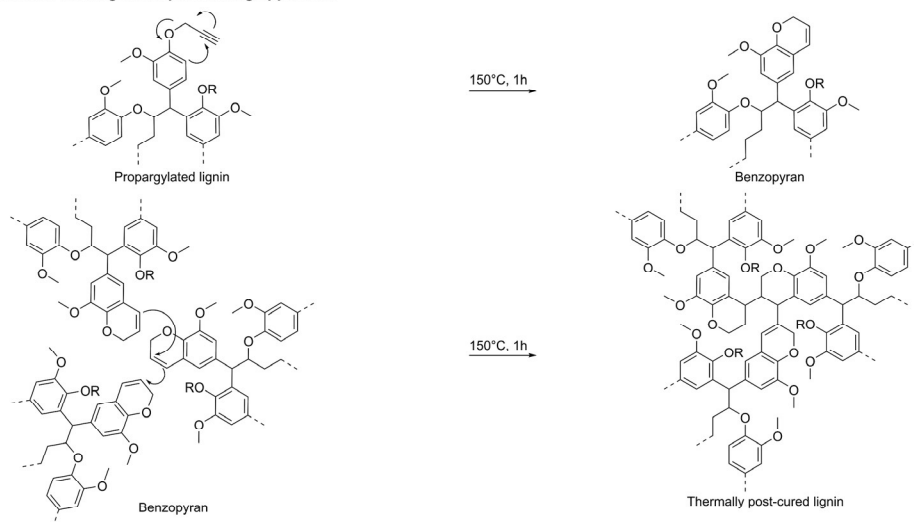
Scheme 1 *Lignin cross-linking via thiol-yne chemistry approach and post-curing strategy via Claisen rearrangement*

Experimental section

Materials

Protobind P1000 soda lignin (P1000) extracted from wheat straw was provided by Green Value S.A. Propargyl bromide solution (80 wt.% in toluene solution, with 0.3% magnesium oxide as a stabilizer), potassium iodide (99.5%), potassium carbonate (99.0%), acetic anhydride (99%), pentaerythritol tetrakis(3-mercaptopropionate) (PETMP, 95%), azobisisobutyronitrile (AIBN, 98%), pyridine (99%), sodium chloride (99%), cholesterol (99%), chromium (III) acetylacetonate (99.99%),

2-chloro-4,4,5,5-tetramethyl-1,3,2-dioxaphospholane (TMDP, 95%) and calcium hydride (95%) were purchased from Sigma Aldrich. 4-Methylsyringol (97%) was purchased from Acros. Acetone, methanol, and ethyl acetate were purchased from Biosolve. Molecular sieves 3Å (0.3 nm, beads 2 mm) were purchased from Merck. Chloroform-*d* (dried over molecular sieves, D, 99.96%) was purchased from Cambridge Isotope Laboratories. Pyridine was dried by distillation over calcium hydride. AIBN was purified by recrystallization from methanol and stored in the freezer. Both lignin fractions, P1000 lignin and CLO MeOH, were vacuum dried (80 °C, overnight) prior to use and analysis. Birch wood specimens (115 mm x 20 mm x 3 mm) were purchased from Interieurbouw Maastricht BV.

Methods

Lignin mild solvolysis

Crude lignin oil (CLO) was obtained from P1000 lignin by solvolysis in methanol in mild conditions.[35, 36] 300 g of P1000 lignin was loaded in a 4 L Parker stirred high-pressure autoclave reactor and mixed with 1500 mL of methanol (1:5 w/v), the solvolysis was carried out at 200 °C, under 10 bar of nitrogen gas for 30 min. After the reaction, the reaction mixture was filtered, and the CLO was collected. The solvent was removed from the CLO by evaporation and methanol-soluble lignin (CLO MeOH) was isolated as a solid.

Synthesis of propargylated lignin[37]

The reaction was performed in a 4 L reactor, equipped with a cooler and mechanical stirrer, under nitrogen flow. First, P1000 lignin (200 g, 1.29 mol, 1 equiv of the sum of phenolic OH, aliphatic OH, and COOH groups) was dissolved in 2 L acetone, then, potassium carbonate (941 g, 6.88 mol, 5 equiv) and potassium iodide (113 g, 0.68 mol, 0.5 equiv) were dispersed in the lignin solution. Subsequently, the temperature was increased to 60 °C, and propargyl bromide (80 wt.% solution in toluene, 759 mL, 6.88 mol, 5 equiv) was added dropwise into the reaction mixture. The reaction mixture was then refluxed for 24 h. Afterward, the reaction mixture was cooled, and the product was filtered. The solid residue from the reaction mixture was washed with acetone, the filtrates were combined, and the solvent was removed using the rotavapor. The solid residue was dried at 80 °C in the vacuum oven overnight. The crude product was dissolved in 500 mL of ethyl acetate and washed twice with deionized water and with brine. The solvent was removed in the rotavapor, and the product was dried in the vacuum oven at 80 °C overnight. 142 g of the propargylated lignin was obtained as a brown powder, yielding 57%.[37] The propargyl moiety content was determined by measuring the conversion of the phenolic OH, aliphatic OH, and COOH by [31]P Nuclear Magnetic Resonance (NMR) spectroscopy. The spectra before and after modification are presented in Figures S1 and S2

(Appendix). CLO MeOH was propargylated according to the same procedure, with a yield of 66%.

Synthesis of reactive diluent, 4-methylsyringyl propargyl ether (P-4MS)

The propargylation of 4-methylsyringol was performed in a 4 L reactor, equipped with a cooler and mechanical stirrer, under nitrogen flow. First, 4-methylsyringol (100 g, 0.6 mol, 1 equiv) was dissolved in 1.5 L of acetone, and then, potassium carbonate (103 g, 0.74 mol, 1.25 equiv) and potassium iodide (12 g, 0.07 moles, 0.13 equiv) were dispersed in the solution. Subsequently, the temperature was increased to 60 °C, and propargyl bromide (80 wt.% solution in toluene, 82 mL, 0.74 moles, 1.25 equiv) was added dropwise into the reaction mixture. The reaction mixture was then refluxed for 24 h. Afterward, the reaction mixture was cooled, and the product was filtered. The solid residue from the reaction mixture was washed with acetone, the filtrates were combined, and the solvent was removed using the rotavapor. The crude product was dissolved in 500 of mL ethyl acetate and washed twice with deionized water and with brine. The solvent was evaporated, and the product was dried in the vacuum oven at 80 °C overnight. 114 g of the product was isolated as an orange liquid, with 93% yield. The ^{1}H and ^{13}C NMR spectra are presented in Figures S3 and S4 (Appendix).

Thiol-yne resins preparation

Propargylated P1000 lignin (1.50 g, 4.66 mmol/g of the propargyl moiety) was mixed with 4-methylsyringyl propargyl ether (P-4MS, 0.5 g, 2.42 mmol), pentaerythritol tetrakis(3-mercaptopropionate) (PETMP, 1.87 g, 3.83 mmol, 2 eq of thiol per propargyl moiety), and azobisisobutyronitrile (AIBN, 0.19 g, 0.73 mmol, 5 wt.% based on the total weight of the mixture) in a 20 mL vial and dissolved in 5 mL of acetone to ensure good homogeneity of the mixture. Then, the solvent was evaporated and the resin was flushed with nitrogen for 30 min. The prepared thiol-yne resin was subsequently used in the curing studies, specimen preparation, and application testing. The other resins were prepared according to the same procedure, with varying amounts of propargylated lignin (75-100%, 0%) and of P-4MS (0-25%, 100%). The specimens were cured in a Collin P 200 E hydraulic press at 125 °C for 15 min with the applied pressure of 10 bar. Approximately 0.5g of each resin was placed between biaxially-oriented polyethylene terephthalate (BoPET) sheets limited with silicone spacers. BoPET sheets were placed between the wood specimens to mimic the application testing conditions. Post-curing of the specimens was performed in an oven at 150 °C for 1 h. Samples were named using the following formula: TY/PC_lignin fraction_lignin%, where TY is used for thiol-yne cured resins and PC is used when post-curing was additionally performed.

Synthesis of PF reference resin

The resin was prepared, as described by Chen *et al.*[38] Briefly, to phenol (0.94 g, 10 mmol), a formaldehyde solution was added (1.41 mL, 19 mmol, F/P ratio = 1.9) and stirred at room temperature for 15 min. Then, sodium hydroxide (0.08 mL, 0.5 mmol, 50% solution) was added and the reaction mixture was heated up to 70 °C (over 30 min) and kept at that temperature for 15 min. Finally, the reaction was heated up to 85 °C (over 15 min) and stirred for 30 min at 85 °C.

Characterization

The aromatic and aliphatic hydroxyl groups, as well as the carboxylic acids (before and after modification) of lignin were determined by ^{31}P NMR spectroscopy after sample derivatization, according to the method described by Korntner *et al.*[39] 10 mg of dried (in a vacuum oven at 80 °C, overnight), lignin-based material was dissolved in a 500 µL of anhydrous pyridine and deuterated chloroform mixture (1.6:1, v:v). Then, 100 µL of internal standard solution, cholesterol (19.7 mg/mL in the anhydrous pyridine and deuterated chloroform mixture, 1.6/1, v/v, 0.0051 mmol), 50 µL of the relaxation agent, chromium (III) acetylacetonate (10 mg/mL, in the anhydrous pyridine and deuterated chloroform mixture, 1.6:1, v:v), and 50 µL of the derivatizing agent (2-chloro-4,4,5,5-tetramethyl-1,3,2-dioxaphospholane) were added to the solution. The solution was stirred for 10 min, transferred into a dry 5 mm NMR tube and measured. The measurement was performed on Bruker Avance III HD Nanobay 300 MHz apparatus (121.49 MHz for ^{31}P NMR experiments) using the standard phosphorus pulse program, at ambient temperature, with 512 scans, a relaxation delay of 5 s, an acquisition time of 2 s, a transmitter excitation fre RE: Monika Jedrzejczyk (14256) - Notification start production today - PMquency of 140 ppm, and a spectral width of 396 ppm. The chemical shifts were reported in ppm. Chemical shifts were referenced from the sharp signal of the reaction product between residual water and 2-chloro-4,4,5,5-tetramethyl-1,3,2-dioxaphospholane at 132.2 ppm. ^{1}H and ^{13}C NMR experiments were recorded with 16 and 1024 scans, respectively, on the same apparatus.

The molecular weight of lignin and its dispersity were obtained from gel permeation chromatography (GPC) analysis. GPC analysis was performed at 40 °C using a Waters GPC equipped with a Waters 2414 refractive index detector. Tetrahydrofuran was used as the eluent at a flow rate of 1 mL/min. Three linear columns were used (Styragel HR1, Styragel HR4, and Styragel HR5), preceded by a precolumn Styragel THF. Lignin samples were acetylated by acetic anhydride in the presence of pyridine before the measurement using the protocol described by Gosselink *et al.*[40] Acetylated lignin samples (approximately 7 mg) were dissolved in 1.5 mL of tetrahydrofuran and filtered with a PTFE syringe filter (pore size 0.2 µm) prior to the measurement. Molecular weights were given relative to polystyrene standards.

Chapter 2

Rheological curing experiments were performed using a TA Instruments Discovery HR 2 rheometer to determine the gel point (curing temperature) and the vitrification temperature. The resin curing was studied in the temperature range of 25-150 °C (heating rate of 10 °C/min) in a 25mm parallel plate geometry, with a 440 µm gap, under a 0.1% strain and an angular frequency of 1.0 rad/s. The gel point is defined as the intersection of the storage and loss modulus, G' and G" curves, while the vitrification temperature is observed at the plateau of the complex viscosity curve.

FT-IR spectra of the resins before and after curing were recorded on a PerkinElmer Frontier spectrometer, equipped with Pike technologies GladiATR accessory in the range of 600-4000 cm^{-1}, with a resolution of 2 cm^{-1} using 32 accumulative scans. Curing kinetics were determined at 115 °C, and the spectra were recorded in 15 s intervals. The conversion was determined by following the disappearance of the alkyne C≡C-H peak at 3300 cm^{-1}, while the peak of the aromatic C=C at 1590 cm^{-1} was used as the internal standard.

Thermogravimetric analysis (TGA) was performed using a TA Instruments Q500 instrument. Approximately 10 mg of the sample was heated at 10 °C/min from 25 to 700 °C in nitrogen flow. The maximum of the first derivative of the weight loss over the temperature curve is reported as the maximum degradation temperature of the polymers and the 5% degradation temperature of the polymers is determined from the weight loss over the temperature curve.

The glass transition temperature (T_g) was determined by differential scanning calorimetry (DSC). Thermographs were recorded on a Netzsch Polyma 2014 DSC. DSC data were obtained from approximately 10 mg of the dried lignin sample. Two heating/cooling cycles were performed at the rate of 10 °C/min in the range of -40 to 150 °C. The T_g of each lignin fraction was determined as the temperature at the midpoint of the transition in the second heating cycle. Indium, zinc, tin, and bismuth were used as standards for temperature and enthalpy calibration.

Insoluble fractions were determined by swelling experiments. 50 mg of the cured or post-cured, dried network sample was weighed and placed in a vial. Then 10 mL of acetone (a good solvent for propargylated lignin and PETMP) was added, and the sample was kept at room temperature for 24h. Afterward, the sample was collected and dried under vacuum at 80 °C for another 24h and weighed again. The insoluble fractions were calculated as follows:

$$insoluble\ fraction = \frac{material\ weight\ (after\ dissolution)}{material\ weight\ (initial)} \cdot 100\%$$

Scanning Electron Microscopy - Energy Dispersive X-Ray Spectroscopy (SEM-EDX) was used to analyze the morphology and map the elemental composition of the cured resin. Microscopic images and elemental profiles were recorded using Jeol IT2000 SEM equipped with an EDX detector, operated at 20 kV of an accelerating voltage for compositional analysis.

Application testing as wood adhesive was performed via lap-shear test experiments according to the ASTM D 5868 standard test method using a Zwick/Roell Z020 tensile machine equipped with a 50kN cell. Birch wood specimens (115 mm x 20 mm x 3 mm) were used in these studies, and they were conditioned before and after the application of the resin and hot-pressing. Conditioning of the wood veneer: specimens were conditioned in a Binder MFK 240 climate chamber at 20 °C and 65% relative humidity for 7 days before applying the adhesive and hot-pressing and 7 days afterward, before the tensile strength measurements. Hot-pressing and lap-shear specimen preparation: wood specimens were coated with 250 g/m^2 of adhesive on an area of 5 cm^2, and a second veneer specimen was applied. The specimens were then hot-pressed using a Collin P 200 E hydraulic press at 125 °C for 15 min with the applied pressure of 10 bar. Post-curing of the specimens was performed in an oven at 150 °C for 1h. Tensile strength measurements: lap-shear specimens were tested on a Zwick/Roell Z020 tensile machine using a 50kN cell according to ASTM D 5868. The data for each sample were obtained from an average of three specimens.

Results and discussion

The ultimate goal of this research is to synthesize novel thermoset materials based on lignin, which are suitable as wood adhesives. The thiol-yne "click"-chemistry approach was used to achieve this goal, with and without an additional post-curing step by Claisen rearrangement. Moreover, the use of the monomeric lignin-derived reactive diluent (P-4MS) is also investigated to tune the properties of the thermosets and their performance. Reactive diluent also helps decrease the adhesive formulation's viscosity before curing.

Lignin modification

In this study, two lignin fractions were used as a precursor for the thiol-yne thermosets. The first one is commercial P1000 soda lignin, and the second one is P1000 lignin fractionated using mild thermal solvolysis in methanol (CLO MeOH).[36] As it can be seen in Table 1, CLO MeOH slightly decreased in functionality compared to P1000 lignin, and the molecular weight almost halved which leads to a decrease in T_g by 60 °C. This behavior is in accordance with the findings reported in the literature.[41-43] Thermal stability of lignin fractions was studied by TGA (Figure S5,

Appendix). Both lignins show similar degradation profiles, which is typical for lignins. In lower temperatures, below 180 °C, the weight loss is mainly caused by the release of water, while at higher temperatures, the lignin backbone starts to degrade.[44, 45] In temperatures between 200 and 280 °C, propanoid side chains degrade, followed by the main pyrolytic degradation with the formation of volatile products such as aromatic hydrocarbons and phenolic compounds (up to 400 °C). Degradation in temperatures up to 800 °C is mostly associated with the formation of highly condensed aromatic structures resulting in char formation.

Table 1 Lignin fractions characterization

Lignin fraction	Phen. OH [mmol/g]	Aliph. OH [mmol/g]	COOH [mmol/g]	Total OH + COOH [mmol/g]	M_w [kDa]	M_n [kDa]	Đ [-]	T_g [°C]
P1000	3.71	1.80	0.95	6.46	4.3	1.9	2.6	126.8
CLO MeOH	3.29	1.10	0.23	4.62	2.3	1.1	2.1	66.6

In order to incorporate lignin into the polymeric network via thiol-yne chemistry, aromatic and aliphatic OH groups have to be modified (Scheme 1). Williamson etherification with propargyl bromide has been selected for this purpose. ^{31}P NMR and FT-IR spectroscopies provide the evidence of the successful conversion (Table 2, Figures S1 and S2, Appendix). ^{31}P NMR spectroscopy revealed the disappearance of both aliphatic and aromatic OH groups, while in the FT-IR spectra, an additional peak can be observed at wavenumber 3300 cm^{-1} originating from the propargyl moiety. The reaction was more selective toward phenolic hydroxyl groups than toward aliphatic ones, as seen in Table 2, leading to nearly quantitative conversion of phenolic OH and only partial conversion of aliphatic OH despite the used of the propargyl bromide. In our synthesis method, we observe modification of both phenolic and aliphatic OHs, unlike in a study by Sen *et al.*, where only phenolic OH groups were modified.[31]

Table 2 Summary of the lignin propargylation

Lignin fraction	Phenolic OH conversion[a] [%]	Aliphatic OH conversion[a] [%]	Propargyl moiety content [mmol/g]
P1000	94.9	56.6	4.66
CLO MeOH	99.8	30.3	3.49

[a] Calculated as described by Koivu et al.[46] based on a theoretical lignin mass percentage in a lignin ether. $m(\%)lignin = \frac{1-m(H\%)}{1-m(H\%)+m(R\%)} \times 100\% = \frac{1-[(\frac{PropBr}{Lignin}) \times (OH) \times M(H)]}{1+[(\frac{PropBr}{Lignin}) \times (OH) \times M(R)]} \times 100\%$, Where: PropBr/Lignin is the molar ratio of added propargyl bromide (equiv, excess is counted as 1); (OH) is the total hydroxyl content of lignin; m(H%) and m(R%) are mass effects related to hydrogen and propargyl groups, where M(H)=1 g/mol and M(R)=38 g/mol.

Lignin-based resins curing

Thanks to the derivatization with propargyl groups, lignin fractions can be thermally cross-linked using a thiol-yne chemistry approach. In this study, a set of thermosets was synthesized with tetrafunctional thiol, PETMP, used as a cross-linker, and varying amounts of the reactive diluent, P-4MS (Scheme 1).

To determine the curing parameters, such as the curing temperature and time, a combination of rheology and FT- IR spectroscopy was applied. First, the curing gel point was determined using oscillatory shear rheology. In thermoset systems, upon the cross-linking reaction the storage modulus (G') increases significantly, while the increase in loss modulus (G'') is less pronounced, as it is caused by the change in molecular weight.[47] The crossover point of storage and loss modulus is considered as the gel point representing the transition from a liquid to a solid system and, therefore the inception of the gelation process. An example of storage and loss modulus dependence over temperature in the studied lignin-based thermosets can be seen in Figure 1A. In general, the thiol-yne system was starting to cure at temperatures ranging between 105-115 °C (Figure 1B): P1000-based systems have slightly lower gel point than CLO-based systems, and P-4MS reactive diluent causes an increase in the gel point, which is especially noticeable in the TY_P-4MS_100% system. Based on these observations, 115 °C was selected as the curing temperature for all the resins for the time-resolved FT-IR studies. In Figure 2, an example of the IR spectra can be seen. The disappearance of alkyne and thiol bonds, at 3300 and 2572 cm^{-1}, respectively, provides an evidence of the reaction of those functional groups during the thiol-yne cross-linking reaction. It can be seen in Figure S6 (Appendix) that the reaction conversion reaches a plateau after 5 min, indicating the cross-linking reaction completion. Similar to a study by Jawerth *et al*. in lignin-based thermally cured thiol-ene, full conversion of the functional groups was not accomplished, which may be a result of a high cross-linking density in the already cured systems.[24] The addition of the reactive diluent, P-4MS, leads to improved conversion rates which may be associated to increased mobility and lower viscosity of the system caused by the presence of monomeric components. Additionally, in order to achieve even higher conversions, a post-curing strategy was investigated. Thermal post-curing at 150 °C was chosen to carry out the Claisen rearrangement reaction of remaining propargyl groups in lignin and to further enhance the chain mobility resulting in higher conversion and even higher cross-linking density.[31]
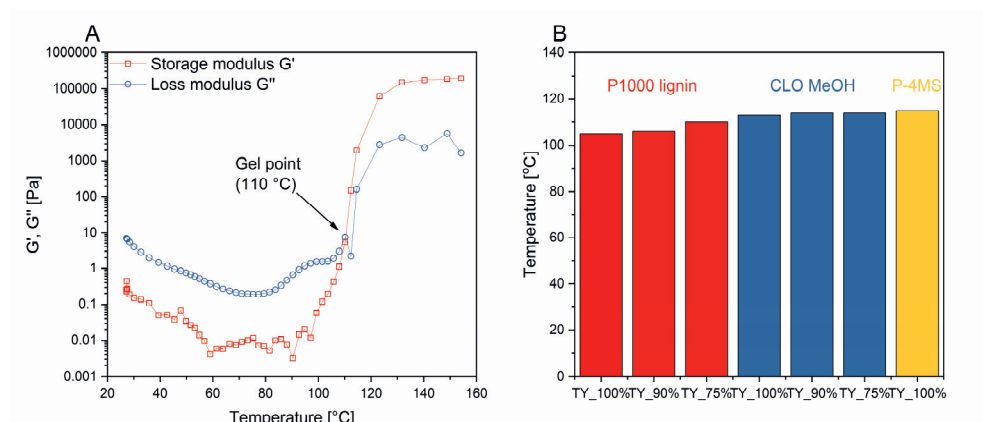
Figure 1 *A: Rheology of curing of thiol-yne resins (Example: P1000_75%), B: Summary of the rheological curing results*
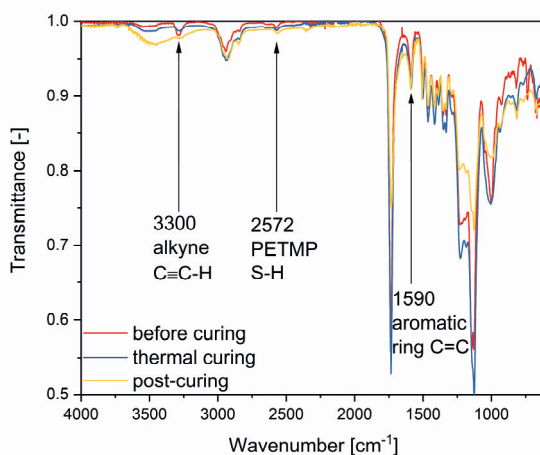

Figure 2 *Example of IR spectra before and after thermal curing and post-curing (example: P1000_75% resin)*

Lignin-based thermosets characterization and application testing

Once the curing parameters were optimized, the specimens were prepared in order to study the characteristics of such prepared thiol-yne networks. The findings are summarized in Table 3. In general, the thermal curing step leads to the alkyne conversion ranging between 65 and 92%, and it increased to 92-100% after the thermal post-curing step. These findings suggest that after the post-curing step, the network density further increased, which is also reflected in the increased insoluble fraction content (in acetone) and T_g. The insoluble fraction increases from 53-85% to 92-100% after post-curing. Unfortunately, there is no trend in how the monomeric reactive diluent influences the conversion and insoluble fraction content. T_g, on the

other hand, is closely related to the composition of the thermoset resin, as it can be seen in Figure 3. An increase in the monomeric reactive diluent content, P-4MS, leads to a decreased T_g. Additionally, lignin is known for its rigidity and it is not surprising to see that higher lignin loading in the network brings a higher T_g. For those lignin-based thermosets, the T_g is 21 °C and 13 °C for TY_P1000_100% and TY_CLO MeOH_100% networks, respectively, whereas for TY_P-4MS_100% networks the T_g is -7 °C. Upon thermal post-curing, the T_g increases by 30 to 40 °C for lignin-based networks and by 27 °C for PC_P-4MS_100% thermoset. In studies performed by Jawerth *et al*. with the thermally cross-linked lignin with a trifunctional thiol [trimethylolpropane tris(3-mercaptopropionate)] using thiol-ene chemistry, the resulting networks exhibited higher T_g (45-65 °C) compared to the ones presented in this study.[24] This phenomena may be associated with higher loading of the thiol used in the thiol-yne approach compared to the thiol-ene approach (46-55% vs. 35% of the resin mass) and another lignin type used in those studies which makes it difficult to make a fair comparison and draw solid conclusions.[24, 28, 48] It was reported that a higher thiol/ene ratio decreases the T_g of the networks indicating the plasticizing effect of the thiol on the network.[24] In both studies, lignin-based networks have a lower T_g than that in the lignin starting material. Thermal stability of the prepared lignin-based materials was evaluated by TGA (Figure S7, Appendix). There is a clear trend that lignin incorporation leads to improved thermal stability of the thermally cured thiol-yne networks increasing from $T_{5\% \text{ degradation}}$ of 120 °C for the TY_P-4MS_100% network, to 235 °C for the TY_P1000_100% thermoset. After post-curing, the thermal stability increases by 60-100 °C for lignin-based thermosets. The difference is more pronounced for networks containing more P-4MS, and the TY_P-4MS_100% improved by 126 °C after post-curing. The $T_{\text{max degradation}}$ ranges from 326 to 345 °C, and it is clearly neither related with the thermoset composition nor with the curing strategy, but rather with the intrinsic properties of the building components, such as lignin which is degrading at similar temperatures.

Additionally, the surface analysis performed by SEM-EDX mapping (Figure 4) shows that lignin and thiol cross-linker are homogeneously dispersed within PC_CLO MeOH_100% resin, with no visible lignin agglomerates. The following can be concluded based on the uniform distribution of sulfur within the cured network. However, in the picture certain porosity of the material can be observed. The observed bubbles originate from the AIBN decomposition during the initiation step when next to the initiator radicals, and molecular nitrogen gas is formed, which is trapped in resin upon curing.

Chapter 2

Table 3 Summary of the thermoset thermal properties

| Sample	Composition [wt.%]		Alkyne conversion [%]		Insoluble fraction [%]		T_g [°C]		$T_{5\%}$ degradation [°C]		T_{max} degradation [°C]	
	Lignin	*P-4MS*	TY	PC	TY	PC	TY	PC	TY	PC	TY	PC
P1000 100%	100	0	80	99	85	100	20.7	55.9	235	296	331	331
P1000 90%	90	10	92	96	83	92	16.1	42.6	215	292	331	332
P1000 75%	75	25	78	93	93	100	5.6	45.1	171	276	330	326
CLO MeOH 100%	100	0	98	100	53	99	12.5	42.2	211	270	345	331
CLO MeOH 90%	90	10	65	92	69	100	8.9	46.8	177	275	326	332
CLO MeOH 75%	75	25	82	93	70	97	10.2	42.7	177	270	326	327
P-4MS 100%	0	100	89	98	72	99	-7.0	19.5	120	246	336	325
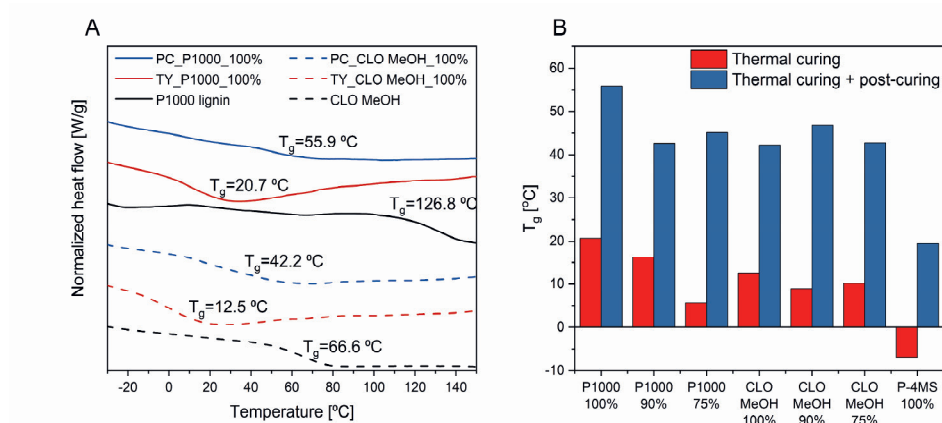
Figure 3 *A: Thermographs of the specimens and of the native lignin fraction (thermogravimetric analysis in nitrogen atmosphere at a heating rate of 10 °C/min), B: Summary of the T_g of the specimens with various amounts of the reactive diluent*
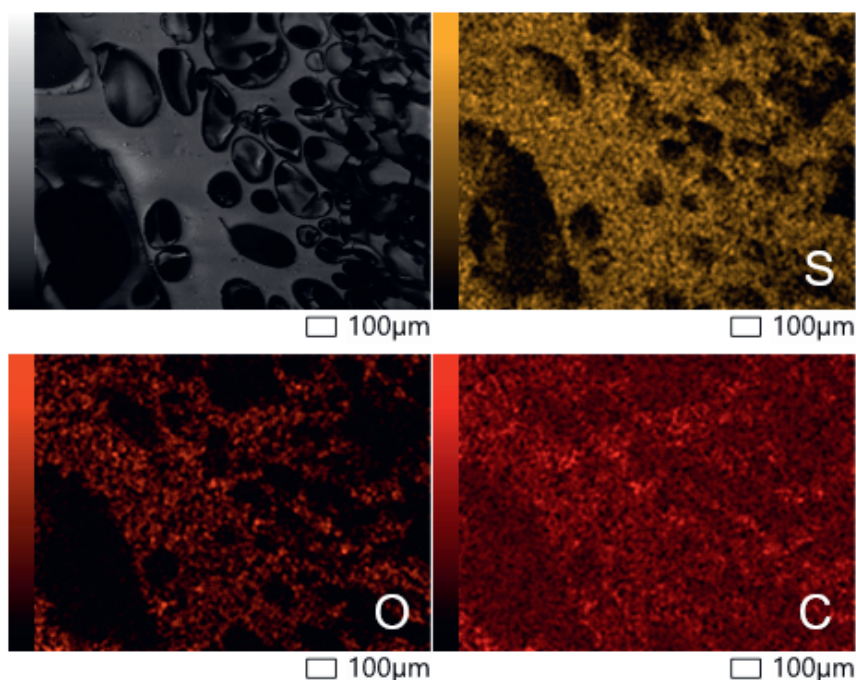
Figure 4 *SEM image and EDX mapping of PC_CLO MeOH_100% resin specimen*

In this study, next to the development of lignin-based thermosets, the proof-of-concept application as wood adhesive is demonstrated. For this purpose, the resin was applied between birch wood specimens and assembled in the hot press. Half of the samples were subjected to thermal post-curing to evaluate its effect. The performance was assessed based on lap-shear experiments according to ASTM D 5868 and compared with (PF) resin. Phenolic resins are one of the most applied types of wood adhesives because of their excellent performance, which makes them a great benchmark for lignin-based thermosets.[49] The findings are summarized in Figure 5. All lignin-based thermosets have the acceptable shear lap strength as required by the GB/T 14732-2006 National standard (>0.7 MPa).[17] All tested specimens exhibited cohesive type of adhesive bond failure, indicating very good interaction of cured resin with the surface. Compared with PF resins, all thiol-yne cured resins have worse performance in terms of tensile strength, but once they are thermally post-cured, their performance increased significantly and becomes similar or even better than PF resins. This is probably caused by the increased cross-linking density obtained after thermal post-treatment. The addition of P-4MS to the formulation led to maintained (CLO MeOH based-resins) or slightly decreased performance (P1000 based-resins) of the thermally cured resins, while after post-curing, the reactive diluent presence improved the adhesive strength in both cases. It may be partially associated with the T_g below room temperature of the

thermosets after thiol-yne curing, which decreases with the P-4MS content. The CLO MeOH series has slightly better performance than the P1000 series, which may be a result of lower molecular weight of the precursor. This phenomenon is often observed for phenolic resins, where lower molecular weight lignin causes a decrease in the application viscosity of the adhesive formulation and therefore improves the penetration in the wood.[18] This may also contribute to the better performance of the P-4MS-containing thermosets after post-curing. The thermoset based on P-4MS exhibits a performance similar to the PF resin once it is thermally post-cured.
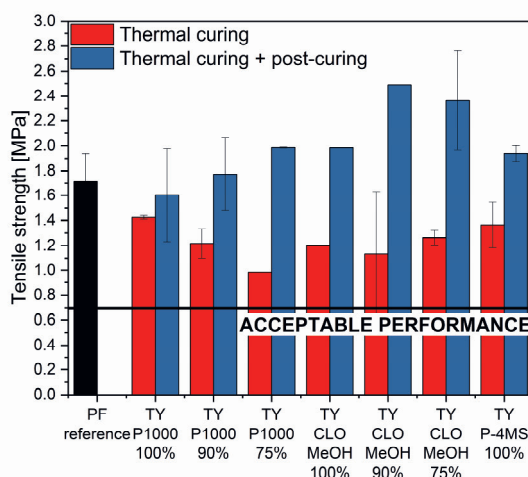
Figure 5 Tensile strength of the adhesive bond for cured and post-cured thiol-yne resins assessed by the lap-shear test according to the ASTM D 5868 standard test method

Conclusions

In this work, a proof-of-concept for novel, lignin-based thermoset resins suitable for the application as wood adhesives was developed. Their curing can be executed in two scenarios: as thermal thiol-yne curing with and without the post-curing via Claisen rearrangement. The post-curing improved the conversion and therefore properties of the thermosets due to the increased cross-linking density. Additionally, it was shown that the properties of the networks can be tuned by the selection of the curing scenario and the composition of the formulation (amount of reactive diluent, P-4MS). The presented resins show good performance in wood adhesive applications fulfilling the required specifications. The performance of the lignin-based thermosets was in a similar range or better than the PF reference resin. The outcome of this research contributes to the valorization of lignin as value-added application and extends the scope of possibilities for its utilization.

References

1.   Ferdosian, F.; Pan, Z.; Gao, G.; Zhao, B., Bio-Based Adhesives and Evaluation for Wood Composites Application. *Polymers* 2017, *9* (2), 1-29.

2.   Wang, H.; Gong, X.; Gong, J., Current and Future Challenges of Bio-Based Adhesives for Wood Composite Industries. In *Eco-Friendly Adhesives for Wood and Natural Fiber Composites: Characterization, Fabrication and Applications*, Jawaid, M.; Khan, T. A.; Nasir, M.; Asim, M., Eds. Springer Singapore: Singapore, 2021; pp 147-164.

3.   Kumar, R. N.; Pizzi, A., Thermosetting Adhesives Based on Bio-Resources for Lignocellulosic Composites. In *Adhesives for Wood and Lignocellulosic Materials*, Pizzi, R. N. K. a. A., Ed. 2019; pp 267-291.

4.   Vanholme, R.; Demedts, B.; Morreel, K.; Ralph, J.; Boerjan, W., Lignin Biosynthesis and Structure. *Plant Physiol.* 2010, *153* (3), 895-905.

5.   Figueiredo, P.; Lintinen, K.; Hirvonen, J. T.; Kostiainen, M. A.; Santos, H. A., Properties and chemical modifications of lignin: Toward lignin-based nanomaterials for biomedical applications. *Prog. Mater Sci.* 2018, *93*, 233-269.

6.   Kai, D.; Tan, M. J.; Chee, P. L.; Chua, Y. K.; Yap, Y. L.; Loh, X. J., Toward lignin-based functional materials in a sustainable world. *Green Chem.* 2016, *18* (5), 1175-1200.

7.   Liu, X.; Bouxin, F. P.; Fan, J.; Budarin, V. L.; Hu, C.; Clark, J. H., Recent Advances in the Catalytic Depolymerization of Lignin toward Phenolic Chemicals: A Review. *ChemSusChem* 2020, *13* (17), 4296-4317.

8.   Chio, C.; Sain, M.; Qin, W., Lignin utilization: A review of lignin depolymerization from various aspects. *Renewable Sustainable Energy Rev.* 2019, *107*, 232-249.

9.   Schutyser, W.; Renders, T.; Van den Bosch, S.; Koelewijn, S. F.; Beckham, G. T.; Sels, B. F., Chemicals from lignin: an interplay of lignocellulose fractionation, depolymerisation, and upgrading. *Chem. Soc. Rev.* 2018, *47* (3), 852-908.

10.   Wang, C.; Kelley, S. S.; Venditti, R. A., Lignin-Based Thermoplastic Materials. *ChemSusChem* 2016, *9* (8), 770-783.

11.   Zhao, S.; Abu-Omar, M. M., Materials Based on Technical Bulk Lignin. *ACS Sustain. Chem. Eng.* 2021, *9* (4), 1477-1493.

12.   Sun, Z.; Fridrich, B.; de Santi, A.; Elangovan, S.; Barta, K., Bright Side of Lignin Depolymerization: Toward New Platform Chemicals. *Chem. Rev.* 2018, *118* (2), 614-678.

13.   Jedrzejczyk, M. A.; Van den Bosch, S.; Van Aelst, J.; Van Aelst, K.; Kouris, P. D.; Moalin, M.; Haenen, G. R. M. M.; Boot, M. D.; Hensen, E. J. M.; Lagrain, B.; Sels, B. F.; Bernaerts, K. V., Lignin-Based Additives for Improved Thermo-Oxidative Stability of Biolubricants. *ACS Sustain. Chem. Eng.* 2021, *9* (37), 12548-12559.

14.   Zhao, M.; Jing, J.; Zhu, Y.; Yang, X.; Wang, X.; Wang, Z., Preparation and performance of lignin–phenol–formaldehyde adhesives. *Int. J. Adhes. Adhes.* 2016, *64*, 163-167.

15.   Pang, B.; Yang, S.; Fang, W.; Yuan, T.-Q.; Argyropoulos, D. S.; Sun, R.-C., Structure-property relationships for technical lignins for the production of lignin-phenol-formaldehyde resins. *Ind. Crops Prod.* 2017, *108*, 316-326.

16.   Younesi-Kordkheili, H.; Pizzi, A., A Comparison among Lignin Modification Methods on the Properties of Lignin-Phenol-Formaldehyde Resin as Wood Adhesive. *Polymers* 2021, *13* (20), 3502.

17.   Kalami, S.; Arefmanesh, M.; Master, E.; Nejad, M., Replacing 100% of phenol in phenolic adhesive formulations with lignin. *J. Appl. Polym. Sci.* 2017, *134* (30), 45124-45133.

18.   Kalami, S.; Chen, N.; Borazjani, H.; Nejad, M., Comparative analysis of different lignins as phenol replacement in phenolic adhesive formulations. *Ind. Crops Prod.* 2018, *125*, 520-528.

19.   Sternberg, J.; Sequerth, O.; Pilla, S., Green chemistry design in polymers derived from lignin: review and perspective. *Prog. Polym. Sci.* 2021, *113*, 101344-101348.

20.   Buono, P.; Duval, A.; Avérous, L.; Habibi, Y., Clicking Biobased Polyphenols: A Sustainable Platform for Aromatic Polymeric Materials. *ChemSusChem* 2018, *11* (15), 2472-2491.

Chapter 2

21.   Panovic, I.; Montgomery, J. R. D.; Lancefield, C. S.; Puri, D.; Lebl, T.; Westwood, N. J., Grafting of Technical Lignins through Regioselective Triazole Formation on β-O-4 Linkages. *ACS Sustain. Chem. Eng.* 2017, *5* (11), 10640-10648.

22.   Yuan, L.; Zhang, Y.; Wang, Z.; Han, Y.; Tang, C., Plant Oil and Lignin-Derived Elastomers via Thermal Azide–Alkyne Cycloaddition Click Chemistry. *ACS Sustain. Chem. Eng.* 2018, *7* (2), 2593-2601.

23.   Duval, A.; Lange, H.; Lawoko, M.; Crestini, C., Reversible crosslinking of lignin via the furan–maleimide Diels–Alder reaction. *Green Chem.* 2015, *17* (11), 4991-5000.

24.   Jawerth, M.; Johansson, M.; Lundmark, S.; Gioia, C.; Lawoko, M., Renewable Thiol–Ene Thermosets Based on Refined and Selectively Allylated Industrial Lignin. *ACS Sustain. Chem. Eng.* 2017, *5* (11), 10918-10925.

25.   Liu, H.; Chung, H., Visible-Light Induced Thiol–Ene Reaction on Natural Lignin. *ACS Sustain. Chem. Eng.* 2017, *5* (10), 9160-9168.

26.   Ribca, I.; Jawerth, M. E.; Brett, C. J.; Lawoko, M.; Schwartzkopf, M.; Chumakov, A.; Roth, S. V.; Johansson, M., Exploring the Effects of Different Cross-Linkers on Lignin-Based Thermoset Properties and Morphologies. *ACS Sustain. Chem. Eng.* 2021, *9* (4), 1692-1702.

27.   Jawerth, M.; Lawoko, M.; Lundmark, S.; Perez-Berumen, C.; Johansson, M., Allylation of a lignin model phenol: a highly selective reaction under benign conditions toward a new thermoset resin platform. *RSC Advances* 2016, *6* (98), 96281-96288.

28.   Jawerth, M. E.; Brett, C. J.; Terrier, C.; Larsson, P. T.; Lawoko, M.; Roth, S. V.; Lundmark, S.; Johansson, M., Mechanical and Morphological Properties of Lignin-Based Thermosets. *ACS Appl. Polym. Mater.* 2020, *2* (2), 668-676.

29.   Buono, P.; Duval, A.; Averous, L.; Habibi, Y., Lignin-Based Materials Through Thiol-Maleimide "Click" Polymerization. *ChemSusChem* 2017, *10* (5), 984-992.

30.   Jin, C.; Zhang, X.; Xin, J.; Liu, G.; Wu, G.; Kong, Z.; Zhang, J., Clickable Synthesis of 1,2,4-Triazole Modified Lignin-Based Adsorbent for the Selective Removal of Cd(II). *ACS Sustain. Chem. Eng.* 2017, *5* (5), 4086-4093.

31.   Sen, S.; Sadeghifar, H.; Argyropoulos, D. S., Kraft Lignin Chain Extension Chemistry via Propargylation, Oxidative Coupling, and Claisen Rearrangement. *Biomacromolecules* 2013, *14* (10), 3399-3408.

32.   Wang, M.; Yang, L., Lignin Functionalized by Thermally Curable Propargyl Groups as Heat-Resistant Polymeric Material. *J. Polym. Environ.* 2012, *20* (3), 783-787.

33.   Sadeghifar, H.; Sen, S.; Patil, S. V.; Argyropoulos, D. S., Toward Carbon Fibers from Single Component Kraft Lignin Systems: Optimization of Chain Extension Chemistry. *ACS Sustain. Chem. Eng.* 2016, *4* (10), 5230-5237.

34.   van Baarle, D. Vertoro scales up oil production from lignin. https://www.industryandenergy.eu/biobased-economy/vertoro-scales-up-oil-production-from-lignin/ (accessed 01.07.2021).

35.   Kouris, P. D.; Boot, M. D.; Hensen, E. J. M.; Oevering, H. A method for obtaining a stable lignin: polar organic solvent composition via mild solvolytic modifications. WO/2019/053287, 2019.

36.   Kouris, P. D.; van Osch, D. J. G. P.; Cremers, G. J. W.; Boot, M. D.; Hensen, E. J. M., Mild thermolytic solvolysis of technical lignins in polar organic solvents to a crude lignin oil. *Sustainable Energy Fuels* 2020, *4* (12), 6212-6226.

37.   Jedrzejczyk, M. A.; Engelhardt, J.; Djokic, M. R.; Bliznuk, V.; Van Geem, K. M.; Verberckmoes, A.; De Clercq, J.; Bernaerts, K. V., Development of Lignin-Based Mesoporous Carbons for the Adsorption of Humic Acid. *ACS Omega* 2021, *6* (23), 15222-15235.

38.   Chen, Y. F., Charles R.; Cai, Zhiyong; Lorenz, Linda F.; Stark, Nicole M. In *Lignin-based Phenol-Formaldehyde Resins from Purified CO_2 Precipitated Kraft lignin (PCO_2KL)*, International Conference on Wood Adhesives, Toronto, Ontario, Canada, October 9-11; Toronto, Ontario, Canada, 2013; pp 601-610.

39.   Korntner, P.; Sumerskii, I.; Bacher, M.; Rosenau, T.; Potthast, A., Characterization of technical lignins by NMR spectroscopy: optimization of functional group analysis by 31P NMR spectroscopy. *Holzforschung* 2015, *69* (6), 807-814.

40.   Gosselink, R. J. A.; Abächerli, A.; Semke, H.; Malherbe, R.; Käuper, P.; Nadif, A.; van Dam, J. E. G., Analytical protocols for characterisation of sulphur-free lignin. *Ind. Crops Prod.* 2004, *19* (3), 271-281.

41.   Sadeghifar, H.; Ragauskas, A., Perspective on Technical Lignin Fractionation. *ACS Sustain. Chem. Eng.* 2020, *8* (22), 8086-8101.

42.   Passoni, V.; Scarica, C.; Levi, M.; Turri, S.; Griffini, G., Fractionation of Industrial Softwood Kraft Lignin: Solvent Selection as a Tool for Tailored Material Properties. *ACS Sustain. Chem. Eng.* 2016, *4* (4), 2232-2242.

43.   Jiang, X.; Abbati de Assis, C.; Kollman, M.; Sun, R.; Jameel, H.; Chang, H.-m.; Gonzalez, R., Lignin fractionation from laboratory to commercialization: chemistry, scalability and techno-economic analysis. *Green Chem.* 2020, *22* (21), 7448-7459.

44.   Brebu, M.; Vasile, C., Thermal degradation of lignin – A Review. *Cellul. Chem. Technol.* 2010, *44*, 353-363.

45.   Watkins, D.; Nuruddin, M.; Hosur, M.; Tcherbi-Narteh, A.; Jeelani, S., Extraction and characterization of lignin from different biomass resources. *J. Mater. Res. Technol.* 2015, *4* (1), 26-32.

46.   Koivu, K. A. Y.; Sadeghifar, H.; Nousiainen, P. A.; Argyropoulos, D. S.; Sipilä, J., Effect of Fatty Acid Esterification on the Thermal Properties of Softwood Kraft Lignin. *ACS Sustain. Chem. Eng.* 2016, *4* (10), 5238-5247.

47.   Dörr, D.; Kuhn, U.; Altstädt, V., Rheological Study of Gelation and Crosslinking in Chemical Modified Polyamide 12 Using a Multiwave Technique. *Polymers* 2020, *12* (4), 855-865.

48.   Lowe, A. B., Thiol-yne "click"/coupling chemistry and recent applications in polymer and materials synthesis and modification. *Polymer* 2014, *55* (22), 5517-5549.

49.   Yang, W.; Jiao, L.; Wang, X.; Wu, W.; Lian, H.; Dai, H., Formaldehyde-free self-polymerization of lignin-derived monomers for synthesis of renewable phenolic resin. *Int. J. Biol. Macromol.* 2021, *166*, 1312-1319.

Chapter 2

Appendix for Chapter 2
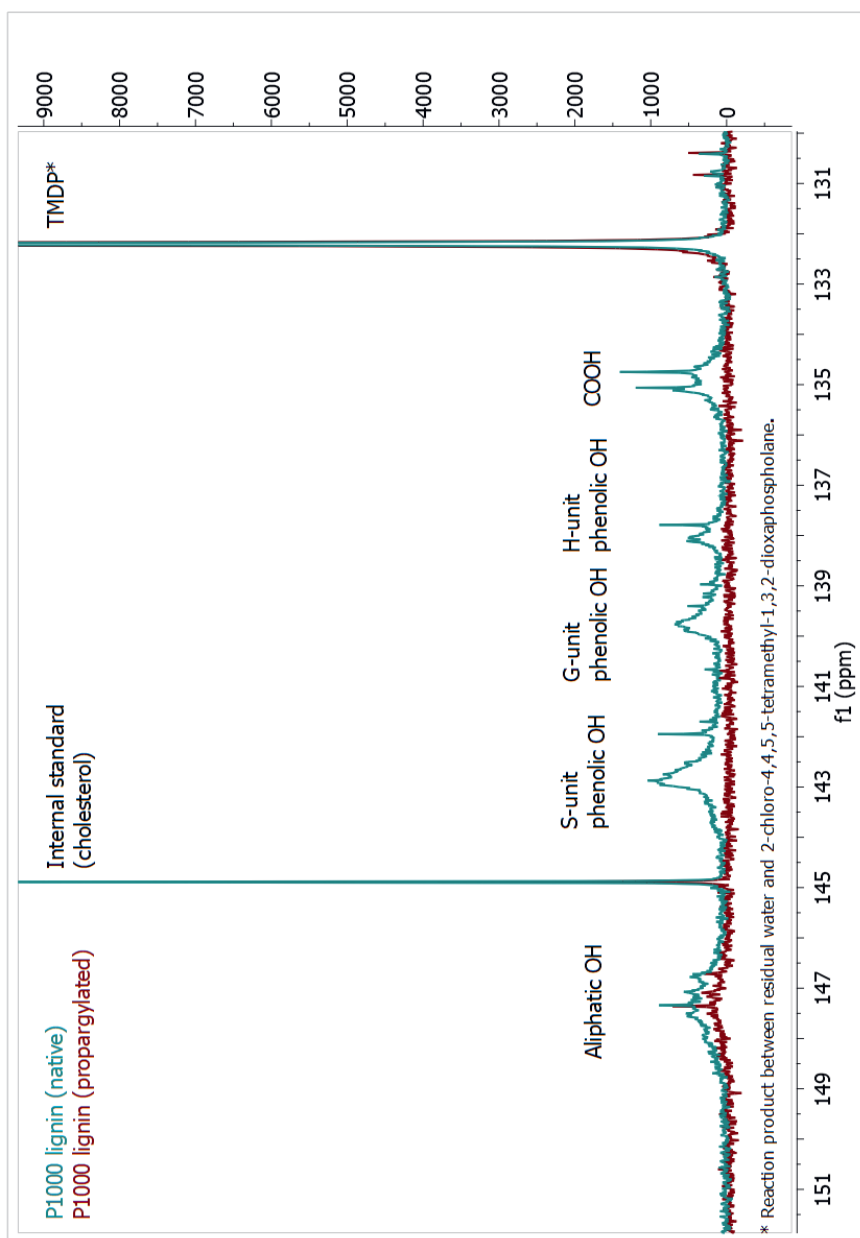
Figure S1 *Example of ^{31}P NMR spectra (in CDCl$_3$) before and after propargylation of P1000 lignin*
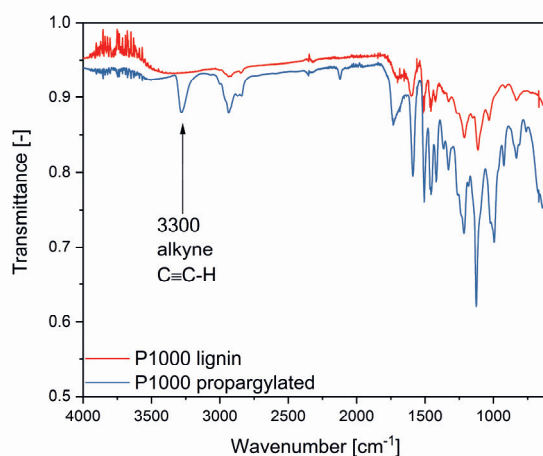
Figure S2 *Example of FT-IR spectra before and after propargylation of P1000 lignin*
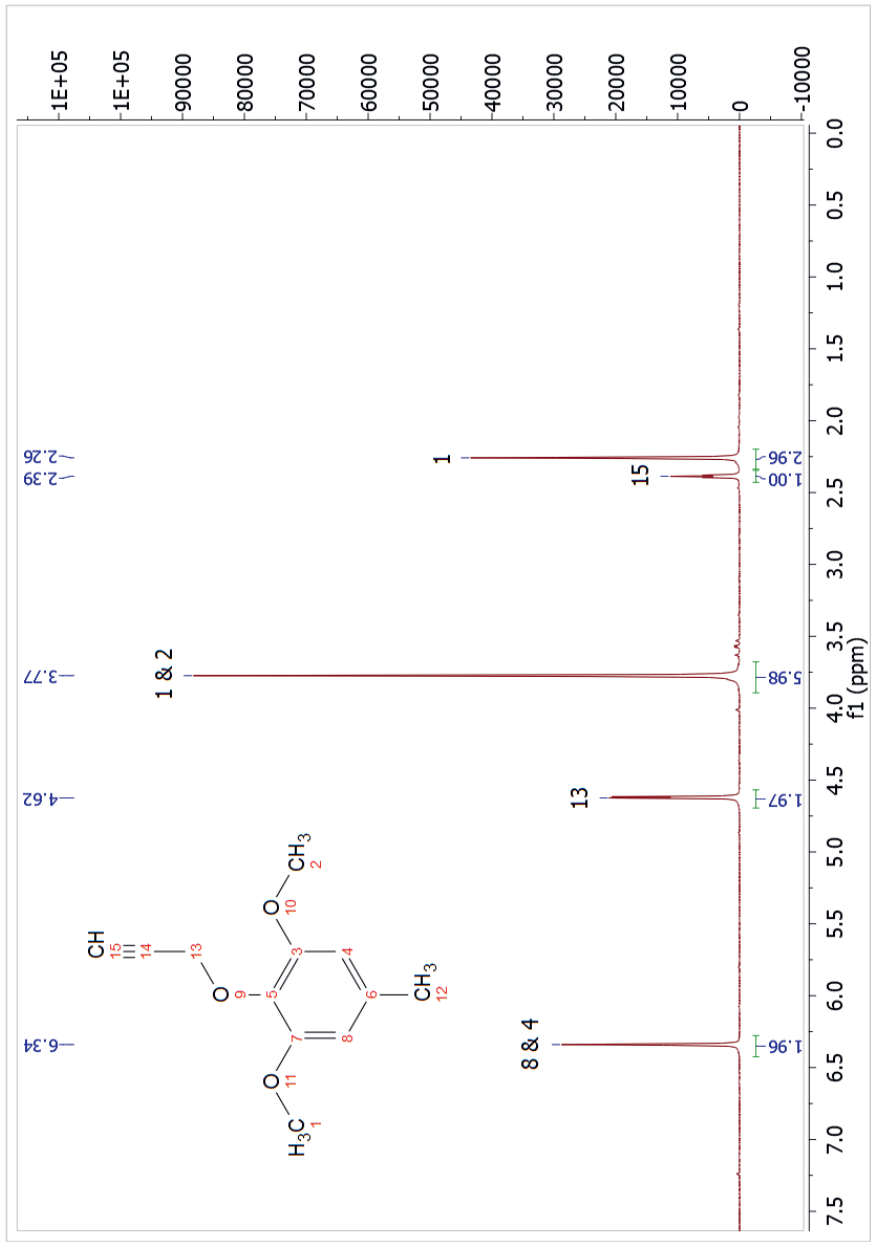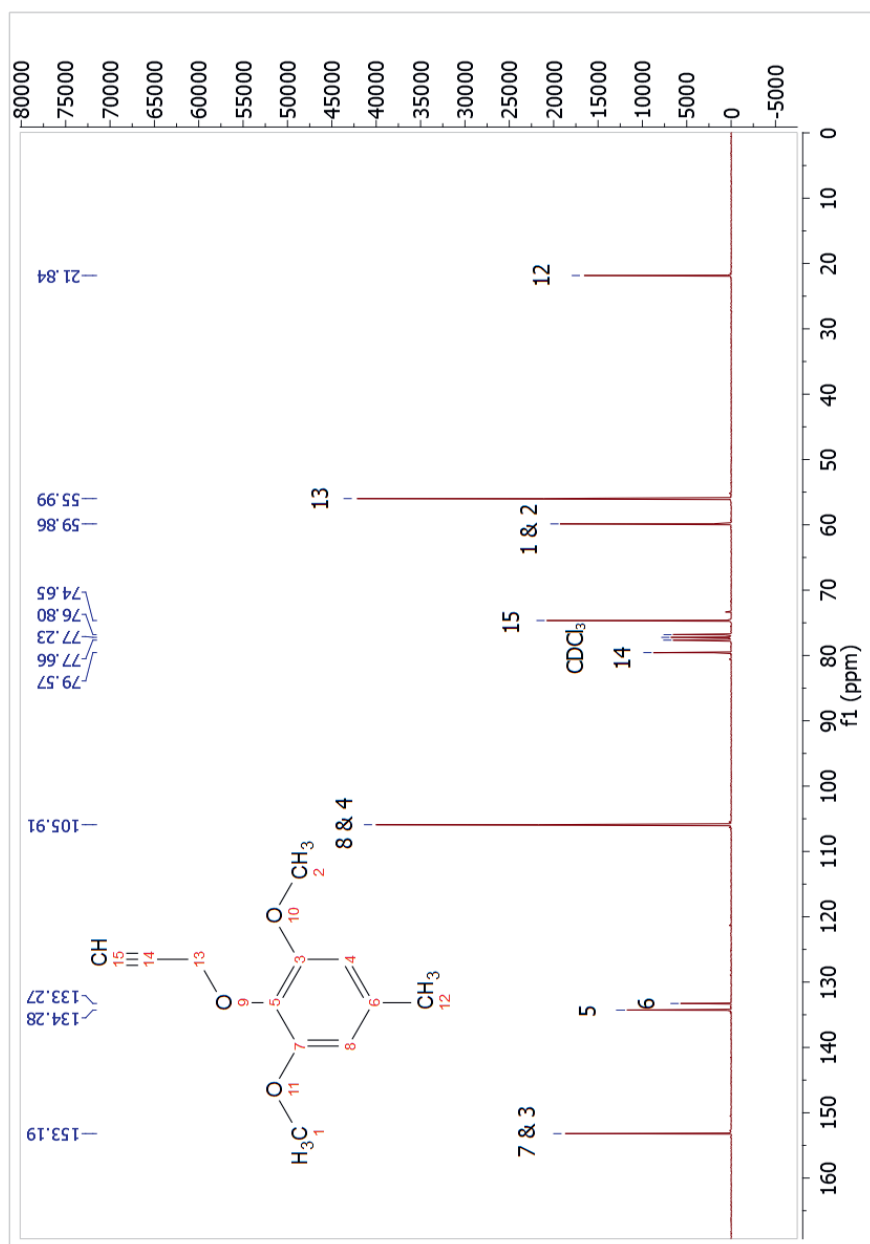
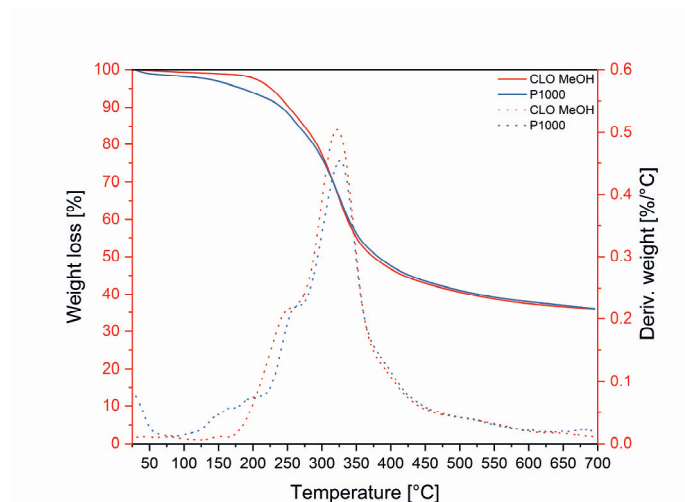**Figure S3** ^1H NMR spectrum (in CDCl$_3$) of propargylated 4-methylsyringol (P-4MS)

*Figure S4* ^{13}*C NMR spectrum (in CDCl$_3$) of propargylated 4-methylsyringol (P-4MS)*

Figure S5 *Thermographs of P1000 lignin and CLO MeOH (thermogravimetric analysis in nitrogen atmosphere at a heating rate of 10 °C/min), weight loss is displayed as a solid line, derivative of weight loss is displayed as a dotted line*
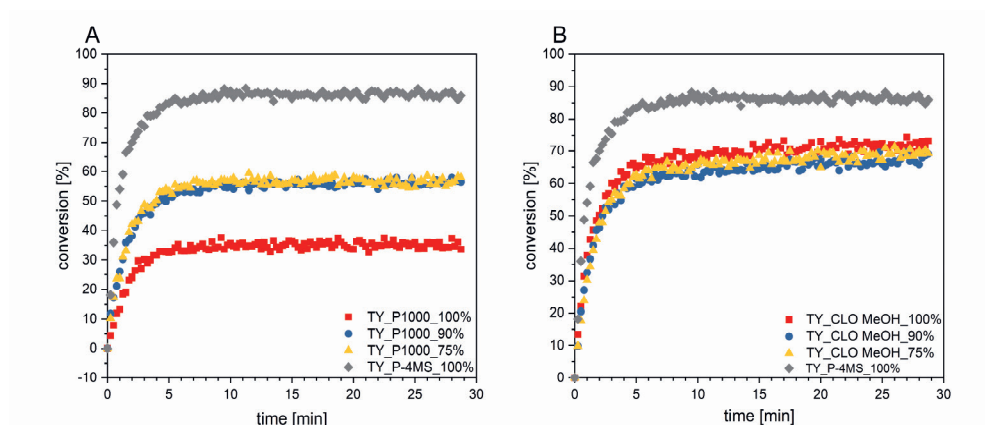
Figure S6 *FT-IR curing kinetic studies of the thiol-yne resins with various amounts of reactive diluent at 115ºC. A: P1000 resins series, B: CLO MeOH resins series*
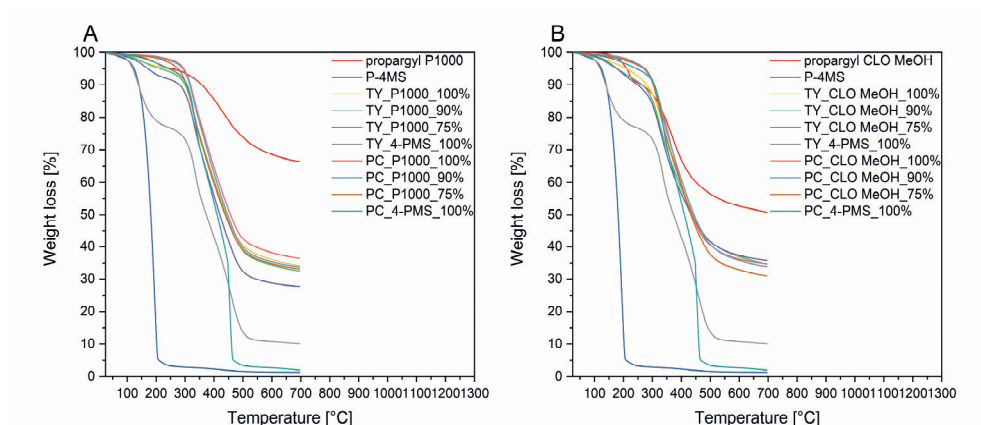
Figure S7 *Thermographs of P1000 lignin thiol-yne resins (thermogravimetric analysis in nitrogen atmosphere at a heating rate of 10 °C/min), propargylated lignin and P-4MS for A: P1000 resins series, B: CLO MeOH resins series*

Chapter 2

3

Preparation of renewable thiol-yne "click" networks based on fractionated lignin for anticorrosive protective film applications
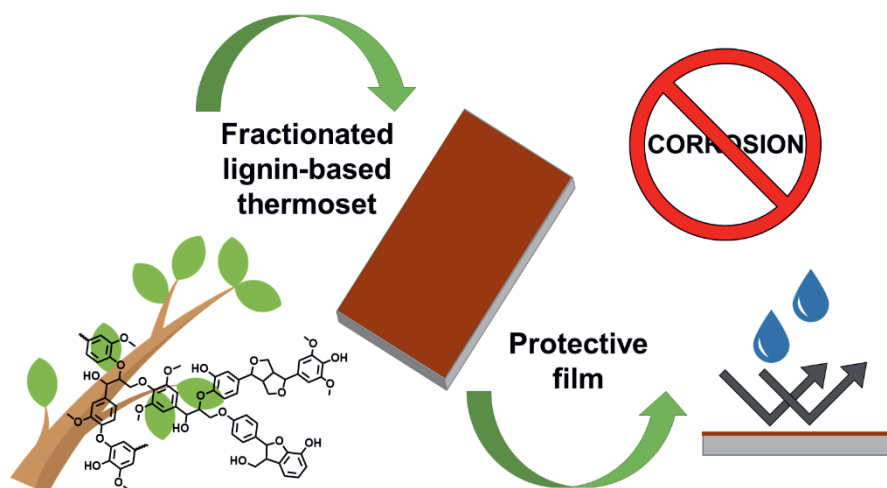
The synthesis of novel, renewable lignin-based protective films with anticorrosive properties is presented in this chapter. Thermosetting films are prepared by means of tandem UV-initiated thiol-yne "click" synthesis and Claisen rearrangement strategy. These films contain high lignin loading, 46-61%, originating from a birch wood reductive catalytic fractionation process using a nickel catalyst. Lignin fractions with varying monomer content are compared before resins preparation, namely a mixture of monomers and oligomers without fractionation, or after fractionation via extraction and membrane separation. The goal is to determine if separation of lignin monomers and oligomers is necessary for the application as a thermosetting resin. The resulting protective films exhibit remarkable adhesion to a steel surface and excellent solvent resistance, even after exposure to a corrosive environment. Moreover, those films show superior barrier properties, studied with Odd Random Phase Electrochemical Impedance Spectroscopy. After 21 days of exposure, the examined films still show impressive high corrosion protection with the low frequency impedance around 10^{10} Ωcm^2 and capacitive behavior. This work demonstrates a proof-of-concept where laborious, costly, and energy-intensive separation of the depolymerized lignin mixture is not necessary for successful resin synthesis with excellent properties using the applied synthetic strategy.

Introduction

In light of the proceeding climate change, more and more attention is being paid to the transition toward a circular and sustainable chemical industry, which is based on natural resources instead of fossil fuels.[1] One of the platform materials suitable for this purpose is lignin, originating from lignocellulosic biomass, which is not competing with food production.[2] Currently, the majority of almost 90 million metric tons of lignin produced each year is used for energy with only 2% used for added-value applications.[3] There is a great potential to increase this number, as lignin is known to have unique properties, such as antioxidant, UV-blocking, and antimicrobial properties, among others, thanks to its polyphenolic structure.

There are multiple applications in which lignin can be incorporated: adhesives, coatings, dispersants, additives, chemical products such as benzene-toluene-xylene (BTX) and vanillin, lignin-based polymers, and carbon materials.[3-6] An application on which we focus in this work is in the field of coatings, which can be used to protect metal surfaces against corrosion. It is a topic of great importance due to the widespread use of metallic substrates, which require appropriate protection to extend their safe lifespan and limit environmental pollution. Lignin has been reported in corrosion protection applications, and it can be incorporated in various ways: either as a corrosion inhibitor used in solution,[7-9] as a deposited layer on a coating surface,[10, 11] as a part of a polymeric blend applied on a metal surface,[10] or as a part of a resin used as a protective, anticorrosive coating.[10] Although lignin applied directly on the metal surface provides corrosion inhibition because of the formation of a lignin-metal complex, it lacks long-term corrosion inhibition in aggressive conditions, which may limit its use.[10] Therefore, in this work, we concentrate on the use of lignin integrated in the resin of protective coatings.

There are some state-of-the-art examples where lignin was incorporated in protective, anticorrosive coatings. Lignin can become part of the coating formulation in multiple ways, including being part of the cross-linked thermoset composition,[12-15] as an additive in a thermoplastic system,[16, 17] deposited on the metal surface as such,[18, 19] or lignin can be used as an anticorrosive additive.[20] In this research, lignin is incorporated in the coating formulation as a component of the thermoset resin, and for that reason, only the examples of works where lignin is a part of the thermoset resin are further described.

The work of Cao *et al*. has shown an example where lignin was incorporated in the preparation of thermosetting polyurethane anticorrosive coatings.[13] Enzymatic hydrolysis lignin used in that study was modified in order to increase the OH content and the resulting lignin-based polyol was later cross-linked with hexamethylene diisocyanates to fabricate polyurethane films and coatings with high lignin-based

polyol (up to 55%) content. The resulting coatings exhibited corrosion resistance with good long-term stability, up to 40 days. Another example is the work of Fang *et al*., in which polyurea coatings containing up to 30% polyetheramine-grafted lignin, exhibited corrosion resistance, and excellent UV-aging properties were demonstrated.[14] Carlos de Haro *et al.* described silanized lignin cross-linked films by tetraethylorthosilicate.[12] In that study, the silanized lignin loading was very high, 95%, and the resulting cross-linked, hydrophobic film showed good adhesion and corrosion inhibition properties on aluminum surfaces. Ding *et al*. showed that epoxidized lignin can improve the corrosion resistance of epoxy coatings.[15] Unfortunately, only the addition below 2% of epoxidized lignin resulted in good compatibility with the epoxy resin and resulted in good quality metal coatings.

The novelty of our approach lies in not only an alternative approach with respect to the applied protective film chemistry (tandem thiol-yne "click" chemistry and Claisen rearrangement, Figure 1), but also in the lignin sourcing and fractionation. This work presents a proof-of-concept for using the depolymerized lignin monomers and oligomer mixture as such without fractionation for resin synthesis and benchmarks its usability with lignin oligomeric fractions separated via either extraction or membrane separation. The anticorrosive performance and some basic film properties of the resulting lignin-based thermoset resins are studied as well.
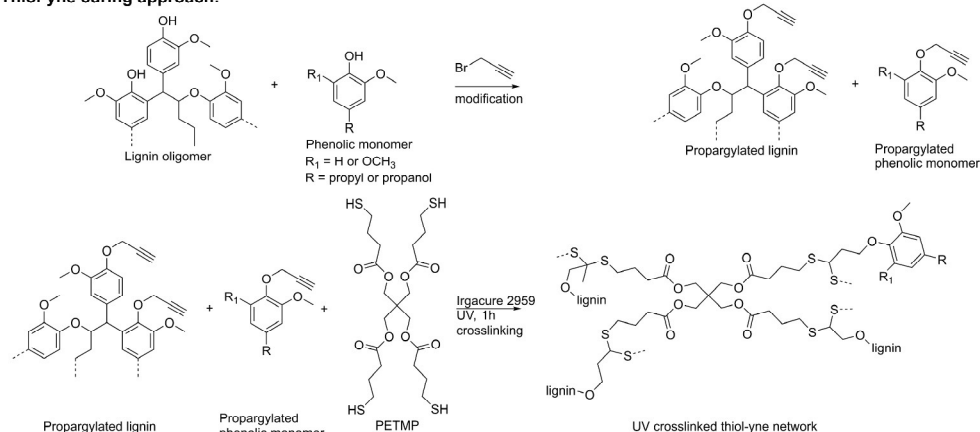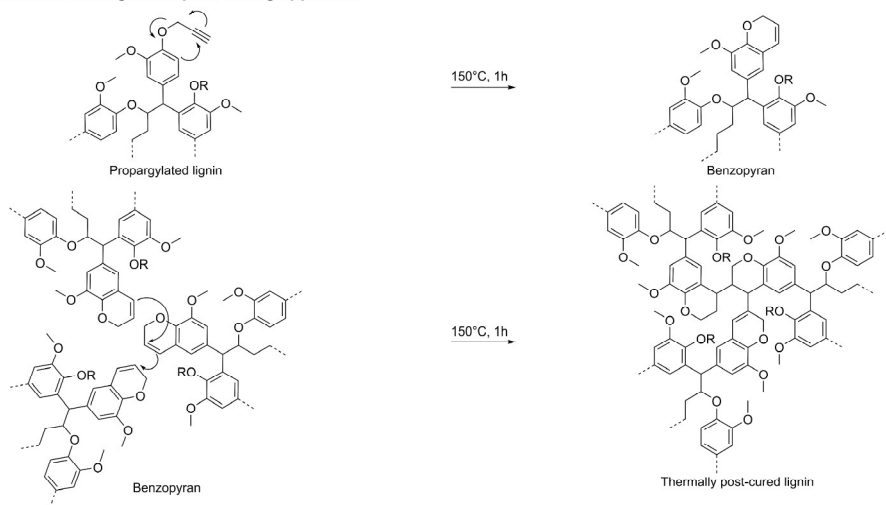
Chapter 3

Thiol-yne curing approach:

Claisen rearrangement post-curing approach:

Figure 1 *Synthetic approach for lignin-based protective films via tandem UV-initiated thiol-yne chemistry and Claisen rearrangement*

Experimental Section

Materials

The chemicals were obtained from TCI, Acros, Alfa Aesar, Biosolve, Sigma Aldrich, Cambridge isotopes, SAFC Global, VWR, and Honeywell. 2-Chloro-4,4,5,5-tetramethyl-1,3,2-dioxaphospholane (>95%), cholesterol (>99%), and chromium(III)acetylacetonate (>97%) were obtained from TCI. 2-Hydroxy-4′-(2-hydroxyethoxy)-2-methylpropiophenone (Irgacure 2959, 98%), dry pyridine (99.8%), and pentaerythritol tetrakis(3-mercaptopropionate) (PETMP, >95%) were obtained from Sigma Aldrich. 2-Methyltetrahydrofuran

(2-MeTHF, 99+%), N-methyl-N-(trimethylsilyl)trifluoroacetamide (≥98.5%), potassium carbonate (99+%), potassium iodide (99+%), propargyl bromide (80% weight in toluene), and pyridine (≥99.8%) were obtained from Acros. 4-Methylcatechol (>97%), 4-methylguaiacol (>97%), and 4-methylsyringol (>97%) were obtained from Alfa Aesar. 2-Isopropylphenol (≥98%) was obtained from SAFC Global. Methanol was purchased from VWR. Acetone (99.8%), dichloromethane (DCM, 99.8%), ethyl acetate (99.8%), and *n*-hexane (>95%) were obtained from Biosolve. *d*-Chloroform (99.88%) was obtained from Cambridge isotopes. Sodium hydroxide (≥98%) was obtained from Honeywell. All chemicals were used as received. Cold-rolled steel Q-panels (R-46) were obtained from Benelux Scientific BV. Kimtech science delicate task wipes were used to clean the steel panels. 3M polyester tape 8402 used in corrosion studies was bought from Hoffmann Group. The tubular ceramic membrane 0.9 nm TiO_2 was purchased at Inopor and modified by VITO's proprietary grafting method (FunMem). The ceramic membrane was a 1-channel tube with an active titania top layer at the lumen side, an outer diameter of 10 mm, an inner diameter of 7 mm and a length of 10 cm, providing a surface area of approx. 25 cm².

Methods

Lignin depolymerization by Reductive Catalytic Fractionation (RCF)

The depolymerized lignin fraction, namely BN_mixture, was obtained by RCF of lignocellulose biomass.[21-23] The RCF experiment was performed in a 2 L stainless steel batch reactor (Parr Instruments & Co.). 150 g of birch wood chips, milled with a Retsch cutting mill with a 2 mm screen, was loaded into the reactor, together with 15.0 g Ni/SiO_2 and 800 mL methanol. Subsequently, the reactor was sealed, flushed three times with nitrogen gas (10 bar), and then pressurized with hydrogen gas (30 bar at room temperature). Next, the reaction mixture was stirred (750 rpm) and simultaneously heated to 235 °C (~30 min heating time). After a reaction time of 3 h, the reactor was cooled and depressurized at room temperature. The reactor contents were quantitatively collected by washing the reactor with ethanol. The solid pulp was separated by filtration and washed thoroughly with ethanol. Next, the standard protocol for the separation of carbohydrates, monomers, and lignin oligomers was applied.[24] The resulting filtrate was evaporated and a brown oil was obtained, which was solubilized in dichloromethane (DCM) and subjected to liquid-liquid extractions using DCM and water: per 1 equiv of DCM 4 equiv of water were used, after DCM fraction was separated and the aqueous fraction was extracted with fresh DCM three times in total. To obtain the RCF lignin oil, these combined DCM-extracted phases were evaporated and dried in an oven at 80 °C.

Chapter 3

Lignin fractionation via extraction

BN_mixture obtained according to the procedure described above was subjected to the separation of monomers, dimers and oligomers via extraction. This BN_mixture lignin oil (1 gram equiv) was fourfold extracted with a mixture of hexane (3 mL equiv) for 30 min at 80 °C.[24] After each extraction, the soluble hexane phase was removed and fresh hexane was added. The residue after the four hexane extractions was obtained after drying in a vacuum oven at 80 °C.

Lignin fractionation via membrane separation

The nanofiltration trials were carried out on a bench-top stainless steel high-pressure cross-flow filtration unit, consisting of a temperature-controlled feed tank (capacity of approx. 1 L), a magnetically driven circulation pump (type D-10, Hydra-Cell, USA) with max. feed flow of approximately 800 L/h, a suitable in-house constructed membrane housing and fitted with pressure and temperature transducers. Nitrogen gas was used for pressurization. Approximately 95 mL of BN_mixture in methanol (50/50 wt.%) was received and diluted to 750 mL in methanol. The filtration tests were carried out in batch mode, at a cross flow velocity of approx. 2 ms^{-1}, a temperature of 25 °C and transmembrane pressures of 10 bar. The proprietary ceramic membrane was selected for trials in diafiltration mode. Approximately 2 to 5 diavolumes (DV) of methanol were added to 750 mL feed on a constant volume basis by means of a volumetric metering pump (ProMinent, type Delta, ProMinent Belgium N.V.) and a level switch on the feed tank. Permeate and retentate samples were taken at regular intervals during diafiltration. The retentate sample was drained from the filtration unit and coded as BN_membrane.

Lignin modification

Propargylation of lignin was performed according to the procedure similar to the one described by Sen *et al.*.[25] A total of 7.00 g (1 equiv, 45.4 mmol OH groups) of solvent-free BN_mixture lignin fraction was dissolved in 110 mL NaOH (0.5 M) at room temperature under stirring in a nitrogen atmosphere. Next, the mixture was heated up to 80 °C and 25 mL (5 equiv, 226.8 mmol) of 80% propargyl bromide in toluene was added to the reaction mixture. The reaction was performed for 24 h at 85 °C under nitrogen flow. After 24 hours, the reaction mixture was extracted with 200 mL of 2-methyltetrahydrofuran. The organic layer was then washed with 200 mL brine twice. The organic layer was dried over magnesium sulfate before 2-MeTHF was evaporated. The product was dried in vacuo at 80 °C overnight. The yield was 5.10 g (56%) of black oil. The same procedure was applied for the modification of BN_extracted and BN_membrane lignin fractions.

Preparation of the protective films

To a 10 mL vial 1.50 g (7.28 mmol propargyl moiety, 1 equiv) of propargylated BN_mixture was added, followed by the addition of 1.78 g (3.64 mmol, 0.5 equiv) of

PETMP and 3.3 mg (0.1% wt) of Irgacure 2959. To this mixture 2 mL of acetone was added in order to dissolve all the components end ensure good homogeneity of the resin. Then, the solvent was evaporated and the resin was flushed with nitrogen for 30 min. The steel Q-panels (R-46) were cleaned thoroughly by rinsing them with acetone, wiping with a dust-free optical lens cleaning wipe, and drying with a heat gun prior to formulation application. A 30 μm thick formulation layer was applied on the steel Q-panel (R-46) using a bar coater (3520, Elcometer). The plate was cured in an Analytik Jena UV curing system (equipped with UVP 3UV 8 Watt lamp, 365 nm wavelength) for two hours at 10 cm distance from the lamp, under a nitrogen flow. After 2 h, the plate was post-cured in a Memmert UF55 oven for 1 h at 150 °C. The same procedure was applied for BN_extracted and BN_membrane protective films.

Films conditioning in a corrosive environment

All coated metal (steel) panels were cut in half and one half was conditioned in the corrosive environment (3.5% NaCl) and the other half was used as a reference. In order to determine films performance and resistance to a corrosive environment, all coated metal panels were secured with 3M polyester tape and submerged in 3.5% sodium chloride solution for 7 days. Afterward, the following properties of the cured film on the steel substrate were evaluated: cross-cut adhesion (ISO 2409) and MEK solvent resistance via the MEK double rub test with a cotton swab (ASTM D5402).

Characterization

Samples before and after propargylation were measured by GC to determine the monomer content in the lignin fractions using the procedure described by Van Aelst *et al.*[23] Therefore, a weighed amount of external standard (2-isopropylphenol; ~20 mg) was added to a GC-vial containing a weighed amount of lignin (~40 mg). Subsequently, 0.3 mL of pyridine and 0.3 mL of N-methyl-N-(trimethylsilyl)trifluoroacetamide were added, next to 0.6 mL of acetonitrile. The vial was sealed and put in an oven at 80 °C for 30 min. Afterward, the samples were analyzed on a gas chromatograph (Agilent 6890 series) equipped with an HP5 column and a flame ionization detector (FID). The following operating conditions were used: injection temperature of 300 °C, column temperature program: 50 °C (1 min), 15 °C/min to 150 °C, 10 °C/min to 300 °C (12 min), with a detection temperature of 300 °C. Sensitivity factors of the products were obtained by calibration with commercial standards or estimated, based on effective carbon number (ECN) calculations or trends within the response factors (RF's) of commercial standards.

The aromatic and aliphatic hydroxyl groups as well as the carboxylic acids (before and after modification) of lignin were determined by ^{31}P NMR spectroscopy after sample derivatization, according to the method described by Korntner *et al.*[26] 10 mg

of dried (in a vacuum oven at 80 °C, overnight), lignin-based material was dissolved in 500 μL anhydrous pyridine and deuterated chloroform mixture (1.6:1, v:v). Then, 100 μL of internal standard solution, cholesterol (19.7 mg/mL in anhydrous pyridine and deuterated chloroform mixture, 1.6/1, v/v, 0.0051 mmol), 50 μL of relaxation agent, chromium (III) acetylacetonate (10 mg/mL, in anhydrous pyridine and deuterated chloroform mixture, 1.6:1, v:v), and 50 μL of derivatizing agent, 2-chloro-4,4,5,5-tetramethyl-1,3,2-dioxaphospholane were added to the solution. The solution was stirred for 10 min, transferred into a dry 5 mm NMR tube and measured. The measurement was performed on a Bruker Avance III HD Nanobay 300 MHz apparatus (121.49 MHz for ^{31}P NMR experiments) using the standard phosphorus pulse program, at ambient temperature, with 256 scans, relaxation delay 5 s, acquisition time 2 s, transmitter excitation frequency 140 ppm, and spectral width 396 ppm. The chemical shifts were reported in ppm. Chemical shifts were referenced from the sharp signal of the reaction product between residual water and 2-chloro-4,4,5,5-tetramethyl-1,3,2-dioxaphospholane at 132.2 ppm. The signals were assigned as follows: 144.8 ppm - cholesterol OH group (internal standard), 133.8-135.5 ppm - carboxyl groups, 137-138.5 ppm - hydroxyphenyl units, 138.5-140.4 ppm - guaiacyl units, 140.4-144.8 ppm - syringyl and condensed guaiacyl units, 145-151 ppm - aliphatic hydroxyl groups.[26] The quantification of the hydroxyl groups was performed according to the protocol described in the literature.[27]

The molecular weight distribution of lignin was obtained from GPC analysis. It was performed at 40 °C using a Waters GPC equipped with a Waters 2414 refractive index detector. Tetrahydrofuran was used as an eluent at a flow rate of 1 mL/min. Three linear columns were used (Styragel HR1, Styragel HR4 and Styragel HR5) Lignin samples were acetylated by acetic anhydride in the presence of pyridine before the measurement using the protocol described by Gosselink *et al*.[28] Acetylated lignin samples (approx. 7 mg) were dissolved in 1.5 mL of tetrahydrofuran and samples were filtered with a PTFE syringe filter (pore size 0.2 μm) prior to measurement. Molecular weights were given relative to polystyrene standards within the calibration range of 500 – 2 520 000 Da.

FT-IR spectra of the resins before and after curing were recorded on a PerkinElmer Frontier spectrometer, equipped with Pike technologies GladiATR accessory in a range of 600-4000 cm-1, with a resolution of 2 cm-1 using 32 accumulative scans. The conversion was determined by following the disappearance of the alkyne C≡C-H peak at 3300 cm^{-1}, while the peak of the aromatic C=C at 1590 cm^{-1} was used as an internal standard.

Glass transition temperature (T_g) was determined by DSC. Thermographs were recorded on a Netzsch Polyma 2014 DSC. DSC data were obtained from

approx. 10 mg of dried lignin sample. Two heating/cooling cycles were performed at the rate of 10 °C/min in the range of -40 to 150 °C. The T_g of each lignin fraction was determined as the temperature at the midpoint of the transition in the second heating cycle. Indium, zinc, tin, and bismuth were used as standards for temperature and enthalpy calibration.

Film solvent resistance was evaluated before and after exposure to a corrosive environment according to the protocol described in ASTM D5402 using MEK as a solvent. When the film was not deteriorated after 200 double rubs with MEK further testing was not continued and the quality of the exposed trace was evaluated (checked if the surface was matted or remained unchanged).

Film thickness was measured using an Elcometer 456 separate coating thickness gauge using a dual FNF probe. The thickness was measured on five different spots.

Film adhesion to the metal (steel) surface was evaluated before and after exposure to the corrosive environment according to the protocol described in ISO 2409:2013. Briefly, a grid incision was cut on the coated surface using a 1 mm with cutter, and a pressure-sensitive tape (Elcometer, adhesive tape ISO 2409 type) was applied over the cut. 5 min after the application of the tape, the tape was removed under an angle of 60° within 0.5-1 s. The adhesion of the film was assessed on a 0-5 scale depending on the damage.

The electrochemical Odd Random Phase Electrochemical Impedance Spectroscopy (ORP-EIS) measurements were performed in a BioLogic flat cell (EL-FLAT-3) with an exposed area of 1 cm^2. The electrolyte was a 0.05 M NaCl to study barrier properties of the coatings in a corrosive environment. The measurements were started shortly after immersion, typically after 20-120 s. The OCP of the system was then measured for 10 s. The signal with an amplitude of 10 mV (rms) and a frequency range of 5 mHz^{-1} kHz is imposed at the electrode around OCP during 6 periods. Data acquisition for the ORP-EIS measurements was done using an NI PCI-4461 data acquisition card, connected to a custom-built compact analog potentiostat placed in a Faraday cage to avoid leakage currents and electromagnetic interference. The measurements were run using custom software running under Python 3.7. The counter electrode and reference electrode consisted of a Pt mesh and an Ag/AgCl (sat. KCl, E_0 = 0.197 V vs. NHE) electrode, respectively.

Chapter 3

Results and discussion

Lignin mixture separation and characterization

Lignin depolymerization and fractionation is a hot topic in scientific research and valorization of depolymerized and/or fractionated lignin is gaining more and more importance. The reductive catalytic fractionation (RCF) process of native birch wood using Ni/SiO$_2$ applied in this work, results in a mixture of lignin oligomers and monomers. One of the possible applications for depolymerized lignin is coatings. Often lignin is fractionated prior to being used in the final application; however, this research concentrates on the evaluation of whether or not separation of RCF lignin fraction is really necessary. The direct use of the mixture of monomers and oligomers after the RCF process for resin synthesis would be a big advantage since laborious, costly, and energy-intensive fractionation steps can be avoided. Moreover, the presence of monomers in the RCF lignin mixture reduces the viscosity, which avoids the addition of solvents or additional reactive diluents in order to reach the required application viscosity of the coating formulation. The three lignin fractions used in this study are the mixture of monomers and oligomers as such without fractionation (BN_mixture), separated via hexane extraction (BN_extracted), or separated via membrane technology. (BN_membrane). Different separation methods resulted in different chemical compositions of those fractions and different functionality. Figure 2 and Table 1 summarize those characteristics. GC data indicate that after the RCF process on birch wood, the resulting mixture is composed of oligomers and various substituted methoxyphenols such as ethylsyringol, syringol, propylsyringol, propanolsyringol, propylguaiacol, propanolguaiacol, and methoxypropylsyringol (Table S1, Appendix). The most abundant monomers present in the mixture are propanolsyringol and propylsyringol followed by propanolguaiacol and propylguaiacol, which is in line with previous findings.[29] Upon hexane extraction, the total monomer content decreased from 31.68% to 19.28% (removal of 39% of monomers from the RCF lignin mixture), and most of the propylguaicol and propylsyringol present in the mixture were removed via the extractive workup. On the other hand, propanolguaiacol and propanolsyringol were not isolated from the hexane residue via the extraction and remained in the residue that can be explained by the polarity difference and possibly poor solubility of alcohol-substituted methoxyphenols in nonpolar solvent like hexane. As shown by Van Aelst *et al.,* through liquid extraction with solvents of varying polarity, the monomers can be selectively removed and the lignin oil can be fractionated into distinct fractions, which is in line with the results shown here.[23] Membrane separation is the most effective method in monomeric fraction removal and it results in the removal of 65% of the monomers from the RCF lignin mixture, leading to the monomer content of 11.18% in BN_membrane fraction. In this case, the polarity of the solvent seems not to influence which monomers were isolated, and the remaining monomers and their

ratio are similar to the original composition of the mixture. Membrane separation processes rely on the physical principle of permeability of the feed components through the porous membrane, and therefore the difference between retentate and permeate composition is based on the membrane characteristics such as the molecular weight cut-off. Those results are in line with the functionality analysis determined by ^{31}P NMR analysis. A decrease in phenolic OH content is observed upon fractionation, which can be correlated with the decreased monomer content for BN_extracted and BN_membrane fractions compared with BN_mixture fraction. The molecular weight of the oligomeric part in those separated fractions is almost the same, which indicates that the separation did not significantly discriminate the structure of the lignin oligomers. GPC traces (Figure S1, Appendix) show that the shape of the oligomeric peaks overlaps in those three fractions and that the most significant differences are observed in the low molecular weight region where monomers and dimers are detected. It should be noted that monomers and dimers are outside the calibration range and, therefore not quantified in M_n and M_W calculation.
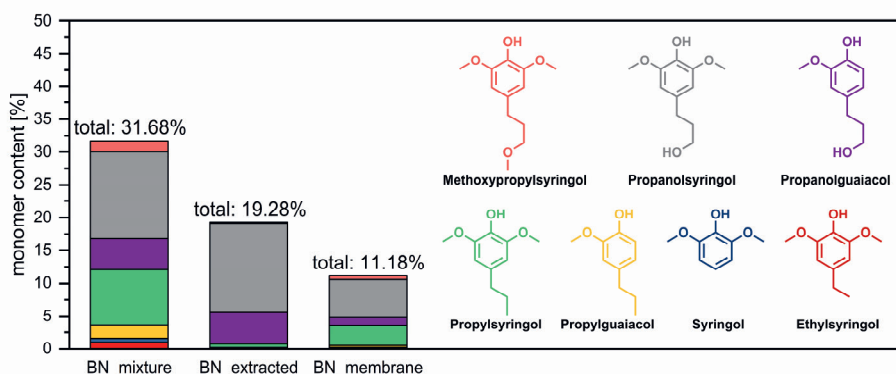
Figure 2 Comparison of the monomer composition in different lignin fractions as determined via GC

Table 1 Summary of lignin fractions characterization

Lignin fraction	Mono.[a]	Phen. OH[b]	Aliph. OH[b]	COOH[b]	OH + COOH)	M_n [c]	M_w [c]	Đ[c]
	[wt.%]	[mmol/g]	[mmol/g]	[mmol/g]	[mmol/g]	[kDa]	[kDa]	[-]
BN_mix.	31.68	2.99	3.36	0.13	6.48	1.4	1.9	1.32
BN_extr.	19.28	2.83	2.84	0.02	5.69	1.3	1.8	1.33
BN_mem.	11.18	2.71	2.97	0.03	5.71	1.4	1.9	1.37

[a] determined by GC, [b] determined by ^{31}P NMR spectroscopy, [c] based on THF GPC, after acetylation, only the oligomeric fraction (with molecular weight higher than 500 Da) was quantified, therefore it is not fully representative for the whole sample.

Chapter 3

Preparation and characterization of the lignin-based protective films

In order to synthesize lignin-containing protective film using tandem thiol-yne and Claisen rearrangement chemistries, lignin fractions were modified first with a triple bond bearing moiety. Aliphatic and phenolic OH groups in lignin monomers and oligomers were etherified with a propargyl group via a Williamson etherification reaction. This conversion was confirmed by means of ^{31}P NMR and GC (Table 2 and Table S1, Appendix). It can be clearly seen that the amount of phenolic and aliphatic OH groups is significantly decreased, indicating high conversion, especially in the case of phenolic OH etherification, showing 67-95% conversion (Figure S2, Appendix). Aliphatic OH, due to their lower reactivity, were modified to a lower extent, with conversion rates of 24-58%, resulting in an overall concentration of propargyl moieties in the propargylated fractions between 2.59 and 4.85 mmol/g. Due to the initial highest hydroxyl group concentration, BN_mixture contains the most propargyl moieties, followed by BN_membrane and BN_extracted, which had similar functionality. GC data indicate that part of the monomers was removed during the extractive workup procedure upon the etherification reaction. However, the modified fractions still show the same trend in monomer content as the unmodified fractions, BN_mixture>BN_extracted>BN_membrane. BN_mixture and BN_membrane show a low content (1.17-1.93 %) of unmodified phenolic monomers that cannot be incorporated in the polymeric network upon cross-linking, while the BN_extracted fraction contains a slightly higher amount of unmodified phenolic monomers (4.08%), which is in line with ^{31}P NMR observations regarding the conversion of hydroxyl groups.

Table 2 Lignin propargylation ^{31}P NMR results summary

Lignin fraction	Phen. OH[a] [mmol/g]	Aliph. OH[a] [mmol/g]	Phen. OH conv.[b] [mmol/g]	Aliph. OH conv.[b] [mmol/g]	Phen. OH[a] [mmol/g]	Isolated mod. mono.[c] [wt.%]	Isolated unmod. mono.[c] [wt.%]
BN_mix.	0.16	1.53	95	58	4.85	9.99	1.93
BN_extr.	0.93	2.15	67	24	2.59	4.39	4.08
BN_mem.	0.31	1.98	90	33	3.18	4.40	1.17

[a] determined by ^{31}P NMR spectroscopy, [b] calculated as described by Koivu et al.[30] Calculations are based on a theoretical lignin mass percentage in a lignin ester.

$$m(\%)lignin = \frac{1-m(H\%)}{1-m(H\%)+m(R\%)} \times 100\% = \frac{1-[(\frac{PropBr}{Lignin}) \times (OH) \times M(H)]}{1+[(\frac{PropBr}{Lignin}) \times (OH) \times M(R)]} \times 100\%$$, Where: PropBr/Lignin

is the molar ratio of added propargyl bromide to lignin (equiv); (OH) is the total hydroxyl content of lignin in mmol/g; m(H%) and m(R%) are mass effects related to the hydrogen (H) and propargyl ether group (R), where M(H) = 1 g/mol and M(R) = 39 g/mol, [c] determined by GC.

The next step in the protective film fabrication was mixing modified lignin fractions with the multifunctional thiol pentaerythritol tetrakis(3-mercaptopropionate) (PETMP)

to give a 1:2 relationship between the reactive groups as one alkyne moiety reacts with two thiol groups. The system was cured to create a polymeric network via UV-initiated thiol-yne "click" chemistry followed by thermal Claisen rearrangement post-curing.[25] Post-curing was required due to the low UV-curing conversion, possibly caused by UV-blocking properties of lignin and/or scavenging of the initiator radicals by the residual phenolic compounds with known antioxidant properties.[31, 32] The cross-linking reaction was followed by FT-IR (Figure 3). The BN_mixture resin formulation shows bands at 3300 and 2572 cm^{-1} associated with alkyne moieties in modified lignin fractions and the thiol group in PETMP, respectively. After the curing, both bands almost completely disappeared, confirming the successful conversion, as summarized in Table 3. Considering the intensity of the peaks, alkyne conversion determination is more accurate than thiol conversion determination. Alkyne conversion decreases with increasing lignin content, in the order BN_extracted<BN_membrane<BN_mixture. This phenomenon can be explained by steric hindrance in systems containing more bulky oligomeric fractions and limited mobility in the cured systems leading to incomplete conversion.[33] This incomplete conversion may lead to decreased T_g of the cross-linked networks. While fully cross-linked (96.9% conversion of alkyne) BN_mixture formulations show a T_g of 83.9 °C, BN_extracted and BN_membrane exhibit lower T_g, 63.6 and 66.8 °C, respectively, which correlates well with the lower conversion of alkyne moiety (79.9 and 89.5%, respectively). Moreover, the differences in T_g may originate from the mass ratio of lignin:thiol and varying monomer content in the system. In this study, we did not study full coating formulations, which also contain colorants and additives next to the resin and carrier liquid; clear coating systems in the form of polymeric protective films were studied in this proof-of-principle. However, we still performed several application tests, which are typical for coatings. To investigate the performance of the films, methyl ethyl ketone (MEK) solvent resistance and cross-cut adhesion tests were performed before and after exposure to a corrosive environment (3.5% NaCl). Overall, the protective films were not destroyed after 200 double rubs indicating good MEK solvent resistance. In all cases, the solvent resistance remained unchanged after conditioning in the corrosive environment. All cured films exhibit outstanding adhesion to the metal (steel) surface and result in class 0 test results in cross-cut adhesion, which means there is no detachment of the coating at all after the test. After conditioning in a corrosive, salty water environment, the adhesion of the protective films to the steel surface marginally decreased to class 1, which can be associated with water uptake of the polymeric film and decreased adhesion. Based on the evaluation of those basic film properties, there is no significant advantage in fractionating the mixture of lignin oligomers and monomers after the RCF process (via extraction or membrane separation).
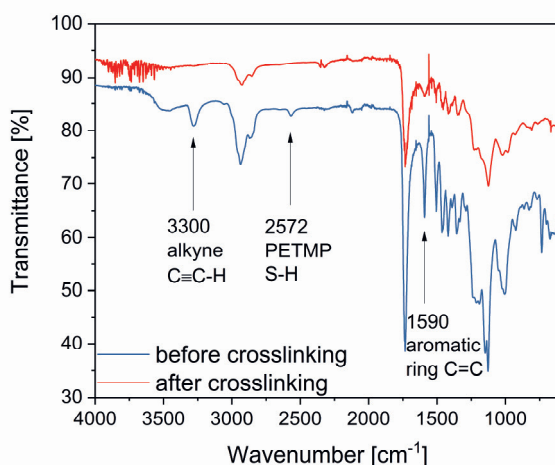
Chapter 3

Figure 3 *FT-IR spectra of the BN_mixture protective film resin formulation before and after curing*

Table 3 *FT-IR spectra of the BN_mixture protective film resin formulation before and after curing*

Film	Lignin cont.	Conv. alkyne	Conv. thiol	T_g	Film thickn.	MEK resistance[a]		Cross-cut adhesion[b]	
	[wt %]	[%]	[%]	[°C]	[µm]	Before exp.	After exp.	Before exp.	After exp.
BN_mix.	46	96.9	83.5	83.9	28.0± 2.4	200+	200+	class 0	class 1
BN_extr.	61	79.6	97.9	63.6	44.6± 3.8	200-	200-	class 0	class 1
BN_mem.	57	89.5	67.2	66.8	77.9± 10.1	200+	200+	class 0	class 1

[a] after 200 double rubs with MEK: + sample appearance was unchanged, - sample was slightly matte in rubbing area, [b] the adhesion is classified with class 0 – class 5 scale where class 0: no damage to the surface, class 1: small flakes of film have detached at intersections and not more than 5% of the cross-cut area is affected, class 5: severe flaking of the film exceeding 65% of the cross-cut area

Corrosion resistance of lignin-containing films

Electrochemical impedance spectroscopy (EIS) is a well-known technique to assess corrosion resistance of the coatings and predict their service lifetime. EIS data provide insights into the transport of corrosive species through the coating while indicating changes in buried metal oxide/coating interface. Odd Random Phase multisine EIS (ORP-EIS) is a multisine technique that provides vital information on the linearity and stationarity state of the system.[34] Measurements are started shortly after exposure (within 20 - 120 s). Measuring shortly after the exposure is necessary, considering that uptake of the electrolyte and electrochemical reactions can introduce non-stationarities on the electrochemical state of the coating/metal system.

In the presence of non-stationarities, calculation of the instantaneous impedance allows following the impedance of the system resolved over the measurement time.[35]

Results acquired with the ORP-EIS technique are used to evaluate barrier properties of the three lignin-based protective films: BN_extracted, BN_membrane, and BN_mixture. Figure 4 shows an example of the ORP EIS measurement (BN_mixture) presented in bode plot format with different noise levels. The overlap between the noise + non-linearities with the stochastic noise shows the system behaves linearly in the measurement frequency range while the noise + non-stationarities exceed the stochastic noise. This is an indication of the non-stationary state of the system. Considering that the non-stationarity at high frequency originates from the change in the capacitance of the polymer film and uptake of the electrolyte affects the polymer film capacitance, this non-stationarity can originate from the uptake of the electrolyte (water and/or ions).[36]
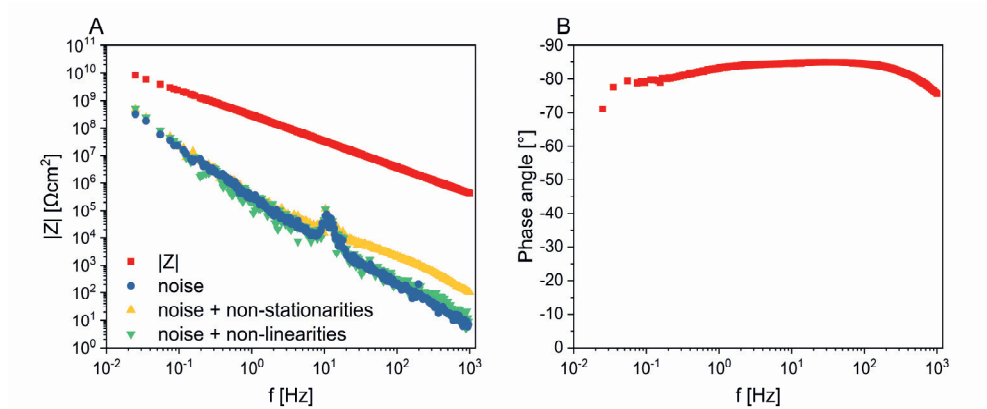
Figure 4 *ORP EIS results of the first measurement of the BN_mixture sample after 60 s of immersion in 0.05 M NaCl. A: Modulus and noise levels; B: phase angle*

To compare the short-term barrier properties of these three protective films, in the first 24 h of exposure to 0.05 M NaCl, the evolution of the impedance at low frequency (0.025 Hz) versus time is depicted in Figure 5. The impedance at 0.01 Hz is a well-known indicator of the film condition being exposed to the corrosive electrolyte. In the used ORP-EIS excitation signal, the closest frequency to 0.01 Hz existing in the generated signal for these series of experiments is 0.025 Hz. Figure 5 illustrates that $|Z_{0.025Hz}|$ for all three protective films are similar, the impedance is relatively stable within 24 h. This behavior can be attributed to the high barrier properties and corrosion performance of these protective films. These results also indicate that the fractionation of the BN_mixture does not imply a significant improvement in the anticorrosive performance of these films in short 24 h exposure.
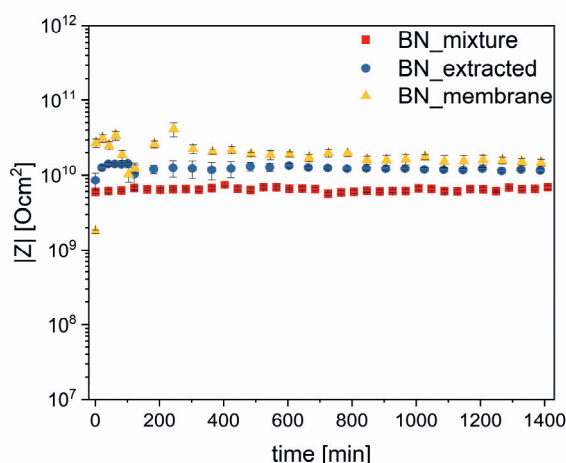
Figure 5 *Evolution of impedance, |Z0.025Hz| versus time for BN_mixture (red), BN_extracted (blue) and BN_membrane (yellow). Noise + non-stationarities are plotted as error bars*

In order to further demonstrate the corrosion resistance of these three protective films, the long-term anticorrosive behavior was investigated by ORP EIS measurements on the 2nd, 3rd, 10th, and 21st day after exposure. As illustrated in Figure 6, after 21 days of exposure, the films maintained their high corrosion performance with $|Z_{0.025Hz}|$ around 10^{10} Ωcm^2. Comparing the impedance values of the lignin-based films obtained in this study with the systems reported in the literature, it can be concluded that these protective films exhibit an impressive corrosion resistance. Rahman *et al.* reported the use of lignin nanoparticles in epoxy resins where impedance was around 10^5 Ωcm^2.[37] Ding *et al.* showed that films in which lignin was incorporated in epoxy resin could exhibit the impedance of around 10^{10} after 20 days of exposure.[15] In both reported systems, the lignin content was below 2%. Cao *et al.* studied polyurethane coatings containing 35-53% lignin with impedances of around 10^{10} Ωcm^2 after 40 days of exposure, which is similar to the results presented here.[13]

Protective films based on BN_extracted and BN_membrane did not show a significant difference with film based on BN_mixture regarding the impedance at low frequencies. However, considering the phase angle of these three samples in the low frequency region, after 21 days of exposure, only the BN_mixture is still close to -80. This means this sample has the main contribution from the capacitance of the coating, while in the two other films, BN_extracted and BN_membrane, the phase angle is shifting toward lower angles, showing deviation from capacitive behavior toward more resistive behavior; this behavior indicates the beginning of the lowering of the barrier properties of these two protective films in comparison with BN_mixture, however, the difference is not significant yet.
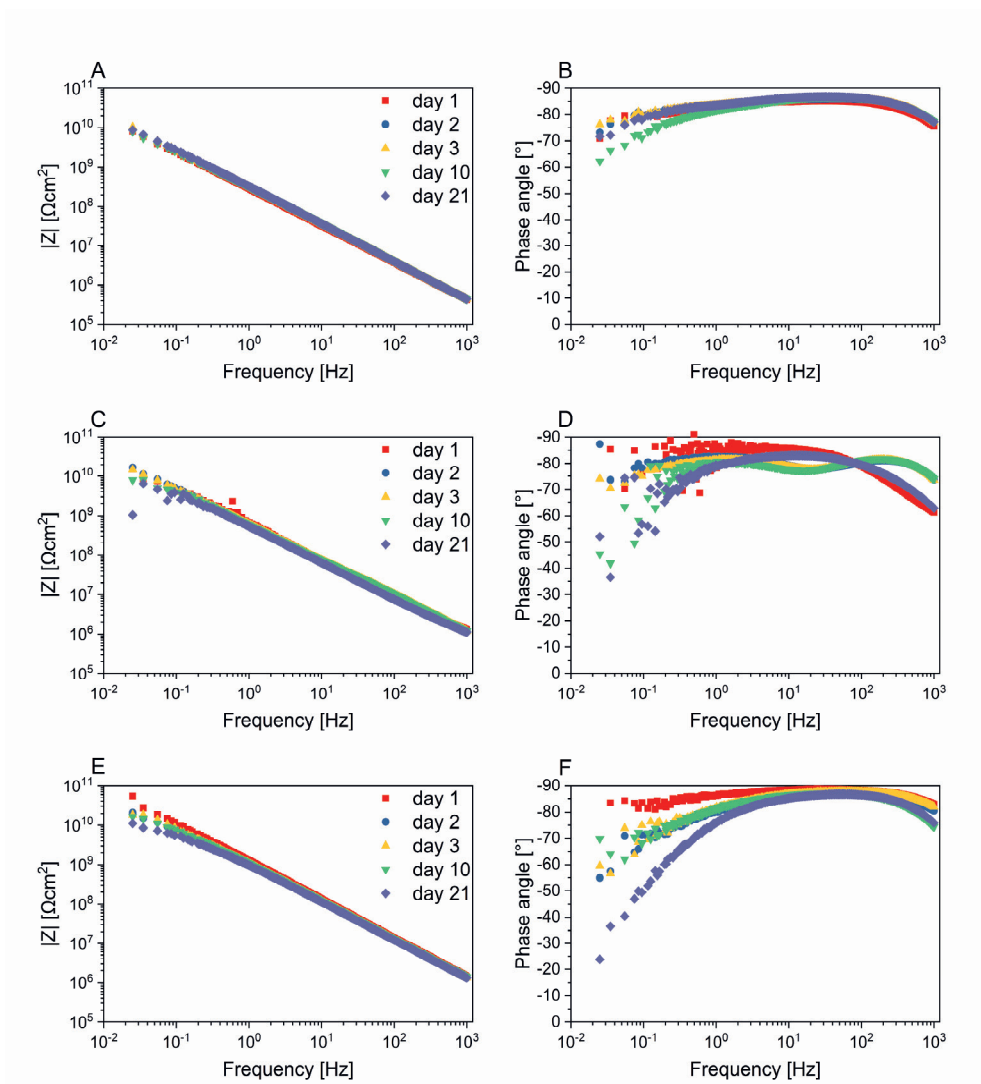
Figure 6 *ORP EIS results of (a) BN_mixture, (b) BN_membrane and (c) BN_extracted in the 1st, 2nd, 3rd, 10th, and 21th day after exposure*

Conclusions

In this work, the synthesis and characterization of novel lignin-based films as anticorrosive protection for metal substrates was described. The lignin fractions used in this study were obtained from the birch wood RCF process using Ni/SiO$_2$ catalyst. Three fractions were compared, namely the mixture of lignin oligomers and monomers after the RCF process without fractionation, or fractionated samples via extraction and membrane separation processes. The resulting fractions differed in

the monomer content and composition. Membrane separation is more effective than extraction in order to reduce the monomer content in the RCF mixture of monomers and oligomers after depolymerization. Fractionated lignin samples were used as a precursor in polymeric network synthesis using tandem UV-initiated thiol-yne "click" synthesis and Claisen rearrangement. All networks were obtained with high conversion and exhibited outstanding performance in cross-cut adhesion test and solvent resistance both before and after exposure to corrosive environment. To further study this behavior, ORP-EIS was used to determine the barrier properties of the films. The films exhibited excellent barrier and corrosion protection even after 21 days. The goal of this work was to determine if the laborious, costly, and energy-intensive separation of the lignin monomeric and oligomeric mixture obtained after depolymerization is necessary in order to efficiently act as anticorrosive polymer film. This study shows that the separation is unnecessary and does not bring improved performance of the polymer film compared with the unseparated sample, which is an advantage in terms of process sustainability and techno-economics. This is a very interesting proof-of-concept showing the application potential of unfractionated RCF lignin as a component in thermoset polymeric films. This concept can be easily transferred to real coating formulations and other cross-linking chemistries than the thiol-yne/Claisen approach studied in this work.

References

1.   Finley, J. W.; Seiber, J. N., The Nexus of Food, Energy, and Water. *J. Agric. Food Chem.* **2014,** *62* (27), 6255-6262.

2.   Bajwa, D. S.; Pourhashem, G.; Ullah, A. H.; Bajwa, S. G., A concise review of current lignin production, applications, products and their environmental impact. *Ind. Crops Prod.* **2019,** *139*, 111526.

3.   Poveda-Giraldo, J. A.; Solarte-Toro, J. C.; Cardona Alzate, C. A., The potential use of lignin as a platform product in biorefineries: A review. *Renewable Sustainable Energy Rev.* **2021,** *138*, 110688.

4.   Jedrzejczyk, M. A.; Engelhardt, J.; Djokic, M. R.; Bliznuk, V.; Van Geem, K. M.; Verberckmoes, A.; De Clercq, J.; Bernaerts, K. V., Development of Lignin-Based Mesoporous Carbons for the Adsorption of Humic Acid. *ACS Omega* **2021,** *6* (23), 15222-15235.

5.   Schutyser, W.; Renders, T.; Van den Bosch, S.; Koelewijn, S. F.; Beckham, G. T.; Sels, B. F., Chemicals from lignin: an interplay of lignocellulose fractionation, depolymerisation, and upgrading. *Chem. Soc. Rev.* **2018,** *47* (3), 852-908.

6.   Sternberg, J.; Sequerth, O.; Pilla, S., Green chemistry design in polymers derived from lignin: review and perspective. *Prog. Polym. Sci.* **2021,** *113*, 101344-101348.

7.   Gao, C.; Zhao, X.; Liu, K.; Dong, X.; Wang, S.; Kong, F., Construction of eco-friendly corrosion inhibitor lignin derivative with excellent corrosion-resistant behavior in hydrochloric acid solution. *Mater. Corros.* **2020,** *71* (11), 1903-1912.

8.   Gao, C.; Zhao, X.; Fatehi, P.; Dong, X.; Liu, K.; Chen, S.; Wang, S.; Kong, F., Lignin copolymers as corrosion inhibitor for carbon steel. *Ind. Crops Prod.* **2021,** *168*.

9.   Shahini, M. H.; Ramezanzadeh, B.; Mohammadloo, H. E., Recent advances in biopolymers/carbohydrate polymers as effective corrosion inhibitive macro-molecules: A review study from experimental and theoretical views. *J. Mol. Liq.* **2021,** *325*, 115110.

10.   Jedrzejczak, P.; Collins, M. N.; Jesionowski, T.; Klapiszewski, L., The role of lignin and lignin-based materials in sustainable construction - A comprehensive review. *Int. J. Biol. Macromol.* **2021,** *187*, 624–650.

11.   Cao, Y.; Zheng, D.; Lin, C., Construction of ecofriendly anticorrosive composite film ZnAl-LDH by modification of lignin on AA 7075 surface. *Mater. Corros.* **2021,** *72* (10), 1595-1606.

12.   Carlos de Haro, J.; Magagnin, L.; Turri, S.; Griffini, G., Lignin-Based Anticorrosion Coatings for the Protection of Aluminum Surfaces. *ACS Sustain. Chem. Eng.* **2019,** *7* (6), 6213-6222.

13.   Cao, Y.; Liu, Z.; Zheng, B.; Ou, R.; Fan, Q.; Li, L.; Guo, C.; Liu, T.; Wang, Q., Synthesis of lignin-based polyols via thiol-ene chemistry for high-performance polyurethane anticorrosive coating. *Compos. Part B* **2020,** *200*, 108295.

14.   Fang, C.; Liu, W.; Qiu, X., Preparation of Polyetheramine-Grafted Lignin and Its Application in UV-Resistant Polyurea Coatings. *Macromol. Mater. Eng.* **2019,** *304* (10), 1900257.

15.   Ding, J., Epoxidation Modification of Renewable Lignin to Improve the Corrosion Performance of Epoxy Coating. *Int. J. Electrochem. Sci.* **2016,** 6256-6265.

16.   Kulkarni, P.; Ponnappa, C. B.; Doshi, P.; Rao, P.; Balaji, S., Lignin from termite frass: a sustainable source for anticorrosive applications. *J. Appl. Electrochem.* **2021,** *51*, 1491–1500.

17.   Deng, Y.; Chen, J.; Zhang, X.; Wei, F.; Zhang, J.; Lin, J.; Xu, Y., Preparation of water-dispersible corrosion inhibitors for composite lacquer coatings with excellent properties. *Prog. Org. Coat.* **2019,** *127*, 276-285.

18.   Dastpak, A.; Lourençon, T. V.; Balakshin, M.; Farhan Hashmi, S.; Lundström, M.; Wilson, B. P., Solubility study of lignin in industrial organic solvents and investigation of electrochemical properties of spray-coated solutions. *Ind. Crops Prod.* **2020,** *148*, 112310.

19.   Dastpak, A.; Yliniemi, K.; de Oliveira Monteiro, M.; Höhn, S.; Virtanen, S.; Lundström, M.; Wilson, B., From Waste to Valuable Resource: Lignin as a Sustainable Anti-Corrosion Coating. *Coatings* **2018,** *8* (12), 454.

Chapter 3

20.   Tan, Z.; Wang, S.; Hu, Z.; Chen, W.; Qu, Z.; Xu, C.; Zhang, Q.; Wu, K.; Shi, J.; Lu, M., pH-Responsive Self-Healing Anticorrosion Coating Based on a Lignin Microsphere Encapsulating Inhibitor. *Ind. Eng. Chem. Res.* **2020,** *59* (7), 2657-2666.

21.   Liao, Y.; Koelewijn, S.-F.; Van den Bossche, G.; Van Aelst, J.; Van den Bosch, S.; Renders, T.; Navare, K.; Nicolaï, T.; Van Aelst, K.; Maesen, M.; Matsushima, H.; Thevelein, J. M.; Van Acker, K.; Lagrain, B.; Verboekend, D.; Sels, B. F., A sustainable wood biorefinery for low–carbon footprint chemicals production. *Science* **2020,** *367* (6484), 1385-1390.

22.   Abu-Omar, M. M.; Barta, K.; Beckham, G. T.; Luterbacher, J. S.; Ralph, J.; Rinaldi, R.; Román-Leshkov, Y.; Samec, J. S. M.; Sels, B. F.; Wang, F., Guidelines for performing lignin-first biorefining. *Energy Environ. Sci.* **2021,** *14* (1), 262-292.

23.   Van Aelst, K.; Van Sinay, E.; Vangeel, T.; Cooreman, E.; Van den Bossche, G.; Renders, T.; Van Aelst, J.; Van den Bosch, S.; Sels, B. F., Reductive catalytic fractionation of pine wood: elucidating and quantifying the molecular structures in the lignin oil. *Chem. Sci.* **2020,** *11* (42), 11498-11508.

24.   Van den Bosch, S.; Schutyser, W.; Vanholme, R.; Driessen, T.; Koelewijn, S. F.; Renders, T.; De Meester, B.; Huijgen, W. J. J.; Dehaen, W.; Courtin, C. M.; Lagrain, B.; Boerjan, W.; Sels, B. F., Reductive lignocellulose fractionation into soluble lignin-derived phenolic monomers and dimers and processable carbohydrate pulps. *Energy Environ. Sci.* **2015,** *8* (6), 1748-1763.

25.   Sen, S.; Sadeghifar, H.; Argyropoulos, D. S., Kraft Lignin Chain Extension Chemistry via Propargylation, Oxidative Coupling, and Claisen Rearrangement. *Biomacromolecules* **2013,** *14* (10), 3399-3408.

26.   Korntner, P.; Sumerskii, I.; Bacher, M.; Rosenau, T.; Potthast, A., Characterization of technical lignins by NMR spectroscopy: optimization of functional group analysis by 31P NMR spectroscopy. *Holzforschung* **2015,** *69* (6), 807-814.

27.   Meng, X.; Crestini, C.; Ben, H.; Hao, N.; Pu, Y.; Ragauskas, A. J.; Argyropoulos, D. S., Determination of hydroxyl groups in biorefinery resources via quantitative 31P NMR spectroscopy. *Nat. Protoc.* **2019,** *14* (9), 2627-2647.

28.   Gosselink, R. J. A.; Abächerli, A.; Semke, H.; Malherbe, R.; Käuper, P.; Nadif, A.; van Dam, J. E. G., Analytical protocols for characterisation of sulphur-free lignin. *Ind. Crops Prod.* **2004,** *19* (3), 271-281.

29.   Van den Bosch, S.; Renders, T.; Kennis, S.; Koelewijn, S. F.; Van den Bossche, G.; Vangeel, T.; Deneyer, A.; Depuydt, D.; Courtin, C. M.; Thevelein, J. M.; Schutyser, W.; Sels, B. F., Integrating lignin valorization and bio-ethanol production: on the role of Ni-Al2O3catalyst pellets during lignin-first fractionation. *Green Chem.* **2017,** *19* (14), 3313-3326.

30.   Koivu, K. A. Y.; Sadeghifar, H.; Nousiainen, P. A.; Argyropoulos, D. S.; Sipilä, J., Effect of Fatty Acid Esterification on the Thermal Properties of Softwood Kraft Lignin. *ACS Sustain. Chem. Eng.* **2016,** *4* (10), 5238-5247.

31.   Majira, A.; Godon, B.; Foulon, L.; Putten, J. C.; Cézard, L.; Thierry, M.; Pion, F.; Bado-Nilles, A.; Pandard, P.; Jayabalan, T.; Aguié-Béghin, V.; Ducrot, P. H.; Lapierre, C.; Marlair, G.; Gosselink, R. J. A.; Baumberger, S.; Cottyn, B., Enhancing the Antioxidant Activity of Technical Lignins by Combining Solvent Fractionation and Ionic-Liquid Treatment. *ChemSusChem* **2019,** *12* (21), 4799-4809.

32.   Jedrzejczyk, M. A.; Van den Bosch, S.; Van Aelst, J.; Van Aelst, K.; Kouris, P. D.; Moalin, M.; Haenen, G. R. M. M.; Boot, M. D.; Hensen, E. J. M.; Lagrain, B.; Sels, B. F.; Bernaerts, K. V., Lignin-Based Additives for Improved Thermo-Oxidative Stability of Biolubricants. *ACS Sustain. Chem. Eng.* **2021,** *9* (37), 12548-12559.

33.   Jawerth, M.; Johansson, M.; Lundmark, S.; Gioia, C.; Lawoko, M., Renewable Thiol–Ene Thermosets Based on Refined and Selectively Allylated Industrial Lignin. *ACS Sustain. Chem. Eng.* **2017,** *5* (11), 10918-10925.

34.   Van Gheem, E.; Pintelon, R.; Vereecken, J.; Schoukens, J.; Hubin, A.; Verboven, P.; Blajiev, O., Electrochemical impedance spectroscopy in the presence of non-linear distortions and non-stationary behavior: Part I: theory and validation. *Electrochim. Acta* **2004,** *49* (26), 4753-4762.

35.   Breugelmans, T.; Lataire, J.; Muselle, T.; Tourwé, E.; Pintelon, R.; Hubin, A., Odd random phase multisine electrochemical impedance spectroscopy to quantify a non-stationary behavior: Theory and validation by calculating an instantaneous impedance value. *Electrochim. Acta* **2012,** *76*, 375-382.

36.   Wouters, B.; Jalilian, E.; Claessens, R.; Madelat, N.; Hauffman, T.; Van Assche, G.; Terryn, H.; Hubin, A., Monitoring initial contact of UV-cured organic coatings with aqueous solutions using odd random phase multisine electrochemical impedance spectroscopy. *Corros. Sci.* **2021,** *190*, 109713.

37.   Rahman, O. u.; Shi, S.; Ding, J.; Wang, D.; Ahmad, S.; Yu, H., Lignin nanoparticles: synthesis, characterization and corrosion protection performance. *New J. Chem.* **2018,** *42* (5), 3415-3425.

Chapter 3

Appendix for Chapter 3

Table S1 Comparison of lignin fractions monomer composition determined via GC before and after propargylation

Monomer	BN_ mix. [wt.%]	BN_ extr. [wt.%]	BN_ mem. [wt.%]	BN_ mix. proparg. [wt.%]	BN_ extr. proparg. [wt.%]	BN_ mem. proparg. [wt.%]
Ethylsyringol	0.98	0.12	0.24	0.00	0.00	0.00
Syringol	0.55	0.00	0.00	0.00	0.00	0.00
Propylguaiacol	2.09	0.09	0.31	0.00	0.00	0.00
Propylsyringol	8.48	0.59	3.01	0.72	0.23	0.28
Propanolguaiacol	4.73	4.83	1.32	0.00	1.29	0.00
Propanolsyringol	13.17	13.45	5.69	0.34	2.56	0.29
Methoxypropylsyringol	1.68	0.20	0.60	0.87	0.00	0.60
Propanolguaiacol propargylated	NA	NA	NA	1.78	1.64	0.85
Propanolsyringol propargylated	NA	NA	NA	2.40	2.38	1.20
Propylguaiacol propargylated	NA	NA	NA	1.52	0.00	0.31
Propylsyringol propargylated	NA	NA	NA	3.71	0.37	1.71
Methoxypropylsyringol propargylayed	NA	NA	NA	0.58	0.00	0.33
Total monomer content	**31.68**	**19.28**	**11.18**	**11.92**	**8.47**	**5.57**
Total modified monomer content	**NA**	**NA**	**NA**	**9.99**	**4.39**	**4.40**
Total unmodified monomer content	**NA**	**NA**	**NA**	**1.93**	**4.08**	**1.17**
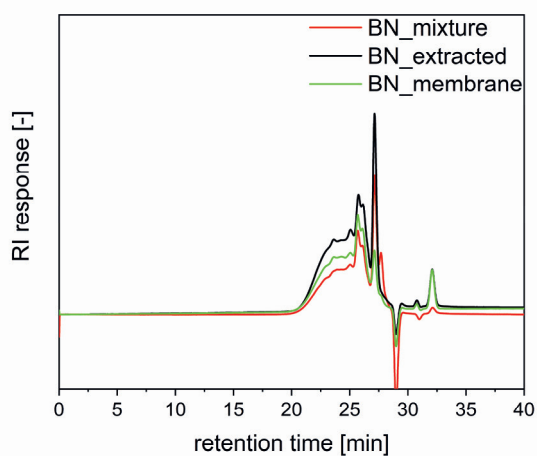
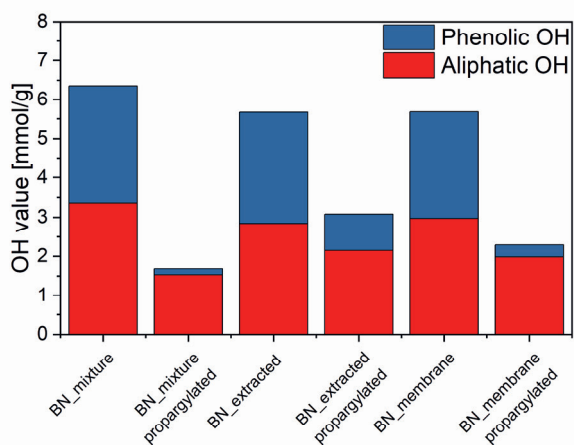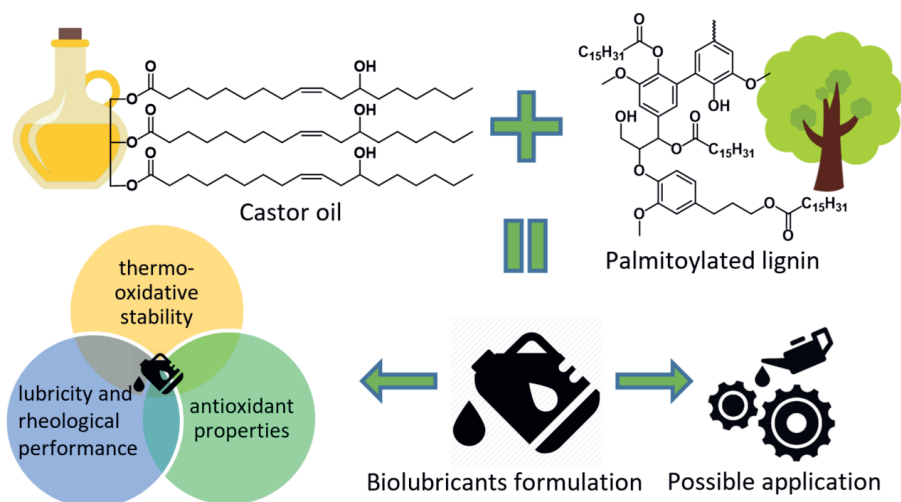***Figure S1*** *GPC curves of lignin fractions used in this study*

Figure S2 *Comparison of phenolic and aliphatic OH content before and after modification*

Chapter 3

Lignin based additives for improved thermo-oxidative stability of biolubricants

Castor oil

Palmitoylated lignin

thermo-oxidative stability

lubricity and rheological performance

antioxidant properties

Biolubricants formulation   Possible application

There is an environmental concern regarding the use of petroleum-based lubricants, which are generally toxic and nonbiodegradable. Biobased lubricants, such as vegetable oils, are the alternative: they show excellent lubricity, are readily biodegradable and nontoxic. A major disadvantage of using vegetable oils in lubricant applications is their lack of thermo-oxidative stability, which can be improved by antioxidant additives. We propose the use of lignin-based additives in biolubricant formulations to improve this feature due to lignin's antioxidant properties. To ensure a stable dispersion in vegetable oil, lignin was partially esterified. Antioxidant properties of lignin before and after palmitoylation were demonstrated in a 2,2-diphenyl-1-picrylhydrazyl (DPPH) assay. Four different lignin-based fractions, commercial Protobind P1000 soda lignin from straw, solvolytically fractionated Protobind P1000 lignin, and two lignin fractions from reductively catalyzed fractionation (RCF) of native birch wood, were tested in biolubricant formulations with castor oil as base oil. Those lignin fractions exhibited excellent performance compared to butylated hydroxytoluene (BHT), a commonly used petroleum-based antioxidant. Formulations of modified lignin in castor oil possess improved thermo-oxidative stability, as illustrated by their increased oxidation induction time. Additionally, rheological and tribological tests demonstrate similar, or in some cases improved, lubricating properties compared to castor oil. This study showcases the successful incorporation of lignin-based antioxidants in biolubricant formulations, tackling the major disadvantage of vegetable oils as environment-friendly lubricants.

Introduction

The main purpose of lubricants is to protect moving parts in, for example, engines and machinery by reducing heat, friction, and wear when they are in motion. There is a constant growth in the use of lubricants, which are primarily used by the automotive industry, and the estimated global market size is 30-40 million tons annually.[1] About 90-95% of lubricants are petroleum-based products.[2] Approximately half of these products end up in the environment due to total-loss applications, spillage, evaporation and mishandling, polluting soil, water, and air as a result of their toxicity and lack of biodegradability.

An environment-friendly alternative to synthetic petroleum-based lubricants are biolubricants such as vegetable oils. Promising oils for this application include sunflower, rapeseed, soybean, castor, jatropha, and neem oils, among others.[1, 3] Next to their biodegradability, renewable, and nontoxic character, vegetable oils possess advantageous performance features: excellent lubricity, low volatility, high flash point, and viscosity.[2, 4] Nonetheless, their biggest drawback is limited thermo-oxidative and hydrolytic stability, which can be overcome by the use of additives or chemical modification of the oil by transesterification, epoxidation, estolide formation, or hydrogenation.[1, 2, 4]

In our view, the focus should be pointed toward biolubricants originating from nonedible vegetable oils to avoid competition with feed and food resources. Castor oil is a good example of such an oil. It is mostly composed of the triglyceride of ricinoleic acid (Figure 1). Hydroxyl groups present in its structure lead to increased polarity and provide it with improved properties, such as enhanced lubricity, affinity to metals, increased viscosity, better low-temperature performance, and a generally higher additive solubility compared to other vegetable oils.[5] Such features make castor oil a preferred base oil for lubricant formulations.[6] Castor oil finds applications in various fields, including lubricants, fuels, paints, coatings, polymer synthesis, fertilizers, and pharmaceuticals.[6, 7, 8, 17]
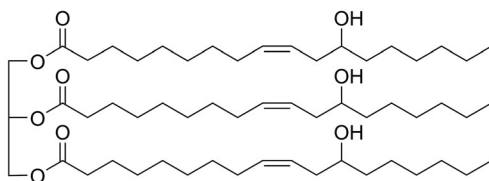

Figure 1 *Chemical structure of the triglyceride of ricinoleic acid, which is the main triglyceride in castor oil*

Low oxidation stability is one of the major obstacles hampering industrial acceptance of vegetable oil-based lubricants.[1, 3] In this work, the activity of natural antioxidants, like lignin and its derivatives, in vegetable oil-based lubricants was evaluated.

Lignin is the most abundant polyphenolic material on earth, present in land-based biomass. It is biosynthesized by cross-linking of monolignols (syringyl (S), guaiacyl (G), and p-hydroxyphenyl (H) units, Figure 2).[9] Next to the antioxidant properties of lignin and lignin-derived products, also enhanced antimicrobial and antifungal activity against certain species has been indicated for lignin.[9, 10] Moreover, lignin is already proven to have low toxicity and to be biocompatible under certain circumstances.[9, 10] Lignin can be produced by various isolation, fractionation, and depolymerization approaches, as reviewed by Liu *et al.* and Chio *et al.*[9, 11, 12] Lignin products have been valorized as a building block in polymeric materials, adhesives, coatings, fuels, antioxidants, additives, and platform chemicals among others.[9, 13-15]
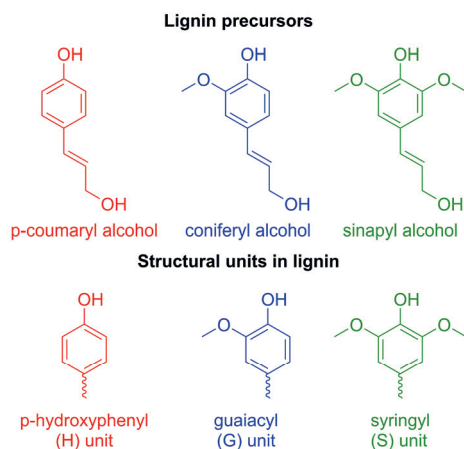
Figure 2 *Lignin building blocks and structural units*

It has been reported that lignin can be incorporated into various biolubricant formulations. Gallego *et al.*, Acar *et al.,* and Borrero-López *et al*. demonstrated that lignin derivatives (hexamethylene diisocyanate cross-linked, epoxide, or isocyanate functionalized lignin) act as thickening agents in castor and sunflower oils.[16-18] Delgado *et al*. showed that epoxidized lignin can be used as a thickener in castor oil biogreases exhibiting improved tribological and antiwear performance.[19] Hua *et al.* and Mu *et al.* investigated the effect of lignin on thermal and tribological properties of ionic liquid-based biolubricants.[20, 21] Mu *et al.* also studied the influence of lignin in ethylene glycol and polyethylene glycol (PEG) matrices on lubricating performance.[22] Cortés-Triviño *et al.* showed that epoxidized lignin can be used as a rheology modifier in castor oil-based gel-like dispersions.[23] Unfortunately, the thermo-oxidative stability of those formulations was not investigated.

Chandrasekaran *et al*. reported the use of phenolic bio-oils, obtained after slow pyrolysis of birchwood and Kraft lignin, as an antioxidant additive in soy biodiesel.[24] In that research, the bio-oil was a mixture of phenolic monomers and dimers, and this mixture exhibited slightly better antioxidant activity than BHT in soybean oil,

while physical properties were not affected by the additive.[24] This study was followed up by Larson *et al*., who showed that bio-oil from softwood lignin pyrolysis exhibits antioxidant properties similar to those of BHT in soybean methyl ester biodiesel.[25] In that work, the authors recognized dimeric phenolic compounds as the most potent antioxidants in the pyrolisate, while monomeric phenolic compounds were less active. Dimers were more active as their double functionality enables separate hydrogen bonding and radical quenching, while monomeric phenols predominantly interact with oils via hydrogen bonding, which reduces their activity. Cesari *et al*. evaluated the antioxidant activity of the model phenolic compounds which could be obtained after lignin depolymerization and showed that all of them exhibit antioxidant performance in multiple antioxidant property assays.[26] Similarly, Quinchia *et al*. showed that natural antioxidants such as (+)-α-tocopherol, propyl gallate, or ascorbyl palmitate can be used in biolubricant formulations, improving the oxidative stability of the high-oleic sunflower and castor oils.[27] The main difference between those works and this study is that we evaluate the performance of lignin-based oligomeric fractions as well, not only phenolic monomers and dimers. Polymeric lignin has been proven by Kaur and Uppal to possess radical scavenging activity, and Kasprzycka-Guttman and Odzeniak have shown that it can inhibit auto-oxidation of arachide nut oil; in both studies the lignin performance was slightly better than that with BHT.[28, 29]

Here, we propose an alternative approach toward the development of lignin-containing biolubricants by improving their main disadvantage, suboptimal thermo-oxidative stability. To improve this property, we apply lignin-based antioxidant additives, which were modified by palmitoylation to increase their lipophilicity. In this research, we investigated several lignin types to derive structure-property-function relationships, i.e., (i) commercial Protobind P1000 soda lignin from straw, (ii) solvolytically fractionated Protobind P1000 lignin from straw[30] and (iii) lignin fractions from reductively catalyzed fractionation (RCF) of native birch wood.[17, 31-33] P1000 lignin was selected as a representative sample of commercially available lignins and because it is a starting material for the solvolysis of the lignin fraction used in this study. As a source of biomass for RCF, birch wood was selected since it is a significant wood source in the Scandinavian region, and it is a good benchmark often used in RCF literature.[15] These fractions were selected due to ongoing scale-up initiatives and coming commercialization of these types of lignin, and their application development is required.[34, 35] Our goal is to assess the potential of palmitoylated lignin as an antioxidant additive in castor oil formulations to improve thermo-oxidative stability, while maintaining the required rheological and tribological performance.

Experimental section

Materials

Protobind P1000 lignin, soda lignin extracted from wheat straw was provided by Green Value S.A. Palmitoyl chloride (98%), acetic anhydride (99%), pyridine (99%), hydrochloric acid (37%), sodium chloride (99%), butylated hydroxytoluene (BHT) (99%), cholesterol (99%), chromium (III) acetylacetonate (99.99%), calcium hydride (95%), 2-chloro-4,4,5,5-tetramethyl-1,3,2-dioxaphospholane(95%), 1,4-dioxane (99%), N-methyl-N-(trimethylsilyl) trifluoroacetamide (98%), 2-methoxyphenol (98%), 4-n-propylguaiacol (99%), 2,6-dimethoxyphenol (99%), 4-methylsyringol (97%), 2-isopropylphenol (98%), 5 wt.% Ru on carbon and 5 wt.% Pd on carbon, were purchased from Sigma Aldrich. 4-Ethylguaiacol (98%) was purchased from Acros Organics. 3-(4-hydroxy-3-methoxyphenyl)-1-propanol (98%) and 2,2-diphenyl-1-picrylhydrazyl (DPPH) (97%) were purchased from TCI. Methanol, hexane, dichloromethane (DCM), acetonitrile, and tetrahydrofuran were purchased from Biosolve. Molecular sieves 3Å (0.3 nm, beads 2 mm) were purchased from Merck. Chloroform-d (dried over molecular sieves, D, 99.96%) was purchased from Cambridge Isotope Laboratories. Dichloromethane and pyridine were dried by distillation over calcium hydride prior to use. Castor oil (pure) was purchased from Fisher Chemicals. Castor oil typically contains approximately 1% stearic acid, 1% palmitic acid, 3% oleic acid, 4% linoleic acid, and 90% ricinoleic acid.[8, 36] It has an iodine value between 85-90, hydroxyl value between 160-168, viscosity of 889 cSt, density of 0.959 g/mL, thermal conductivity of 4.727 W/m°C, specific heat of 0.089 kJ/kg/K, refractive index of 1.48, flash, cloud and melting points of 145°C, 2.7 °C and between -2 °C and -5 °C, respectively.[8, 37]

Methods

P1000 lignin solvolysis: CLO MeOH fraction was obtained from P1000 lignin (wheat straw soda lignin) by solvolysis in MeOH under mild conditions.[30, 38] A total of 300 g of P1000 lignin was loaded in a 4 L batch reactor (Parr Instruments & Co.) and mixed with 1500 mL of MeOH [1:5 w/v]; the solvolysis was carried out at 200 °C, with 10 bar of nitrogen gas for 30 min. After the reaction, the reaction mixture was filtered, and the solvent was removed by rotary evaporation (45-50 °C, 5 mbar) for 1 h. The final oligomeric fractions were dried at 80 °C until a stable weight was achieved.

Reductive Catalytic Fractionation (RCF)

The depolymerized lignin fractions, namely Ru/C and Pd/C hexane residues, were obtained by RCF of lignocellulose biomass.[31-33] The RCF experiment was performed in a 2 L stainless steel batch reactor (Parr Instruments & Co.). A total 150 g of birch wood chips, milled with a Retsch cutting mill with a 2 mm screen, was loaded into the reactor, together with 15.0 g of Pd/C or 15.0 g of Ru/C and 800 mL of methanol. Subsequently, the reactor was sealed, flushed three times with nitrogen gas (10 bar),

and then pressurized with hydrogen gas (30 bar at room temperature). Next, the reaction mixture was stirred (750 rpm) and simultaneously heated to 235 °C (~30 min. heating time). After the reaction time of 3 h, the reactor was cooled and depressurized at room temperature. The reactor contents were quantitatively collected by washing the reactor with ethanol. The solid pulp was separated by filtration and washed thoroughly with ethanol. Next, the standard protocol for the separation of carbohydrates, monomers, and lignin oligomers was applied.[39] The resulting filtrate was evaporated, and a brown oil was obtained, which was solubilized in dichloromethane (DCM) and subjected to a liquid-liquid extraction using DCM and water: per 1 equiv of DCM 4 equiv of water was used; after the DCM fraction was separated and the aqueous fraction was extracted with fresh DCM three times in total. To obtain the RCF lignin oil, the combined DCM-extracted phases were evaporated and dried in an oven of 80 °C. This RCF lignin oil (1 g equiv) was 4-fold extracted with a mixture of hexane (3 mL equiv) and water (3 mL equiv) for 30 min at 80 °C.[39] After each extraction, the soluble hexane phase was removed, and fresh hexane was added. The residue after the four hexane extractions was obtained by rotavap evaporation of water and drying in a vacuum oven. All lignin fractions, P1000 lignin, CLO MeOH, and Ru/C and Pd/C hexane residues, were vacuum-dried (80 °C, 5-10 mbar, overnight) prior to use and analysis.
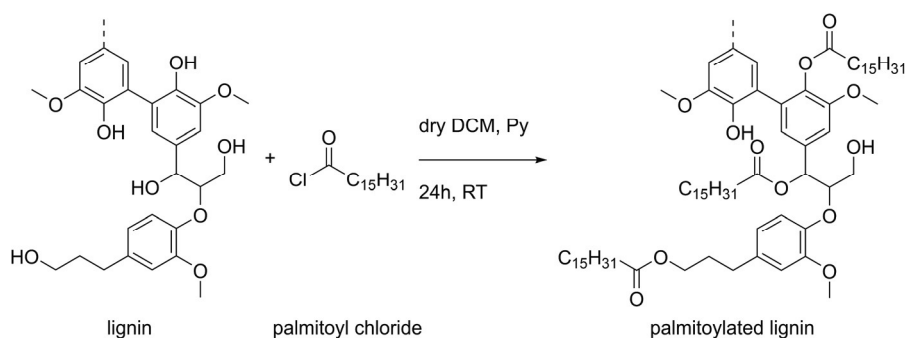
Scheme 1 *Lignin esterification reaction scheme*

All lignin fractions were partially modified with palmitoyl chloride (Scheme 1) in order to make them compatible with the biolubricants matrix (castor oil) while maintaining their antioxidant properties. The general procedure was as follows: 1.0 g of lignin sample was dissolved in 40 mL of dry dichloromethane and stirred under a nitrogen atmosphere. Next, 0.5 equiv* (based on the total phenolic and aliphatic OH content per lignin source, *0.4 equiv was used for Pd/C hexane residue sample) of dry pyridine was added to the reaction mixture, followed by the addition of equimolar equiv of palmitoyl chloride. The reaction was carried out under a nitrogen atmosphere at room temperature for 24 h. Afterward, the reaction mixture was washed with 40 mL of 10% hydrochloric acid, and brine (3 x 40 mL). The product

was dried in vacuum before analysis by GC (Appendix, Table S1) and ^{31}P nuclear magnetic resonance (NMR) spectroscopy (Table 2). Fully modified P1000 lignin was prepared using the same procedure, but 1.5 equiv of palmitoyl chloride was used.

Esterified lignin was dispersed in castor oil by adding the appropriate amount of components at room temperature, and subsequently they were sonicated using a Branson 3800 Ultrasonic bath at 70 °C for 1 h. The concentrations of lignin fractions were adjusted to have the same free phenolic OH content originating from the lignin fraction per 1g of castor oil. The concentrations were 0.007, 0.034, and 0.071 mmol OH/g castor oil; the weight percentage corresponding to this can be found in Table S1 (Appendix).

Characterization

The aromatic and aliphatic hydroxyl groups as well as the carboxylic acids (before and after modification) of lignin were determined by ^{31}P NMR spectroscopy after sample derivatization, according to the method described by Korntner *et al.*[40] Approx. 10 mg of dried (in vacuum a oven at 80 °C, overnight) lignin-based material was dissolved in 500 µL of anhydrous pyridine and deuterated chloroform mixture (1.6:1, v:v). Then, 100 µL of internal standard solution, cholesterol (19.7 mg/mL in anhydrous pyridine and deuterated chloroform mixture, 1.6/1, v/v, 0.0051 mmol), 50 µL of relaxation agent, chromium (III) acetylacetonate (10 mg/mL, in anhydrous pyridine and deuterated chloroform mixture, 1.6:1, v:v), and 50 µL of derivatizing agent, 2-chloro-4,4,5,5-tetramethyl-1,3,2-dioxaphospholane were added to the solution. The solution was stirred for 10 min, transferred into a dry 5 mm NMR tube and measured. The measurement was performed on a Bruker Avance III HD Nanobay 300 MHz apparatus (121.49 MHz for ^{31}P NMR experiments) using the standard phosphorus pulse program, at ambient temperature, with 256 scans, a relaxation delay of 5 s, an acquisition time of 2 s, a transmitter excitation frequency of 140 ppm, and a spectral width of 396 ppm. The chemical shifts were reported in ppm. Chemical shifts were referenced from the sharp signal of the reaction product between residual water and 2-chloro-4,4,5,5-tetramethyl-1,3,2-dioxaphospholane at 132.2 ppm. The signals were assigned as follows: 144.8 ppm - cholesterol OH group (internal standard), 133.8-135.5 ppm - carboxyl groups, 137-138.5 ppm - hydroxyphenyl units, 138.5-140.4 ppm - guaiacyl units, 140.4-144.8 ppm - syringyl and condensed guaiacyl units, 145-151 ppm - aliphatic hydroxyl groups.[40] The quantification of the hydroxyl groups was performed according to the protocol described in the literature.[41]

The molecular weight distribution of lignin was obtained from gel permeation chromatography (GPC) analysis. It was performed at 40 °C using a Waters GPC equipped with a Waters 2414 refractive index detector. Tetrahydrofuran was used as an eluent at a flow rate of 1 mL/min. Three linear columns were used (Styragel

Chapter 4

HR1, Styragel HR4, and Styragel HR5). Lignin samples were acetylated by acetic anhydride in the presence of pyridine before the measurement using the protocol described by Gosselink *et al.*[42] Acetylated lignin samples (approx. 7 mg) were dissolved in 1.5 mL of tetrahydrofuran, and samples were filtered with a PTFE syringe filter (pore size 0.2 µm) prior to measurement. Molecular weights were given relative to polystyrene standards within the calibration range of 370 – 2 520 000 Da.

Samples before and after palmitoylation were measured by gas chromatography (GC) to determine the monomer content in the lignin fractions using the procedure described by Van Aelst *et al.*[33] Therefore, a weighed amount of external standard (2-isopropylphenol; ~20 mg) was added to a GC-vial containing a weighed amount of lignin (approx. 40 mg). Subsequently, 0.3 mL of pyridine and 0.3 mL of N-methyl-N-(trimethylsilyl)trifluoroacetamide were added, next to 0.6 mL of acetonitrile. The vial was sealed and put in an oven at 80 °C for 30 min. Afterward, the samples were analyzed on a gas chromatograph (Agilent 6890 series) equipped with an HP5 column and a flame ionization detector (FID). The following operating conditions were used: injection temperature of 300 °C, column temperature program: 50 °C (2 min), 15 °C/min to 150 °C, 10 °C/min to 220 °C and 20 °C/min to 290 °C (12 min), with a detection temperature of 300 °C. Sensitivity factors of the products are obtained by calibration with commercial standards or estimated, based on effective carbon number (ECN) calculations or trends within the response factors (RF's) of commercial standards.

DPPH free radical scavenging assays of all modified and unmodified lignins were performed using the procedure described by de Menezes *et al.*[43] Lignin and BHT solutions were prepared at the same molar concentration (0.005 mmol/mL, the equiv of 1 mg/mL of BHT, based on phenolic OH content) in a 90% (v/v) 1,4-dioxane-water solution. A DPPH radical working solution in 90% (v/v) 1,4-dioxane-water of 0.04 mg/mL was prepared from a 10 mg/mL stock solution. To 1350 µL of the DPPH radical working solution, the lignin solution was added (10, 30, 75, 150, or 300 µL) to start a reaction, and subsequently a mixture of 90% (v/v) of 4-dioxane in water was added to a total volume of 3 mL with a 90% (v/v) 1,4-dioxane-water solution. The reaction mixture was mixed and kept in the dark for 30 min after starting the reaction before absorption of light of λ=520 nm was determined, using a Jasco V-650 spectrometer. The reduction in absorption reflects the amount of DPPH radicals that have been scavenged by the antioxidant compound. The antioxidant activity is expressed as IC_{50} values in µmol/mL or µg/mL, which is the concentration of the antioxidant compound that is needed to scavenge half of the DPPH radical in 30 min. The IC_{50} was determined using the logarithmic regression of the inhibition calculated using the equation below versus the antioxidant concentration in the 3 mL reaction mixture. The analyses were performed in triplicate.

$$Inhibition\ [\%] = \frac{Abs_{DPPH} - Abs_{antiox}}{Abs_{DPPH}} * 100$$

Where: Abs_{DPPH} the absorbance after 30 min of the DPPH radical solution at 520 nm in the absence of the antioxidant compound and Abs_{antiox} the absorbance after 30 min of the DPPH radical solution in the presence of the antioxidant compound.

Oxidation induction time (OIT) was determined by differential scanning calorimetry (DSC). Thermographs were recorded on a Netzsch Polyma 2014 DSC apparatus. DSC data were obtained from about 10 mg of biolubricant sample, which was heated to 180 °C at a heating rate of 30 °C/min and kept isothermally at 180 °C for 6 h under a constant air flow of 75 mL/min. OIT is reported as the onset time of the sample oxidation. The onset time of the oxidation reaction was taken as the intersection of the extrapolated baseline and the tangent line (leading edge) of the exotherm. An example of OIT determination for castor oil is presented in Figure S1A (Appendix). OIT was determined using the oxidation induction time function in the Proteus Analysis (Netzsch) software. The experiments were performed in a triplex.

The biolubricant viscosity within a shear rate range of 1-1000 s^{-1} was reported using a TA Instruments Discovery HR 2 rheometer at 25 °C in a Newtonian regime. A parallel plate geometry was used, using a 40 mm diameter stainless steel plate on a Peltier temperature control plate.

The evaluation of the tribological properties of the prepared biolubricants was conducted using an SRV4 Test Machine (Optimol Instruments Priiftechnik GmbH). The test method, according to ASTM D 6425, has been implemented at the SRV test machine using a test ball (AISI 52100 steel, 60 HRC hardness, 10 mm diameter) oscillated at a constant frequency (50 Hz) and stroke amplitude (1 mm) and under a constant load (50 N for 30 s, then 300 N for 2h), against a test disk (AISI 521000 steel) that had been moistened with the lubricant (0.3 mL). The platform to which the disc is attached is held at a constant temperature (80 °C). Balls and disks were washed in petroleum ether in an ultrasonic cleaner for 10 min. Peak values of coefficients of friction are determined and recorded as a function of time (Figure S6, Appendix). After the test, the wear scar on the ball was measured by means of an optical microscope (Nikon). The planimetric wear of the wear track was determined employing a profilometer (Talysurf CCI optical profiler) in the center of the track length. All experiments were performed in a triplex.

Chapter 4

Results and discussion

In this study, four different lignin samples: P1000 (soda pulping lignin from wheat straw), CLO MeOH (solvolitically fractionated P1000 lignin), and Ru/C and Pd/C hexane residues (lignin fractions obtained after Reductive Catalytic Fractionation (RCF), using Ru/C or Pd/C catalysts on birch wood, respectively) are used as antioxidant additives in biolubricant formulations and compared with a commercial reference BHT. Here, we compare wheat straw lignins (P1000 and CLO MeOH) with birch wood lignins (Ru/C and Pd/C hexane residues) processed *via* either soda pulping (P1000 lignin), solvent fractionation (CLO MeOH), or RCF Ru/C and Pd/C hexane residues. The protocols describing how those fractions were obtained are reported in the Experimental part. Those fractions were selected because upscaling of those processes is currently ongoing, and application development is needed for their commercialization. Ru/C and Pd/C hexane residues contain oligomeric and monomeric fractions (10% and 50% of monomers are present in Ru/C and Pd/C hexane residue, respectively), while P1000 lignin and CLO MeOH consist of oligomeric fractions exclusively (Table S2, Appendix).

Lignin fractions characterization and modification

Table 1 summarizes the characteristics of each lignin fraction. In general, all of the samples have a similar amount of phenolic hydroxyl groups, while a larger variation, ranging from 1.27 to 4.33 mmol OH/g lignin, is observed for the aliphatic hydroxyl groups. These aliphatic hydroxyl groups are most abundant in Pd/C hexane residue, followed by Ru/C hexane residue, P1000 lignin, and CLO MeOH. Carboxylic groups are most abundant in P1000 lignin, followed by CLO MeOH, and Pd/C and Ru/C hexane residues. A difference in (S+G)/H (syringyl (S), guaiacyl (G), and *p*-hydroxyphenyl (H)) unit ratios can be observed. Ru/C and Pd/C hexane residues have a higher amount of syringyl and guaiacyl units, while P1000 lignin and CLO MeOH contain higher amounts of p-hydroxyphenyl units. This difference is the effect of the used feedstock: birch wood, a hard wood (Ru/C and Pd/C hexane residues), versus wheat straw (P1000 lignin and CLO MeOH). The weight average molecular weight (M_w) and dispersity are the highest for P1000 wheat straw soda lignin, while CLO MeOH, obtained after P1000 lignin methanolysis, demonstrates a lower molecular weight by a factor of 2 compared to P1000 lignin, along with a narrower dispersity. The Ru/C and Pd/C hexane residues exhibited very low molecular weights. Monomers, dimers, and oligomers were present in the sample as a result of RCF depolymerization (Figure S2, Appendix). The observed differences in functional group content and M_w between the four lignin fractions are explained mainly by application of the different process technologies and to a minor extent the biomass source, i.e., lignin isolation from wheat straw *via* the soda process, followed by methanolysis of the obtained P1000 soda lignin *versus* the RCF of birch wood.

Table 1 *Characterization of lignin-based fractions by ^{31}P NMR spectroscopy and GPC*

Sample	Source	Phen. OH[a]	Aliph. OH[a]	COOH[a]	Phen. OH of (S+G)/H type ratio[a]	M_w[b]	M_n[b]	Đ[b]
		[mmol/g]	[mmol/g]	[mmol/g]	[%]	[kDa]	[kDa]	[-]
Ru/C hexane residue	Birch wood (hardwood)[c]	3.47	2.70	0.09	96/4	1.7	0.7	2.6
Pd/C hexane residue	Birch wood (hardwood)[d]	3.43	4.33	0.12	98/2	0.8	0.6	1.4
CLO MeOH	P1000 lignin (wheat straw)[e]	3.22	1.27	0.35	85/15	2.3	1.1	2.1
P1000 lignin	wheat straw[f]	3.71	1.80	0.95	85/15	4.3	1.9	2.6

[a] phenolic OH of syringyl (S), guaiacyl (G) and p-hydroxyphenyl (H) contemt and ratio determined by ^{31}P NMR spectroscopy, [b] based on THF GPC, after acetylation, only the oligomeric fraction was quantified therefore it is not fully representative for the whole sample (monomers and dimers are outside the quantification region of 370 – 2 520 000 Da) [c] depolymerized over Ru/C catalyst, extracted, hexane residue, [d] depolymerized over Pd/C catalyst, extracted, hexane residue, [e] mild solvolysis fractionation, [f] soda pulping, commercial lignin sample

The above-described lignin fractions could not be dissolved in castor oil, and the resulting dispersions obtained instead were not stable. Therefore, the lignin fractions had to be modified with aliphatic chains to improve the compatibility (miscibility or dispersibility) with castor oil. To increase the lipophilicity of lignin, esterification by palmitic chloride was chosen.[14, 44, 45] Importantly, only partial esterification of the phenolic OH moieties in the lignin structure was performed, as these OH groups are responsible for the targeted antioxidant properties. The results of lignin palmitoylation are summarized in Table 2. In all cases, aliphatic hydroxyl groups were modified to a higher extent than phenolic hydroxyl groups. This can be attributed to a depletion of palmitoylating agent and competition between aliphatic and aromatic OH groups. Pyridine as the catalyst was indeed previously described to favor aliphatic rather than aromatic hydroxyl moieties.[46] The molecular weight of all the modified fractions increased compared to the unmodified fractions which is expected (Figure S3, Appendix). Additionally, GC-FID analysis of palmitoylated lignin fractions (detailed data available in Appendix, Table S2) revealed that there were no lignin monomers in P1000 or CLO MeOH palmitoylated fractions and almost no nonpalmitolyated monomeric compounds in Ru/C and Pd/C samples (below 3.5%). All of the samples contained some free palmitic acid (4-16 wt.%).

Chapter 4

Table 2 *Summary of the esterification results based on ^{31}P NMR spectroscopy*

Sample	Palm. moieties	Esterif. degr.[b]	Free phen. OH[a]	Free aliph. OH[a]	Phen. OH of (S+G)/H type ratio[a]	M_w[c]	M_n[c]	Đ[c]
	[mmol/g]	[% total OH]	[mmol/g]	[mmol/g]	[%]	[kDa]	[kDa]	[-]
Ru/C hexane residue, palmitoylated	1.91	75	0.82	0.06	100/0	2.8	2.2	1.29
Pd/C hexane residue, palmitoylated	1.5	40	2.02	0.63	99/1	1.7	2.0	1.20
CLO MeOH, palmitoylated	1.61	73	0.74	0.06	79/21	3.9	2.1	1.82
P1000 lignin, palmitoylated	1.72	71	0.67	0.26	90/10	9.8	5.3	1.84

[a] phenolic OH of syringyl (S), guaiacyl (G) and p-hydroxyphenyl (H) type ratio determined by ^{31}P NMR spectroscopy, [b] Calculated as described by Koivu et al.[45] Calculations are based on a theoretical lignin mass percentage in a lignin ester.

$$m(\%)lignin = \frac{1-m(H\%)}{1-m(H\%)+m(R\%)} \times 100\% = \frac{1-[(\frac{PalmCl}{Lignin}) \times (OH) \times M(H)]}{1+[(\frac{PalmCl}{Lignin}) \times (OH) \times M(R)]} \times 100\%$$, Where: PalmCl/Lignin

is the molar ratio of added palmitoyl chloride to lignin (equiv); (OH) is the total hydroxyl content of lignin in mmol/g; m(H%) and m(R%) are mass effects related to the hydrogen (H) and palmitic acyl group (R), where M(H) = 1 g/mol and M(R) = 239 g/mol, [c] based on THF GPC, after acetylation, only the oligomeric fraction was quantified, therefore it is not fully representative for the whole sample (palmitoylated monomers and dimers with molecular weight below 1000 Da were not quantified).

Lignin fractions antioxidant activity

Limited oxidative stability is the main disadvantage of the current industrial use of vegetable oils as lubricants. Therefore, this aspect needs to be improved by either chemical modification of the base oils or by the addition of an antioxidant. Butylated hydroxytoluene (BHT) is a commonly used synthetic antioxidant, next to other antioxidants such as propyl gallate, ascorbyl palmitate, butylated hydroxyanisole, mono-tert-butylhydroquinone, and 4,4′-methylenebis(2,6-di-tert-butylphenol), whose role is to increase oxidative stability in lubricants.[27, 45 47] The mechanism of BHT's antioxidant activity is free radical scavenging by hydrogen atom transfer.[48] The radical of a phenolic compound such as BHT is more stable than a lipid or a lipid peroxy radical due to the delocalization of the unpaired electron throughout the π system in the phenolic ring structure, which is additionally stabilized by the *tert*-butyl substituent in the para position. Additionally, hydrogen atom transfer between antioxidants like BHT and the lipid peroxy or lipid radicals of oil is thermodynamically driven, hereby blocking the propagation of peroxy radicals within oil structures. Lignin is known for its antioxidant properties: in reactions with free radicals it forms resonance-stabilized radicals *via* a mechanism similar to BHT (Figure 3).[49, 50] Since

lignin has a more complex chemical structure than BHT, additional factors influence lignin's antioxidant activity, such as the molecular weight, the amount of phenolic OH and methoxy groups (introducing more resonance stabilization), the possible presence of conjugated carbonyl groups in the side chain and aliphatic OH groups (both having a negative effect on antioxidant activity).[10, 49-57] Moreover, carbohydrate impurities can decrease the antioxidant activity due to hydrogen bonding with lignin phenolic groups.[50, 58] The results presented in available literature suggest that the phenolic hydroxyl group content is a very important factor, next to molecular weight, and is responsible for the antioxidant activity of lignin. [53, 54, 56] Therefore, all the lignin concentrations in the antioxidant activity assay and the oxidative induction time studies were based only on the phenolic hydroxyl group content. [21]
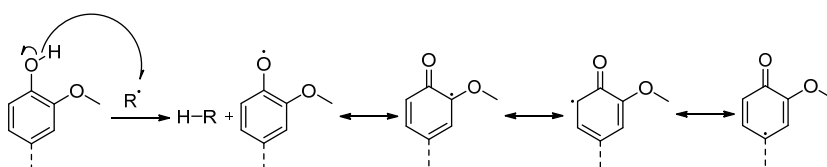
Figure 3 *Radical formation on lignin via hydrogen atom transfer mechanism. Adapted from ref. 52*

To compare the antioxidant activity of the lignin fractions under study, the 2,2-diphenyl-1-picrylhydrazyl (DPPH) assay was used to determine radical scavenging activity of the lignin fractions. The activity of each fraction, before and after palmitoylation, was benchmarked with BHT, which is a commonly used antioxidant. The inhibition profile as a function of antioxidant concentration (available in Appendix, Figure S4) was used to determine IC_{50} values. The corresponding data are summarized in Figure 3. IC_{50} is the concentration of the antioxidant compound required to scavenge 50% of DPPH radicals. The lower the IC_{50} value is, the higher the radical scavenging activity of the component. Pure castor oil and fully palmitoylated P1000 lignin references did not exhibit significant antioxidant activity (available in Appendix, Figure S4).

As palmitoylation will change the chemical properties of the samples, the IC_{50} values of all samples were presented as both molar and mass concentrations. Generally, antioxidant properties are compared based on IC_{50} mass concentration, however, in this case we aimed to compare the samples before and after palmitoylation based on molar concentration of the phenolic OH as well. Palmitoylation of lignin caused a significant decrease in the amount of the phenolic OH groups, which is the moiety responsible for antioxidant activity. Therefore, to fairly compare the antioxidant potential of these samples both manners were used. In Figure 4A and B, it is shown that the best results, i.e., the lowest IC_{50}, are obtained for Pd/C hexane residue, followed by Ru/C hexane residue, CLO MeOH, and P1000 lignin. The same trend is

Chapter 4

observed before and after palmitoylation, irrespective of the IC_{50} calculation on a molar or weight basis. The results on weight basis in Figure 4B-D reveal that, for each lignin sample, modification has a negative influence on the antioxidant activity, as could be expected due to the reduction of free phenolic OH groups as well as the contribution of the incorporated palmitoyl chain to the increase of M_W. BHT shows similar antioxidant activity compared to palmitoylated CLO MeOH and is better than palmitoylated P1000 lignin. Notably, the palmitoylated Ru/C and Pd/C hexane residues outperform BHT in terms of radical scavenging activity on a weight basis with a factor of 2.5 to 6, respectively. When the results are standardized based on the molar concentration of free phenolic OH, all lignin-based samples outperform BHT by a factor between 4 (palmitoylated P1000 lignin) and 20 (palmitoylated Pd/C hexane residue sample). Although it was reported in literature that lignin could have lower an IC_{50} than BHT, usually the difference was not that pronounced.[29, 51, 59, 60]

The molecular weight of the lignin fractions (Figure 4C) partly explains the observed IC_{50} values: a decreasing molecular weight favors better performance of lignin as an antioxidant, a trend that is in line with the literature.[51, 59, 61, 62] Moreover, methoxy-substituted phenolic units exhibit increased stabilization of the radicals. Therefore, lignin fractions with higher syringyl (two methoxy groups) and guaiacyl (one methoxy group) units are reported to contribute to the increased antioxidant property compared to fractions with higher content of p-hydroxyphenyl (one OH and zero methoxy groups) units.[10, 49-51, 53] Thus, the higher content of phenolic OH of the S+G type in nonpalmitoylated RCF samples (Ru/C and Pd/C hexane residues) compared to P1000 samples (CLO MeOH and P1000 lignin) can explain why RCF samples have lower IC_{50} values than P1000 derived samples (Table 2). For the Ru/C and Pd/C hexane residues, the presence of low molecular weight fractions and higher monomer content (10% vs. 50%, respectively) may lead to improved antioxidant properties. [55]
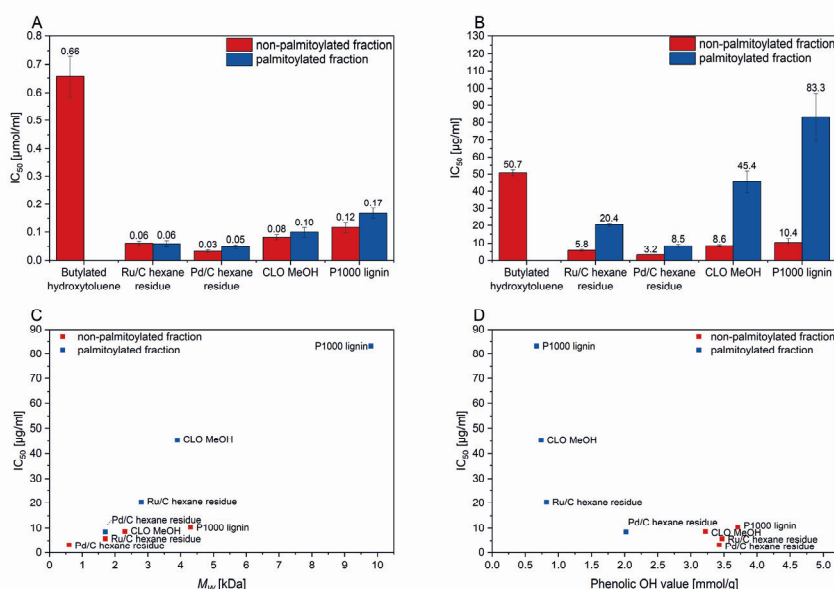
Figure 4 *IC$_{50}$ values of lignin-based modified and unmodified fractions obtained in the DPPH antioxidant activity assays, A: molar-based comparison, B: weight-based comparison, C: IC$_{50}$ as a function of MW, D: IC$_{50}$ as a function of phenolic OH value for the different lignin fractions (modified and unmodified)*

The use of lignin fractions in biolubricant formulations

Next to the evaluation of antioxidant capabilities of the different lignin fractions, the antioxidant effect of lignin vs. BHT in castor oil-based lubricants was assessed in oxidative induction time (OIT) studies. This allows for direct evaluation of the resistance to oxidation of formulated lubricants, instead of measuring the scavenging activity of pure antioxidants, as is the case for the DPPH assay. In OIT studies, the radicals are generated *in situ* during the exposure of the material to oxygen at elevated temperatures. The antioxidant effect is observed by delay of the starting point of the material oxidation. Oil oxidation is an exothermic process involving release of heat, which is recorded by DSC. Thermal oxidation of triglyceride-based vegetable oils is related to the unsaturation degree of the fatty acid chains.[48, 63] Double bonds are the active sites of oxidation by the free radical mechanism.[48, 63] First, a hydrogen atom from a methylene group next to a double bond in the fatty acid is abstracted and a lipid radical is formed. This radical subsequently reacts with oxygen, and peroxy radicals are formed. The lipid peroxy radicals can then remove a hydrogen atom from the next fatty acid chain, forming a lipid hydroperoxide and new lipid radical, propagating the autoxidation process. The O-O bond in a hydroperoxide functional group can break easily homolytically, explaining that hydroperoxides are a source of more free radicals. Such a branching step leads to the proliferation of radicals and assists in the propagation of more hydroperoxides,

Chapter 4

which continue to build up in the oil *via* propagation and branching steps. Ultimately, the hydroperoxides are decomposed into volatile and nonvolatile low molecular weight compounds. Alternatively, polymerization reactions may result in polymeric film formation.[48, 63]

To ensure a fair comparison between the lignin samples with varying phenolic OH content, the amount of palmitoylated lignin dispersed in castor oil was adjusted accordingly. Each lignin sample set was tested with a final concentration of 0.007, 0.034, and 0.071 mmol of free phenolic OH per 1 g of castor oil. The effect of various lignin-based antioxidants in different concentrations in a castor oil matrix on the thermal oxidation stability was illustrated by OIT studies, visualized in Figure 5 (examples of DSC OIT curves for a concentration of 0.034 mmol antioxidant/g oil are presented in Figure S1, Appendix). In general, for all tested additives, there is a clear trend of increased OIT with an increased amount of antioxidant within the tested concentration range. The OIT of pure castor oil is 22 min, and the OIT increases slightly after the addition of 0.007 mmol of antioxidant/g of oil. Notably, at higher antioxidant concentrations of 0.034 mmol/g oil, the OIT improves almost 3-fold for all of the antioxidants. A further increase to 86-118 min, or a 3.8-5.4 times improvement over pure castor oil, is observed at a concentration of 0.071 mmol/g. As shown in Figure 5, at various concentrations, the tested lignin-based antioxidants have a similar antioxidative influence on castor oil at 180 °C, compared to BHT, except for the highest loading of Pd/C palmitoylated hexane residue, which provides superior thermal oxidative stability to the oil, by almost 1.5 times compared to BHT. OIT of fully palmitoylated P1000 lignin was 25 and 27 min for 5 and 10 wt.%, respectively. This difference is insignificant compared with other lignin fractions described in this study, and we prove that lignin antioxidant performance is strongly related to its phenolic OH content. Other works, such as the findings of Kasprzycka-Guttman and Odzeniak, showed that the addition of lignin to arachide oil improves OIT slightly more than BHT.[28] Chandrasekaran *et al.* showed that the addition of lignin pyrolisate bio-oil exhibited similar antioxidant performance to BHT in soy methyl ester biodiesel.[24]
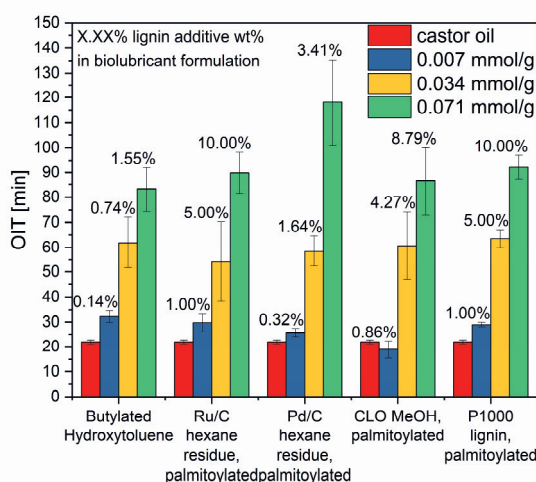
Figure 5: *Oxidation induction time of castor oil and biolubricant formulations with varying concentrations of esterified lignin-based additives, determined by DSC at 180 °C under an air flow*

Viscosity is an important rheological lubricant parameter, since it determines the lubricant's resistance to flow. The rheological behavior of a given lubricant is determined by the base oil and the additives. For instance, most of the oils exhibit Newtonian behavior, while lubricating greases and multigrade oils containing viscosity modifiers are often characterized by non-Newtonian behavior, such as shear thinning.[64] As depicted in Figure 6A, the difference between viscosities at high and low shear rates is marginal for BHT, modified Ru/C and Pd/C hexane residues in castor oil-based dispersions, indicating Newtonian behavior. The dispersions containing CLO MeOH and P1000 modified fractions, show shear thinning behavior, which becomes more pronounced at higher additive concentrations (see the example in Figure 6B). Shear thinning is generally considered to be a result of microscale structural rearrangements and changes in molecular conformations within the fluid that facilitate shearing.[65] Shear thinning is often observed in lubricants and can affect the behavior of the lubricant at different deformation rates. Non-Newtonian samples were fitted in the Sisko model (Table S3, Appendix) to determine their infinite shear viscosity, which is comparable with their viscosity at 1000 s^{-1}. Moreover, the addition of lignin-based additives affects the viscosity of the biolubricant formulation (Figure 6B). Relative to castor oil, the increase of the relative viscosity is the most pronounced for P1000 and CLO MeOH palmitoylated lignins (Figure 6C) rather than Ru/C and Pd/C palmitoylated hexane residues. BHT, and Ru/C and Pd/C lignin oligomers have a small effect on the viscosity of the formulations; the increase is below 6% for the highest concentrations, while for P1000 lignin we observe up to an 80% increase. This phenomenon correlates well

with the increased molecular weights of P1000 and CLO MeOH lignins compared to BHT, and Ru/C and Pd/C palmitoylated hexane residues (Figure 6D).
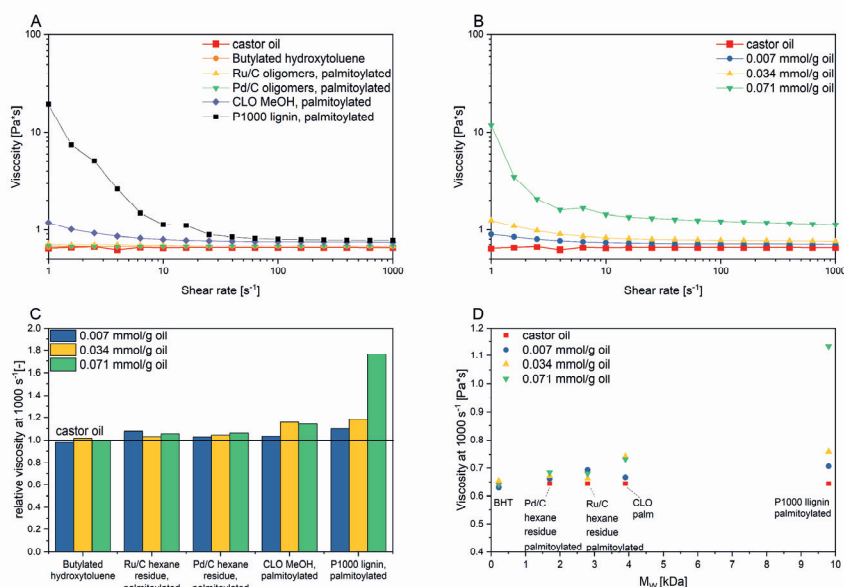
Figure 6 A: Viscosity as a function of shear rate of castor oil and biolubricant formulations with esterified lignin-based additives (0.034 mmol/g oil additive), B: comparison of the viscosity difference as a function of lignin concentration (example: P1000 lignin palmitoylated), C: relative viscosity of the biolubricant formulations compared to pure castor oil, D: viscosity at high shear rate of castor oil and biolubricant formulations as a function of molecular weight of esterified lignin-based additives

Vegetable oils are known for their excellent tribological performance, and the aim of this work was to maintain them in the lubricants formulations with lignin-based antioxidative additives. The main goal of using lubricants in the first place is protection of the metal surface and heat transfer from friction spots. In the case of vegetable oils, consisting of triglycerides, surface protection is attained through adsorption of the polar part of the oil molecules (ester groups in triglycerides) to the metal surface, resulting in the creation of a barrier, which is responsible for decreasing the coefficient of friction.[4, 66] Previously, lignin was demonstrated to possess antiwear properties in matrices such as various ionic liquids,[67, 68] PEG, and ethylene glycol.[22, 69, 70]

As shown in Figure 7A, lignin-based additives and BHT demonstrate minor to no effect in decreasing the coefficient of friction between the metal surfaces, compared to castor oil. A similar coefficient of friction, ranging between 0.10 and 0.13, was obtained for all formulations, in line with other vegetable oils.[71, 72] A desired reduction of the wear volume (Figure 7B-D) was also observed in several of the tested

biolubricant formulations. It ranges from 0.004 to 0.006 mm^3 for the formulations containing lignin-based additives, while for pure castor oil the value is 0.006 mm^3. BHT and the palmitoylated Pd/C hexane residue demonstrate the biggest reduction in wear volume, which is 30-40% decreased compared to the wear volume caused by castor oil. The remaining lignin samples caused a reduction of the wear volume, while at some concentrations no significant difference was observed compared to castor oil. However, the wear scar diameter is slightly higher when the additive is wear volume by less than 25%, added, in the range of 1.04-1.19 mm, while pure castor oil caused a 1.07 mm scar (Figure S5, Appendix). Most of the formulations with lignin additives exhibited a similar wear scar diameter as the BHT-containing formulations. Although the scar diameter is similar or slightly higher, its depth is lower than for the castor oil reference (Figure 7C-D, Table S4 in Appendix), which results in a reduction of the wear volume. Overall, when considering the three tested tribological parameters, Pd/C palmitoylated hexane residue demonstrated the best results, and it is comparable with BHT performance. Those results indicate that lignin-based antioxidants have the potential to create a good quality lubricating film, and some of them bring antiwear properties to the above-mentioned biolubricant formulations.

Chapter 4
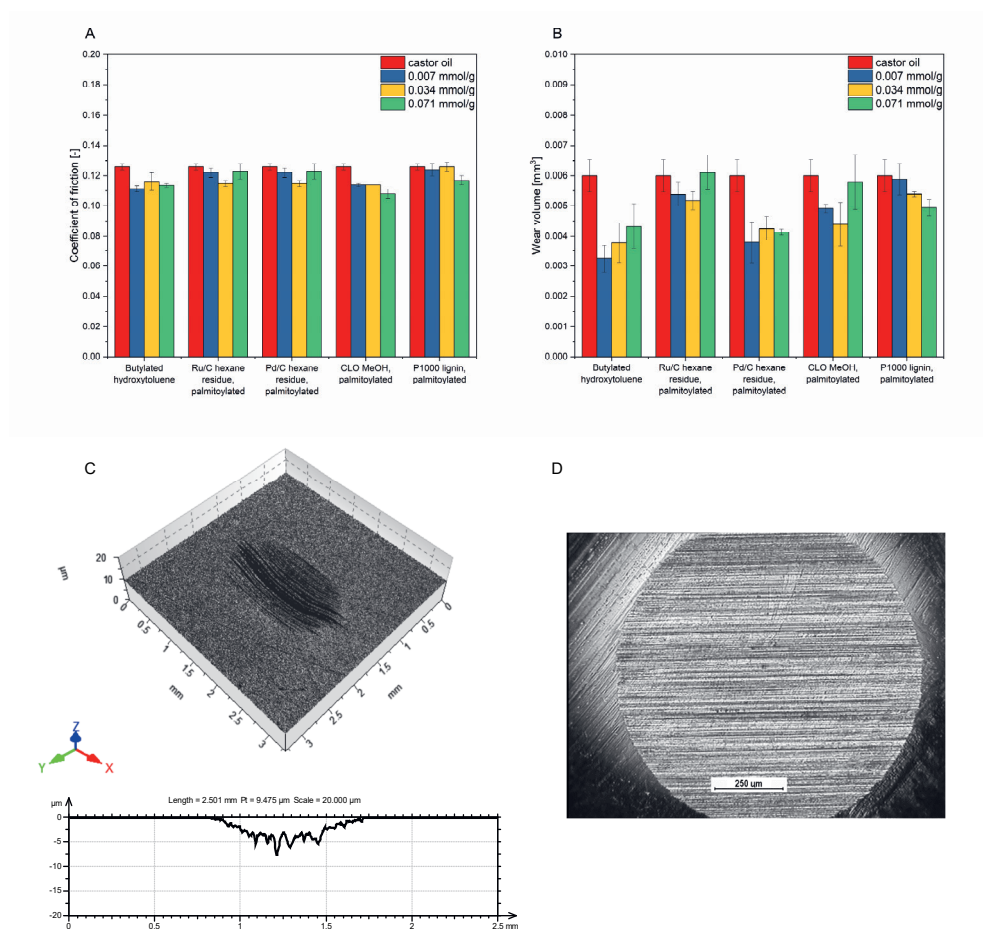
Figure 7 *Tribology results of castor oil and biolubricant formulations with esterified lignin-based additives: A: Coefficient of friction, B: Wear volume, C: 3D image and profile of the wear track in the disc, D: scars in the ball (C, D: example: Pd/C hexane residue, palmitoylated, 0.034mmol/g oil biolubricant)*

Conclusions

Poor thermo-oxidative stability is the main disadvantage of the use of pure vegetable oil as a biolubricant. In this work, we successfully demonstrate the use of novel, lignin-based antioxidant additives in vegetable oil formulations. Four different lignin fractions were partially modified by the introduction of palmitoyl moieties, in order to increase their lipophilicity, after which good dispersibility in the castor oil matrix was demonstrated. All studied lignin-based antioxidants were benchmarked with BHT, a commercially used antioxidant. DPPH assays on modified and unmodified lignin fractions proved increased radical scavenging properties of these lignins compared

to BHT. The best results were obtained with low molecular weight lignin-based fractions possessing a high S+G hydroxyl content. From the biolubricant perspective, an especially interesting additive was palmitoylated Pd/C hexane residue obtained by reductive catalytic fractionation (RCF) of birch wood, which showed better OIT than BHT, while the rest of the additives showed similar performance with BHT. Moreover, formulations with modified lignin-based additives exhibited lubrication properties comparable to BHT in tribological and rheological tests. This proof-of-principle application research is providing an added value for both biomaterials, lignin and castor oil by showing more possibilities in their valorization. We believe that it is possible to use these materials for other applications than biolubricants, such as cosmetics and pharmaceutics, due to lignin's biocompatibility and low cytotoxicity.

Chapter 4

References

1.   Syahir, A. Z.; Zulkifli, N. W. M.; Masjuki, H. H.; Kalam, M. A.; Alabdulkarem, A.; Gulzar, M.; Khuong, L. S.; Harith, M. H., A review on bio-based lubricants and their applications. *J. Cleaner Prod.* **2017,** *168*, 997-1016.

2.   Murru, C.; Badía-Laíño, R.; Díaz-García, M. E., Oxidative Stability of Vegetal Oil-Based Lubricants. *ACS Sustainable Chem. Eng.* **2021,** *9* (4), 1459-1476.

3.   Zainal, N. A.; Zulkifli, N. W. M.; Gulzar, M.; Masjuki, H. H., A review on the chemistry, production, and technological potential of bio-based lubricants. *Renewable Sustainable Energy Rev.* **2018,** *82*, 80-102.

4.   Panchal, T. M.; Patel, A.; Chauhan, D. D.; Thomas, M.; Patel, J. V., A methodological review on bio-lubricants from vegetable oil based resources. *Renewable Sustainable Energy Rev.* **2017,** *70*, 65-70.

5.   Quinchia, L. A.; Delgado, M. A.; Reddyhoff, T.; Gallegos, C.; Spikes, H. A., Tribological studies of potential vegetable oil-based lubricants containing environmentally friendly viscosity modifiers. *Tribol. Int.* **2014,** *69*, 110-117.

6.   Suhane, A.; Sarviya, R. M.; Rehman, A.; Khaira, H. K., Suitability of Alternative Lubricants for Automotive Gear Applications. *Int. J. Eng. Res. Appl.* **2014,** *4* (3), 64-67.

7.   Sels, B.; Philippaerts, A., *Conjugated Linoleic Acids and Conjugated Vegetable Oils*. Royal Society of Chemistry: 2014; p 117-130.

8.   Patel, V. R.; Dumancas, G. G.; Kasi Viswanath, L. C.; Maples, R.; Subong, B. J. J., Castor Oil: Properties, Uses, and Optimization of Processing Parameters in Commercial Production. *Lipid insights* **2016,** *9*, 1-12.

9.   Kai, D.; Tan, M. J.; Chee, P. L.; Chua, Y. K.; Yap, Y. L.; Loh, X. J., Toward lignin-based functional materials in a sustainable world. *Green Chem.* **2016,** *18* (5), 1175-1200.

10.   Kim, J.-Y.; Johnston, P. A.; Lee, J. H.; Smith, R. G.; Brown, R. C., Improving Lignin Homogeneity and Functionality via Ethanolysis for Production of Antioxidants. *ACS Sustain. Chem. Eng.* **2019,** *7* (3), 3520-3526.

11.   Liu, X.; Bouxin, F. P.; Fan, J.; Budarin, V. L.; Hu, C.; Clark, J. H., Recent Advances in the Catalytic Depolymerization of Lignin toward Phenolic Chemicals: A Review. *ChemSusChem* **2020,** *13* (17), 4296-4317.

12.   Chio, C.; Sain, M.; Qin, W., Lignin utilization: A review of lignin depolymerization from various aspects. *Renewable Sustainable Energy Rev.* **2019,** *107*, 232-249.

13.   Sun, Z.; Fridrich, B.; de Santi, A.; Elangovan, S.; Barta, K., Bright Side of Lignin Depolymerization: Toward New Platform Chemicals. *Chem. Rev.* **2018,** *118* (2), 614-678.

14.   Wang, C.; Kelley, S. S.; Venditti, R. A., Lignin-Based Thermoplastic Materials. *ChemSusChem* **2016,** *9* (8), 770-783.

15.   Schutyser, W.; Renders, T.; Van den Bosch, S.; Koelewijn, S. F.; Beckham, G. T.; Sels, B. F., Chemicals from lignin: an interplay of lignocellulose fractionation, depolymerisation, and upgrading. *Chem. Soc. Rev.* **2018,** *47* (3), 852-908.

16.   Acar, N.; Kuhn, E.; Franco, J., Tribological and Rheological Characterization of New Completely Biogenic Lubricating Greases: A Comparative Experimental Investigation. *Lubricants* **2018,** *6* (2), 45-56.

17.   Gallego, R.; Arteaga, J. F.; Valencia, C.; Díaz, M. J.; Franco, J. M., Gel-Like Dispersions of HMDI-Cross-Linked Lignocellulosic Materials in Castor Oil: Toward Completely Renewable Lubricating Grease Formulations. *ACS Sustain. Chem. Eng.* **2015,** *3* (9), 2130-2141.

18.   Borrero-López, A. M.; Martín-Sampedro, R.; Ibarra, D.; Valencia, C.; Eugenio, M. E.; Franco, J. M., Evaluation of lignin-enriched side-streams from different biomass conversion processes as thickeners in bio-lubricant formulations. *Int. J. Biol. Macromol.* **2020,** *162*, 1398-1413.

19.   Delgado, M. A.; Cortés-Triviño, E.; Valencia, C.; Franco, J. M., Tribological study of epoxide-functionalized alkali lignin-based gel-like biogreases. *Tribol. Int.* **2020,** *146*, 106231.

20.   Hua, J.; Shi, Y., Non-corrosive Green Lubricant With Dissolved Lignin in Ionic Liquids Behave as Ideal Lubricants for Steel-DLC Applications. *Front. Chem.* **2019,** *7* (857), 1-8.

21.   Mu, L.; Shi, Y.; Guo, X.; Wu, J.; Ji, T.; Chen, L.; Feng, X.; Lu, X.; Hua, J.; Zhu, J., Enriching Heteroelements in Lignin as Lubricating Additives for Bioionic Liquids. *ACS Sustain. Chem. Eng.* **2016,** *4* (7), 3877-3887.

22.   Mu, L.; Shi, Y.; Wang, H.; Zhu, J., Lignin in Ethylene Glycol and Poly(ethylene glycol): Fortified Lubricants with Internal Hydrogen Bonding. *ACS Sustainable Chem. Eng.* **2016,** *4* (3), 1840-1849.

23.   Cortés-Triviño, E.; Valencia, C.; Franco, J. M., Influence of epoxidation conditions on the rheological properties of gel-like dispersions of epoxidized kraft lignin in castor oil. *Holzforschung* **2017,** *71* (10), 777-784.

24.   Chandrasekaran, S. R.; Murali, D.; Marley, K. A.; Larson, R. A.; Doll, K. M.; Moser, B. R.; Scott, J.; Sharma, B. K., Antioxidants from Slow Pyrolysis Bio-Oil of Birch Wood: Application for Biodiesel and Biobased Lubricants. *ACS Sustain. Chem. Eng.* **2016,** *4* (3), 1414-1421.

25.   Larson, R. A.; Sharma, B. K.; Marley, K. A.; Kunwar, B.; Murali, D.; Scott, J., Potential antioxidants for biodiesel from a softwood lignin pyrolyzate. *Ind. Crops Prod.* **2017,** *109*, 476-482.

26.   Cesari, L.; Mutelet, F.; Canabady-Rochelle, L., Antioxidant properties of phenolic surrogates of lignin depolymerisation. *Ind. Crops Prod.* **2019,** *129*, 480-487.

27.   Quinchia, L. A.; Delgado, M. A.; Valencia, C.; Franco, J. M.; Gallegos, C., Natural and Synthetic Antioxidant Additives for Improving the Performance of New Biolubricant Formulations. *J. Agric. Food Chem.* **2011,** *59* (24), 12917-12924.

28.   Kasprzycka-Guttman, T.; Odzeniak, D., Antioxidant properties of lignin and its fractions. *Thermochim. Acta* **1994,** *231*, 161-168.

29.   Kaur, R.; Uppal, S. K., Structural characterization and antioxidant activity of lignin from sugarcane bagasse. *Colloid Polym. Sci.* **2015,** *293* (9), 2585-2592.

30.   Kouris, P. D.; van Osch, D. J. G. P.; Cremers, G. J. W.; Boot, M. D.; Hensen, E. J. M., Mild thermolytic solvolysis of technical lignins in polar organic solvents to a crude lignin oil. *Sustainable Energy Fuels* **2020,** *4* (12), 6212-6226.

31.   Liao, Y.; Koelewijn, S.-F.; Van den Bossche, G.; Van Aelst, J.; Van den Bosch, S.; Renders, T.; Navare, K.; Nicolaï, T.; Van Aelst, K.; Maesen, M.; Matsushima, H.; Thevelein, J. M.; Van Acker, K.; Lagrain, B.; Verboekend, D.; Sels, B. F., A sustainable wood biorefinery for low–carbon footprint chemicals production. *Science* **2020,** *367* (6484), 1385-1390.

32.   Abu-Omar, M. M.; Barta, K.; Beckham, G. T.; Luterbacher, J. S.; Ralph, J.; Rinaldi, R.; Román-Leshkov, Y.; Samec, J. S. M.; Sels, B. F.; Wang, F., Guidelines for performing lignin-first biorefining. *Energy Environ. Sci.* **2021,** *14* (1), 262-292.

33.   Van Aelst, K.; Van Sinay, E.; Vangeel, T.; Cooreman, E.; Van den Bossche, G.; Renders, T.; Van Aelst, J.; Van den Bosch, S.; Sels, B. F., Reductive catalytic fractionation of pine wood: elucidating and quantifying the molecular structures in the lignin oil. *Chem. Sci.* **2020,** *11* (42), 11498-11508.

34.   Cooreman, E.; Vangeel, T.; Van Aelst, K.; Van Aelst, J.; Lauwaert, J.; Thybaut, J. W.; Van den Bosch, S.; Sels, B. F., Perspective on Overcoming Scale-Up Hurdles for the Reductive Catalytic Fractionation of Lignocellulose Biomass. *Ind. Eng. Chem. Res.* **2020,** *59* (39), 17035-17045.

35.   van Baarle, D. Vertoro scales up oil production from lignin. https://www.industryandenergy.eu/biobased-economy/vertoro-scales-up-oil-production-from-lignin/ (accessed 01.07.2021).

36.   Mannari, V.; Patel, C. J., *Understanding Coatings Raw Materials*. Vincentz Network: 2015.

37.   Naik, S. N.; Saxena, D. K.; Dole, B. R.; Khare, S. K., Chapter 21 - Potential and Perspective of Castor Biorefinery. In *Waste Biorefinery*, Bhaskar, T.; Pandey, A.; Mohan, S. V.; Lee, D.-J.; Khanal, S. K., Eds. Elsevier: 2018; pp 623-656.

38.   Kouris, P. D.; Boot, M. D.; Hensen, E. J. M.; Oevering, H. A method for obtaining a stable lignin: polar organic solvent composition via mild solvolytic modifications. WO 2019/053287, 2019.

Chapter 4

39.   Van den Bosch, S.; Schutyser, W.; Vanholme, R.; Driessen, T.; Koelewijn, S. F.; Renders, T.; De Meester, B.; Huijgen, W. J. J.; Dehaen, W.; Courtin, C. M.; Lagrain, B.; Boerjan, W.; Sels, B. F., Reductive lignocellulose fractionation into soluble lignin-derived phenolic monomers and dimers and processable carbohydrate pulps. *Energy Environ. Sci.* **2015,** *8* (6), 1748-1763.

40.   Korntner, P.; Sumerskii, I.; Bacher, M.; Rosenau, T.; Potthast, A., Characterization of technical lignins by NMR spectroscopy: optimization of functional group analysis by 31P NMR spectroscopy. *Holzforschung* **2015,** *69* (6), 807-814.

41.   Meng, X.; Crestini, C.; Ben, H.; Hao, N.; Pu, Y.; Ragauskas, A. J.; Argyropoulos, D. S., Determination of hydroxyl groups in biorefinery resources via quantitative 31P NMR spectroscopy. *Nat. Protoc.* **2019,** *14* (9), 2627-2647.

42.   Gosselink, R. J. A.; Abächerli, A.; Semke, H.; Malherbe, R.; Käuper, P.; Nadif, A.; van Dam, J. E. G., Analytical protocols for characterisation of sulphur-free lignin. *Ind. Crops Prod.* **2004,** *19* (3), 271-281.

43.   de Menezes Nogueira, I.; Avelino, F.; de Oliveira, D. R.; Souza, N. F.; Rosa, M. F.; Mazzetto, S. E.; Lomonaco, D., Organic solvent fractionation of acetosolv palm oil lignin: The role of its structure on the antioxidant activity. *Int. J. Biol. Macromol.* **2019,** *122*, 1163-1172.

44.   Pawar, S. N.; Venditti, R. A.; Jameel, H.; Chang, H.-M.; Ayoub, A., Engineering physical and chemical properties of softwood kraft lignin by fatty acid substitution. *Ind. Crops Prod.* **2016,** *89*, 128-134.

45.   Koivu, K. A. Y.; Sadeghifar, H.; Nousiainen, P. A.; Argyropoulos, D. S.; Sipilä, J., Effect of Fatty Acid Esterification on the Thermal Properties of Softwood Kraft Lignin. *ACS Sustain. Chem. Eng.* **2016,** *4* (10), 5238-5247.

46.   Guo, Z.-X.; Gandini, A.; Pla, F., Polyesters from lignin. 1. The reaction of kraft lignin with dicarboxylic acid chlorides. *Polym. Int.* **1992,** *27* (1), 17-22.

47.   Yehye, W. A.; Rahman, N. A.; Ariffin, A.; Abd Hamid, S. B.; Alhadi, A. A.; Kadir, F. A.; Yaeghoobi, M., Understanding the chemistry behind the antioxidant activities of butylated hydroxytoluene (BHT): A review. *Eur. J. Med. Chem.* **2015,** *101*, 295-312.

48.   Choe, E.; Min, D. B., Mechanisms of Antioxidants in the Oxidation of Foods. *Compr. Rev. Food Sci. Food Saf.* **2009,** *8* (4), 345-358.

49.   Ponomarenko, J.; Dizhbite, T.; Lauberts, M.; Viksna, A.; Dobele, G.; Bikovens, O.; Telysheva, G., Characterization of Softwood and Hardwood LignoBoost Kraft Lignins with Emphasis on their Antioxidant Activity. *BioResources* **2014,** *9* (2), 2051-2068.

50.   Espinoza-Acosta, J. L.; Torres-Chávez, P. I.; Ramírez-Wong, B.; López-Saiz, C. M.; Montaño-Leyva, B., Antioxidant, Antimicrobial, and Antimutagenic Properties of Technical Lignins and Their Applications. *BioResources* **2016,** *11* (2), 5452-5481.

51.   Majira, A.; Godon, B.; Foulon, L.; van der Putten, J. C.; Cezard, L.; Thierry, M.; Pion, F.; Bado-Nilles, A.; Pandard, P.; Jayabalan, T.; Aguie-Beghin, V.; Ducrot, P. H.; Lapierre, C.; Marlair, G.; Gosselink, R. J. A.; Baumberger, S.; Cottyn, B., Enhancing the Antioxidant Activity of Technical Lignins by Combining Solvent Fractionation and Ionic-Liquid Treatment. *ChemSusChem* **2019,** *12* (21), 4799-4809.

52.   Pan, X.; Kadla, J. F.; Ehara, K.; Gilkes, N.; Saddler, J. N., Organosolv Ethanol Lignin from Hybrid Poplar as a Radical Scavenger: Relationship between Lignin Structure, Extraction Conditions, and Antioxidant Activity. *J. Agric. Food Chem.* **2006,** *54* (16), 5806-5813.

53.   Alzagameem, A.; Khaldi-Hansen, B. E.; Buchner, D.; Larkins, M.; Kamm, B.; Witzleben, S.; Schulze, M., Lignocellulosic Biomass as Source for Lignin-Based Environmentally Benign Antioxidants. *Molecules* **2018,** *23* (10), 2664-2689.

54.   Dizhbite, T.; Telysheva, G.; Jurkjane, V.; Viesturs, U., Characterization of the radical scavenging activity of lignins--natural antioxidants. *Bioresour. Technol.* **2004,** *95* (3), 309-317.

55.   Sadeghifar, H.; Argyropoulos, D. S., Correlations of the Antioxidant Properties of Softwood Kraft Lignin Fractions with the Thermal Stability of Its Blends with Polyethylene. *ACS Sustain. Chem. Eng.* **2015,** *3* (2), 349-356.

56.   Qin, Z.; Liu, H.-M.; Gu, L.-B.; Sun, R.-C.; Wang, X.-D., Lignin as a Natural Antioxidant: Property-Structure Relationship and Potential Applications. In *Reactive and Functional Polymers Volume One : Biopolymers, Polyesters, Polyurethanes, Resins and Silicones*, Gutiérrez, T. J., Ed. Springer International Publishing: Cham, 2020; pp 65-93.

57.   Ponomarenko, J.; Dizhbite, T.; Lauberts, M.; Volperts, A.; Dobele, G.; Telysheva, G., Analytical pyrolysis – A tool for revealing of lignin structure-antioxidant activity relationship. *J. Anal. Appl. Pyrolysis* **2015**, *113*, 360-369.

58.   Ugartondo, V.; Mitjans, M.; Vinardell, M. P., Comparative antioxidant and cytotoxic effects of lignins from different sources. *Bioresour. Technol.* **2008**, *99* (14), 6683-6687.

59.   Li, Z.; Zhang, J.; Qin, L.; Ge, Y., Enhancing Antioxidant Performance of Lignin by Enzymatic Treatment with Laccase. *ACS Sustain. Chem. Eng.* **2018**, *6* (2), 2591-2595.

60.   Kaur, R.; Uppal, S. K.; Sharma, P., Antioxidant and Antibacterial Activities of Sugarcane Bagasse Lignin and Chemically Modified Lignins. *Sugar Tech* **2017**, *19* (6), 675-680.

61.   Sadeghifar, H.; Wells, T.; Le, R. K.; Sadeghifar, F.; Yuan, J. S.; Jonas Ragauskas, A., Fractionation of Organosolv Lignin Using Acetone:Water and Properties of the Obtained Fractions. *ACS Sustain. Chem. Eng.* **2016**, *5* (1), 580-587.

62.   Guo, Z.; Li, D.; You, T.; Zhang, X.; Xu, F.; Zhang, X.; Yang, Y., New Lignin Streams Derived from Heteropoly Acids Enhanced Neutral Deep Eutectic Solvent Fractionation: Toward Structural Elucidation and Antioxidant Performance. *ACS Sustain. Chem. Eng.* **2020**, *8* (32), 12110-12119.

63.   Fox, N. J.; Stachowiak, G. W., Vegetable oil-based lubricants—A review of oxidation. *Tribol. Int.* **2007**, *40* (7), 1035-1046.

64.   Jang, J. Y.; Khonsari, M. M., Lubrication with a Non-Newtonian Fluid. In *Encyclopedia of Tribology*, Wang, Q. J.; Chung, Y.-W., Eds. Springer US: Boston, MA, 2013; pp 2146-2151.

65.   Daugan, S.; Talini, L.; Herzhaft, B.; Allain, C., Aggregation of particles settling in shear-thinning fluids. *Eur. Phys. J. E* **2002**, *7* (1), 73-81.

66.   Adhvaryu, A.; Biresaw, G.; Sharma, B. K.; Erhan, S. Z., Friction Behavior of Some Seed Oils: Biobased Lubricant Applications. *Ind. Eng. Chem. Res.* **2006**, *45* (10), 3735-3740.

67.   Mu, L.; Ma, X.; Guo, X.; Chen, M.; Ji, T.; Hua, J.; Zhu, J.; Shi, Y., Structural strategies to design bio-ionic liquid: Tuning molecular interaction with lignin for enhanced lubrication. *J. Mol. Liq.* **2019**, *280*, 49-57.

68.   Mu, L.; Shi, Y.; Guo, X.; Ji, T.; Chen, L.; Yuan, R.; Brisbin, L.; Wang, H.; Zhu, J., Non-corrosive Green Lubricants: Strengthened Lignin-[Choline][Amino Acid] Ionic Liquids Interaction via Reciprocal Hydrogen Bonding. *RSC Advances* **2015**, *5*, 66067–66072.

69.   Mu, L.; Wu, J.; Matsakas, L.; Chen, M.; Rova, U.; Christakopoulos, P.; Zhu, J.; Shi, Y., Two important factors of selecting lignin as efficient lubricating additives in poly (ethylene glycol): Hydrogen bond and molecular weight. *Int. J. Biol. Macromol.* **2019**, *129*, 564-570.

70.   Mu, L.; Wu, J.; Matsakas, L.; Chen, M.; Vahidi, A.; Grahn, M.; Rova, U.; Christakopoulos, P.; Zhu, J.; Shi, Y., Lignin from Hardwood and Softwood Biomass as a Lubricating Additive to Ethylene Glycol. *Molecules* **2018**, *23* (3), 537-547.

71.   McNutt, J.; He, Q., Development of biolubricants from vegetable oils via chemical modification. *J. Ind. Eng. Chem.* **2016**, *36*, 1-12.

72.   Ortega-Álvarez, R.; Aguilar-Cortés, G. E.; Hernández-Sierra, M. T.; Aguilera-Camacho, L. D.; García-Miranda, J. S.; Moreno, K. J., Physical and rheological investigation of vegetable oils and their effect as lubricants in mechanical components. *MRS Advances* **2019**, *4* (59-60), 3291-3297.

Chapter 4

Appendix for Chapter 4

Table S1 Comparison of weight percentage of modified lignin in biolubricants formulations

Lignin fraction	Wt.% of lignin fraction for 0.007 mmol OH/g castor oil [%]	Wt.% of lignin fraction for 0.034 mmol OH/g castor oil [%]	Wt.% of lignin fraction for 0.071 mmol OH/g castor oil [%]
Ru/C hexane residue, palmitoylated*	1	5	10
Pd/C hexane residue, palmitoylated	0.32	1.67	3.53
CLO MeOH, palmitoylated	0.88	4.57	9.64
P1000 lignin, palmitoylated	1	5	10

* actual mmol OH/g oil for this fraction is 0.008, 0.043 and 0.091 mmol/g oil for 1, 5 and 10%, respectively
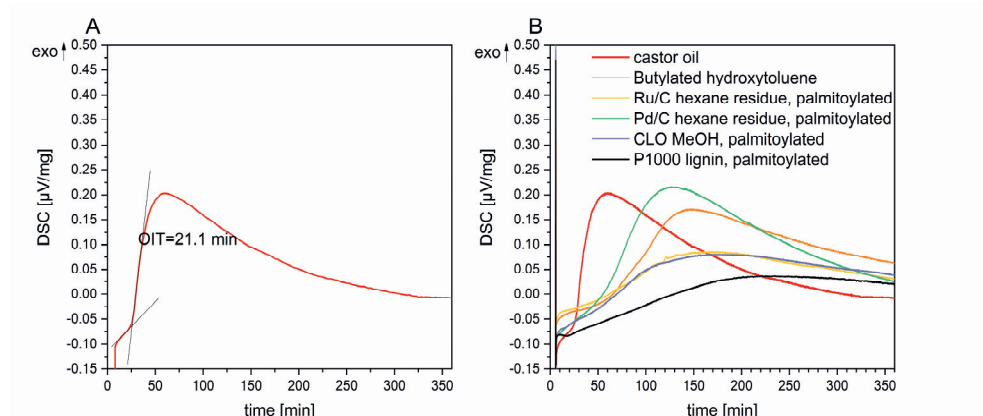
Figure S1 Examples of DSC oxidation induction time curves of A: castor oil, B: biolubricant formulations with 0.034 mmol/g oil esterified lignin-based additives (obtained by isothermal DSC analysis at 180 °C in air flow)

Table S2 *Monomer composition of the oligomeric lignin-based fractions before and after esterification determined by GC-FID analysis*

	Ru/C hex. res. [wt.%]	Pd/C hex. res. [wt.%]	CLO MeOH [wt.%]	P1000 [wt.%]	Ru/C hex. res. palm. [wt.%]	Pd/C hex. res. palm. [wt.%]	CLO MeOH, palm. [wt.%]	P1000, palm. [wt.%]
4-propyl syringol	7.67	0.35	-	-	2.62	0.20	-	-
4-propyl guaiacol	0.50	0.01	-	-	0.48	0.07	-	-
4-propanol guaiacol	0.38	11.71	-	-	-	0.57	-	-
4-propanol syringol	0.98	37.83	-	-	-	1.55	-	-
4-ethyl syringol	0.23	0.36	-	-	0.08	0.04	-	-
palmitic acid	-	-	-	-	8.85	3.89	15.61	6.95
total monomers	9.76	50.26	-	-	3.18 [a]	2.43 [a]	-	-
oligomers[b]	90.24	49.74	100	100	87.97	93.68	84.39	93.05

[a] Palmitoylated monomers in the Ru/C and Pd/C palmitoylated fractions were detected, however, quantification is not performed due to their unknown response factors, caused by large errors on effective carbon number (ECN) calculations of large molecules and unknown volatility, [b] calculated as: oligomers = 100% - (monomers% + palmitic acid%)
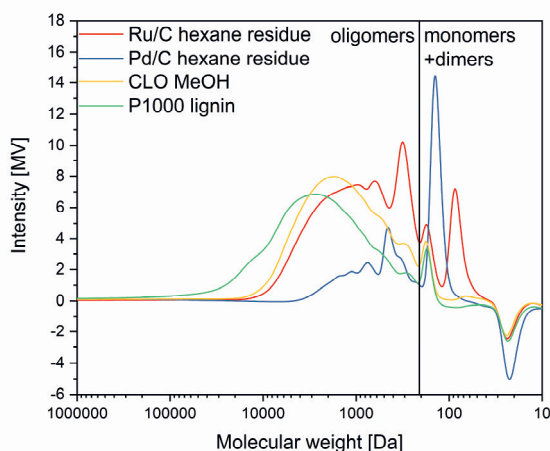
Figure S2 *Overlay of the GPC traces of the unmodified lignin fractions*
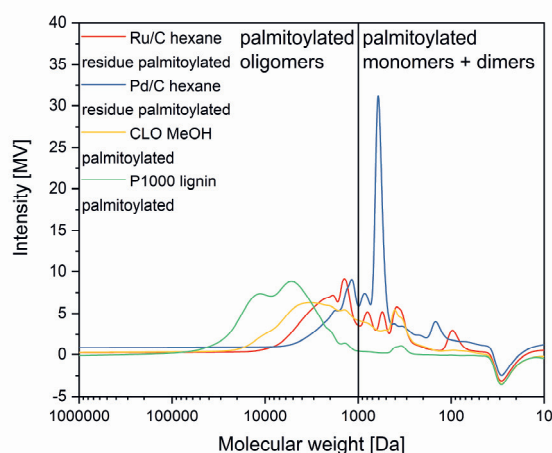
Figure S3 *Overlay of the GPC traces of the modified lignin fractions*
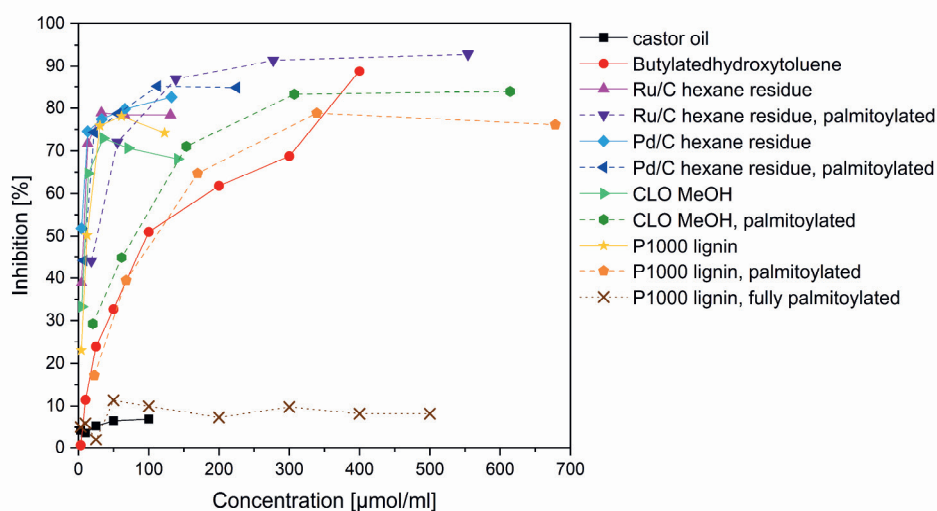
Figure S4 *Inhibition curves of castor oil, BHT, modified and non-modified lignin fractions obtained in the DPPH antioxidant activity assay*

Table S3 *Parameters of the Sisko model for non-Newtonian biolubricants formulations*

Biolubricant formulation	η_∞ [s^{-1}]	k [-]	n [-]
CLO MeOH, palmitoylated, 0.007 mmol/g oil	0.658	0.069	0.828
CLO MeOH, palmitoylated, 0.034 mmol/g oil	0.748	0.434	0.003
CLO MeOH, palmitoylated, 0.071 mmol/g oil	0.736	0.482	0.073
P1000 lignin, palmitoylated, 0.007 mmol/g oil	0.712	0.190	0.163
P1000 lignin, palmitoylated, 0.034 mmol/g oil	0.768	0.483	0.094
P1000 lignin, palmitoylated, 0.071 mmol/g oil	1.141	7.761	0.001

Where: η is viscosity, η_∞ is the infinite viscosity, k is the consistency, γ is the shear rate, and n is the power law index according to Sisko model: $\eta = \eta_\infty + k \cdot \gamma^{n-1}$
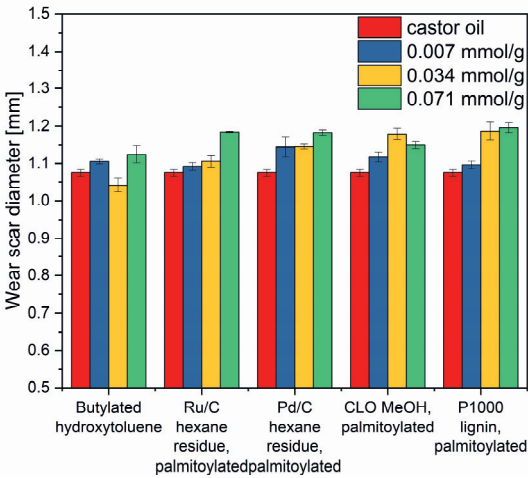
Figure S5 *Tribology results of castor oil and biolubricant formulations with esterified lignin-based additives: wear scar diameter*
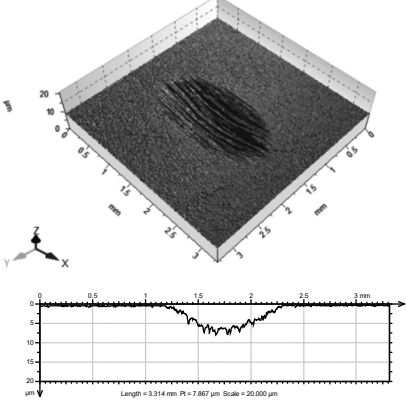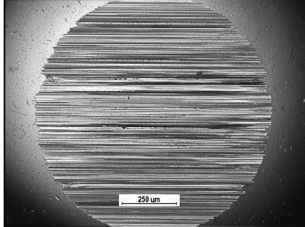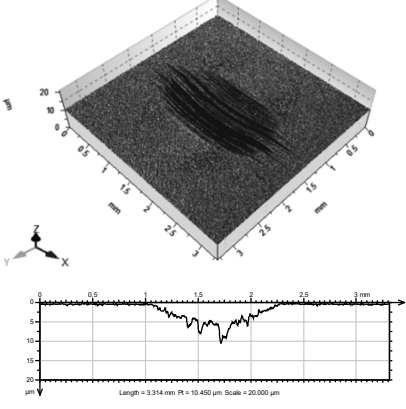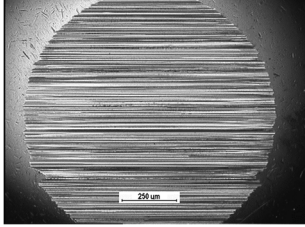
Chapter 4
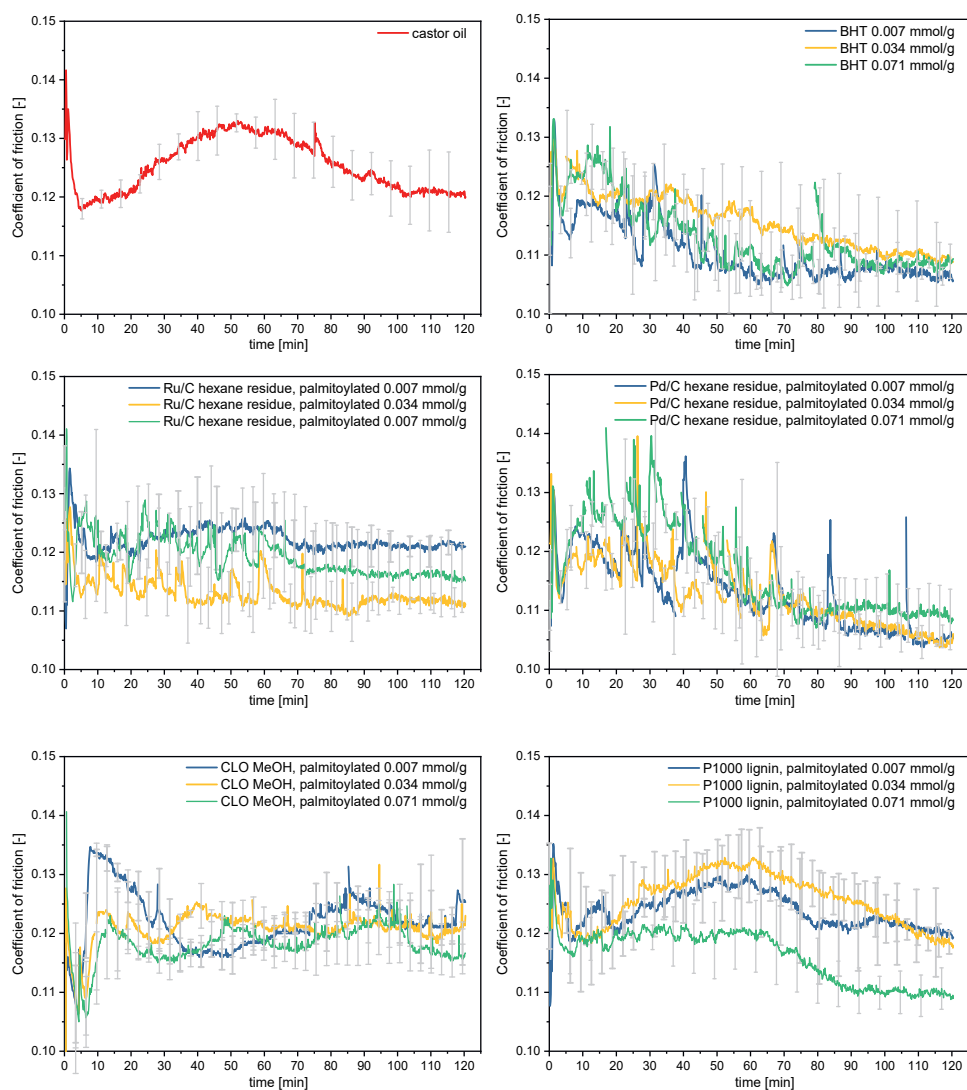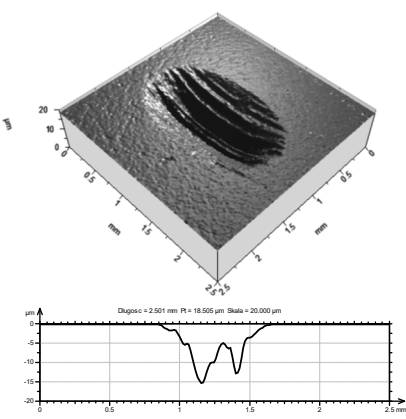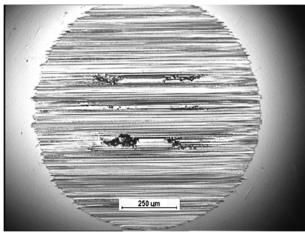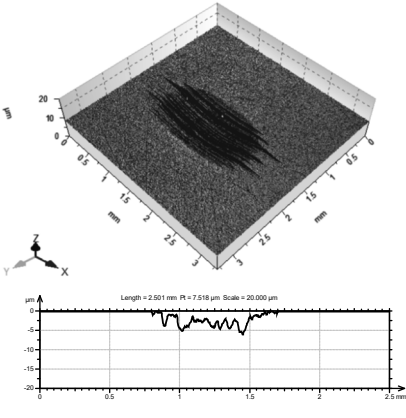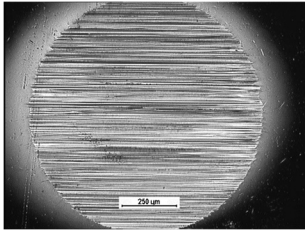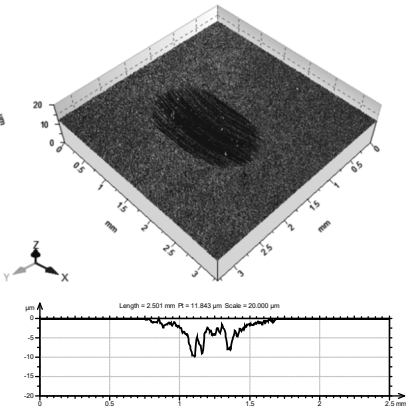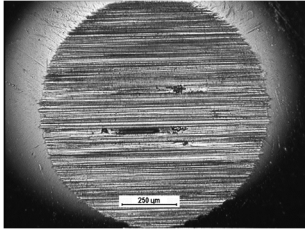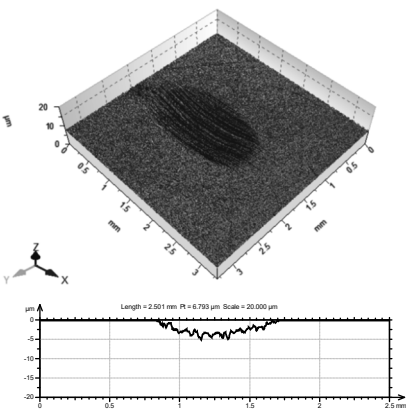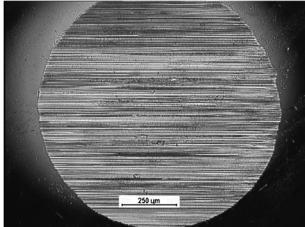
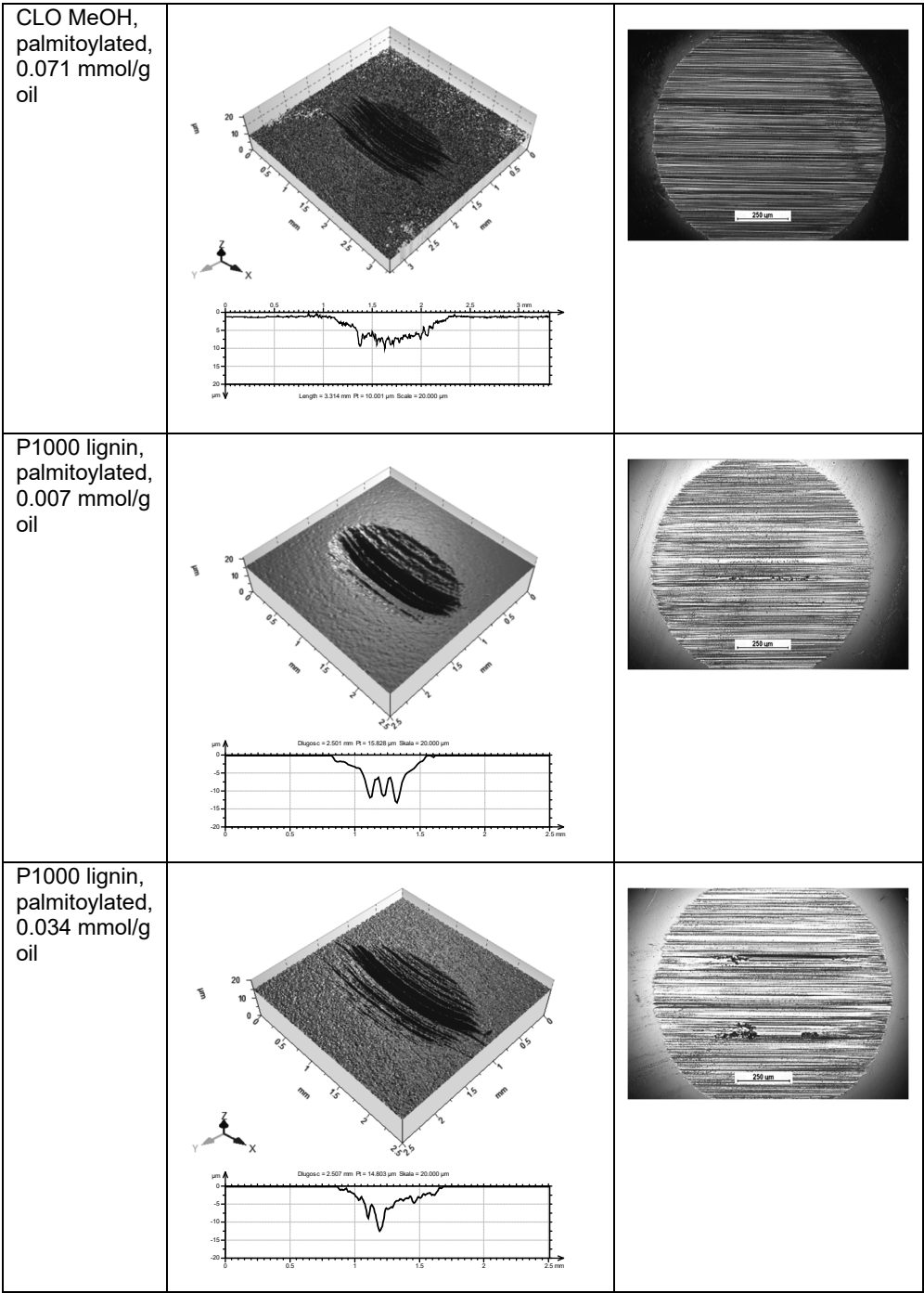**Figure S6** *Evolution of the coefficient of friction as a function of time*

Table S4 *3D images and profiles of the wear track in the disc and scars in the balls*

Lubricant formulation	3D image and profile of the wear track	Scars in the balls
Castor oil		
BHT, 0.007 mmol/g oil		
BHT, 0.034 mmol/g oil		

Chapter 4

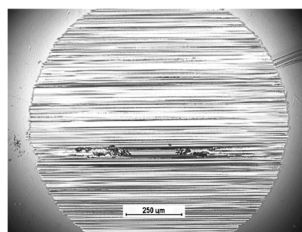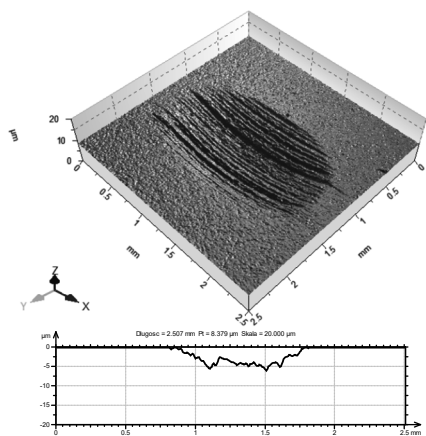| BHT, 0.071 mmol/g oil | | |
| Ru/C hexane residue, palmitoylated, 0.007 mmol/g oil | | |
| Ru/C hexane residue, palmitoylated, 0.034 mmol/g oil | | |

Ru/C hexane residue, palmitoylated, 0.071 mmol/g oil		
Pd/C hexane residue, palmitoylated, 0.007 mmol/g oil		
Pd/C hexane residue, palmitoylated, 0.034 mmol/g oil		

Pd/C hexane residue, palmitoylated, 0.071 mmol/g oil		
CLO MeOH, palmitoylated, 0.007 mmol/g oil		
CLO MeOH, palmitoylated, 0.034 mmol/g oil		

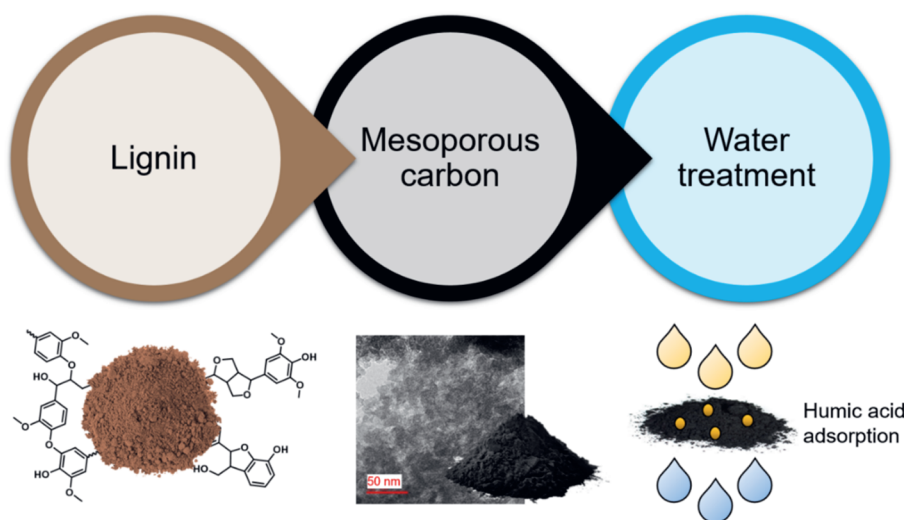|		
CLO MeOH, palmitoylated, 0.071 mmol/g oil		
P1000 lignin, palmitoylated, 0.007 mmol/g oil		
P1000 lignin, palmitoylated, 0.034 mmol/g oil		

Chapter 4

| P1000 lignin, palmitoylated, 0.071 mmol/g oil | | |

CHAPTER 5

Development of lignin based mesoporous carbons for the adsorption of humic acid

There is an increasing urge to make the transition toward biobased materials. Lignin, originating from lignocellulosic biomass, can be potentially valorized as humic acid adsorbents via lignin-based mesoporous carbon. In this work, these materials were synthesized for the first time starting from modified lignin as the carbon precursor, using the soft-template methodology. The use of a novel synthetic approach, Claisen rearrangement of propargylated lignin, and a variety of surfactant templates (Pluronic®, Kraton™, Solsperse™) have been demonstrated to tune the properties of the resulting mesoporous carbons. The obtained materials showed tunable properties (BET surface area: 95-367 m^2/g, pore size: 3.3-36.6 nm, V_{BJH} pore volume: 0.05-0.33 m^3/g, and carbon and oxygen content: 55.5-91.1% and 3.0-12.2%, respectively) and good performance in terms of one of the highest humic acid adsorption capacities reported for carbon adsorbents (up to 175 mg/g).

Introduction

The transition from a petroleum-based economy toward a biobased economy gained a lot of interest in recent years, both from industry and the academic world, due to environmental and sustainability concerns. Lignocellulosic biomass is an especially interesting feedstock because it is not competing with food and feed production.[1] Depending on the biomass source, plant cell wall material is composed of cellulose (35-80%), hemicellulose (5-35%), and lignin (15-35%).[2] There are multiple possibilities for their conversion from both cellulose and hemicellulose to ethanol, furfural, platform sugars and their derivatives,[3-5] and from lignin to fuels, chemicals, and materials.[4, 6-8]

Lignin is an amorphous material consisting of highly branched aromatic macromolecules based on three basic phenylpropanoid components (coumaryl, coniferyl, and sinapyl alcohols) bonded together.[9] In nature, lignin provides lignocellulosic materials with inner strength, rigidity and dimensional stability due to the chemical bonding with cellulose and hemicellulose, water impermeability and its transport within the plant, and it also has antioxidant, antimicrobial and antifungal properties among others.[10, 11] Currently, lignin is considered as a by-product of the lignocellulose bioethanol production and paper industry, and it has a relatively low value and quality. From the approx. 70-100 million tons of lignin produced annually, only less than 5% is not used as an energy source.[12] To valorize lignin and improve its use, high value applications are being developed, and lignin biorefineries converting lignin into high value products are increasingly drawing attention.[13] Possible value-added applications of lignin include its conversion to chemicals, fuels and carbonous materials, its applications in polymeric materials for adhesives, coatings, composites, and as antioxidant or flame retardant among others.[7, 8, 11-15]

Carbonous materials, such as mesoporous carbons (MCs), are widely used in multiple fields, such as adsorption, separation, catalysis, drug delivery, fuel cells, and energy storage, and in electronics as a result of their excellent properties: unique morphology, high specific area, pore volume, and excellent mechanical, chemical, and thermal stability.[16-21] They can be obtained via different routes: soft- and hard-templating, physical and chemical activation, sol-gel method, hydrothermal carbonization, or direct carbonization.[16, 19, 20, 22-24] In this research, the soft-templating method of a lignin precursor was applied. In this method a carbon precursor is cross-linked in the presence of a structure directing agent (surfactant, block copolymer) after their self-assembly, to form an organized mesophase. Afterward, the surfactant is removed by means of a thermal treatment, followed by the carbonization of the cross-linked resins, as presented in Figure 1. One of the most common synthetic routes in soft-templating methods is evaporation-induced self-assembly (EISA). The principle of the EISA method is as follows: polymerizable

precursors and structure-directing agents form micelles in the solution, and upon solvent evaporation, their concentration is increasing, promoting more organic-organic self-assembly of the components.[25] Effective self-assembly is driven by the concentration gradient in EISA.[26] Tunability of the mesoporous carbon (MC) properties is related to the selection of the precursor, synthetic route, surfactant type and concentration, and carbonization temperature.[20, 27]
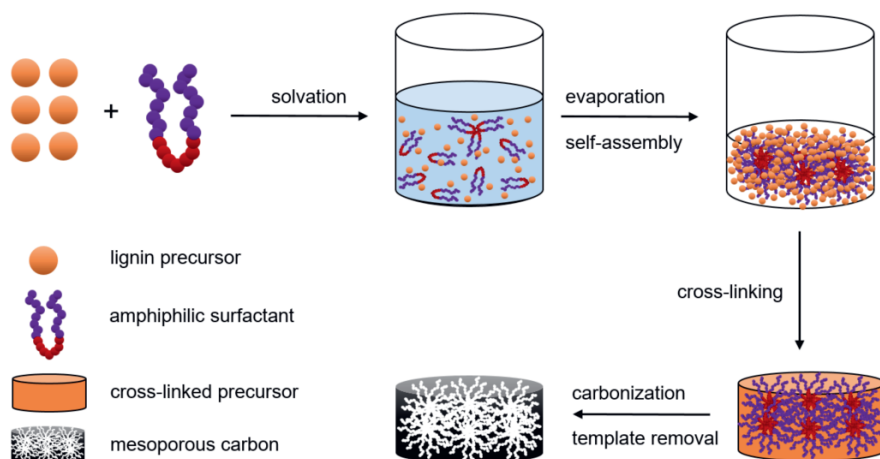

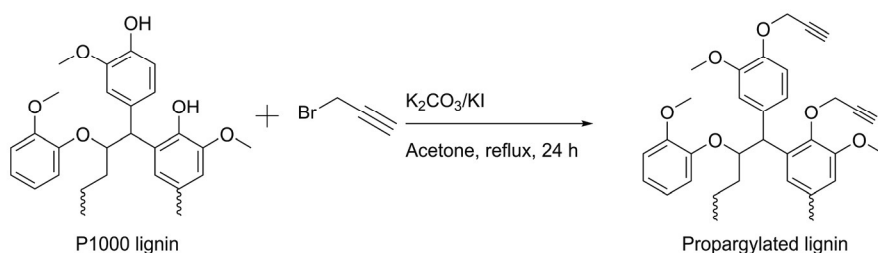*Figure 1* *MC synthesis via the soft-templating EISA method. Adapted from ref. 28*

Commonly used petroleum-based carbon precursors for MCs are phenolic resins, such as phenol-, resorcinol -, or phloroglucinol- formaldehyde resins, phenolic functionalized melamine, and (phenol)-urea-formaldehyde resins.[16, 20, 25, 29-32] The synthesis of MCs from biobased precursors is gaining interest in modern materials science research and it was described in multiple reviews. Precursors, such as plant biomass, lignin, fungus, algae, chitin, chitosan, gelatin, ionic liquids, various sugars, amino acids, and their derivatives, have been demonstrated.[16, 19, 20, 24, 33-37] Use of lignin in this application has an advantage of using a nontoxic, renewable and widely available resource, which is structurally similar to phenol-formaldehyde, one of the well-established precursors. Lignin can be incorporated in MCs fabrication using various pathways, such as templating methods, and physical and chemical activation.[15, 38, 39]

Lignin-based MCs fabricated via the soft-templating have been reported in the literature.[40-45] In these reports, lignin-formaldehyde or lignin-phenol/phloroglucinol-formaldehyde resins are synthesized, and cured in the presence of a surfactant (Pluronic® type), with the disadvantage of the use of toxic phenol and/or formaldehyde. In the next step, carbonization of the resin is performed. Such MCs have relatively high surface area (81-685 m^2/g) and pore volume (0.075-0.62 cm^3/g).[40-45] In general, lignin-based mesoporous carbons find

their application in the fields of supercapacitors, conductive and energy storage materials,[40, 41, 46-48] catalysis,[44] delivery systems,[78, 43] adsorption of organic molecules or heavy metals from water,[49, 50] or air pollutant adsorption.[50, 51]

In contrast to state-of-the-art,[41-44, 50, 52] where the toxic formaldehyde is used to cross-link the system, we developed a formaldehyde-free method to cross-link lignin and for further MC fabrication. Here, propargyl-modified lignin was cross-linked via the Claisen rearrangement, in the presence of a surfactant, using the soft-templating EISA strategy (Figure 2). Propargylated lignin has been reported to self-cross-link via the Claisen rearrangement,[53, 54] and it can be used as a precursor in single-component carbon fiber preparation.[55] This is the first report of the Claisen rearrangement approach for lignin cross-linking used for MCs precursor synthesis. Four different surfactants were selected as a template: Pluronic®® F127 and P123, Kraton™ G1652, and Solsperse™ M387. The most widely used surfactants are represented by the Pluronic® family, consisting of poly(ethylene oxide) (PEO) and poly(propylene oxide) (PPO) block copolymers. The Pluronics ® were selected because they are up to now the workhorses for the preparation of MCs. While PPO orients toward the core of the micelles, PEO stretches out into the aqueous medium where it undergoes H-bonding with, for example OH-groups in the carbonous precursor resin. In this work, we investigated surfactants with various levels of hydrophobicity. Therefore, more hydrophobic surfactants like Kraton™ G1652 and Solsperse™ M387 were tested. Those surfactants have not yet been reported as a template for MCs synthesis. Kraton™ G1652 is a hydrogenated triblock copolymer with polystyrene end blocks and a poly(ethylene/butadiene) middle block (SEBS), while Solsperse™ M387 is a basic and weakly cationic and H-bonding dispersant with known affinity for aromatics.[56] They were selected based on their foreseen possibility to interact with the lignin precursor via π-π stacking. Cured resins were carbonized at three different temperatures (600, 800 and 1000 °C), characterized, and applied as adsorbent for humic acid (HA).

Lignin propargylation:

P1000 lignin → Propargylated lignin

Lignin based resins preparation and curing via Claisen rearrangement:

Propargylated lignin → Benzopyran
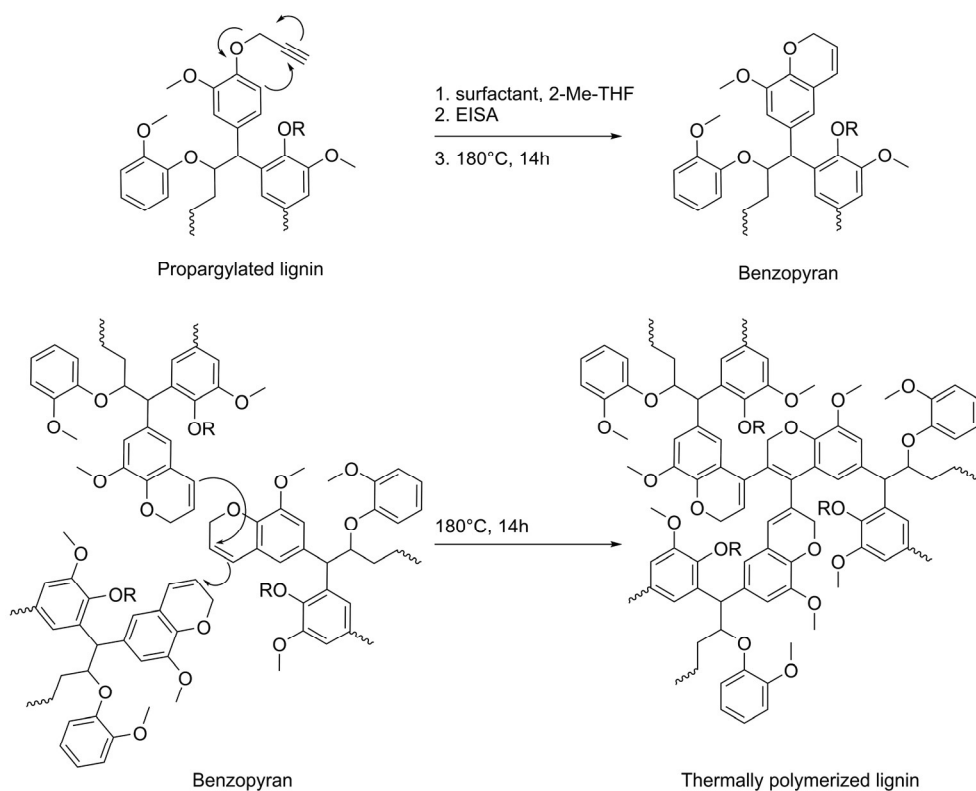

Benzopyran → Thermally polymerized lignin

Figure 2 Synthetic route of obtaining the lignin-based MCs precursor via the soft-templating method. The resin is cured via Claisen rearrangement after lignin propargylation

HA is one of the components of the surface and ground water. It is a complex, polydisperse biomacromolecule, categorized as dissolved organic carbon.[57] HA dissolved in water not only influences the color, taste, and odor of water, but also causes fouling during water purification, resulting in a potential hazard for human health during potable water processing.[58] It is a precursor to potentially carcinogenic trihalomethanes and haloacetic acids produced as byproducts during water

disinfection by chlorine or chloramines.[58, 59] Moreover, HA tends to form organometallic complexes with heavy metals, increasing their bioavailability.[60] There are multiple ways to remove HA from water, including adsorption, membrane filtration, coagulation, flocculation, electrochemical methods, catalytic oxidation, and decomposition.[57, 61] Adsorption is an important HA elimination technique. Examples, advantages and disadvantages of the various adsorbents are a topic of multiple reviews.[57, 62, 63] Those adsorbents can be categorized in the following groups: carbonaceous, mineral, and polymeric materials, and (nano)composites, and nanomaterials (nanoparticles and nanotubes). The examples of such materials are mesoporous and activated carbons, clays and zeolites, ion-exchange membranes, carbon nanotubes, and metallic nanoparticles and their composites, respectively.[57, 62, 63] The MCs synthesized in this article will be benchmarked with state-of-the-art MC synthesized using the lignin-formaldehyde approach (soft templated with Pluronic® F127)[42], and commercial activated carbon, to evaluate their performance as HA adsorbents.

The main objective of this work is the development of lignin-derived MCs suitable for the adsorption of HA. The strategy is to synthesize carbonous materials from lignin by its cross-linking via the Claisen rearrangement, in the presence of different surfactants, using the soft-templating EISA approach. The investigated surfactants varied in structure and hydrophobicity. The ultimate goal is to correlate the MCs properties with their HA adsorbent capacity.

Experimental section

Materials

All chemicals were used as received, unless stated otherwise. Protobind P1000 Lignin, soda lignin extracted from wheat straw (M_w=4.3 kDa, Đ=2.6, measured on a gel permeation chromatograph (GPC) with RI detection, calibrated with polystyrene standards, using tetrahydrofuran as the eluent, after acetylation of the lignin[64]), was provided by Green Value S.A. It contains less than 4 wt.% carbohydrates and less than 2 wt.% ash. Elemental analysis of this lignin yields the following composition: 59% C, 6% H, 26% O, 1% N, and 0.1% S.[65] 2-Chloro-4,4,5,5-tetramethyl-1,3,2-dioxaphospholane (95%), propargyl bromide solution (80 wt.% in toluene solution, with 0.3% magnesium oxide as stabilizer), potassium iodide (≥99.5%), potassium carbonate (≥99.0%), Pluronic® F127 (poly(ethylene oxide)$_{106}$-poly(propylene oxide)$_{70}$-poly(ethylene oxide)$_{106}$, M_w=12,600 g mol^{-1}), Pluronic® P123 (poly(ethylene oxide)$_{20}$-poly(propylene oxide)$_{70}$-poly(ethylene oxide)$_{20}$, M_w = 5,800 g mol^{-1}), formalin solution (37% in H_2O, with 10-15% methanol as stabilizer), sodium hydroxide (≥98%), nitric acid (70%),

2-methyltetrahydrofuran (2-Me-THF) (anhydrous >99.0%), cyclohexanol (99%), pyridine (dried over molecular sieves, 99.8%), chromium(III) acetylacetonate (99.99%), humic acid (>99%), and hydrochloric acid (37%) were purchased from Sigma Aldrich. Acetone, ethyl acetate and tetrahydrofuran were purchased from Biosolve. Molecular sieves 3Å were purchased from Merck. Chloroform-d (dried over molecular sieves, D, 99.96%) was purchased from Cambridge Isotope Laboratories. The linear triblock copolymer based on styrene and ethylene/butylene (SEBS) with a styrene/rubber ratio of 30/70 Kraton™ G1652 (Kraton Cooperation) was kindly provided by Kraton Polymers Belgium. The Solsperse™M387 dispersant (Lubrizol Corporation) was kindly provided by Integrated Chemicals Specialties BV. Activated carbon, Organosorb 200-1, was kindly provided by Desotec.

Methods

Lignin propargylation

The propargylation of P1000 lignin (Figure 2) was performed in a 4 L reactor, equipped with a reflux condenser and mechanical stirrer, under nitrogen flow. First, 200 g (1.29 mol, 1 eq of the sum of phenolic, aliphatic OH and COOH groups) of P1000 lignin was dissolved in 2 L acetone, then 941.2 g (6.88 mol, 5 equiv) of potassium carbonate and 113.1 g (0.68 mol, 0.5 equiv) of potassium iodide were dispersed in the lignin solution. Subsequently, the temperature was increased to 60 °C and 759 mL (6.88 mol, 5 equiv) of 80 wt.% propargyl bromide solution in toluene was added dropwise into the reaction mixture. The reaction mixture was then refluxed for 24 h. Afterward, the reaction mixture was cooled down and the product was filtered. The solid residue from the reaction mixture was washed with acetone, the filtrates were combined, and the solvent was evaporated. The solid residue was dried at 80°C in the vacuum oven overnight. The crude product was dissolved in 500 mL ethyl acetate and washed three times with brine. The solvent was evaporated, and the product was dried in the vacuum oven at 80 °C overnight. 141.5 g of the propargylated lignin was obtained as a brown powder (yield 64%). The propargyl moiety content was determined by measuring the conversion of the phenolic OH, aliphatic OH, and COOH by ^{31}P NMR spectroscopy. The conversion of phenolic OH, aliphatic OH, and COOH was 96, 64 and 96%, respectively, which equals to 4.38 mmol/g of propargyl moieties. The spectra before and after modification are presented in Figure S1, Appendix.

Preparation of lignin-based resins and curing

Propargylated lignin can be cross-linked via Claisen rearrangement above 150 °C.[53] Here, propargylated P1000 lignin was cured in bulk, in the presence of the corresponding surfactant to obtain the mesoporous carbons precursor. 3.75 g of propargylated P1000 lignin and 11.13 g of surfactant (Pluronic® P123, Pluronic® F127, Kraton™ G1652, or Solsperse™ M387) in a 1:3 weight ratio lignin:surfactant

Chapter 5

were dissolved in 60 mL of the green solvent 2-methyltetrahydrofuran to ensure proper mixing of the components. After dissolution, the solvent was evaporated, and the material was transferred to a Binder oven. The Claisen rearrangement reaction (Figure 2) was carried out at 180 °C for 14 h. The samples were named by the surfactant name. The conversion was determined via FT-IR analysis (Figure S2, Appendix).

Preparation of mesoporous carbons

Carbonization of the cured resins was performed in a Carbolite tube furnace type TFZ 12/65/550 according to the procedure described by Libbrecht et al.[66] 2.5 g resin was weighed into two ceramic pans and the oven was flushed with nitrogen for 30 min. Then, there were two heating steps: the first to remove the surfactant template, and the second to fully carbonize the material. During the first heating step, the sample was heated up to the template decomposition temperature, at a heating rate of 1 °C/min. When the desired temperature was reached, it was kept isothermal for 2 h. A second heating step with a heating rate of 2°C/min was performed until the desired carbonization temperature was reached (600, 800, or 1000 °C). Then, the temperature was maintained for 3h to ensure full carbonization of the sample. After carbonization, the material was cooled to ambient temperature at 5°C/min. Flushing, heating, and cooling steps were performed under a constant nitrogen flow of 0.4 NL/min. The obtained material was weighed, grinded and stored under dry conditions. The different carbons were named by surfactant name_carbonization temperature.

The decomposition temperature of the surfactants was investigated using TGA analysis. Thermal stability of the samples was determined on a TA TGA Q500 instrument in nitrogen atmosphere, from 25 to 700 °C at a heating rate of 10 °C/min. The thermographs of the surfactants are presented in Figure S3, Appendix.

Characterization

The aromatic and aliphatic hydroxyl groups as well as the carboxylic acids (before and after modification) of lignin were determined by ^{31}P NMR spectroscopy after sample derivatization, according to the method described by Korntner et al.[67] 10 mg of dried (in vacuum oven at 80 °C, overnight) lignin-based material was dissolved in a 500 µL anhydrous pyridine and deuterated chloroform mixture (1.6:1, v:v). Then, 100 µL of internal standard solution, cholesterol (19.7 mg/mL in anhydrous pyridine and deuterated chloroform mixture, 1.6/1, v/v, 0.0051 mmol), 50 µL of relaxation agent chromium (III) acetylacetonate (10 mg/mL, in anhydrous pyridine and deuterated chloroform mixture, 1.6:1, v:v), and 50 µL of derivatizing agent, 2-chloro-4,4,5,5-tetramethyl-1,3,2-dioxaphospholane were added to the solution. The solution was stirred for 10 min, transferred into a dry 5 mm NMR tube and measured. The measurement was performed on a Bruker Avance III HD Nanobay

300 MHz apparatus (121.49 MHz for ^{31}P NMR experiments) using the standard phosphorus pulse programme, at ambient temperature, with 512 scans, relaxation delay 5 s, acquisition time 2 s, transmitter excitation frequency 140 ppm, and spectral width 396 ppm. The chemical shifts were reported in ppm, and the raw data was processed in MestReNova software. Chemical shifts were referenced from the sharp signal of the reaction product between residual water and 2-chloro-4,4,5,5-tetramethyl-1,3,2-dioxaphospholane at 132.2 ppm.

Molecular weight of lignin and its dispersity was obtained from GPC analysis. It was performed at 40 °C using a Waters GPC equipped with a Waters 2414 refractive index detector. Tetrahydrofuran was used as eluent at a flow rate of 1 mL/min. Three linear columns were used (Styragel HR1, Styragel HR4, and Styragel HR5). Lignin samples were dissolved in 1.5 mL of tetrahydrofuran and samples were filtered with a PTFE syringe filter (pore size 0.2 μm) prior to measurement. Molecular weights were given relative to polystyrene standards. Lignin was acetylated prior to the measurement according the procedure described by Gosselink et al.[64]

IR spectra of the resins before and after curing were recorded on a PerkinElmer Frontier spectrometer, equipped with Pike technologies GladiATR accessory in a range of 600-4000 cm^{-1}, with a resolution of 2 cm^{-1} using 32 accumulative scans. The conversion was determined by following the disappearance of the alkyne C≡C-H peak at 3320 cm^{-1}, while the peak of the aromatic C=C at 1600 cm^{-1} was used as internal standard (Figure S2, Appendix). The conversion was determined based on the integration of the representative peaks with SpectraGryph 1.2 software.

Elemental analysis was performed to investigate the chemical composition of the carbon. The measurement was performed with a UNICUBE (Elementar Analysensysteme GmbH). For the carbon, hydrogen, nitrogen and sulfur content, the elemental composition of the synthesized materials was determined by the analysis of the combustion products (CO_2, H_2O, SO_2 and NO_2). Oxygen content was determined by pyrolysis of the sample in a pyrolysis chamber in a separate experiment. The calibration of the instrument was performed with sulfanilamide as model compound. Data were analyzed with EAS UNICUBE software.

The nitrogen sorption studies were performed on a Micromeritics Tristar II 3020 surface area and porosimeter analyser at 77K. Samples were pretreated at 300°C to remove moisture under nitrogen flow for 6 h. The relative pressure range was measured from 2.5*10^{-3} to 0.99. The total pore volume V_{tot} was calculated as the amount of nitrogen adsorbed at a relative pressure of 0.95. The pore volumes of micropores V_{micro} was calculated from the V−t plot. The pore volumes of mesopores and macropores, V_{BJH} was calculated using Barrett-Joyner-Halenda (BJH) desorption cumulative volume of pores between 17.000 Å and 3,000.000 Å width.

The total surface area S_{BET} was determined using the Brunauer−Emmett−Teller (BET) method. The average pore size (D_p BJH) and the pore size distribution (PSD) were calculated from the desorption branch using the Barrett-Joyner-Halenda (BJH) method. The reported data including S_{BET}, V_{tot}, V_{micro}, V_{BJH} and PSD were calculated by the software MicroActive from Micromeritics.

The morphology of the synthesized materials was investigated via transmission electron microscopy (TEM). The TEM images were acquired on a JOEL JEM 2200-FS TEM with high tension of 200 kV and 0.1s exposure time. For the measurement, the powdered sample was placed on a copper grid (Lacey F/C 200 mesh Cu, Ted Pella Inc.).

X-ray Photoelectron Spectroscopy (XPS) measurements were carried out in an Ultra AxisTM spectrometer, (Kratos Analytical). The samples were irradiated with monoenergetic Al Kα1,2 radiation (1486.6 eV) and the spectra were taken at a power of 144 W (12 kV x 12 mA). The aliphatic carbon (C-C, C-H) at a binding energy of 285 eV (C 1s photoline) was used to determine the charging. The spectral resolution - i.e. the Full Width of Half Maximum (FWHM) of the Ester carbon from poly(ethylene terephthalate) (PET) - was better than 0,68 eV for the elemental spectra. The elemental concentration is given in weight %, but it should be considered that this method can detect all elements except hydrogen and helium. The information depth is about 10 nm.

The HA adsorption capacity of the synthesized carbons was determined using the methodology described by Libbrecht et al.[66] First, a 500 mg/L HA solution was prepared by dispersing 500 mg HA in 1L of deionized water. HA was dissolved by adding 0.1 M sodium hydroxide solution until pH 12 and ultrasonic treatment for 30 min. After dissolution, the solution was neutralized to pH 7 with 0.1 M hydrochloric acid solution. Next, 10 mg of adsorbent was added to 50 mL of the 500 mg/L HA-solution. These mixtures were incubated in a thermostatic shaker (Infors HT Multitron Standard) at 25°C and 200 rpm for 7 days to ensure equilibrium. After incubation, the solution was filtered through a 0.45 µm PET syringe filter and its HA concentration was measured by UV-Vis at 254 nm by a Thermo Scientific Evolution 60 UV/VIS spectrometer with VISIONlight 4 software. The HA concentration of the 500 mg/L solution was determined by the same procedure (filtration and UV/VIS analysis). All adsorption experiments were performed in triplicate. The adsorption capacity was calculated using the equation:

$$q_e \ = \ \frac{(C_0 - C_e)\, V}{m}$$

Where: q_e (mg/g) is the HA adsorption capacity at equilibrium, C_0 and C_e (mg/L) the initial and equilibrium concentration of HA, m (mg) the mass of the adsorbent, and V (L) the solution volume.

Results and discussion

Mesoporous carbons precursor synthesis

The propargylated lignin is expected to interact with the surfactant and form micelles via self-assembly in the solvent (2-methyltetrahydrofuran), which is subsequently evaporated. Upon heating above 150 °C, Claisen rearrangement of the propargylated lignin takes place.[53] First, benzopyran structures are formed through [3,3] and [1,5]-sigmatropic, and oxa-Diels-Alder reactions.[68] Then, benzopyran moieties present in the modified lignin structure were thermally polymerized at 180 °C for 14 h to ensure maximal conversion (Figure 2). The conversion has been determined by means of FT-IR, by observing the disappearance of the alkyne moiety band (3300 cm^{-1}). The conversion was high, in the range of 88-99%, as shown in Figure 3. Examples of the spectra before and after cross-linking are shown in Figure S2, Appendix.
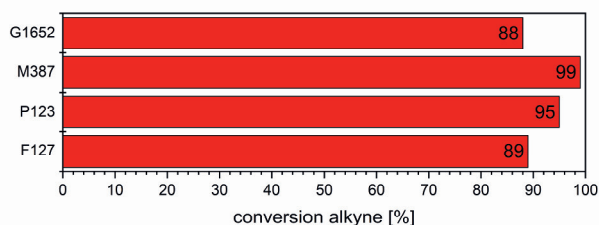

Figure 3 *Claisen rearrangement conversion determined by FT-IR of P1000 lignin in the presence of the four surfactants*

Mesoporous carbons synthesis and characterization

Once the lignin-based resins were cross-linked, they were carbonized at three different temperatures: 600, 800, and 1000 °C. As lignin is carbonized, various pyrolyzates are formed at high temperatures: lignin dehydration and decarboxylation takes place, followed by the formation of polycyclic aromatic hydrocarbons (PAHs), coke, tar, and char. Above 400 °C, methoxy groups in lignin are transformed to catecholic and pyrogallolic structures, together with side chain C-C and C-O bond cleavage, resulting in the start of lignin depolymerization and repolymerization, and initial PAHs, char, and coke formation.[69] Around 550 °C, catecholic and pyrogallolic structures tend to be transformed into coke, together with increased PAH formation,

especially when the temperature increases above 700 °C. At elevated temperatures, larger molecular weight PAHs are being formed. At temperatures above 1000 °C PAHs are the dominant product of lignin tar decomposition.[70]

It was generally observed that the carbon content as determined by elemental analysis, increased with increasing carbonization temperature (Table 1). For instance, the MC P123 carbonized at 600 °C had 67.1 wt.% carbon, while the same resin carbonized at 800 and 1000 °C had a carbon content of 69.0 and 91.1 wt.%, respectively. G1652 and F127 resin sets were an exception, with a similar carbon content for 600 and 800 °C carbonized materials.

During lignin carbonization, oxygen containing moieties, such as hydroxyl, methoxy, and carbonyl groups, are removed, and the remaining carbon network is transformed to PAH, while the carbon framework remains. This explains the increased carbon content with carbonization temperature.[66] This effect was observed for all the surfactants used in this study. Mesoporous carbons carbonized at 1000 °C exhibited a similar carbon content as the reference activated carbon, except for MC F127_1000.

Characterization of the synthesized MCs by elemental analysis did not yield a complete mass balance of H, O, N, S, and C atoms in most cases. Therefore, additional XPS experiments were performed on P1000 lignin, propargylated P1000 lignin, and the P123 MC set to investigate this issue. Elemental analysis provides information about the content of carbon, hydrogen, nitrogen, sulfur, and oxygen, while XPS can detect all elements except hydrogen and helium. XPS showed that sodium and chlorine are present in the MCs samples (but not in P1000 lignin), up to 4.6 and 4.4 wt.%, respectively. Since the workup includes use of concentrated sodium chloride solution, those findings are plausible.

Table 1 Characteristics of the MCs and activated carbon

Material	$S_{BET}{}^a$ [m²/g]	$V_{BJH}{}^b$ [m²/g]	$V_{micro}{}^c$ [m²/g]	D_p BJH^d [nm]	C^e [wt.%]	H^e [wt.%]	N^e [wt.%]	O^e [wt.%]
Activated carbon	1126	0.32	0.22	2.7	86.0	0.3	4.5	9.1
G1652_600	136	0.05	0.04	34.4	58.5 ±0.6	1.6 ±0.1	<1	3.0 ±0.1
G1652_800	102	0.08	0.03	22.5	55.5 ±2.1	<1	1.4	12.2 ±N.A.
G1652_1000	107	0.07	0.03	36.6	91.0 ±1.2	<1	1.6	8.2 ±0.3
M387_600	242	0.14	0.06	5.8	58.9 ±0.8	1.7 ±0.1	3.8 ±0.1	6.1 ±0.5
M387_800	95	0.12	0.02	5.4	63.9 ±2.2	<1	4.6 ±0.3	9.6 ±0.4
M387_1000	142	0.15	0.03	5.4	84.7 ±0.8	1.2 ±0.1	3.0 ±0.1	11.4 ±0.2
P123_600	371	0.30	0.10	10.2	67.1 ±0.3	1.7 ±0.1	<1	5.8 ±0.2
P123_800	277	0.28	0.07	12.2	69.0 ±0.3	1.1 ±0.1	<1	8.5 ±0.1
P123_1000	291	0.33	0.06	10.7	91.1 ±1.7	1.1 ±0.1	<1	9.0 ±0.1
F127_600	367	0.14	0.09	3.7	63.9 ±0.5	1.7 ±0.1	<1	5.5 ±0.2
F127_800	348	0.12	0.09	3.3	72.2 ±0.4	<1	<1	3.6 ±0.2
F127_1000	217	0.12	0.04	3.5	77.4 ±1.1	<1	<1	7.4 ±0.1

^{a} determined using the Brunauer−Emmett−Teller (BET) method, ^{b} BJH desorption cumulative volume of pores between 17.000 Å and 3,000.000 Å width. No pore volume was detected above 50 nm in pore size distribution, ^{c} calculated by the BJH model from the desorption branches of the isotherm; ^{d} calculated by the *V-t* method; ^{e} determined by elemental analysis.

Nitrogen sorption measurements (Figure 4 for the materials carbonized at 800 °C, and Figures S4 and S5 in Appendix for the materials carbonized at 600 and 1000 °C) exhibited isotherms of type IVa for all the synthesized MCs, or isotherm type Ib for the commercial activated carbon, as expected. Materials with isotherm type IV are classified as mesoporous, while those which exhibit isotherm type I are considered to be microporous to mesoporous (with small mesopores, up to 2.5 nm).[71] It can be noticed that for F127 and P123 materials the hysteresis is not closing. This phenomenon has been reported for calcinated phenol-formaldehyde resins made with F127 template and may be related to swelling of the polymer in nonsolvent (here: condensed nitrogen).[72, 73] The carbonized materials exhibited different hysteresis loops, associated with capillary condensation, pore blocking, and/or cavitation controlled evaporation. A H2a hysteresis loop was observed for F127 carbonized materials, which is typical for the materials exhibiting pores blocking in a narrow range of pore necks or cavitation-induced evaporation.[71] M387 carbonized materials showed a combination of H2a and H2b hysteresis loops, which indicates

pores blocking caused by both narrow and wide pore necks, what can be supported by the pore size distribution.[71] Another type of hysteresis loop, which was found for G1652 and P123 carbonized materials, was type H4, often seen for micro-mesoporous carbon systems.[71] Together with a shift of the hysteresis position to higher p/p_0 values, an increase in the pore size was observed (Figure 4).
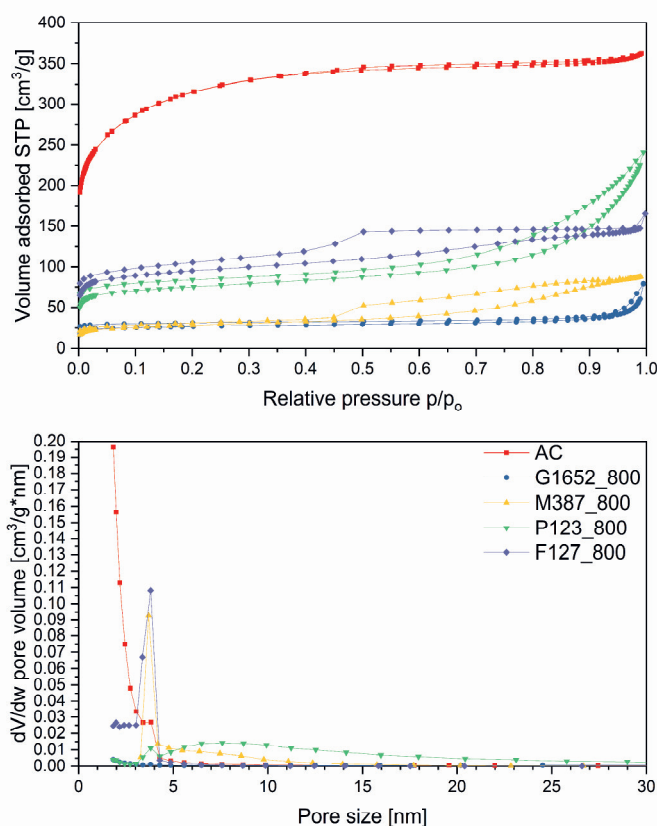

Figure 4 *Nitrogen sorption isotherm (top) and pore size distribution (PSD) (bottom) of the resins carbonized at 800 °C*
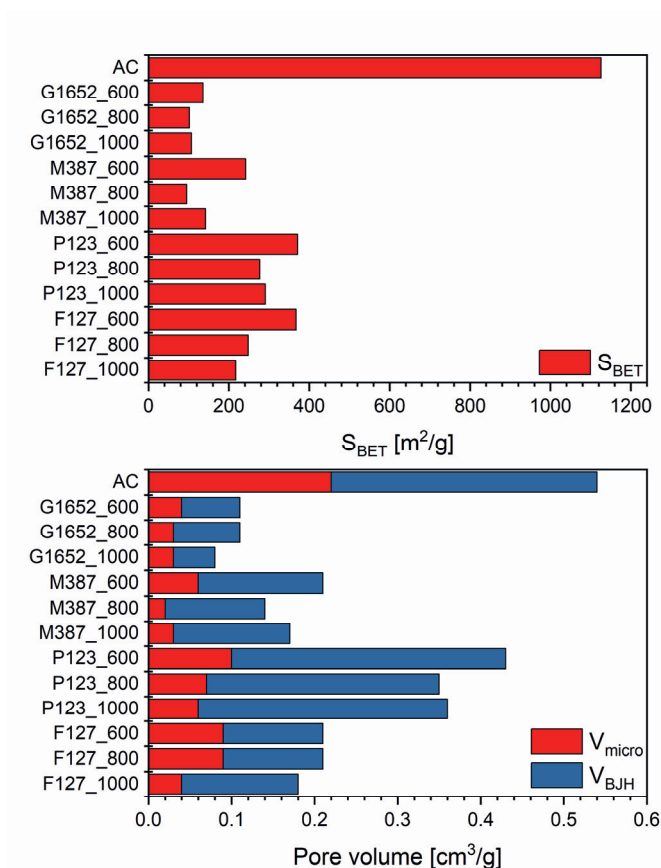
Figure 5 Summary of total BET surface areas (top) and pore volumes (bottom) of the synthesized MCs

The results, as listed in Table 1, clearly indicate the importance of the selection of the right surfactant in order to tune the pore size and volume. Exceptionally good results in terms of BJH pore volume were obtained for P123, followed by F127. Possibly, the interaction of those two surfactants, characterized by the different length of the PPO-PEO-PPO units (Pluronic® F127 PEO_{106}-PPO_{70}-PEO_{106}, Pluronic® P123 PEO_{20}-PPO_{70}-PEO_{20}), results in different micellization efficiency due to the ratio of PEO to PPO units. Overall, the Pluronic® surfactants in Claisen rearrangement-based lignin cross-linking tend to be a better precursor to mesoporous materials as the MCs templated by them exhibited higher BET surface areas and higher pore volumes (Figure 5).

The difference in material properties may arise due to different properties of the surfactant, such as chemical structure, chain architecture, chain lengths and ratio, and so forth, which result in different types of interactions (self-assembly of the structure directing agent and the precursor) influencing the structure of the resulting

Chapter 5

MCs.[74] For instance, there is hydrogen bonding between the hydroxyl functional groups of lignin (phenolic OH and aliphatic OH groups) and the ethers of the hydrophilic PEO outer blocks of the micelles, with the hydrophobic PPO buried inside to avoid contact with the hydrophilic hydroxyl groups in lignin Pluronics®.[27, 75] Kraton™ G1652, a poly(styrene-ethylene/butadiene-styrene) (SEBS) elastomer, and Solsperse™ M387, a basic and weakly cationic and H-bonding dispersant, may interact via weaker hydrophobic interactions and/or π-π stacking with aromatic moieties in the modified lignin. The stronger interactions between lignin and Pluronics® can explain the better material properties obtained with those surfactants compared to the hydrophobic surfactants. Especially interesting MCs were obtained with Pluronic® P123 used as a template. These MCs had the highest surface area S_{BET}, combined with the highest V_{BJH} pore volume. Another interesting case was the MCs templated with Pluronic® F127. Those materials showed similar surface area and slightly lower V_{BJH} pore volume. Interestingly, materials templated with Pluronic® F127 exhibited narrow PSD, with a major peak at 4 nm, while Pluronic® P123 had a wide peak with a maximum at 8 nm, tailing to 80 nm. The broader PSD with Pluronic® P123 as template can be correlated to the shorter hydrophilic PEO segment (PEO_{20}) compared to that of F127 (PEO_{106}), resulting in weaker hydrogen bonding between the template and the precursor.[76] Materials prepared with those two surfactants showed a decrease in surface area with increasing carbonization temperature, which can be a result of the pore shrinking and/or collapse during the carbonization process. This may also cause a lower pore volume.

The obtained TEM images (Figure 6) confirm the observations from nitrogen sorption data regarding the morphology of the pores. Activated carbon consists of a bulky structure, with visible numerous micropores and small size mesopores. In the TEM micrographs of M387_800, the porous domains are visible in a limited amount. Mostly small, uniform mesopores are observed, which is supported by the nitrogen sorption data. P123_800 consists of a more confined structure, with clearly visible larger mesopores and possibly macropores. A high number of pores are visible, which was also observed in the nitrogen sorption data, represented by the high pore volume. In F127_800, randomly distributed mesoporous domains can be observed. The number of pores seems to be moderate, but the pores tend to have a relatively narrow size range and small size.
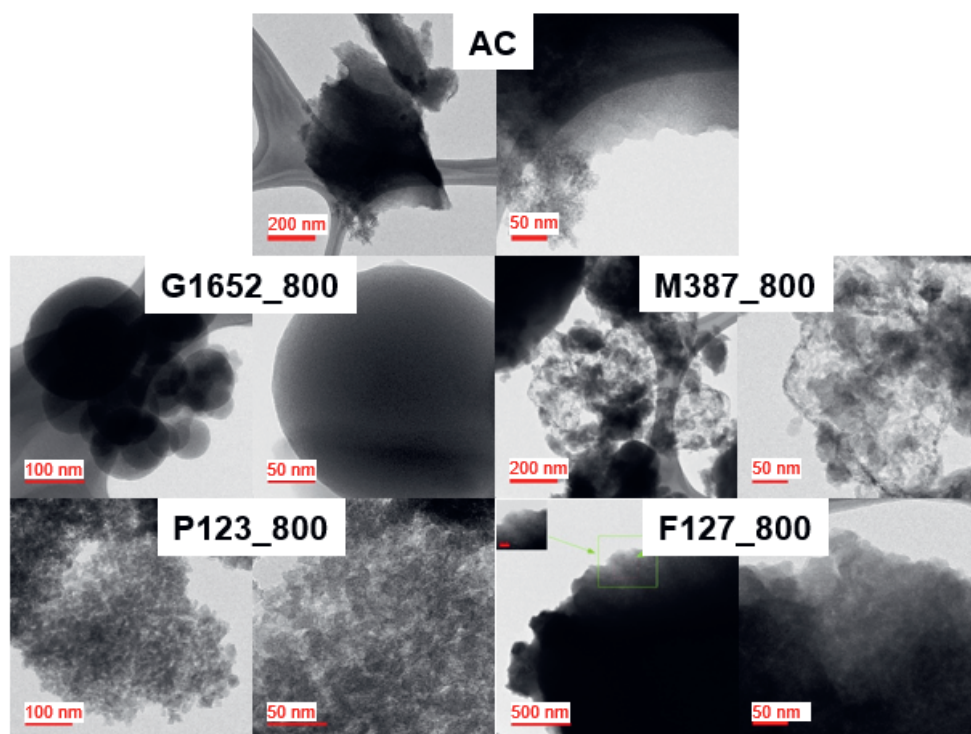
Figure 6 TEM micrographs of activated carbon and lignin-based resins carbonized at 800°C

Surprisingly, Kraton™ G1652 templated MCs exhibited spherical carbon domains along the agglomerated structures. These spherical structures range from 20 nm to 1 µm in diameter. These kind of structures are observed only in the G1652 templated carbons. Due to the dense structure of the species, visualization of pores is hindered, which can be correlated with the low pore volume determined in the nitrogen sorption experiments. This morphology could originate from the interaction with the surfactant, which may enable lignin to rearrange in these spherical structures during the EISA step. Kraton™ G1652 consists of SEBS units and is consequently hydrophobic. During the resin synthesis, the surfactant is interacting with the hydrophobic and aromatic domains of the lignin precursor. The hydrophilic domains, for example remaining hydroxyl groups in lignin, could have been repelled by the surfactant and agglomerated together via hydrogen bonding. This self-assembly could have resulted in the spherical structures, which are observed for the carbonized materials. Li *et al.* reported the synthesis of MC spheres, with 1320 m^2/g specific surface area and 3.5 cm^3/g pore volume with a hierarchical pore size of 3.5-60 nm via a dual templating method, soft and hard templating.[77] The carbon spheres exhibited a more defined pore structure compared to the material obtained by Kraton™ G1652, and the spheres they obtained were in the range of 3-5 µm.[77]

Chapter 5

The synthesized novel material could open an alternative way to synthesize porous carbon nanospheres.

The synthesized carbons can be benchmarked with literature results where a soft-templating approach with lignin as a precursor and Pluronic® F127 as a template was used (Table 2). The resin cross-linking uses very harmful formaldehyde or less harmful glyoxal, while the lignin precursor is different in all the reported cases. Here, we propose lignin cross-linking via the Claisen rearrangement as an alternative. The surface area of the MCs obtained in our study is similar to the phenol-formaldehyde references, except from the one reported by Chen *et al.*[40] In that study, a high amount of KOH was used, which can increase the porosity by chemical activation in the MC synthesis combined with the soft-templating methodology. The total pore volume of our materials is comparable with that reported by Saha *et al.*[43] and lower than that reported by Chen *et al.*[40] and Qin *et al.*[42], but better than the ones obtained by Herou *et al.*[41] When the pore volume of the mesopores is compared, the best performing materials from this study are superior to all the references, except for that reported by Saha *et al.*[43] and Chen *et al.*[40] showing similar or slightly better characteristics. Pore sizes of our MCs vary between 3.3 and 36.6 nm. PSD is related to the surfactant used as a template. All the literature references using the lignin-formaldehyde cross-linking approach used Pluronic® F127 as a template and the pore size was in the range of 3.4-3.8 nm, which is in the same range as our materials templated with Pluronic® F127 (3.3-3.7 nm). The use of another template enables to tune this property, as presented in Table 1. In general, materials presented in this study exhibit good performance compared with what has been reported already in the field of porous lignin materials, with the advantage that our materials are prepared via a formaldehyde-free synthesis route.

Table 2 Lignin-based MCs obtained via the soft-templating with Pluronic® F127 method summary

Lignin precursor	Cross-linking method, carbonization temperature	S_{BET} [m²/g]	V_{tot} [cm³/g]	V_{BJH} [cm³/g]	V_{micro} [cm³/g]	D_p BJH [nm]	Ref.
P1000 lignin	Claisen rearrangement, 600 °C	367[a]	0.23[b]	0.14[c]	0.09[d]	3.7[e]	Best result from this article
Lignosulfonate (Sigma Aldrich)	lignin with formaldehyde, 600 °C	685[a]	0.44[b]	0.21[g]	0.23[d]	3.7[g]	40
Kraft lignin (Sigma Aldrich)	lignin-phenol-formaldehyde (lignin: phenol 1:3), 900 °C	260[a]	NA	0.08[g]	NA	3.4[g]	44
Softwood lignin (Nanjing Forest University)	lignin with formaldehyde, 600 °C	236-466[a]	0.48-0.62[g]	NA	NA	3.8[g]	42
Methanol soluble fraction obtained from Kraft lignin	lignin with formaldehyde, 1000 °C	205-418[a]	0.19-0.50[h]	0.11-0.34[h]	0.02-0.16[h]	NA	43
Masson pine alkali lignin (Nanping Paper-making Co. Ltd)	lignin with formaldehyde, 900 °C	345[a]	NA	0.03[f]	NA	3.4[e]	45
Organosolv Lignin (Fraunhofer Institute Iena)	lignin with glyoxal, 900 °C	81[a]	0.11[i]	0.09[g]	NA	3.6[i]	41

[a] determined using the Brunauer−Emmett−Teller (BET) method, [b] calculated as the amount of nitrogen adsorbed at a relative pressure of 0.95, [c] BJH desorption cumulative volume of pores between 17.000 Å and 3,000.000 Å width, [d] calculated by the *V-t* method, [e] calculated by the BJH model from the desorption branches of the isotherm, [f] not defined in the experimental section how this value was obtained, [g] derived from the adsorption branches of the isotherms by the BJH method, [h] calculated by employing nonlocal density functional theory (NLDFT), [i] calculated from the adsorption line using a DFT model.

Unfortunately, none of our synthesized MCs exhibited an ordered porous structure, which has been reported by Qin *et al.*[42] and Wang *et al.*[45] The formation of ordered pores arises from the high hydroxyl group content of the used low molecular weight lignin (1-1.5 kDa used by Qin *et al.*,[42] and M_w of lignin used Wang *et al.*[45] was not reported), which enables conductive self-assembly of the micelles.[28] Therefore, the observed non-ordered pore structure in our case could arise from a lower amount of hydroxyl groups (0.79 mmol/g, unmodified P1000 5.51 mmol/g) after the functionalization of the lignin precursor with propargyl units and its relative higher molecular weight (4.3 kDa) compared to the lignin used by Qin *et al.*[42]

By consequence, the H-bond interaction between our propargylated lignin precursors and the surfactant is weaker (there are less hydrogen bonds), resulting in less ordered porous materials because the interactions are already destroyed in the heating process.

Humic acid adsorption studies

The main objective of this work was the development of the MCs suitable for the adsorption of HA and to correlate their properties with the adsorbent capacity. The synthesized MCs are compared with activated carbon by benchmarking their HA adsorption capacities. The results are summarized in Figure 7.
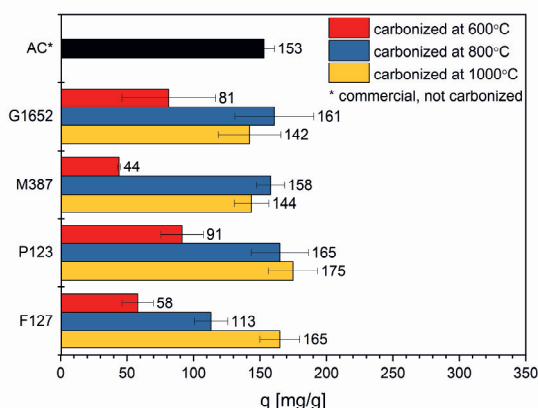

Figure 7 Comparison of HA adsorption of activated carbon and mesoporous materials synthesized in this study

Activated carbon showed a HA adsorption capacity of 153 mg/g. Other reported commercial activated carbons exhibited lower HA adsorption capacities (up to 56 mg/g) than the activated carbon used in this study, probably because of lower specific surface area, (V_{BJH}) pore volume, and pore size of those activated carbons.[79-83] The HA adsorption on activated carbon is hindered by the size exclusion effect due to the small pore size.[84] The adsorption capacity of activated carbon is in the same range as the G1652_800, G1652_1000 M387_800, M387_1000, P123_800, P123_1000 and F127_1000 MCs. HA adsorption for materials carbonized at 800 and 1000°C is comparable for most of the materials, except for the F127 set, where adsorption of the material carbonized at 1000°C is significantly increased compared to the 800°C one. Materials carbonized at 600°C showed the lowest HA adsorption in each set, with pronounced difference in the performance compared to materials carbonized at higher temperatures and reference activated carbon. This could be attributed to the fact that the materials carbonized at 600°C showed the lowest carbon content (Table 1).

Libbrecht *et al.* reported that an increase in the pore size and carbon content promote higher HA adsorption due to the hydrophobic π-π stacking adsorption mechanism.[66] Unfortunately, we do not observe it for our materials, which have a lower carbon content than the ones reported by Libbrecht *et al.* which have 77-95% carbon. The lower carbon content in the reported materials would be expected to yield in lower adsorption, since carbon enhances the hydrophobic character of the material and therefore the van der Waals and hydrophobic interactions.[66] Upon a pH increase, the carboxyl groups of the HA deprotonate first (pK_a=5), and at higher pH values the phenolic hydroxyl groups (pK_a=10) deprotonate as well. This makes HA more hydrophilic. The adsorption experiments were performed at a pH of 7, therefore, the HA will be charged and become more hydrophilic. It was observed that the MCs, which had an oxygen content above 7wt.%, showed good HA adsorption if they exhibited moderate to good material properties, such as surface area and mesoporous volume. A possible explanation might be the presence of non-covalent interactions between HA and the adsorbent, for example, hydrogen bonding. The hydrogen bonding could enhance the interaction strength between the adsorbent and the adsorbate and increase the adsorption capacity. Therefore, the increased oxygen content can be beneficial for HA adsorption. Additionally, the large pore size enables the adsorption of HA, whose reported hydrodynamic radius is 7.1 nm.[27] For materials with a pore size lower than 7.1 nm, the size exclusion effect may prevent the adsorption of large amounts of HA.

Unfortunately, it is difficult to draw general conclusions regarding the relationship between synthesis route (used approach, surfactant, and experimental conditions), materials properties, and HA adsorption. For each case, the surfactant had a different effect on the properties of the materials, and therefore, the combination of different factors (BET surface area, pore volume, pore diameter, and elemental composition) influenced the adsorption properties. As multiple properties influence HA adsorption, it is very difficult to understand the interplay between them and the HA adsorption. The G1652 MCs exhibited good to very good HA adsorption, despite the low pore volume. Their performance can be connected with the high oxygen content in those MCs, combined with big pore sizes. M387 materials on the other hand exhibited low pore sizes, but their good performance can be attributed to the high oxygen content and moderate mesoporous volume. P123 MCs have the best performance from all the synthesized materials and the excellent performance can be the result of the combination of the highest mesoporous volume, high BET surface area, pore size above 10 nm, and high oxygen content. F127 materials exhibited moderate to good performance, which can be correlated with the high BET surface area and moderate mesoporous volume.

Chapter 5

When compared with other carbon materials used for HA adsorption (Table 3), it turns out that the performance of the materials synthesized in this study is relatively good, in the same range as the AC reference, but significantly better than the majority of other activated carbons. The shown materials are outperformed only by the materials synthesized from resorcinol-formaldehyde resin by Libbrecht *et al.* and coal-based mesoporous activated carbons prepared by Lorenc-Grabowska *et al.*[66, 85] Other materials have significantly lower HA adsorption capacity than presented materials, despite their usually higher surface areas and pore volumes.[84, 86-89] In comparison to the other commercial activated carbons repoted in the literature, their performance is drastically lower than the MCs presented in this study.[79-83]

Table 3 Comparison of carbon materials used as HA adsorbents

Material	S_{BET}^{a} [m²/g]	D_p BJH [nm]	V_{tot} [cm³/g]	HA adsorption [mg/g]	Conditions (pH, Temp [°C])	Ref.
Commercial Filtrasorb 200 activated carbon	NA	NA	NA	24	5.0, 25	79
Commercial adsorbent JZN	149	NA	0.63^b	3	7.0, 25	86
Commercial, treated coconut shell–based activated carbons	NA	NA	NA	8-70	NA, 30	83
Commercial activated carbon treated with sulphuric and phosphoric acids	659-724	NA	NA	19-26	NA, RT	80
Commercial cellulose and powdered activated carbon	102-834	NA	NA	89-30	2.0, 37	82
Chitosan treated granular activated carbon (Filtrasorb 400)	NA	NA	NA	56-71	7.0, 25	81
Chitosan-encapsulated activated carbon	316^b	3.28^b	0.26^b	72	6.4, 30	88
Ammonia and hydrogen treated mesoporous activated carbons	415-518	NA	0.51-0.53^c	90-137	NA, RT	87
Coal-based mesoporous activated carbons	367-850	NA	0.24-0.47^b	170-200	12.0-12.5, 25	85
Soft templated mesoporous carbons based on resorcinol-formaldehyde resins	422-670	3.5-27^d	0.74-1.56^c	155-352	7.0, 25	66
Hard templated (mesoporous SiO$_2$) ordered mesoporous carbon	988	NA	1.33^c	51	6.0, 25	84
Carbonized rice containing nanosized magnetite	NA	NA	NA	80	7.61, RT	90

Magnetic porous carbon based on pyrolyzed biomass, containing γ-Fe_2O_3	63	NA	NA	96	5.0, NA	[91]
Dual-pore carbon shells synthesized by templating against silica nanospheres	750-1350	2.4-9.5[b]	0.4-1.1[b]	12-100	NA, 25	[89]
P123_1000	290	10.7[d]	0.37[c]	175	7.0, 25	This work
P123_800	277	12.2[d]	0.28[c]	165	7.0, 25	This work
F127_1000	156	3.5[d]	0.12[c]	165	7.0, 25	This work
G1652_800	102	22.5[d]	0.07[c]	161	7.0, 25	This work
M387_800	95	5.4[d]	0.13[c]	158	7.0, 25	This work
AC	1026	2.3[d]	0.50[c]	153	7.0, 25	This work

[a] determined using the Brunauer−Emmett−Teller (BET) method, [b] not defined in the experimental section how this value was obtained, [c] calculated as the amount of nitrogen adsorbed at a relative pressure of 0.95; [d] calculated by the BJH model from the desorption branches of the isotherm.

Conclusions

A series of novel, lignin-based MCs were successfully prepared using a Claisen rearrangement route. The soft-templating method using EISA was applied to obtain mesoporous materials after carbonization. We presented the material characteristics obtained through the synthesis using various surfactants used as a template and at different carbonization temperatures. All the materials are benchmarked as HA adsorbents. The ultimate goal of this study was to correlate carbonous material properties with the HA adsorption capacity. High HA adsorption can be influenced by various properties of MCs, such as carbon and oxygen content, pore size and volume, and BET surface area. These properties can be steered by changing the surfactant type and concentration, resin preparation methodology, and carbonization temperature; however, it is not easy to understand the complex interplay between all these aspects in the materials preparation.

The MCs synthesized in this research exhibited good performance as HA adsorbents compared to other carbonous materials in terms of adsorption capacity. The best results are obtained with Pluronic® P123 surfactant and carbonized at 1000 °C because this material possesses high surface area and pore volume with average pore size above 7 nm, with one of the highest carbon content obtained in this study. This work is one of the examples of lignin use in value-added applications, such as

Chapter 5

adsorbents for water purification, which is an interesting highlight adding to lignin valorization. This is a proof-of-principle application, but we believe that it is possible to use these materials for other applications as well, such as supercapacitors and energy storage materials.[16, 20, 92, 93]

References

1.   Finley, J. W.; Seiber, J. N., The Nexus of Food, Energy, and Water. *J. Agric. Food Chem.* **2014,** *62* (27), 6255-6262.

2.   Azadi, P.; Inderwildi, O. R.; Farnood, R.; King, D. A., Liquid fuels, hydrogen and chemicals from lignin: A critical review. *Renewable Sustainable Energy Rev.* **2013,** *21*, 506-523.

3.   Caes, B. R.; Teixeira, R. E.; Knapp, K. G.; Raines, R. T., Biomass to Furanics: Renewable Routes to Chemicals and Fuels. *ACS Sustain. Chem. Eng.* **2015,** *3* (11), 2591-2605.

4.   Delidovich, I.; Hausoul, P. J.; Deng, L.; Pfutzenreuter, R.; Rose, M.; Palkovits, R., Alternative Monomers Based on Lignocellulose and Their Use for Polymer Production. *Chem. Rev.* **2016,** *116* (3), 1540-1599.

5.   Mika, L. T.; Csefalvay, E.; Nemeth, A., Catalytic Conversion of Carbohydrates to Initial Platform Chemicals: Chemistry and Sustainability. *Chem. Rev.* **2018,** *118* (2), 505-613.

6.   Schutyser, W.; Renders, T.; Van den Bosch, S.; Koelewijn, S. F.; Beckham, G. T.; Sels, B. F., Chemicals from lignin: an interplay of lignocellulose fractionation, depolymerisation, and upgrading. *Chem. Soc. Rev.* **2018,** *47* (3), 852-908.

7.   Sun, Z.; Barta, K., Cleave and couple: toward fully sustainable catalytic conversion of lignocellulose to value added building blocks and fuels. *Chem. Commun.* **2018,** *54* (56), 7725-7745.

8.   Sun, Z.; Fridrich, B.; de Santi, A.; Elangovan, S.; Barta, K., Bright Side of Lignin Depolymerization: Toward New Platform Chemicals. *Chem. Rev.* **2018,** *118* (2), 614-678.

9.   Vanholme, R.; Demedts, B.; Morreel, K.; Ralph, J.; Boerjan, W., Lignin Biosynthesis and Structure. *Plant Physiol.* **2010,** *153* (3), 895-905.

10.   Figueiredo, P.; Lintinen, K.; Hirvonen, J. T.; Kostiainen, M. A.; Santos, H. A., Properties and chemical modifications of lignin: Toward lignin-based nanomaterials for biomedical applications. *Prog. Mater Sci.* **2018,** *93*, 233-269.

11.   Kai, D.; Tan, M. J.; Chee, P. L.; Chua, Y. K.; Yap, Y. L.; Loh, X. J., Toward lignin-based functional materials in a sustainable world. *Green Chem.* **2016,** *18* (5), 1175-1200.

12.   Bajwa, D. S.; Pourhashem, G.; Ullah, A. H.; Bajwa, S. G., A concise review of current lignin production, applications, products and their environmental impact. *Ind. Crops Prod* **2019,** *139*, 111526-111537.

13.   Balakshin, M. Y.; Capanema, E. A.; Sulaeva, I.; Schlee, P.; Huang, Z.; Feng, M.; Borghei, M.; Rojas, O. J.; Potthast, A.; Rosenau, T., New Opportunities in the Valorization of Technical Lignins. *ChemSusChem* **2020,** *14* (4), 1016-1036.

14.   Yu, O.; Kim, K. H., Lignin to Materials: A Focused Review on Recent Novel Lignin Applications. *Applied Sciences* **2020,** *10* (13), 4626-4642.

15.   Chatterjee, S.; Saito, T., Lignin-Derived Advanced Carbon Materials. *ChemSusChem* **2015,** *8* (23), 3941-3958.

16.   Inagaki, M.; Toyoda, M.; Soneda, Y.; Tsujimura, S.; Morishita, T., Templated mesoporous carbons: Synthesis and applications. *Carbon* **2016,** *107*, 448-473.

17.   Lim, E.; Jo, C.; Lee, J., A mini review of designed mesoporous materials for energy-storage applications: from electric double-layer capacitors to hybrid supercapacitors. *Nanoscale* **2016,** *8* (15), 7827-7833.

18.   Suib, S. L., A Review of Recent Developments of Mesoporous Materials. *Chem. Rec.* **2017,** *17* (12), 1169-1183.

19.   Xin, W.; Song, Y., Mesoporous carbons: recent advances in synthesis and typical applications. *RSC Advances* **2015,** *5* (101), 83239-83285.

20.   Benzigar, M. R.; Talapaneni, S. N.; Joseph, S.; Ramadass, K.; Singh, G.; Scaranto, J.; Ravon, U.; Al-Bahily, K.; Vinu, A., Recent advances in functionalized micro and mesoporous carbon materials: synthesis and applications. *Chem. Soc. Rev.* **2018,** *47* (8), 2680-2721.

21.   Gang, D.; Uddin Ahmad, Z.; Lian, Q.; Yao, L.; Zappi, M. E., A review of adsorptive remediation of environmental pollutants from aqueous phase by ordered mesoporous carbon. *Chem. Eng. J.* **2021,** *403*, 126286-126304.

22.   Ferrero, G. A.; Sevilla, M.; Fuertes, A. B., Mesoporous carbons synthesized by direct carbonization of citrate salts for use as high-performance capacitors. *Carbon* **2015,** *88*, 239-251.

23.   Xie, Y.; Kocaefe, D.; Chen, C.; Kocaefe, Y., Review of Research on Template Methods in Preparation of Nanomaterials. *Journal of Nanomaterials* **2016,** *2016*, 1-10.

24.   Lyu, L.; Seong, K.-d.; Ko, D.; Choi, J.; Lee, C.; Hwang, T.; Cho, Y.; Jin, X.; Zhang, W.; Pang, H.; Piao, Y., Recent development of biomass-derived carbons and composites as electrode materials for supercapacitors. *Mater. Chem. Front.* **2019,** *3* (12), 2543-2570.

25.   Chuenchom, L.; Kraehnert, R.; Smarsly, B. M., Recent progress in soft-templating of porous carbon materials. *Soft Matter* **2012,** *8* (42), 10801-10812.

26.   Enterría, M.; Figueiredo, J. L., Nanostructured mesoporous carbons: Tuning texture and surface chemistry. *Carbon* **2016,** *108*, 79-102.

27.   Libbrecht, W.; Verberckmoes, A.; Thybaut, J. W.; Van Der Voort, P.; De Clercq, J., Soft templated mesoporous carbons: Tuning the porosity for the adsorption of large organic pollutants. *Carbon* **2017,** *116*, 528-546.

28.   Saha, D.; Li, Y.; Bi, Z.; Chen, J.; Keum, J. K.; Hensley, D. K.; Grappe, H. A.; Meyer, H. M., 3rd; Dai, S.; Paranthaman, M. P.; Naskar, A. K., Studies on supercapacitor electrode material from activated lignin-derived mesoporous carbon. *Langmuir* **2014,** *30* (3), 900-910.

29.   Chandran, M.; Shamna, I.; Anusha, A.; Bhagiyalakshmi, M., Synthesis of mesoporous carbon-polymeric hybrid material for energy storage application. *SN Appl. Sci.* **2019,** *1* (509), 1-10.

30.   Libbrecht, W.; Deruyck, F.; Poelman, H.; Verberckmoes, A.; Thybaut, J.; De Clercq, J.; Van Der Voort, P., Optimization of soft templated mesoporous carbon synthesis using Definitive Screening Design. *Chem. Eng. J.* **2015,** *259*, 126-134.

31.   Malgras, V.; Tang, J.; Wang, J.; Kim, J.; Torad, N. L.; Dutta, S.; Ariga, K.; Hossain, M. S. A.; Yamauchi, Y.; Wu, K. C. W., Fabrication of Nanoporous Carbon Materials with Hard- and Soft-Templating Approaches: A Review. *J. Nanosci. Nanotechnol.* **2019,** *19* (7), 3673-3685.

32.   Tsouris, C.; Mayes, R.; Kiggans, J.; Sharma, K.; Yiacoumi, S.; DePaoli, D.; Dai, S., Mesoporous carbon for capacitive deionization of saline water. *Environ. Sci. Technol.* **2011,** *45* (23), 10243–10249.

33.   González-García, P., Activated carbon from lignocellulosics precursors: A review of the synthesis methods, characterization techniques and applications. *Renewable Sustainable Energy Rev.* **2018,** *82*, 1393-1414.

34.   Liu, Y.; Chen, J.; Cui, B.; Yin, P.; Zhang, C., Design and Preparation of Biomass-Derived Carbon Materials for Supercapacitors: A Review. *C* **2018,** *4* (4), 53-85.

35.   Varma, R. S., Biomass-Derived Renewable Carbonaceous Materials for Sustainable Chemical and Environmental Applications. *ACS Sustainable Chem. Eng.* **2019,** *7* (7), 6458-6470.

36.   Xie, L.; Jin, Z.; Dai, Z.; Chang, Y.; Jiang, X.; Wang, H., Porous carbons synthesized by templating approach from fluid precursors and their applications in environment and energy storage: A review. *Carbon* **2020,** *170*, 100-118.

37.   Danish, M.; Ahmad, T., A review on utilization of wood biomass as a sustainable precursor for activated carbon production and application. *Renewable and Sustainable Energy Reviews* **2018,** *87*, 1-21.

38.   Puziy, A. M.; Poddubnaya, O. I.; Sevastyanova, O., Carbon Materials from Technical Lignins: Recent Advances. *Top. Curr. Chem.* **2018,** *376* (33), 1-34.

39.   Suhas; Carrott, P. J. M.; Ribeiro Carrott, M. M. L., Lignin – from natural adsorbent to activated carbon: A review. *Bioresour. Technol.* **2007,** *98* (12), 2301-2312.

40.   Chen, F.; Zhou, W.; Yao, H.; Fan, P.; Yang, J.; Fei, Z.; Zhong, M., Self-assembly of NiO nanoparticles in lignin-derived mesoporous carbons for supercapacitor applications. *Green Chem.* **2013,** *15* (11), 3057–3063.

41.   Herou, S.; Ribadeneyra, M. C.; Madhu, R.; Araullo-Peters, V.; Jensen, A.; Schlee, P.; Titirici, M., Ordered mesoporous carbons from lignin: a new class of biobased electrodes for supercapacitors. *Green Chem.* **2019,** *21* (3), 550-559.

42.   Qin, H.; Jian, R.; Bai, J.; Tang, J.; Zhou, Y.; Zhu, B.; Zhao, D.; Ni, Z.; Wang, L.; Liu, W.; Zhou, Q.; Li, X., Influence of Molecular Weight on Structure and Catalytic Characteristics of Ordered Mesoporous Carbon Derived from Lignin. *ACS Omega* **2018,** *3* (1), 1350-1356.

43.   Saha, D.; Payzant, E. A.; Kumbhar, A. S.; Naskar, A. K., Sustainable mesoporous carbons as storage and controlled-delivery media for functional molecules. *ACS Appl. Mater. Interfaces* **2013,** *5* (12), 5868-5874.

44.   Gan, L.; Lyu, L.; Shen, T.; Wang, S., Sulfonated lignin-derived ordered mesoporous carbon with highly selective and recyclable catalysis for the conversion of fructose into 5-hydroxymethylfurfural. *Appl. Catal., A* **2019,** *574*, 132-143.

45.   Wang, S.; Sima, G.; Cui, Y.; Chang, L.; Gan, L., Preparations of lignin-derived ordered mesoporous carbon by self-assembly in organic solvent and aqueous solution: Comparison in textural property. *Mater. Lett.* **2020,** *264*, 127318-127321.

46.   Guo, N.; Li, M.; Sun, X.; Wang, F.; Yang, R., Enzymatic hydrolysis lignin derived hierarchical porous carbon for supercapacitors in ionic liquids with high power and energy densities. *Green Chem.* **2017,** *19* (11), 2595-2602.

47.   Hung, Y.-H.; Liu, T.-Y.; Chen, H.-Y., Renewable Coffee Waste-Derived Porous Carbons as Anode Materials for High-Performance Sustainable Microbial Fuel Cells. *ACS Sustain. Chem. Eng.* **2019,** *7* (20), 16991-16999.

48.   Zhang, L.; You, T.; Zhou, T.; Zhou, X.; Xu, F., Interconnected Hierarchical Porous Carbon from Lignin-Derived Byproducts of Bioethanol Production for Ultra-High Performance Supercapacitors. *ACS Appl. Mater. Interfaces* **2016,** *8* (22), 13918-13925.

49.   Zhang, W.; Cheng, H.; Niu, Q.; Fu, M.; Huang, H.; Ye, D., Microbial Targeted Degradation Pretreatment: A Novel Approach to Preparation of Activated Carbon with Specific Hierarchical Porous Structures, High Surface Areas, and Satisfactory Toluene Adsorption Performance. *Environ. Sci. Technol.* **2019,** *53* (13), 7632-7640.

50.   Supanchaiyamat, N.; Jetsrisuparb, K.; Knijnenburg, J. T. N.; Tsang, D. C. W.; Hunt, A. J., Lignin materials for adsorption: Current trend, perspectives and opportunities. *Bioresour. Technol.* **2019,** *272*, 570-581.

51.   Saha, D.; Van Bramer, S. E.; Orkoulas, G.; Ho, H.-C.; Chen, J.; Henley, D. K., CO2 capture in lignin-derived and nitrogen-doped hierarchical porous carbons. *Carbon* **2017,** *121*, 257-266.

52.   Li, Z.; Xiao, D.; Ge, Y.; Koehler, S., Surface-Functionalized Porous Lignin for Fast and Efficient Lead Removal from Aqueous Solution. *ACS Appl. Mater. Interfaces* **2015,** *7* (27), 15000-15009.

53.   Sen, S.; Sadeghifar, H.; Argyropoulos, D. S., Kraft Lignin Chain Extension Chemistry via Propargylation, Oxidative Coupling, and Claisen Rearrangement. *Biomacromolecules* **2013,** *14* (10), 3399-3408.

54.   Wang, M.; Yang, L., Lignin Functionalized by Thermally Curable Propargyl Groups as Heat-Resistant Polymeric Material. *J. Polym. Environ.* **2012,** *20* (3), 783-787.

55.   Sadeghifar, H.; Sen, S.; Patil, S. V.; Argyropoulos, D. S., Toward Carbon Fibers from Single Component Kraft Lignin Systems: Optimization of Chain Extension Chemistry. *ACS Sustain. Chem. Eng.* **2016,** *4* (10), 5230-5237.

56.   Solsperse™ Hyperdispersants Product Guide. https://www.lubrizol.com/Coatings/Brands/Solsperse-Hyperdispersants (accessed 29.01.2021).

57.   Bhatnagar, A.; Sillanpaa, M., Removal of natural organic matter (NOM) and its constituents from water by adsorption - A review. *Chemosphere* **2017,** *166*, 497-510.

Chapter 5

58.   Matilainen, A.; Gjessing, E. T.; Lahtinen, T.; Hed, L.; Bhatnagar, A.; Sillanpää, M., An overview of the methods used in the characterisation of natural organic matter (NOM) in relation to drinking water treatment. *Chemosphere* **2011,** *83* (11), 1431-1442.

59.   Li, A.; Zhao, X.; Liu, H.; Qu, J., Characteristic transformation of humic acid during photoelectrocatalysis process and its subsequent disinfection byproduct formation potential. *Water Res.* **2011,** *45* (18), 6131-6140.

60.   Tang, W.-W.; Zeng, G.-M.; Gong, J.-L.; Liang, J.; Xu, P.; Zhang, C.; Huang, B.-B., Impact of humic/fulvic acid on the removal of heavy metals from aqueous solutions using nanomaterials: A review. *Sci. Total Environ.* **2014,** *468-469*, 1014-1027.

61.   Sillanpää, M.; Ncibi, M. C.; Matilainen, A.; Vepsäläinen, M., Removal of natural organic matter in drinking water treatment by coagulation: A comprehensive review. *Chemosphere* **2018,** *190*, 54-71.

62.   Islam, M. A.; Morton, D. W.; Johnson, B. B.; Angove, M. J., Adsorption of humic and fulvic acids onto a range of adsorbents in aqueous systems, and their effect on the adsorption of other species: A review. *Sep. Purif. Technol.* **2020,** *247*, 116949-116968.

63.   Reshadi, M. A. M.; Bazargan, A.; McKay, G., A review of the application of adsorbents for landfill leachate treatment: Focus on magnetic adsorption. *Sci. Total Environ.* **2020,** *731*, 138863-138878.

64.   Gosselink, R. J. A.; Abächerli, A.; Semke, H.; Malherbe, R.; Käuper, P.; Nadif, A.; van Dam, J. E. G., Analytical protocols for characterisation of sulphur-free lignin. *Ind. Crops Prod.* **2004,** *19* (3), 271-281.

65.   Constant, S.; Wienk, H. L. J.; Frissen, A. E.; Peinder, P. d.; Boelens, R.; van Es, D. S.; Grisel, R. J. H.; Weckhuysen, B. M.; Huijgen, W. J. J.; Gosselink, R. J. A.; Bruijnincx, P. C. A., New insights into the structure and composition of technical lignins: a comparative characterisation study. *Green Chemistry* **2016,** *18* (9), 2651-2665.

66.   Libbrecht, W.; Verberckmoes, A.; Thybaut, J. W.; Van Der Voort, P.; De Clercq, J., Tunable Large Pore Mesoporous Carbons for the Enhanced Adsorption of Humic Acid. *Langmuir* **2017,** *33* (27), 6769-6777.

67.   Korntner, P.; Sumerskii, I.; Bacher, M.; Rosenau, T.; Potthast, A., Characterization of technical lignins by NMR spectroscopy: optimization of functional group analysis by 31P NMR spectroscopy. *Holzforschung* **2015,** *69* (6), 807-814.

68.   Srinivasadesikan, V.; Dai, J.-K.; Lee, S.-L., Quantum mechanistic insights on aryl propargyl ether Claisen rearrangement. *Org. Biomol. Chem.* **2014,** *12* (24), 4163-4171.

69.   Kawamoto, H., Lignin pyrolysis reactions. *Journal of Wood Science* **2017,** *63* (2), 117-132.

70.   Yu, H.; Zhang, Z.; Li, Z.; Chen, D., Characteristics of tar formation during cellulose, hemicellulose and lignin gasification. *Fuel* **2014,** *118*, 250-256.

71.   Thommes, M.; Kaneko, K.; Neimark Alexander, V.; Olivier James, P.; Rodriguez-Reinoso, F.; Rouquerol, J.; Sing Kenneth, S. W., Physisorption of gases, with special reference to the evaluation of surface area and pore size distribution (IUPAC Technical Report). *Pure Appl. Chem.* **2015,** *87* (9-10), 1051–1069.

72.   Muylaert, I.; Borgers, M.; Bruneel, E.; Schaubroeck, J.; Verpoort, F.; Van Der Voort, P., Ultra stable ordered mesoporous phenol/formaldehyde polymers as a heterogeneous support for vanadium oxide. *Chem. Commun.* **2008,** (37), 4475-4477.

73.   McKeown, N. B.; Budd, P. M.; Msayib, K. J.; Ghanem, B. S.; Kingston, H. J.; Tattershall, C. E.; Makhseed, S.; Reynolds, K. J.; Fritsch, D., Polymers of Intrinsic Microporosity (PIMs): Bridging the Void between Microporous and Polymeric Materials. *Chem. - Eur. J.* **2005,** *11* (9), 2610-2620.

74.   Muylaert, I.; Verberckmoes, A.; De Decker, J.; Van Der Voort, P., Ordered mesoporous phenolic resins: Highly versatile and ultra stable support materials. *Adv. Colloid Interface Sci.* **2012,** *175*, 39-51.

75.   Azadfar, M.; Hiscox, W. C.; Chen, S., Solubilization of lignin in copolymer micelles in aqueous solution. *Colloids and Surfaces A: Physicochemical and Engineering Aspects* **2016,** *503*, 1-10.

76.   Jiao, J.; Cai, Y.; Liu, P.; Liu, P., Influence of template on the structure of mesoporous carbon prepared with novalac resin as carbon precursor. *J. Porous Mater.* **2013,** *20* (5), 1247-1255.

77.   Li, Q.; Jiang, R.; Dou, Y.; Wu, Z.; Huang, T.; Feng, D.; Yang, J.; Yu, A.; Zhao, D., Synthesis of mesoporous carbon spheres with a hierarchical pore structure for the electrochemical double-layer capacitor. *Carbon* **2011,** *49* (4), 1248-1257.

78.   Saha, D.; Warren, K. E.; Naskar, A. K., Soft-templated mesoporous carbons as potential materials for oral drug delivery. *Carbon* **2014,** *71*, 47-57.

79.   Chen, J. P.; Wu, S., Simultaneous adsorption of copper ions and humic acid onto an activated carbon. *J. Colloid Interface Sci.* **2004,** *280* (2), 334-342.

80.   Eustáquio, H.; Lopes, C.; S. da Rocha, R.; D. Cardoso, B.; Pergher, S., Modification of Activated Carbon for the Adsorption of Humic Acid. *Adsorpt. Sci. Technol.* **2015,** *33*, 117-126.

81.   Maghsoodloo, S.; Noroozi, B.; Haghi, A. K.; Sorial, G. A., Consequence of chitosan treating on the adsorption of humic acid by granular activated carbon. *J. Hazard. Mater.* **2011,** *191* (1-3), 380-387.

82.   Tavengwa, N. T.; Chimuka, L.; Tichagwa, L., Equilibrium and kinetic studies on the adsorption of humic acid onto cellulose and powdered activated carbon. *Desalin. Water Treat.* **2015,** *40* (1), 25-32.

83.   Yang, K.; Fox, J. T., Adsorption of Humic Acid by Acid-Modified Granular Activated Carbon and Powder Activated Carbon. *Journal of Environmental Engineering* **2018,** *144* (10), 4018104-4018114.

84.   Liu, F.; Xu, Z.; Wan, H.; Wan, Y.; Zheng, S.; Zhu, D., Enhanced adsorption of humic acids on ordered mesoporous carbon compared with microporous activated carbon. *Environ. Toxicol. Chem.* **2011,** *30* (4), 793-800.

85.   Lorenc-Grabowska, E.; Gryglewicz, G., Adsorption of lignite-derived humic acids on coal-based mesoporous activated carbons. *J. Colloid Interface Sci.* **2005,** *284* (2), 416-423.

86.   Stárek, J.; Zukal, A.; Rathouský, J., Comparison of the adsorption of humic acids from aqueous solutions on active carbon and activated charcoal cloths. *Carbon* **1994,** *32* (2), 207-211.

87.   Kołodziej, A.; Fuentes, M.; Baigorri, R.; Lorenc-Grabowska, E.; García-Mina, J. M.; Burg, P.; Gryglewicz, G., Mechanism of adsorption of different humic acid fractions on mesoporous activated carbons with basic surface characteristics. *Adsorption* **2014,** *20* (5-6), 667-675.

88.   Wu, F.-C.; Tseng, R.-L.; Juang, R.-S., Adsorption of dyes and humic acid from water using chitosan-encapsulated activated carbon. *J. Chem. Technol. Biotechnol.* **2002,** *77* (11), 1269-1279.

89.   Yu, H.; Zhang, Q.; Dahl, M.; Joo, J. B.; Wang, X.; Wang, L.; Yin, Y., Dual-Pore Carbon Shells for Efficient Removal of Humic Acid from Water. *Chemistry* **2017,** *23* (64), 16249-16256.

90.   Anzai, T.; Matsuura, Y.; Sugawara, T.; Miura, O., Removal of Humic Acid in Water by Rice Hull Magnetic Activated Carbon and Magnetic Separation. *IEEE Trans. Appl. Supercond.* **2016,** *26* (4), 1-4.

91.   Wen, T.; Wang, J.; Yu, S.; Chen, Z.; Hayat, T.; Wang, X., Magnetic Porous Carbonaceous Material Produced from Tea Waste for Efficient Removal of As(V), Cr(VI), Humic Acid, and Dyes. *ACS Sustain. Chem. Eng.* **2017,** *5* (5), 4371-4380.

92.   Espinoza-Acosta, J. L.; Torres-Chávez, P. I.; Olmedo-Martínez, J. L.; Vega-Rios, A.; Flores-Gallardo, S.; Zaragoza-Contreras, E. A., Lignin in storage and renewable energy applications: A review. *Journal of Energy Chemistry* **2018,** *27* (5), 1422-1438.

93.   Zhu, J.; Yan, C.; Zhang, X.; Yang, C.; Jiang, M.; Zhang, X., A sustainable platform of lignin: From bioresources to materials and their applications in rechargeable batteries and supercapacitors. *Progress in Energy and Combustion Science* **2020,** *76*, 100788-100812.

Chapter 5

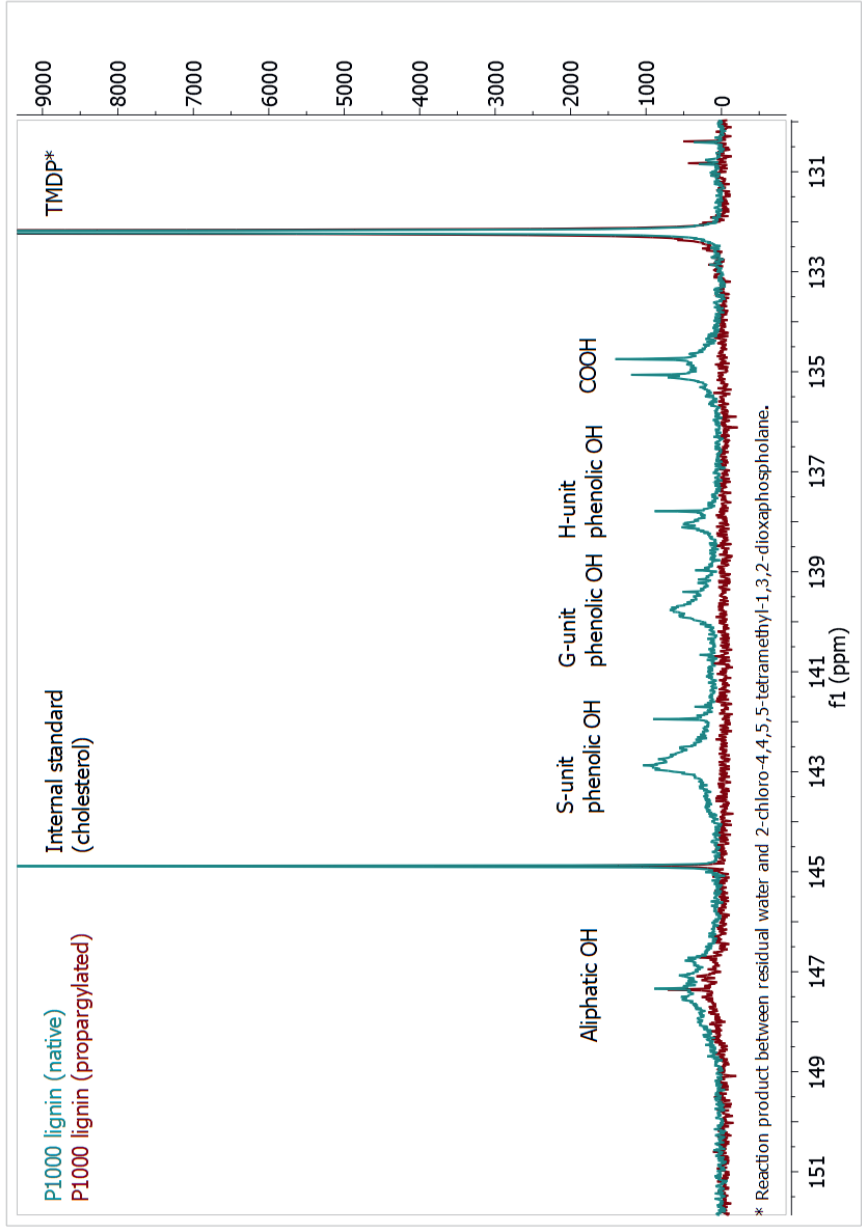## Appendix for Chapter 5

Figure S1 ^{31}P NMR spectra before and after propargylation of P1000 lignin (CDCl$_3$/Pyridine)
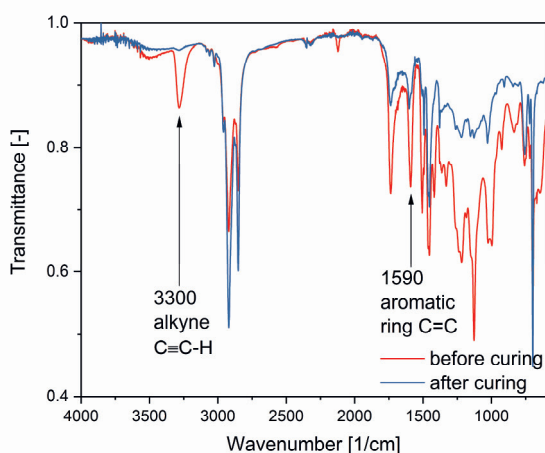
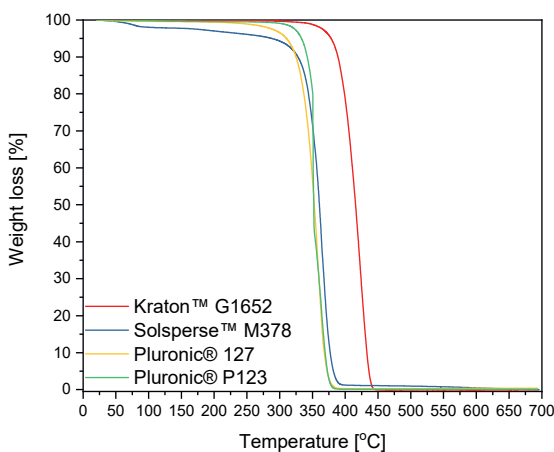**Figure S2** *Example of IR spectra before and after Claisen rearrangement (example: G1652 resin)*

Figure S3 *TGA thermographs of the used surfactants (thermogravimetric analysis in nitrogen atmosphere at a heating rate of 10 °C/min*
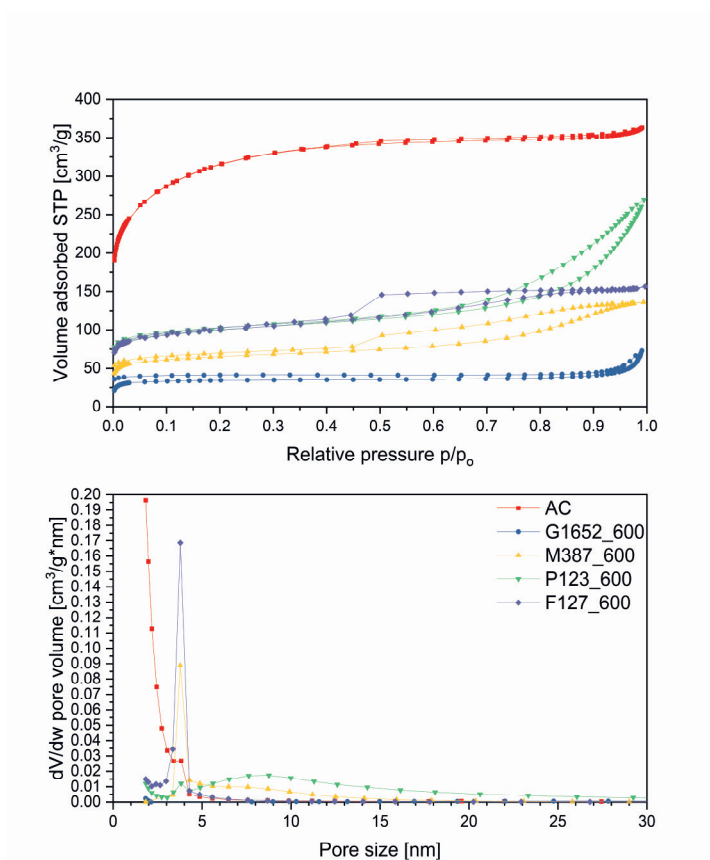
Chapter 5

***Figure S4** Nitrogen sorption isotherm (top) and pore size distribution (PSD) (bottom) of the resins carbonized at 600°C*
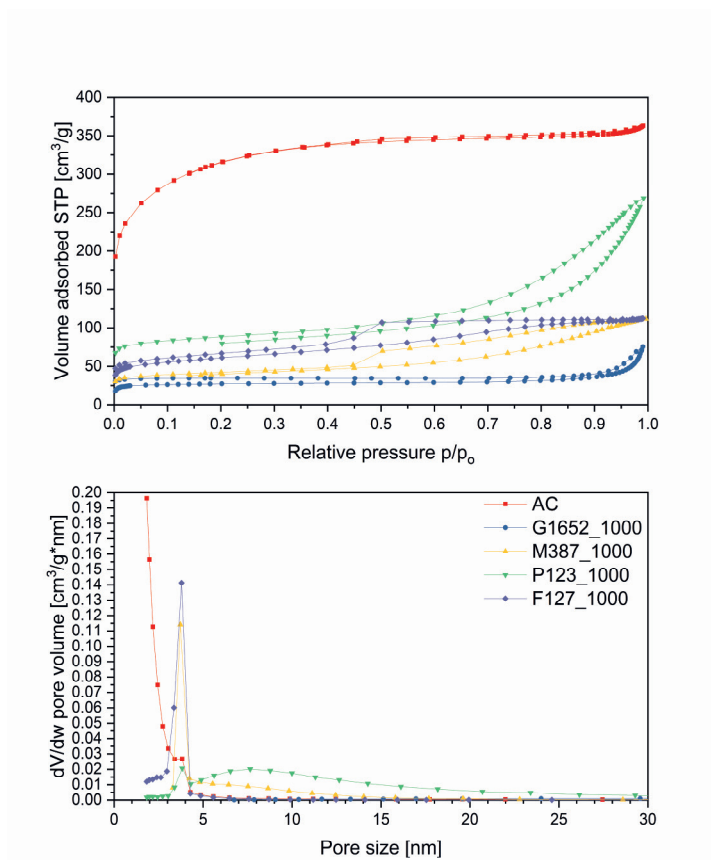
Figure S5 *Nitrogen sorption isotherm (top) and pore size distribution (PSD) (bottom) of the resins carbonized at 1000°C*

Summary

Among multiple biobased platform molecules, lignin plays a special role as one of the most abundant feedstocks available, while at the same time being the most abundant renewable source of aromatic compounds. Despite that, only less than 5% of lignin is used in value-added applications that do not include the energy sector. Commercially available technical lignins often have low quality: they are condensed, have high molecular weight and dispersity, lack in functionality, contain sulphur, and have various impurities, which decrease their solubility in organic solvents and overall limit their application pool, especially in polymeric materials. While incorporation of lignin in polymeric materials by blending or replacement of structural units, can bring added properties to the final materials, such as UV-blocking and antioxidant properties, the mechanical properties typically deteriorate upon incorporating high quantities of lignin in polymeric materials.

A possible solution to that issue is using fractionated or depolymerized lignin fractions, which show advantageous properties in terms of molecular weight, functionality, and purity compared with technical lignins. In this thesis, lignin fractions originating from different biomass feedstocks, obtained via various processing methods such as state-of-the-art isolation of technical lignins, solvolysis of technical lignin, 'lignin-first' process, and separation of lignin fractions were evaluated. Above-mentioned lignins were incorporated in various polymeric materials using novel synthetic approaches. Those materials are suitable for applications such as adhesives, coatings, additives, and adsorbents, and their performance was benchmarked against state-of-the-art equivalent products. The structure-property relationships between the performance and structural features of lignin fractions were also determined.

The focus of chapter 2 was the development of lignin-based resins suitable for wood adhesion applications. This study involved thermal cross-linking of a lignin-based resin via thiol-yne "click" chemistry and investigated a post-curing strategy via Claisen rearrangement. Two lignin fractions were evaluated as a starting material: commercial Protobind 1000 lignin and methanol soluble Protobind 1000 lignin fraction after mild solvolysis. Although these two lignin fractions varied in characteristics such as molecular weight and functionality, the difference in their performance was rather small. It may be connected with the fact, that Protobind 1000 lignin is one of the purest and lowest molecular weight and technical lignins available on the market. It was shown that the properties of the networks (such as T_g, thermal stability, and insoluble fraction) could be tuned by selection of the curing scenario and the composition of the formulation (amount of reactive diluent, P-4MS). Resins prepared in this chapter were tested as a wood adhesive and possessed a desirable

performance, comparable to state-of-the-art phenol-formaldehyde resins. The main benefits over the phenol-formaldehyde approach are that higher lignin loadings are possible to achieve (usually less than 50% of phenol can be replaced by lignin in lignin-phenol-formaldehyde resins, vs 75-100% lignin shown here, in both cases the cross-linker is excluded from the calculations) and no volatiles are emitted during the resins processing and use.

The synthesis and characterization of lignin-based protective coatings with anticorrosive properties was explored in chapter 3. Thermosetting coatings with high amounts of lignin-based components were prepared by means of a tandem UV-initiated thiol-yne "click" synthesis and Claisen rearrangement strategy. Lignin fractions investigated in this study were obtained from the 'lignin-first' process using Ni/SiO$_2$ as a catalyst. Three fractions were benchmarked, namely the mixture of lignin oligomers and monomers after 'lignin-first' process without fractionation, or fractionated samples via extraction and membrane separation processes. The above-mentioned lignin fractions differed in the monomer content and composition. Membrane separation turned out to be more effective than extraction in order to reduce the monomer content in the 'lignin-first' mixture of monomers and oligomers after depolymerization. The obtained protective coatings exhibited remarkable adhesion to steel surfaces and excellent solvent resistance, even after exposure to corrosive environment. Moreover, the coatings showed excellent barrier and corrosion protection even after 21 days of exposure. This chapter revealed that the separation of the 'lignin-first' mixture did not improve the performance of the polymeric coating, compared with the unseparated sample, which is an advantage in terms of process sustainability and techno-economics. The take home message of this chapter is that more efforts should be made in order to utilize mixtures of lignin monomers and oligomers as such in other kinds of resins, especially that separation may not bring improved performance.

While the two previous chapters explored the use of lignin in polymeric resins, chapter 4 concentrated on the application of lignin as antioxidant additive. A potential application of such antioxidant additive was selected in the field of biolubricants. Currently used petroleum-based lubricants are in general toxic and nonbiodegradable. As an alternative, biolubricants such as vegetable oils could be used instead. However, the biggest drawback of using vegetable oils in lubricant applications is their lack of thermo-oxidative stability, which as shown in chapter 4, could be improved by adding lignin-based antioxidant additives. In order to ensure good dispersibility of the additive in a vegetable oil matrix, lignin fractions were partially esterified to increase their lipophilicity. Four lignin-based fractions, namely commercial Protobind P1000 soda lignin, solvolytically fractionated Protobind P1000 lignin and two lignin fractions from the 'lignin-first' process, were studied in

biolubricant formulations after esterification. The evaluated lignin fractions exhibited excellent performance compared to butylated hydroxytoluene, a state-of-the-art antioxidant. One of the 'lignin-first' fractions, palmitoylated Pd/C hexane residue, showed significant improvement of thermo-oxidative stability in a vegetable oil matrix, while other lignin-based additives showed similar performance with BHT. From rheological and tribological perspective, the majority of the biolubricant formulations exhibited lubricating properties comparable with vegetable oil. This study demonstrated the successful incorporation of lignin-based antioxidants in biolubricant formulations, tackling the major disadvantage of vegetable oils as environment-friendly lubricants. Moreover, the relationship between antioxidant properties and structural characteristics was established. The molecular weight of lignin-based fractions and S+G hydroxyl content were the most important characteristics influencing the antioxidant activity.

The last application investigated in chapter 6 is the use of lignin as precursor in the synthesis of carbonous materials suitable for adsorption of contaminations in water. In this chapter, a series of lignin-based mesoporous carbons was successfully prepared using a Claisen rearrangement route via the soft-template methodology. Depending on carbonization conditions and the used template, the properties of the mesoporous carbons such as surface area, elemental composition, pore size, and pore volume could be tuned. Lignin-based mesoporous carbons were evaluated as humic acid adsorbent, and showed excellent performance in water purification, compared with the commercial activated carbon and other carbonous adsorbents reported in the literature. This synthetic route yielding lignin-based mesoporous carbons was demonstrated to be suitable for the preparation of adsorbents, but it is expected that it is possible to use these kind of materials for other applications including supercapacitors and energy storage materials.

Overall, this thesis showcased different possible uses of lignin in polymeric materials and additives. As shown in Chapters 2, 4, and 6, the proof-of-concept products in which technical or fractionated lignin have been incorporated showed comparable or improved performance compared to their state-of-art references. However, upscaling activities and further evaluation of their performance and should be performed to fully evaluate usability of lignin in these applications.

Evaluated lignin fractions originated from novel lignin isolation and processing methods, such as 'lignin-first' processes and solvolysis. It is worth to highlight that lignin fractions used in this thesis had high amounts of functional groups and low molecular weight compared with most of available technical lignins. On the other hand, lignin fractions obtained from 'lignin-first' processes were tested as a mixture of lignin monomers and oligomers. Notably, it was shown that separation of lignin

monomers and oligomers may not be necessary for the successful incorporation of lignin fraction in polymeric materials.

To sum up, the origin of the overall good performance of tested lignin fractions in polymeric and carbonous materials, as well as in antioxidant additives can be related to their advantageous physico-chemical properties. These findings are critical for the evaluation of the marketable applications, where these type of lignin fractions have a high chance to be successful. Up until now, lignin fractions originating from mild solvolysis, 'liginin-first' and fractionation processes were available only at the lab scale, but ongoing scaling-up activities open the possibility to explore other applications in polymeric materials and additives, and their evaluation by the industry. Keeping in mind their improved characteristics, it can be expected that more value-added applications can be developed using those fractions in the near future.

Impact paragraph

The transition from a linear economy to a circular economy is recognized as a crucial way to achieve the 2050 climate neutrality targets of the Paris Agreement.[1, 2] As a result of shifting toward circular economy, the use of biobased starting materials is gaining more and more interest from both industry and academia.[3-6] Here, I intend to highlight the impact of this research on academia, industry, and society.

The ultimate goal of this work was to valorize and benchmark lignin fractions in various applications, including adhesives, coatings, additives, and adsorbents. This research utilized lignin fractions originating from different biomass feedstocks, obtained via different processing methods such as state-of-the-art isolation of technical lignins, solvolysis of technical lignin, 'lignin-first' process, and separation of lignin oils. It is worth to highlight that those fractions were obtained as a result of cross-border collaboration within BIO-HArT and InSciTe Lignin RICHES platforms. Those lignin isolation technologies are currently upscaled or will be upscaled in the near future.[7-9] It is crucial to be pointed out that most of the applications for lignin-based materials are currently developed using technical lignins, possessing higher molecular weights, lower purity, and lower functionality. Therefore, the above-mentioned lignin fractions are significantly different from the commercially available technical lignins, as demonstrated in this thesis. Consequently, valorization of the above-mentioned lignin fractions in different applications is relevant for their commercialization and development of their marketable applications. In this work, I have shown some examples of potential applications in the field of polymeric materials and additives. Having said that, this work is relevant for both academic research, as evaluation of novel lignin fractions, and for industry, by providing a possible application pool of the lignin fractions obtained by modern biorefineries. In the future, the applications of the above-mentioned lignin fractions should not be limited to the ones presented here, but can be further developed and include more types of polymeric resins, such as polyurethane and epoxies. In addition, different applications could be tested, for example, polymeric blends, alternative purpose additives, and surfactants.

Another aspect of the research presented in this thesis is related to the development of suitable methodologies for incorporation of lignin fractions in polymeric materials and additives. Although there are already numerous existing methodologies, this work presents alternative approaches utilizing thiol-yne 'click' chemistry and optionally post-curing for the synthesis of lignin-based resins and lignin esterification for the biolubricants additives. The work demonstrated in this thesis shows how the properties of such materials can be tuned and how those materials compare with state-of-the-art references. Even though the methodologies presented in this thesis

were shown to be suitable for modifying (biobased) materials, their application combined with real-life applications was not demonstrated for lignin-based materials. In my opinion, especially valuable are the results shown in chapter 3. The most surprising result of that chapter is that separation of lignin oil containing monomers and oligomers did not lead to improved performance of the coating. Therefore, the separation of lignin depolymerized fraction is not always necessary for the application in polymeric materials. Using the mixture obtained as such will have a tremendous benefit of reduced environmental impact and lower cost of production of said lignin oil compared with separated lignin oil fractions. I hope that this development will inspire more industrial and academic research on lignin oil mixtures used as such and that lignin separation would be employed when there is an actual benefit or necessity of its use.

The last major objective of this work is to study the relationship between the structure of the lignins obtained in depolymerization and fractionation processes and their properties, which affect their performance in real-life applications. Although this aim is addressed in all the chapters, it is the most pronounced in chapter 4. In that chapter, it was shown which structural features of lignin fractions lead to best antioxidant properties. In this chapter, the antioxidant properties of lignin were utilized to serve as an antioxidant additive in biolubricants, which was possible upon partial lignin esterification. The results of this research are highly relevant in the field of biolubricants given that the tribological properties of said biolubricants were improved or at least maintained, while thermo-oxidative stability was significantly improved. Low thermo-oxidative stability is the biggest downside of the use of vegetable oils in biolubricants, which can be overcome by incorporation of lignin-based additives.

The impact of this work on society is rather indirect. While society acknowledges the need to shift from the linear to the circular economy, it is not always straightforward how to implement this goal. That is why the work of scientists is important in addressing that need by showing the possible solutions on how to utilize biobased materials in everyday applications and what their performance is compared to the known materials. The boom in biobased economy is seen by the increasing amount of biorefinery projects utilizing biomass as a feedstock, which would lead to the increased availability of high-quality lignin fractions. Therefore, the circular ecomony aspect of lignocellulose biorefineries can be seen as the reduction of the amount of waste (for instance, residual biomass) by its reuse and upgrading, which can be achieved by integrating biowaste as a feedstock for fuels, chemicals, and materials.[10-13] The use of lignin-fractions originating from currently scaled-up processes contributes to their valorization in marketable solutions answers the urge to include biobased components in (polymeric) materials, which is contributing to

making biorefineries ecomomy more efficient and circular. I hope that this work will help strengthen the knowledge bridge between academic research and industry, which would benefit society in the long term by making biobased products more available on the market.

References

1.   United Nations, Shifting to a Circular Economy Essential to Achieving Paris Agreement Goals. https://unfccc.int/news/shifting-to-a-circular-economy-essential-to-achieving-paris-agreement-goals (accessed 2022.04.30).

2.   European Commission, Circular economy action plan. https://ec.europa.eu/environment/strategy/circular-economy-action-plan_en (accessed 30.04.2022).

3.   Lange, L.; Connor, K. O.; Arason, S.; Bundgård-Jørgensen, U.; Canalis, A.; Carrez, D.; Gallagher, J.; Gøtke, N.; Huyghe, C.; Jarry, B.; Llorente, P.; Marinova, M.; Martins, L. O.; Mengal, P.; Paiano, P.; Panoutsou, C.; Rodrigues, L.; Stengel, D. B.; van der Meer, Y.; Vieira, H., Developing a Sustainable and Circular Bio-Based Economy in EU: By Partnering Across Sectors, Upscaling and Using New Knowledge Faster, and For the Benefit of Climate, Environment & Biodiversity, and People & Business. *Front. Bioeng. Biotechnol.* **2021,** *8*, 619066.

4.   Baldoni, E.; Philippidis, G.; Spekreijse, J.; Gurría, P.; Lammens, T.; Parisi, C.; Ronzon, T.; Vis, M.; M'Barek, R., Getting your hands dirty: A data digging exercise to unearth the EU's bio-based chemical sector. *Renewable Sustainable Energy Rev.* **2021,** *143*, 110895.

5.   de Jong, E.; Stichnothe, H.; Bell, G.; Jørgenson, H., Biobased Chemicals – a 2020 status update. https://task42.ieabioenergy.com/wp-content/uploads/sites/10/2020/02/Bio-based-chemicals-a-2020-update-final-200213.pdf (accessed 30.04.2022).

6.   Lee, J.-Y.; Lee, S.-E.; Lee, D.-W., Current status and future prospects of biological routes to bio-based products using raw materials, wastes, and residues as renewable resources. *Crit. Rev. Environ. Sci. Technol.* **2021**, 1-57.

7.   van Baarle, D., Vertoro scales up oil production from lignin. https://www.industryandenergy.eu/biobased-economy/vertoro-scales-up-oil-production-from-lignin/ (accessed 01.07.2021).

8.   Biorizon, LignoValue Pilot ready to be built: More than 30 interested companies. https://www.biorizon.eu/news/lignovalue-pilot-ready-to-be-built-more-than-30-interested-companies (accessed 30.04.2022).

9.   Sels Group, Lignin-first biorefinery at pilot-scale: KULeuven and MTSA Technopower finalising detailed design. https://sels-group.eu/lignin-first-biorefinery-at-pilot-scale-kuleuven-and-mtsa-technopower-finalising-detailed-design.

10.   Garlapati, V.K.; Chandel, A.K.; Kumar, S.P.J.; Sharma, S.; Sevda, S.; Ingle, A.P.; Deepak, P., Circular economy aspects of lignin: Towards a lignocellulose biorefinery, *Renewable and Sustainable Energy Rev.* **2020,** 130, 109977.

11.   Velvizhi, G.; Balakumar, K.; Shetti, N.P.; Ahmad, G.; Pant, K.K.; Aminabhavi, T.M., Integrated biorefinery processes for conversion of lignocellulosic biomass to value added materials: Paving a path towards circular economy, *Bioresour. Technol.* **2022**, 343, 126151.

12.   Sarsaiya, S.; Jain, A.; Awasthi, S.K.; Duan, Y.; Awasthi, M.K.; Shi, J., Microbial dynamics for lignocellulosic waste bioconversion and its importance with modern circular economy, challenges and future perspectives, *Bioresour. Technol.* **2019**, 291, 121905.

13.   Guo, Z.; Yan, N.; Lapkin, A.A., Towards circular economy: integration of bio-waste into chemical supply chain, *Curr. Opin. Chem. Eng.* **2019**, 26, 148-156.

Acknowledgments

My journey as a PhD candidate at Maastricht University started in 2016, and ever since, I have received plenty of support from all the wonderful people I had an honor to work with. You influenced me personally and helped me to grow professionally. I'm really grateful for this!

Foremost, I would like to express my deepest gratitude to my promotor and daily supervisor, Assoc. Prof. dr. Katrien Bernaerts. Despite some initial ups and downs, I could always count on your guidance and assistance. It is amazing to see how our relationship developed over these last couple of years. Thank you for the countless brainstorming sessions, for sharing your valuable knowledge, and for helping me to grow. I truly admire your dedication, hard work, and perseverance. I appreciate all the opportunities you gave me.

I would also like to thank my co-promotor Prof. dr. Andrij Pich. I have received a great deal of scientific support and constructive criticism from you ever since you joined Maastricht University back in 2019. Last but not least, I would like to acknowledge Prof. dr. Stefaan De Wildeman, who was one of my promotors when I started my PhD research. It was a very inspiring experience to work with you.

I would like to express my sincere appreciation to the members of my Defense Committee, Prof. dr. Maarten Honing, Assoc. Prof. dr. Hanne Diliën, dr. Richard Gosselink, Prof. dr. Wim Thielemans, and Prof. dr. Luc Avérous for accepting an invitation to join the Committee, taking time to carefully evaluate my thesis, and attending my defense.

The research I conducted would have never been the same without the input of my esteemed project partners within InSciTe Lignin RICHES and BIO-HArT platforms. I wish to especially acknowledge the members of the group of Prof. Bert Sels from Katholieke Universiteit Leuven: Sander Van den Bosch, Joost Van Aelst, Korneel Van Aelst, Svetlana Stepanova, Thijs Vangeel, Bert Lagrain, and Bert Sels, and the team of Prof. Emiel Hansen from Eindhoven University of Technology: Dannie van Osch, Panos Kouris, Michael Boot, and Emiel Hensen. It was a very successful collaboration, full of exchange of lignin samples, knowledge, and experience. Furthermore, I would like to thank Kelly Servaes, Karolien Vanbroekhoven, and Viviana Polizzi from VITO, and Peter Quaedflieg and Jeroen Konings from Innosyn for their scientific inputs and discussions.

Furthermore, I would like to express my gratitude towards my collaborators outside InSciTe Lignin RICHES and BIO-HArT projects. In particular, I would like to thank Jeriffa De Clercq and An Verberckmoes from Ghent University, Herman Terryn,

Curriculum Vitae

Monika Jedrzejczyk was born in Opoczno, Poland on December 12, 1991. In 2014, Monika obtained an Engineering Degree (Bachelor of Science) in Chemical Technology at Lodz University of Technology. During her Engineering Degree she followed the Organic Chemical Technology track. Afterward, Monika continued her studies in the field of Nanotechnology, which she completed with a Master's Degree in 2015. Her Master's thesis project focused on the application of silver nanoparticles in cancer diagnostics. During her studies, Monika gained valuable experience during multiple internships in industry and research facilities. In particular, Monika joined University of Twente, the Netherlands for an internship during which she gained experience in polymer development for biomedical applications. Shortly after, Monika pursued a PhD research project at Maastricht University under the supervision of Assoc. Prof. Katrien Bernaerts, Prof. Stefaan de Wildeman, and Prof. Andrij Pich. Her research focused on the development of lignin-based materials and additives. During her time at Maastricht University, Monika extensively collaborated with an excellent team of scientists within InSciTe Lignin REACHES and Interreg BIO-HArT platforms, among others. This fruitful collaboration resulted in four peer-reviewed publications. In 2020, Monika continued working in the field of lignin-based materials development as a Senior Scientist at Vertoro. As of February 2022, Monika is a Trainee Patent Attorney at V.O. Patents and Trademarks and she aims to contribute to innovative science and technology valorization by assisting in obtaining their intellectual property protection.

List of publications

From this thesis:

M. A. Jedrzejczyk, N. Madelat, B. Wouters, H. Smeets, M. Wolters, S. A. Stepanova, T. Vangeel, K. Van Aelst, S. Van den Bosch, J. Van Aelst, V. Polizzi, K. Servaes, K. Vanbroekhoven, B. Lagrain, B. F. Sels, H. Terryn, K. V. Bernaerts, Preparation of Renewable Thiol-Yne "Click" Networks Based on Fractionated Lignin for Anticorrosive Protective Film Applications. *Macromol. Chem. Phys.* **2022**, *223* (13), 2100461

M. A. Jedrzejczyk, P. D. Kouris, M. D. Boot, E. J. M. Hensen, K. V. Bernaerts, Renewable Thiol–yne "Click" Networks Based on Propargylated Lignin for Adhesive Resin Applications. *ACS Appl. Polym. Mater.* **2022**, *4* (4), 2544-2552

M. A. Jedrzejczyk, S. Van den Bosch, J. Van Aelst, K. Van Aelst, P. D. Kouris, M. Moalin, G. R. M. M. Haenen, M. D. Boot, E. J. M. Hensen, B. Lagrain, B. F. Sels, K. V. Bernaerts, Lignin-Based Additives for Improved Thermo-Oxidative Stability of Biolubricants, *ACS Sustainable Chem. Eng.* **2021**, *9* (37), 12548-12559

M. A. Jedrzejczyk, J. Engelhardt, M. R. Djokic, V. Bliznuk, K. M. Van Geem, A. Verberckmoes, J. De Clercq, K. V. Bernaerts, Development of Lignin-Based Mesoporous Carbons for the Adsorption of Humic Acid, *ACS Omega* **2021**, *6* (23), 15222-15235

Previous publications:

H. Abramczyk, M. Kopec, **M. Jedrzejczyk**, Raman Spectroscopy, Medical Applications: A New Look Inside Human Body With Raman Imaging, In: *Encyclopedia of Spectroscopy and Spectrometry (Third Edition)*, Academic Press, **2017**, 915-918